Vol. 60 JUNE, 1956 No. 6

6no.

THE JOURNAL OF PHYSICAL CHEMISTRY

(Registered in U. S. Patent Office)

SYMPOSIUM ON GEOCHEMISTRY, MINNEAPOLIS, MINN., September 12, 1955

THE JOURNAL OF PHYSICAL CHEMISTRY

(Registered in U. S. Patent Office)

Published monthly by the American Chemical Society at 20th and Northampton Sts., Easton, Pa.

Entered as second-class matter at the Post Office at Easton, Pennsylvania.

The *Journal of Physical Chemistry* is devoted to the publication of selected symposia in the broad field of physical chemistry and to other contributed papers.

Manuscripts originating in the British Isles, Europe and Africa should be sent to F. C. Tompkins, The Faraday Society, 6 Gray's Inn Square, London W. C. 1, England.

Manuscripts originating elsewhere should be sent to W. Albert Noyes, Jr., Department of Chemistry, University of Rochester, Rochester 20, N. Y.

Correspondence regarding accepted copy, proofs and reprints should be directed to Assistant Editor, Allen D. Bliss, Department of Chemistry, Simmons College, 300 The Fenway, Boston 15, Mass.

Business Office: Alden H. Emery, Executive Secretary, American Chemical Society, 1155 Sixteenth St., N. W., Washington 6, D. C.

Advertising Office: Reinhold Publishing Corporation, 430 Park Avenue, New York 22, N. Y.

Articles must be submitted in duplicate, typed and double spaced. They should have at the beginning a brief Abstract, in no case exceeding 300 words. Original drawings should accompany the manuscript. Lettering at the sides of graphs (black on white or blue) may be pencilled in and will be typeset. Figures and tables should be held to a minimum consistent with adequate presentation of information. Photographs will not be printed on glossy paper except by special arrangement. All footnotes and references to the literature should be numbered consecutively and placed in the manuscript at the proper places. Initials of authors referred to in citations should be given. Nomenclature should conform to that used in *Chemical Abstracts*, mathematical characters marked for italic, Greek letters carefully made or annotated, and subscripts and superscripts clearly shown. Articles should be written as briefly as possible consistent with clarity and should avoid historical background unnecessary for specialists.

Symposium papers should be sent in all cases to Secretaries of Divisions sponsoring the symposium, who will be responsible for their transmittal to the Editor. The Secretary of the Division by agreement with the Editor will specify a time after which symposium papers cannot be accepted. The Editor reserves the right to refuse to publish symposium articles, for valid scientific reasons. Each symposium paper may not exceed four printed pages (about sixteen double spaced typewritten pages) in length except by prior arrangement with the Editor.

Remittances and orders for subscriptions and for single copies, notices of changes of address and new professional connections, and claims for missing numbers should be sent to the American Chemical Society, 1155 Sixteenth St., N. W., Washington 6, D. C. Changes of address for the *Journal of Physical Chemistry* must be received on or before the 30th of the preceding month.

Claims for missing numbers will not be allowed (1) if received more than sixty days from date of issue (because of delivery hazards, no claims can be honored from subscribers in Central Europe, Asia, or Pacific Islands other than Hawaii), (2) if loss was due to failure of notice of change of address to be received before the date specified in the preceding paragraph, or (3) if the reason for the claim is "missing from files."

Subscription Rates (1956): members of American Chemical Society, $8.00 for 1 year; to non-members, $16.00 for 1 year. Postage free to countries in the Pan American Union; Canada, $0.40; all other countries, $1.20. $12.50 per volume, foreign postage $1.20, Canadian postage $0.40; special rates for A.C.S. members supplied on request. Single copies, current volume, $1.35; foreign postage, $0.15; Canadian postage $0.05. Back issue rates (starting with Vol. 56): $15.00 per volume, foreign postage $1.20, Canadian, $0.40; $1.50 per issue, foreign postage $0.15, Canadian postage $0.05.

The American Chemical Society also publishes *Journal of the American Chemical Society*, *Chemical Abstracts*, *Industrial and Engineering Chemistry*, *Chemical and Engineering News*, *Analytical Chemistry*, *Journal of Agricultural and Food Chemistry* and *Journal of Organic Chemistry*. Rates on request.

(*Continued from first page of cover*)

THE JOURNAL OF
PHYSICAL CHEMISTRY

(Registered in U. S. Patent Office) (© Copyright, 1956, by the American Chemical Society)

VOLUME 60 JUNE 19, 1956 NUMBER 6

PHYSICAL CHEMISTRY IN GEOCHEMISTRY[1]

BY FARRINGTON DANIELS

Contribution from the Department of Chemistry, University of Wisconsin, Madison, Wisconsin

Received December 27, 1955

The purpose of this symposium is to call attention to the many interesting problems of geochemistry which can be attacked through physical chemistry, and to point out also unique experiments started long ago in the geological past, which are now available for physical chemical studies. Geochemistry is of interest alike to those who want to find new mineral deposits and to those who merely seek an understanding of the geological processes by which nature has laid down our minerals in their present locations.

Many branches of physical chemistry are involved in geochemistry, including thermodynamic equilibria of solids, liquids and gases, phase diagrams, oxidation and reduction, *p*H, solubility, precipitation, crystallization, electrolytic reactions, adsorption, sedimentation, kinetics of rate processes, heat transfer, radioactivity, isotopic tracers, nuclear reactions, radiation damage and thermoluminescence. Only a few of these can be illustrated in this symposium but the general principles are applicable to many geological phenomena. In the paragraphs which follow some of the subjects which were discussed at the symposium will be referred to. Four of them are published in detail in this issue of THIS JOURNAL.

The phenomena mentioned above occur both in the igneous or hard rocks and in the sedimentary formations produced by erosion. The primary rocks are formed by the cooling of molten material and efforts have been made to determine what type of material gives an over-all sample of the composition of the earth taken as a whole. Meteorites and the sun apparently are not satisfactory. Geological material may be transported in several different ways as solids, liquids, solutions, gases and colloidal materials. Rivers carry along both dissolved salts and colloidal particles. At high velocities they move large particles and rocks. The glaciers carry large rocks. Volcanic lava and volcanic dust are also important in the movement of material.

Air is a very important geochemical agent and it penetrates to considerable depth below the surface. The oxidation state of an element can tell much concerning the geochemical history of the mineral in which it is found. Combining a knowledge of *p*H and oxidation–reduction potentials, it is possible to determine the conditions under which a given mineral such as iron oxide or lead sulfide will precipitate. Conversely, when a given mineral is found the conditions of its environment can be accurately ascertained.

The ratio of the sulfur isotopes S^{34} to S^{32} offers a valuable means for studying the geological history. Thode has found that S^{34} is enriched in a fractionating process under oxidizing conditions which give sulfates and that it is depleted under reducing conditions which give sulfides. Native sulfur is in a reduced state and it is depleted in S^{34}. The oxidation history of a mineral deposit or a petroleum deposit may be studied from this isotopic ratio and,

---

(1) The following 4 papers are based on a Symposium on Geochemistry held on Sept. 12, 1955, at a meeting of the American Chemical Society in Minneapolis. In addition to the papers published here, the symposium included the following: H. C. Urey, "Abundances of the Elements and the Composition of the Earth"; R. M. Garrels, "Environments of Mineral Formation"; H. G. Thode, "The Isotopes of Sulfur in Geochemistry"; G. W. Morey, "Experimental Geology"; E. J. Zeller and J. L. Wray, "Factors Influencing the Precipitation of Calcium Carbonate"; A. M. Pommer, "The Reduction of Vanadium(V) Solutions by Wood or Lignite"; G. C. Kennedy, "Equilibrium Relations in the System SiO_2–Al_2O_3–H_2O and Al_2O_3–H_2O"; J. J. Katz and H. R. Hoekstra, "Chemistry of Uranium and the Genesis of Uranium Minerals"; G. Phair, "Some Aspects of the Geological Cycle of Uranium"; J. R. Arnold, "Age Determination and Other Applications of Cosmic-Ray-Produced Radioactivities"; J. A. S. Adams, "The Log-Normal Distribution of Uranium and Alpha Activity in Obsidians, A Metamorphic Sequence and Wisconsin Water"; P. K. Kuroda, "Some Aspects of the Geochemistry of Radium"; D. R. Carr and J. L. Kulp, "Development and Application of the Potassium-Argon Method of Age Determination"; W. R. Eckelmann and J. L. Kulp, "Some Aspects of Age Determination by the Uranium-Lead Ratio."

in fact, it may be possible to determine when in the geological past the atmosphere acquired its oxygen.

Water is another geochemical agent of great importance and it must be remembered that the geological temperatures and pressures have frequently been very high. In fact, some of our valuable mineral deposits are best explained on the basis of transportation in highly superheated water.

The study of the crystallization of molten material to give igneous rocks requires an understanding of the phase relations of at least ten metallic oxides. In the crystallization from the molten magma water is an important factor not only in phase relations but in the generation of high steam pressures and the origin of volcanoes.

It is important but difficult to simulate in the laboratory the conditions of very high pressures and temperatures which existed in the geological formation of igneous rocks. Aluminum silicates and aluminum oxides are among the materials which have been studied in water under extreme conditions.

Coprecipitated impurities are often important in setting the crystal pattern as illustrated in the classical and confused interpretation of calcite and aragonite deposits. Impurities such as iron, manganese and strontium affect the crystal form of the $CaCO_3$, and they in turn are determined by their solubility products and affected by the pH. The pH in turn is influenced by the temperature and the carbon dioxide content of the solution.

Quantitative high temperature chemistry being developed now on a laboratory scale above 1000°, is finding new implications for geochemistry, specifically in the reactions of volatile hydroxides and nitrides.

The second half of the symposium was concerned with the geochemistry of uranium and nuclear geology, including examples of geological dating. It is well recognized that the Atomic Energy Commission's support of research on isotopes has led to important advances in chemistry, biology and physics. In a similar manner, its support of projects connected with uranium has advanced considerably the development of geology and geochemistry. The perfection of electronic and chemical methods for measuring minute traces of uranium has given this element new importance in geological studies. Uranium has in fact become a tracer for use in geochemical processes. The use of the Geiger counter and scintillometer has been invaluable in rapid field studies.

The chemistry of uranium in its various oxidation states and complex ions is much better established because of recent laboratory studies. From these it is possible to predict the geochemical behavior of uranium. In the crystallization of igneous rocks such as granites the uranium is expected to concentrate in the mother liquor because it does not have an ionic radius suitable for fitting into the minerals which crystallize out first. There are still many unsolved problems in explaining the occurrence of the uranium which is found in some minerals. The deposition in veins from hot aqueous solutions is important.

In igneous rocks tetravalent uranium and thorium occur together because they have about the same ionic radii. However, they part company in sedimentary rocks because the uranium is oxidized to a higher valence with a different ionic radius. The hexavalent uranium in solution is precipitated by other ions or adsorbed on the upper layers of lignite beds or concentrated in various other ways to give deposits of minable value. Even the low concentrations of uranium obtained from the rainwater leaching of volcanic ash are sufficient to account for the formation of some secondary uranium deposits.

Studies of the uranium content of various materials are significant because the analytical methods are so accurate even for very low concentrations. The obsidians are interesting because the uranium and daughter elements are sealed in glass so that the effect of weathering is slight. The uranium content of Wisconsin rivers is interesting because it fluctuates seasonally with the rainwater dilution of uranium dissolved from granites, and with the leaching of uranium-rich phosphate fertilizers used on the agricultural land.

The lead–uranium ratio, the helium–uranium ratio and the argon–potassium ratio are important in age tests, but continuing research is necessary to improve their accuracy. It is necessary for example to be sure that all the gases are removed from the sample and analyzed, and it is necessary to know that none of the elements involved in the ratio have escaped as gas nor leached away by weathering.

Certain elements can be created by natural radioactivity and neutron flux in the earth's crust. If mass spectrometric measurements could be made with greater precision than is now possible gadolinium would be an interesting element for dating purposes. An isotope of gadolinium is formed by neutron bombardment and since both isotopes have the same chemical properties and the same chances of loss, a determination of the isotope ratio and the neutron flux and neutron absorptions would give the age without errors due to weathering.

One of the newest and most powerful methods of dating the younger rocks is based on nuclear transitions brought about by cosmic rays in the upper atmosphere. Tritium for decades, $carbon^{14}$ for thousands of years and $beryllium^{10}$ for hundreds of thousands of years are finding important uses in geological dating.

Radiation damage to radioactive materials has been examined as an interesting source of stored heat, but evidence has not been obtained to show that it is geologically significant. Metamict minerals of complex lattice are known which contain up to 130 calories of stored energy per gram and which are so badly damaged as to show no X-ray diffraction pattern until the normal lattice is restored by heating.

Thermoluminescence can be produced in the laboratory by heating rocks which have been subject to α-ray bombardment over long periods of time. The α-ray activity comes from traces, about 1 part per million, of uranium or other radioactive elements which are present as an impurity in the rock. The intensity of thermoluminescent light in limestones, fluorites and certain other rocks can sometimes be used to estimate the age of the rock when the alpha ray activity and the sensitivity of the rock to radiation are also known.

REPORT ON THE OCCURRENCE OF TECHNETIUM ON THE EARTH'S CRUST[1]

BY G. E. BOYD AND Q. V. LARSON

Contribution from the Oak Ridge National Laboratory, Oak Ridge, Tennessee

Received December 27, 1955

A search for primordial technetium has failed to reveal any traces of this element in a variety of terrestrial substances, nor are recent reports of the occurrence of technetium in molybdenite and in yttrotantalite confirmed. Post-war nuclear chemical researches have shown that technetium possesses no beta stable nuclear species, although three long-lived isotopes have been established. Both Tc^{97} and Tc^{99} possess half-lives of less than one million years and hence, if initially present, would have disappeared in the approximately 4.5×10^9 years since the formation of the Earth. The possibility for discovering primordial technetium has therefore appeared to depend on whether or not the half-life of long-lived Tc^{98} exceeds 10^8 years. Results from chemical studies with gram quantities of fission product Tc^{99} suggest that technetium should exhibit a strong geochemical coherence with rhenium, which is known to be siderophile and chalcophile. Extremely sensitive methods for the detection of sub-microgram quantities were developed. The most reliable method is that of isotopic dilution using Tc^{99} and mass spectrometric analysis. The neutron activation method based on the formation of 6.0 h Tc^{99m} from Tc^{98} although more sensitive, is subject to interference, particularly by the Tc^{99} (n,n′) 6.0 h Tc^{99m} reaction. The negative result obtained in this search appears to be supported by a recent study which indicates a fairly positive disproof of the existence of technetium in the Sun, and by the preliminary finding in this Laboratory that the half-life of Tc^{98} is approximately 10^5 years.

The problem of the possible occurrence of element 43, eka-manganese, masurium,[2a] or technetium[2b] on the crust of the Earth has remained one of long standing in the chemistry and geochemistry of the elements. Quite recently, three notices[3-5] of the finding of technetium in terrestrial materials have appeared. The possible occurrence of technetium in the surface of the Sun has been proposed[6] for which support appears to have been afforded recently by quantitative explorations.[7] Easily the most dramatic and possibly the most enduring of all these reports has been that by P. W. Merrill which has established the presence of technetium in Type S stars.[8] Numerous previously unidentified lines in R Andromedae can now be assigned[9] to Tc I, including four of the five strongest lines at 4297.06, 4262.26, 4238.19 and 4031.63 Å., respectively, first accurately measured by W. F. Meggers[10] using synthetic technetium. This discovery has stimulated renewed speculation[11-15] by astrophysicists concerning stellar processes. Technetium has been described by one author[11] as "the touch-stone of cosmological theories."

This report will be concerned with the nuclear chemistry and with the geochemistry of technetium as they pertain to whether or not, and possibly where, this element might be expected on the Earth's crust. Radioactive technetium almost certainly exists in certain terrestrial substances in extremely minute quantities: in uranium ores by virtue of the spontaneous fission of U^{238} and by neutron capture fission of U^{235}; in molybdenum-containing minerals as a result of the capture of cosmic ray neutrons; and possibly in other substances, as the end product of extremely high energy reactions caused by other components of cosmic rays. Here, however, the question is asked as to whether or not *primordial technetium* remains on the Earth today. Does a stable or an extremely long-lived technetium exist? What is the geochemistry of technetium? The answer to the first question would appear to hinge on nuclear stability considerations.

Nuclear Stability of Technetium Isotopes.—A summary of available information, including unpublished results from this Laboratory, on the isotopes of technetium is afforded by Fig. 1. The majority of the data listed have been obtained since 1945 and, in addition to the results from Oak Ridge, have been contributed mainly by Prof. P. Sherrer and associates in Zurich and by Prof. M. L. Pool and associates at Ohio State University. It is readily seen that the nuclear chemistry of technetium is complex: some seventeen activities are known; numerous isomers occur in both the even and odd mass numbers. The information given appears to be consistent with, and explicable in terms of, the single particle model of nuclei.[16] The observed decay energies are consonant with recent nuclear stability systematics.[17,18] In agreement

---

(1) Presented before the Symposium on Geochemistry, 128th National Meeting, American Chemical Society, Minneapolis, Minnesota, September 11-16, 1955.

(2) (a) W. Noddack and I. Tacke, *Sitz. Preuss. Akad. Wissenschaften*. 400 (1925); (b) C. Perrier and E. Segrè, *Nature*, **159**, 24 (1947).

(3) W. Herr, *Z. Naturforschg.*, **9A**, 907 (1954).

(4) W. Noddack and I. Noddack, *Angew. Chem.*, **66**, 752 (1954).

(5) E. Alperovitch and J. M. Miller, *Nature*, **176**, 299 (1955).

(6) C. E. Moore, *Science*, **114**, 59 (1951); see also, *ibid.*, **119**, 449 (1954).

(7) H. Hubenet, C. de Jager and C. Zwaan, *Mem. soc. roy. sci., Liege*, **14**, 471 (1954).

(8) P. W. Merrill, *Astrophys. J.*, **116**, 21 (1952); *Science*, **115**, 484 (1952).

(9) P. W. Merrill, *J. Roy. Astron. Soc. Canada*, **46**, 335 (1952).

(10) W. F. Meggers and B. F. Scribner, *J. Res. Natl. Bur. Standards*, **45**, 476 (1950).

(11) P. Jordan, *Naturwiss.*, **40**, 407 (1953).

(12) T. Gold, *Mem. soc. roy. sci., Liege*, **14**, 68 (1954).

(13) St. Temesvary, *ibid.*, **14**, 122 (1954).

(14) J. L. Greenstein, *ibid.*, **14**, 307 (1954).

(15) A. G. W. Cameron, *Astrophys. J.*, **121**, 144 (1955).

(16) M. Goeppert-Mayer and J. H. Jensen, "Elementary Theory of Nuclear Shell Structure," John Wiley and Sons, New York, N. Y., 1955.

(17) K. Way and M. Wood, *Phys. Rev.*, **94**, 119 (1954).

(18) C. D. Coryell, *Ann. Rev. Nuc. Sci.*, **2**, 305 (1953).

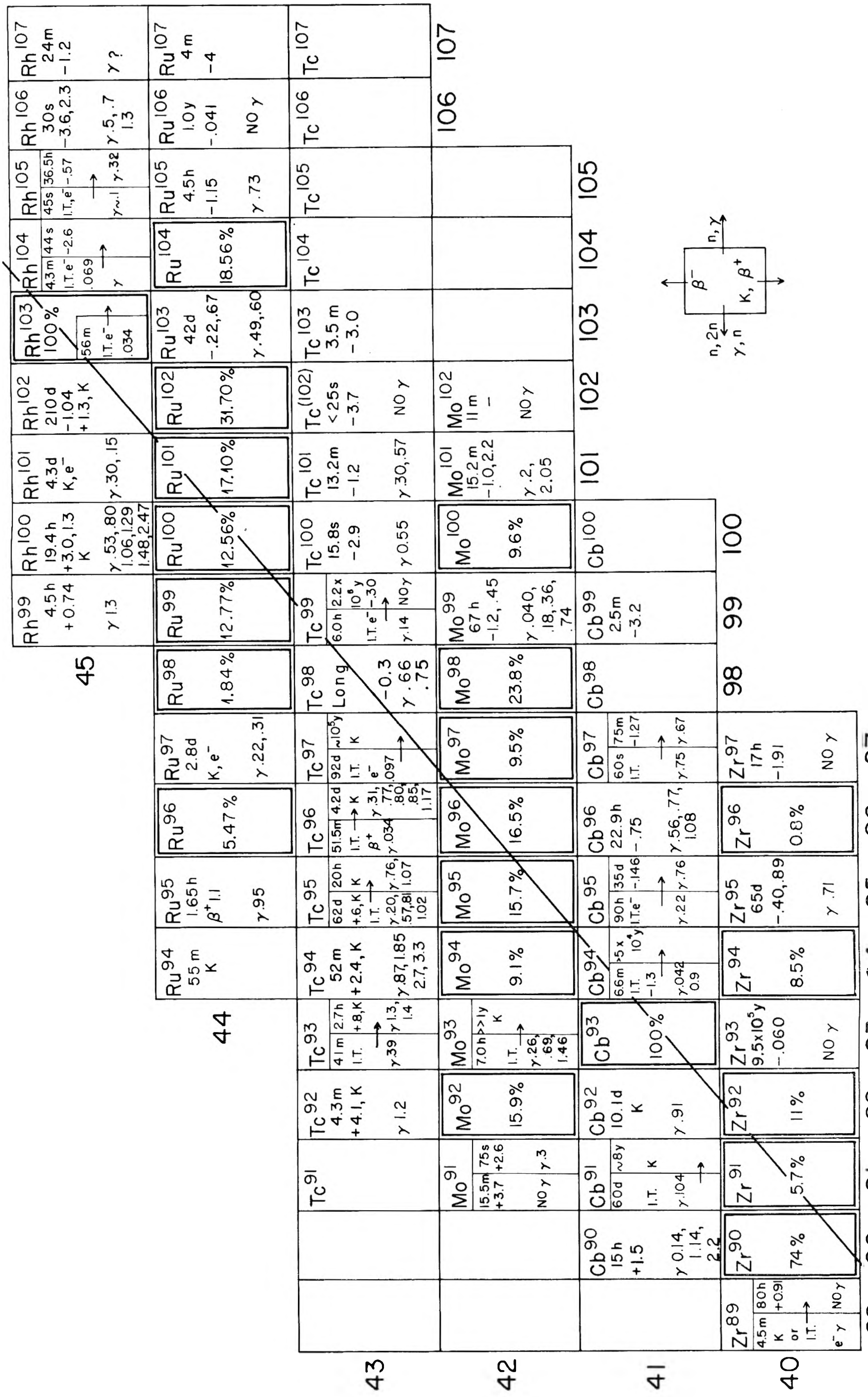

Fig. 1.—Isotope chart in the technetium region (heavy solid indicates maximum stability).

with a long-standing prediction,[19] it has been found that no β-stable isotopes of technetium exist. The nuclides Tc^{97g} and Tc^{99g} decay by orbital electron capture and β-ray emission, respectively, with half-lives of less than one million years, so that these isotopes have virtually disappeared during the approximately 4.5×10^9 years since the formation of the Earth. A remaining possibility is Tc^{98}, which, although β-unstable, may possess a half-life (*ca.* 10^8 years) sufficiently long to permit it to occur on the Earth in detectable amounts.

That Tc^{98} is indeed long-lived has been confirmed recently by a mass spectrometric analysis of the technetium isotopes remaining after nine months decay in a molybdenum metal target subjected to an intense bombardment with 22 Mev. protons.[20] Although microgram quantities of all isotopes with mass numbers between 90 and 101 were produced, only technetium 97, 98, 99 and very small amounts of 60 d Tc^{95m} were observed. Accordingly, it would appear that searches for primordial technetium should be directed specifically toward finding Tc^{98}.

Geochemical Considerations.—A discussion of the possible geochemical behavior of technetium can now be based on the known physical and chemical properties of the element and its compounds obtained during the past five years from studies using fractional gram quantities of fission product, Tc^{99g}. The classification of Goldschmidt[21] will be followed and an attempt will be made to assess the likelihood of a siderophilic, chalcophilic, and/or lithophilic behavior for technetium. These considerations have been of importance as they have appeared to afford a rational basis for the choice of a few out of many terrestrial materials to examine for technetium.

Elemental technetium occurs as a silver-gray metal which is quite similar in many respects to rhenium metal. Both crystallize in a hexagonal close-packed arrangement[22] with metallic radii of 1.358 and 1.373 Å. for Tc and Re, respectively. These radii may be compared with values of 1.322, 1.36, 1.291 Å. for Ru, Mo and Mn, respectively. The melting point of technetium[23] is approximately 2140° compared with values of 1260 and 3180° for manganese and rhenium, respectively. Technetium metal exhibits a weak paramagnetic susceptibility,[24] with $\chi = 270 \times 10^{-6}$ c.g.s. at room temperature compared with values of 527×10^{-6} and 69×10^{-6} for manganese and rhenium, respectively. Rhenium is reported[25] to be strongly siderophilic, and a similar, although perhaps not so pronounced, behavior might be shown by technetium.

A comparison (Fig. 2) of the free energies of formation per gram-atom of oxygen at 298°K. of the various oxides of manganese, technetium and rhenium with that for FeO also supports the expectation of a siderophilic tendency in technetium. Thus, the higher technetium and rhenium oxides will be reduced by an excess of iron, and, if present in relatively small amounts, will dissolve in the latter metal. For exact calculations the free energies of oxidation should be corrected to the temperature of the separation of a silicate slag from fused iron, and the free energy of formation of the corresponding silicates and intermetallic compounds should be employed. These changes, however, will not alter the conclusion already reached.

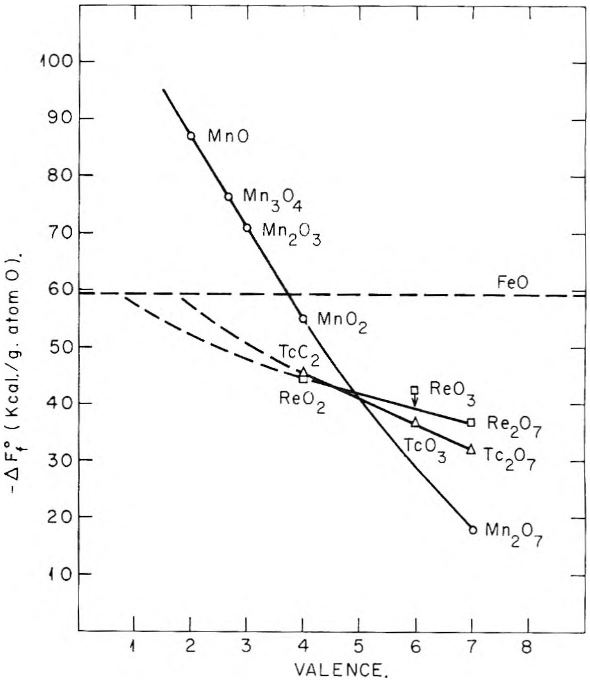

Fig. 2.—Relative stabilities of the oxides of the elements of Group VIIB.

The geochemistry of rhenium is known to be governed also by the pronounced affinity of this element for sulfur. Unfortunately, little quantitative information exists on the thermodynamic stabilities of the sulfides of either technetium or rhenium. The heptasulfides of both elements appear to be unstable relative to their disulfides to which they decompose on gentle heating. Using the known free energy of formation of $\mathrm{ReS_2}$ (-45.8 kcal. mole^{-1}) and an estimated value of -50.2 kcal. mole^{-1} for $\mathrm{TcS_2}$ it may be shown that under possible terrestrial conditions, in the absence of excess free iron, that these two elements will concentrate in the sulfide phase rather than exist as their dioxides. The disulfides, $\mathrm{TcS_2}$ and $\mathrm{ReS_2}$, are isomorphous and form disordered structures related to the $\mathrm{MoS_2}$ structure.[26] The latter structural similarity appears to account for the unusually high rhenium contents of molybdenites, and suggests that such minerals should also concentrate technetium.

The behavior of the upper oxidation states of technetium in aqueous solutions has recently been

---

[19] J. H. D. Jensen, *Naturwiss.*, **26**, 381 (1938); see also H. E. Suess and J. H. D. Jensen, *Arkiv. Fysik*, **3**, 577 (1951).

[20] G. E. Boyd, J. R. Sites, Q. V. Larson and C. R. Baldock, *Phys. Rev.*, **99**, 1030 (1955).

[21] V. M. Goldschmidt (Edited by A. Muir), "Geochemistry," Oxford University Press, 1954.

[22] R. C. L. Mooney, *Acta Cryst.*, **1**, 161 (1948).

[23] G. W. Parker, unpublished researches reported in ORNL-1260, 1951.

[24] C. M. Nelson, G. E. Boyd and W. T. Smith, Jr., *J. Am. Chem. Soc.*, **76**, 348 (1954).

[25] K. Rankama and Th. G. Sahama, "Geochemistry," University of Chicago Press, 1949, Chapter 32.

[26] W. H. Zachariasen, private communication, April, 1952.

elucidated,[27] and a comparison of its potential diagram (Fig. 3) with those of manganese[28] and rhenium[29] emphasizes the great similarity of the behavior of technetium and rhenium in aqueous solution. In acid solutions, however, hexavalent technetium, like hexavalent manganese, disproportionates to yield the quadri- and heptavalent oxidation states. In molar alkaline solutions maximum stability occurs with heptavalent technetium, and, for this reason, the various chemical separations described below were performed in such solutions.

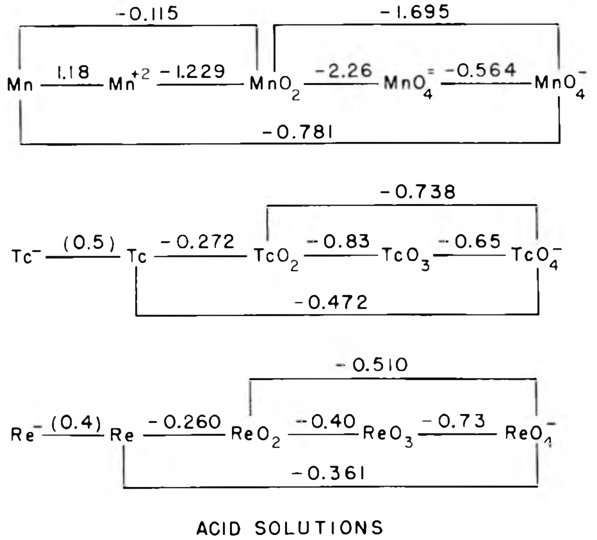

Fig. 3.—Oxidation-reduction diagrams for the elements of Group VIIB.

The occurrence of technetium in extremely low concentrations favors the formation of pertechnetate ion. Thus, for a concentration of 10^{-8} *M*, the potential for the Tc(VII)/Tc(IV) couple is reduced from −0.738 to −0.580 v. in one molar acid, and increased from 0.365 to 0.523 v. in one molar base.

Evidence for other oxidation states of technetium in aqueous solution remains fragmentary, although recently polarographic half-waves for the reduction of Tc(VII) to Tc(V) and of Tc(IV) to Tc(II) at a dropping mercury cathode have been observed.[30] Available chemical evidence suggests that divalent technetium, like divalent rhenium, is unstable toward oxidation by air in a non-complexing acid medium. This valence state is believed, therefore, to be unimportant geochemically. Trivalent technetium may be of importance in acid chloride solutions if this oxidation state resembles Re(III) which forms a stable complex ion.

Considerations based on the hypothesis that elements which have ions of equal valence and similar radius should be closely associated in nature if they have similar ionization potential values[31] also suggest that a fairly marked geochemical coherence between technetium and rhenium may be expected. The "anion affinity index," ϕ, defined as the ratio of the ionization potentials of two such ions, has been proposed[31] as a measure of the association of elements. Thus, only a fair geochemical affinity is indicated for the Tc^{+7} and Re^{+7} ions which have equal radii of 0.56 Å., because $\phi = 1.20$ using the values 95 and 79 e.v. for their respective ionization potentials. This prediction appears to be confirmed by several known divergent properties of the heptavalent compounds of these elements: (a) The solubility of $KTcO_4$ is nearly one hundred times that of $KReO_4$, and experiment has shown that tracer quantities of the former can be separated away from bulk amounts of the latter by fractional crystallization.[32] (b) The volatility of Tc_2O_7 is appreciably greater than that of Re_2O_7.[33] At 250° the vapor pressure exerted by the former compound is approximately 120 mm., while that for the latter is but 10 mm. (c) Heptavalent technetium in concentrated hydrochloric acid solutions in contrast to Re(VII) appears to be reduced to an oxidation state that cannot be coprecipitated by acid insoluble sulfides.[32] A greater degree of geochemical coherence is expected between the tetravalent states of technetium and rhenium for here the ionic radii are 0.69 and 0.72 Å., respectively, and $\phi = 1.13$.

By reason, therefore, of an expected geochemical affinity between technetium and rhenium, materials previously reported to contain the latter element were generally selected for examination. Technetium, because of its very low if not vanishingly small concentrations, was assumed to exhibit a strongly dispersed manner of occurrence. This search consequently was based on the working hypothesis that technetium never forms independent minerals, but is always concealed, in extremely small amounts, in the structure of other minerals.

Experimental

Analytical Methods for Technetium.—The continuing development of increasingly sensitive and reliable methods for the detection of minute quantities of technetium was found to be necessary during the course of this search which began in 1951.[34] Spectrochemical analysis using the emission spectrum of Tc I excited in a condenser discharge between copper electrodes (Cu spark) was employed initially. Fortunately, the spectrum of technetium is simple with relatively few strong lines, and, more important, there are relatively few interferences. As little as 0.1 microgram of technetium electroplated onto copper electrodes may be detected[35] using the line at 4031.63 Å., as was shown by a calibration curve constructed using known quantities. This method is limited, however, in that all technetium isotopes are detected and, further, the sample examined is consumed in the analysis.

---

[27] J. W. Cobble, W. T. Smith, Jr., and G. E. Boyd, *J. Am. Chem. Soc.*, **75**, 5777 (1953); see also, G. H. Cartledge and W. T. Smith, Jr., *Ibid.*, **59**, 1111 (1955).

[28] W. M. Latimer, "The Oxidation States of the Elements and Their Potentials in Aqueous Solutions," 2nd Ed., Prentice-Hall, Inc., New York, N. Y., 1952, Chapter 15.

[29] G. E. Boyd, J. W. Cobble and W. T. Smith, Jr., *J. Am. Chem. Soc.*, **75**, 5783 (1953).

[30] H. H. Miller, "Polarographic Studies of the Reduction of Pertechnetate Ion in Aqueous Solutions," to be published.

[31] L. H. Ahrens, *Geochem. Cosmochem. Acta*, **2**, 155 (1952); **3**, 1 (1953).

[32] G. E. Boyd, E. E. Motta and Q. V. Larson, to be published.

[33] W. T. Smith, Jr., J. W. Cobble and G. E. Boyd, *J. Am. Chem. Soc.*, **75**, 5773 (1953).

[34] G. E. Boyd, *Record Chem. Progr.* (Kresge-Hooker Sci. Libr.), **12**, 67 (1951); see also: Abstracts of Papers, XIIth International Congress of Pure and Applied Chemistry, New York City, Sept. 10–13, 1951, p. 357.

[35] The authors gratefully acknowledge the assistance of Messrs. C. Feldman and M. M. Murray of the Analytical Chemistry Division, ORNL, in numerous spectrochemical examinations of suspected technetium-containing fractions.

The strong, ultraviolet absorption shown by pertechnetate ion in aqueous solutions was employed in an alternative, non-destructive analytical method of considerable sensitivity. Absorption bands at 2470 and 2890 Å. have been observed[36] showing molar absorbancy indices of 6220 and 2360,[36,37] respectively, which obey Beer's law up to concentrations of 10^{-3} M, so that as little as one microgram per ml. may be detected. All technetium isotopes are detected, and, in addition, the method has been found liable to serious interferences by numerous impurities also absorbing the ultraviolet. Spectrophotometric analysis has therefore been of use in this research principally as a means for conveniently checking for technetium in a given aqueous concentrate.

Recently a much more sensitive method for the detection of very small amounts of technetium has been developed[30] based on the polarographic reduction of Tc(VII) to Tc(IV) at a dropping mercury electrode in a phosphate buffer of pH 7. When the ORNL high sensitivity polarograph is employed as little as 0.05 μg./ml. can be detected. Again, however, this method is non-specific in that all technetium isotopes are assayed.

The most sensitive method for the estimation of millimicrogram quantities of technetium is that based on neutron activation analysis using a neutron chain reactor. Further, this method will distinguish between the isotopes Tc^{98} and Tc^{99}. As may be seen in Table I as little as 3×10^{-10} g. of Tc^{98} should be detectable if the neutron capture cross-section to form 6.0 h Tc^{99m} is as large as 1×10^{-24} cm.^{2} (*i.e.*, 1 barn = 1 b.). The sensitivity may actually be somewhat less, for our measurements thus far appear to establish 1 b. only as an upper limit for this activation cross-section. Should this quantity be an order of magnitude smaller, then the method of activation analysis for Tc^{98} will be subject to serious interferences by competing neutron reactions to form 6.0 h Tc^{99m} from the contaminants present in technetium concentrate fractions. The most important of these interfering reactions is the activation arising from an inelastic scattering of neutrons of energy above 140 Kev. on Tc^{99} present as a contaminant to give the excited state Tc^{99m}. Although the cross-section for this (n,n′) process is relatively small, the flux of fast neutrons in many neutron chain reactors may be approximately equal to the flux of thermal neutrons. Such contaminants as Mo^{98} and Ru^{98} must also be reduced to low levels. Fortunately, however, this generally may be accomplished by efficient chemical separations. Extremely minute quantities of Tc^{99g} in technetium concentrates may be detected by reason of the thermal neutron capture reaction (to form 15.8 s Tc^{100}) which occurs with an approximately 20 b. cross-section. An example is afforded by the data recorded in Fig. 4. Here, known small amounts of technetium and technetium–rhenium mixtures mounted between two thin sheets of highly pure polystyrene were irradiated for approximately 15 seconds at the center of the ORNL graphite reactor (flux = 5×10^{11} cm.$^{-2}$ sec.$^{-1}$) and then transferred within 15 seconds to a radiation detector connected with a fast counting rate recorder which gave the traces shown. Use was made of this procedure on several occasions during our search for primordial technetium to exclude as artifacts observations of 6.0 h Tc^{99m} activity induced in technetium concentrates.

TABLE I

INTERFERENCES WITH THE DETECTION OF Tc^{98} USING NEUTRON ACTIVATION ANALYSES[a]

	Activation cross-section	Sensitivity, g.
Tc^{98} (n,γ) 6.0 h Tc^{99m}	≤ 1.0 b	3×10^{-10}
Tc^{99} (n,n′) 6.0 h Tc^{99m}	*ca.* 0.05	5×10^{-9}
Mo^{98} (n,γ) 67 h Mo^{99}		
$\downarrow \beta^-$		
6.0 h Tc^{99m}	0.13	5×10^{-8}
Ru^{99} (n,p) 6.0 h Tc^{99m}	5×10^{-5} (5×10^{-3})	5×10^{-6}

[a] For 200 c./m. at 50% geometry; $\overline{nv} = 2 \times 10^{13}$.

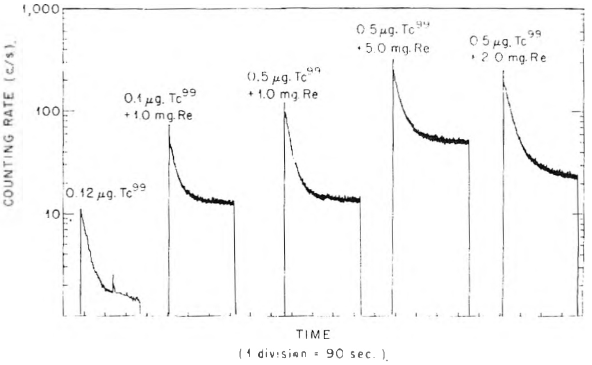

Fig. 4.—Neutron activation analysis for sub-microgram amounts of technetium. Initial rapid decay of induced 15.8 s Tc^{100} followed by decay of longer lived rhenium activities.

A somewhat less sensitive, but much more highly reliable technique is that of isotope dilution analysis.[38] In all of our most recent experiments this method of analysis for Tc^{98} was employed using a 60° mass spectrometer of eight inch radius.[39] In this procedure approximately one microgram of Tc^{99} together with undetectable amounts of 60 d Tc^{95m} tracer were added to the material to be examined. Chemical processing was performed to produce an aqueous technetium concentrate, and the technetium from this solution was electroplated onto an iridium strip which subsequently was heated at 400° in a stream of hydrogen gas to produce an adherent layer of technetium metal. This iridium strip was employed as a filament source in the mass spectrometer in which technetium ions were produced by electron bombardment and by thermal ionization. As may be seen in reference 20 (Fig. 1), where approximately one microgram of element was deposited, as little as 5×10^{-9} g. of either Tc^{97} or Tc^{98} may be detected. Table II affords a summary of the estimated sensitivities and ranges of applicability of the five detection methods for small quantities of technetium used during the course of this search.

TABLE II

METHODS FOR THE DETECTION OF SMALL QUANTITIES OF TECHNETIUM

	Sensitivity, g.	Applicability
Spectrophotometric (u.v. absorption)	10^{-6}	All Tc isotopes
Spectrochemical (Cu spark, Tc-I)	10^{-7}	All Tc isotopes
Polarographic	5×10^{-8}	All Tc isotopes
Mass spectrometric (isotope diln. using Tc^{99})	5×10^{-9}	$Tc^{97,98}$
Neutron activation analysis	3×10^{-10}	Tc^{98}
	2×10^{-11}	Tc^{99}

Analytical Method for Rhenium.—Chemical and geochemical considerations outlined above indicated that rhenium-rich sources might be regarded as the most likely materials to examine for the occurrence of technetium. Accordingly, an analytical method for rhenium was developed[40] and applied to a large number of molybdenum ores, concentrates, and flue dusts, to rare earth-containing minerals, to chromites and to miscellaneous substances. The procedure, which employed 1–5 g. of ore, involved a fusion with sodium peroxide either in an iron, or preferably in a zirconium crucible,[41] followed by solution of the melt in water, concentration of perrhenate ion by absorption onto a strong-base anion-exchange column (Dowex-2) and finally

---

(36) G. E. Boyd, J. W. Cobble, C. M. Nelson and W. T. Smith, Jr., *J. Am. Chem. Soc.*, **74**, 556 (1952).

(37) G. H. Cartledge, *Corrosion*, **11**, 335t (1955).

(38) M. G. Inghram, *Ann. Rev. Nuclear Sci.*, **4**, 81 (1954).

(39) The authors are indebted to Mr. J. R. Sites of the Mass Spectrometer Group, Stable Isotopes Research and Development Division, ORNL, for these mass analyses.

(40) H. H. Miller, unpublished investigations reported in ORNL 1717 and 1788, 1954.

(41) G. J. Petretic, *Anal. Chem.*, **23**, 1183 (1951).

its elution with 2 *N* perchloric acid after molybdate had been thoroughly removed by prior elution with 1 *N* NaOH, $NaNO_3$ or potassium oxalate solutions.[42] The perrhenate fraction was then made 4 *N* in perchloric acid and assayed polarographically. A well defined wave at $E_{1/2} \approx -0.4$ volts against S.C.E. is observed in perchloric acid media, and the diffusion current has been shown proportional to the perrhenate ion concentration.[43] One p.p.m. of rhenium could be estimated reliably (*cf.* Table III).

Chemical Procedures for the Extraction and Concentration of Technetium.—A variety of chemical procedures were required by reason of the varied natures of the terrestrial materials examined. Already, one procedure has been described for the isolation of technetium from molybdenite.[34] Later a much improved method was developed for placing this and other ores into aqueous solution, and for extracting pertechnetate ion from large volumes of this solution. A schematic outline is afforded by Fig. 5 where it may be seen that the initial step was a fusion with sodium peroxide which served among other things to convert technetium to its heptavalent state at the outset. Auxiliary experiments using radio-tracer showed that no technetium was lost during the fusion, and that, with molybdenite, a fivefold quantity by weight of Na_2O_2 was optimum. Fusions were conducted with 25-g. aliquots of ore in iron and with 1-10-g. aliquots in zirconium crucibles. In nearly all cases (*cf.* Table III) γ-emitting radioactive technetium (usually 4.2 d Tc^{96} + 60 d Tc^{95m}) was added to the ore to permit the monitoring of the chemical processing at every step.

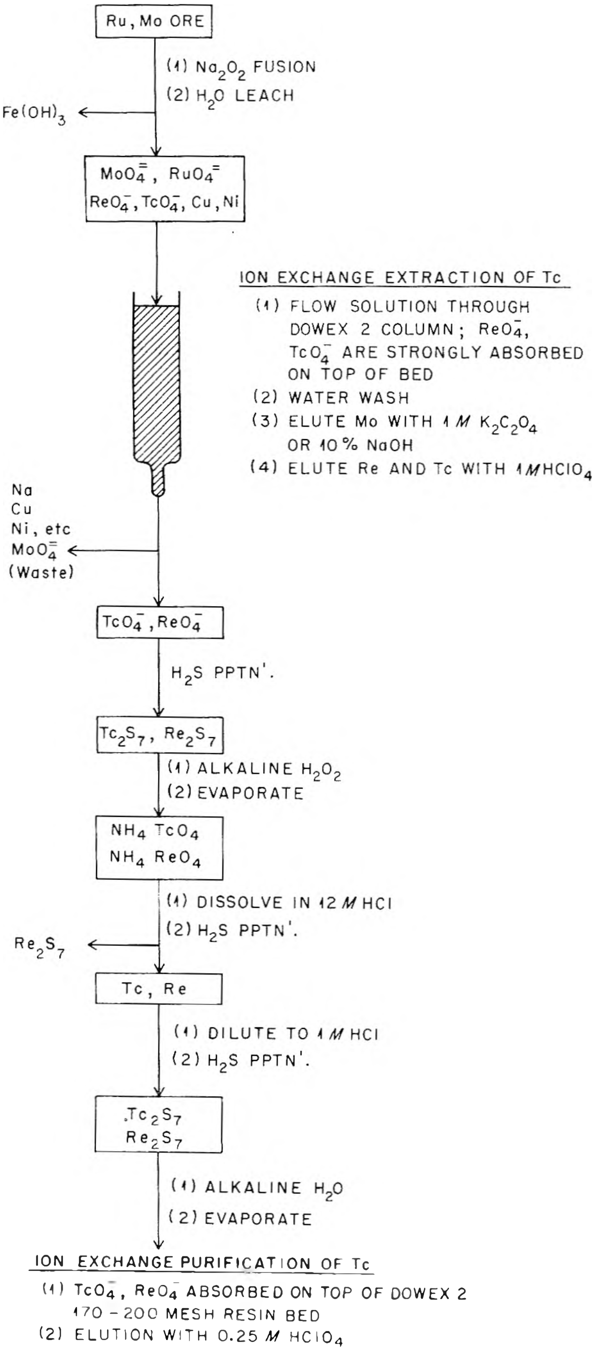

Fig. 5.—Outline of steps in the chemical extraction and concentration of technetium.

The fusion mixture was dissolved in water, and the solution brought to boiling and digested to destroy residual peroxide. Upon cooling to room temperatures, ferric hydroxide from iron originally present in the ore and mainly from the corrosion of the iron crucible was then allowed to settle. Separate tests using radio-tracers showed no technetium was lost by coprecipitation with iron hydroxide. After filtering to remove the iron, volumes of solution ranging from 1 to 45 liters were passed through a 9.6 cm.^{2} by 22 cm. deep bed of strong-base anion exchanger (*viz.*, Dowex-2 or Amberlite IRA 410) which extracted all of the technetium (as proved by tracers), the rhenium, and a small part of the molybdate, sulfate or ruthenate, etc., also formed by the oxidizing, alkaline fusion. Cationic constituents such as Na, Cu, Ni, etc., passed through the resin bed. Molybdate and other anions were eluted with 1 *M* $NaNO_3$ at *p*H 10 or with 2 *N* NaOH solution after rinsing the bed with distilled water.

After a second water rinse, both perrhenate and pertechnetate were displaced quantitatively with 2 *N* $NaClO_4$ or 2 *N* $HClO_4$. The eluent solution usually contained approximately 5–10 mg. of rhenium, and microgram or smaller quantities of technetium, although sometimes as much as one gram of rhenium was present. After acidification (if necessary), the eluate was heated, treated with bromine water to oxidize any reduced technetium, and then treated with H_2S gas to precipitate rhenium and technetium sulfides. Quantitative coprecipitation of technetium was insured by digestion at 90°, then the rhenium sulfide was separated by filtering, dissolved with ammonia and hydrogen peroxide and the solution evaporated to near-dryness on a steam-bath. This residue was taken up in 10 *N* HCl, the solution heated for one hour, and rhenium sulfide again precipitated with hydrogen sulfide. Technetium is not coprecipitated under these conditions,[32,44] and remains in the supernatant acid solution. After filtration, this supernatant was diluted to a concentration of 1 *N*, heated, treated with bromine water, and then with hydrogen sulfide to precipitate residual fractional milligram quantities of rhenium together with technetium which is again coprecipitated. One or more of these cycles served to give a considerable reduction in the amount of rhenium.

Further reduction of the rhenium content of the technetium fraction was accomplished by use of ion-exchange chromatography using a 0.78 cm.^{2} by 30 cm. deep bed of 120–200 mesh strong-base anion exchanger, Dowex-2. The final rhenium sulfide precipitate mentioned above was dissolved in ammoniacal hydrogen peroxide, and the pertechnetate and perrhenate ions in this solution were absorbed on the top of the bed. The chromatographic separation was performed using perchlorate solutions as eluents at flow rates averaging less than 0.5 ml./min. A typical separation of trace quantities of technetium from *ca.* 0.5 mg. of rhenium is illustrated in Fig. 6 where the 92.8 h Re^{186} and the 62 d Tc^{95m} were employed as monitors. Purities of the peak fractions were demonstrated by their γ-ray spectra (see Fig. 7 inserts) measured using a scintillation spectrometer. Fractions containing the technetium were combined, made 1 *N* in HCl, heated and treated with bromine, and then one mg. of copper was precipitated as copper sulfide. This "technetium concentrate" was processed as required by the various assay methods: (1) For spectrochemical analysis, it was dissolved in ammonia and hydrogen peroxide and the technetium electroplated on to the ends of $^1/_4$-inch diameter cylindrical copper electrodes after adjusting the solution to approximate neutrality and adding fluoride ion to assist the electrodeposition.[32] (2) For spectrophoto-

---

[42] V. W. Meloche and A. F. Preuss, *Anal. Chem.*, **26**, 1911 (1954).

[43] J. J. Lingane, *J. Am. Chem. Soc.*, **64**, 1001 (1942).

[44] C. Perrier and E. Segrè, *J. Chem. Phys.*, **7**, 155 (1939).

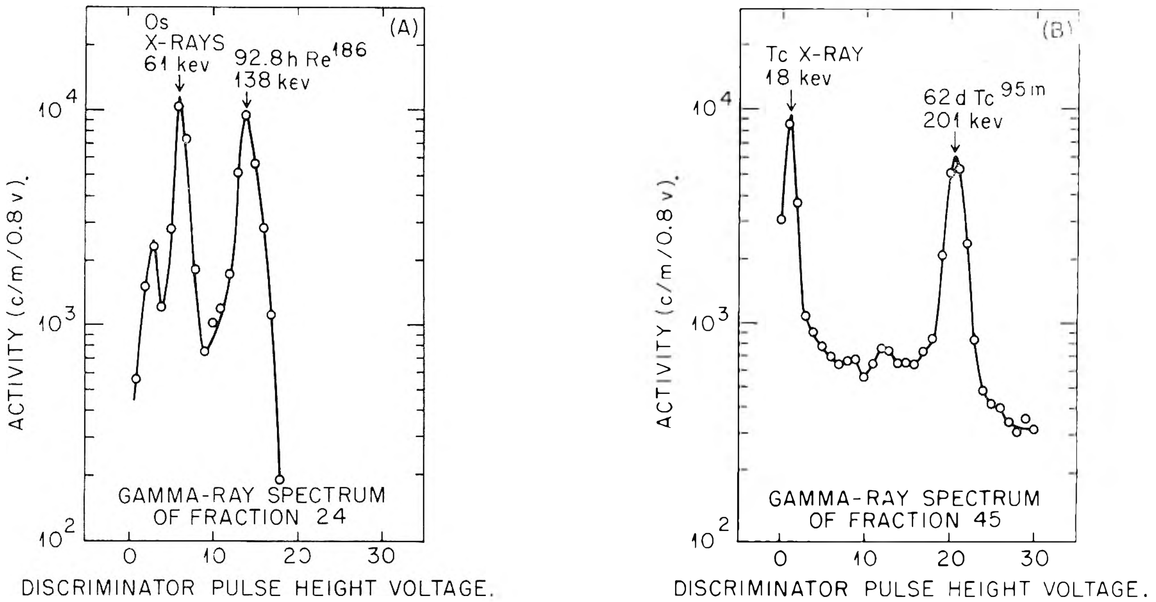

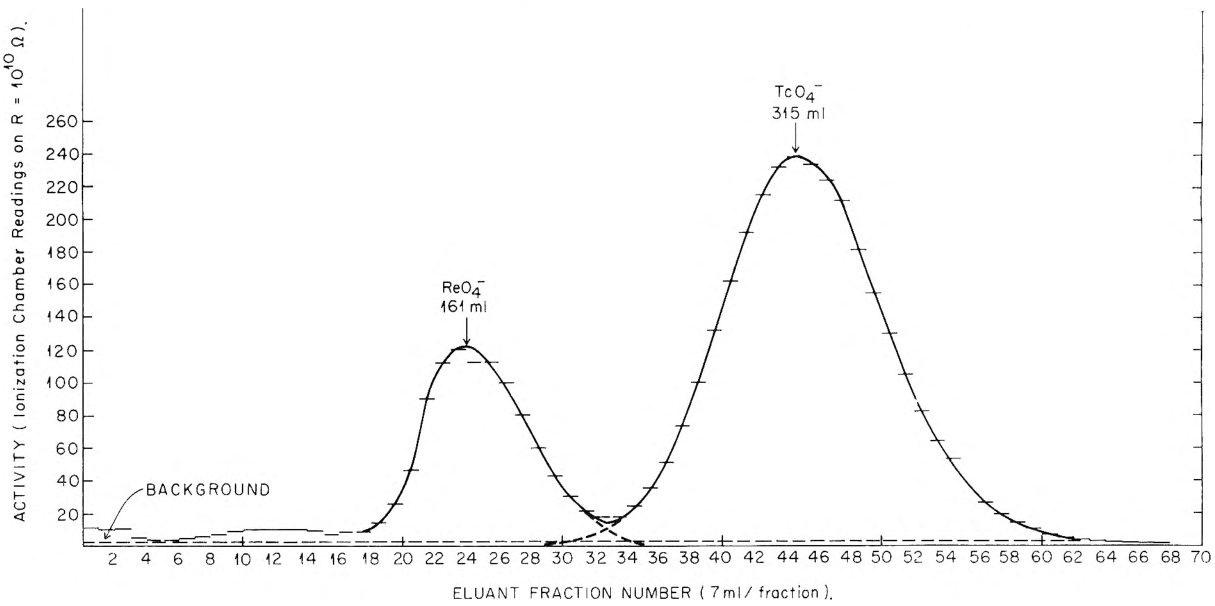

Fig. 6.—Ion exchange chromatographic separation of 5 mg. of rhenium and tracer quantities of technetium (.7 cm.^{2} by 30 cm. deep bed 120/200 mesh Dowex-2 X-10 perchlorate-form; eluent, 0.25 *M* ClO_4^- at 0.47 ml./min.).

metric analysis using a Beckman Model DU spectrophotometer, the copper sulfide was dissolved in ammoniacal peroxide, then copper was removed by passage through a small cation-exchange column (Dowex-50) and finally the solution was evaporated to a volume of one ml. (3) For polarographic analysis the treatment was the same as for (2), except for the omission of the evaporation step. (4) For activation analysis the CuS was carefully wrapped in pure polystyrene foil and irradiated for six hours with neutrons in the Oak Ridge Low Intensity Test Reactor (Flux = *ca.* 3 × 10^{13} cm.$^{-2}$ sec.$^{-1}$) after which it was dissolved in ammoniacal peroxide, treated with a cation exchanger to remove copper and other activated cationic impurities, chromatographed on a small anion-exchange column (Dowex-1) to obtain a pure technetium fraction, and then examined with scintillation spectrometer for the presence of the characteristic 141 Kev. γ-ray of an induced 6.0 h Tc^{99m} activity. (5) For mass spectrometric analysis the CuS was dissolved and copper was removed as before, then the technetium was electroplated onto iridium and finally reduced to its metal in hydrogen gas at about 400°. In all cases above just preceding the assay step the amount of initially added technetium radio-tracer was determined to permit an estimate for the "over-all" chemical yield, or recovery for the separation from the starting material (*cf.* Table III).

The chemical treatment of the iron-nickel meteorite differed from the above only in the initial step where dilute hydrochloric acid was employed to effect a complete dissolution. Subsequently, this solution was made alkaline by adding sodium peroxide, digesting and removing copious amounts of ferric hydroxide.

The potassium perrhenate salt was examined for its possible technetium content[45] by a repeated application of a procedure essentially the same as that outlined above wherein rhenium sulfide is precipitated from 10 *N* HCl under conditions such that technetium is not "carried down."

The reliability of the separation of technetium from molybdenum was tested by an experiment wherein one gram of neutron irradiated Mo metal known to contain 0.5 p.p.m. Tc was processed, and the technetium fraction analyzed spectrochemically. Technetium, in this case, was found, and in the expected amount. Also, repeated spectrochemical analyses on the cyclotron-produced technetium

---

[45] The authors thank Dr. J. W. Cobble for his assistance in the examination of this source.

TABLE III

SEARCH FOR TECHNETIUM IN VARIOUS TERRESTRIAL MATERIALS

No.	Type of material	Wt. processed (g.)	% To recovered	Method of analysis for Tc	Technetium content of final concentrate	Technetium concentration in starting material	Rhenium concn. in starting material (p.p.m.)
16	MoS_2 concentrate	1000	25	Spectrochemical	$<10^{-7}$ g.	$<4 \times 10^{-10}$	20
..	Pure $KReO_4$	30	$\sim$40	Spectrochemical	$<10^{-7}$	$<8 \times 10^{-9}$	..
	Pure $KReO_4$	25	50	Spectrochemical	$<10^{-7}$	$<8 \times 10^{-9}$	..
4	MoS_2 concentrate	100	67.5	Spectrochemical	$<10^{-7}$	$<1.5 \times 10^{-9}$	1030
21	MoS_2 concentrate	100	27.5	Spectrophotometric	$< 5 \times 10^{-6}$	$<1.8 \times 10^{-7}$	152
21	MoS_2 concentrate	250	No tracer	Spectrochemical	$<10^{-7}$	....	152
21	MoS_2 concentrate	250	55.9	Spectrochemical	$<10^{-7}$	$<7.6 \times 10^{-10}$	152
..	Osmiridium concentrate	10	63.4	Spectrochemical	$<10^{-7}$	$<1.6 \times 10^{-8}$	..
21	MoS_2 concentrate	100	74.9	Spectrochemical	$\sim 6 \times 10^{-6}$	6×10^{-8}*	152
17	Flue dust	10	79.3	Spectrochemical	$<10^{-7}$	$<1.3 \times 10^{-8}$	3130
17	Flue dust	100	69	Spectrochemical	$<10^{-7}$	$<1.5 \times 10^{-9}$	3130
23	MoS_2 concentrate	184	No tracer	Activation	$<10^{-9}$	....	150
4	MoS_2 concentrate	100	76	Activation	$\sim 10^{-8}$	$\sim 1.3 \times 10^{-10}$	1030
22	MoS_2 concentrate	100	60.5	Spectrochemical	$<10^{-7}$	$<1.7 \times 10^{-9}$	297
				Activation	$\sim 5 \times 10^{-9}$	$\sim 8.3 \times 10^{-11}$*	
..	Iron-nickel meteorite	1000	22.4	Spectrochemical	$<10^{-7}$	$<4.5 \times 10^{-10}$	$\sim$2
8	MoS_2 concentrate	1000	86	Mass spectrometric	$< 4 \times 10^{-8}$	$<4.6 \times 10^{-11}$	688
4	MoS_2 concentrate	885	92	Activation	$<10^{-9}$	$<1.2 \times 10^{-12}$	1030
				Mass spectrometric	$< 5 \times 10^{-8}$	$<6.1 \times 10^{-11}$	
25	Yttrotantalite	100	68	Mass spectrometric	$<3.7 \times 10^{-7}$	$<5.4 \times 10^{-9}$	..

tracer showed that it contained undetectable quantities of technetium.

Origins of Materials Examined.—The entries in Table II give the chronological order in which the materials were examined. Here, however, information on them will be presented according to geochemical type:

Iron-Nickel Meteorite.—Two approximately 500 g. meteoritic irons (var. Siderite) from Canon Diablo, Arizona, were received through Ward's Natural Science Establishment, Rochester, N. Y. They were Dana 25, No. 34,2194 and 34,2195, respectively.

Osmiridium Concentrate.—This sample of South African osmiridium concentrate was obtained through the generosity of Mr. C. R. Bergherm, Baker and Company, Newark, N. J. The assay also given was: Os, 28.62%; Ru, 13.15%; Rh, 0.77%; Ir, 25.74%; Pt, 11.68%; and Au, 0.73%.

Potassium Perrhenate.—This was laboratory reagent grade salt supplied commercially by the University of Tennessee.[46] Both samples listed in Table III were taken from the same 100-g. shipment of $KReO_4$.

Molybdenite Concentrate No. 16.—This MoS_2 concentrate was taken from the Climax, Colorado, deposit and was kindly given to us by Dr. Arthur Linz of the Climax Molybdenum Corp. of New York, N. Y.

Molybdenite Concentrate No. 4.—This sample was made available from the McGill, Nevada, deposits through the courtesy of the Nevada Mines Division of the Kennecott Copper Corporation, and was collected by Mr. Ralph J. Roberts of the U. S. Geological Survey. It showed one of the highest rhenium contents of all the American molybdenites thus far examined. Spectrochemical analyses supplied by the Geochemistry Branch, U.S.G.S., Washington, D. C., indicated the following additional elements in per cent.: 0.0*x* Ti; 0.00*x* Ag; 0.0*x* Mn; *x*Cu and 0.*x* Mg.

Molybdenite Concentrate No. 21.—This sample was collected from the Miami, Arizona, deposits through the courtesy of the Miami Copper Company by Mr. C. A. Anderson of the U.S.G.S. who reports this molybdenite to be a by-product of the porphyry copper deposit at that locality.

Flue Dust No. 17.—This material was made available to us through the generosity of Prof. A. D. Melaven of the Department of Chemistry, University of Tennessee. It is a by-product from the molybdenite roaster operations of the Miami Copper Company at Miami, Arizona. Other samples have shown rhenium contents varying up to 2% by weight.

Molybdenite Concentrate No. 23.—This concentrate also was collected at Miami, Arizona, and was made available to us through the kindness of Prof. W. T. Smith, Jr., of the University of Tennessee.

Molybdenite Concentrate No. 22.—This sample was collected at Miami, Arizona, by Mr. Nels P. Peterson of the U.S.G.S.

Molybdenite Concentrate No. 8.—This sample from the Miami Copper Company mines at Miami, Arizona, was collected by Mr. Nels P. Peterson approximately one year after the collection of Concentrate No. 22 above.

Yttrotantalite No. 25.—This sample was received through the kindness of Dr. E. Alperovitch of the Department of Chemistry, University of Illinois. Presumably this material comes from Swaziland, West Africa, and is identical with the same material reported on by him.[5]

It is of interest that four of the six molybdenites examined originated from the same general deposit (*i.e.*, No. 8, 21, 22, 23), yet, their rhenium concentrations varied more than fourfold from about 150 to 690 p.p.m.

Experimental Results and Discussion

The results up to this time are brought together in Table III from which it may be seen that apparently technetium was detected in but two instances. The most striking of these was with molybdenite concentrate No. 21 where as much as 6 μg. of technetium was detected spectrochemically. Subsequently, however, neutron activation analysis showed that a contamination by Tc^{99} had occurred. Minute quantities of technetium were also indicated by the appearance of a very small amount of 6.0 h Tc^{99m} activity in the activation analysis of Concentrate No. 22. However, small quantities of rhenium were present so that this result cannot be accepted without reserve. All other analyses on the technetium concentrates failed to reveal the presence of technetium, so that only upper concentration limits are given for the starting material. Either technetium was absent, or, if present, it occurred in concentrations below those which practically could be detected by the means employed in this investigation.

Recent Developments and Conclusions

The failure in this search to find technetium in terrestrial materials appears to have been given sup-

---

[46] A. D. Melaven and J. C. Bacon, U. S. Patent 2,414,965 (January 28, 1947).

port by two developments which have occurred quite recently. Firstly, the evidence for the occurrence of technetium in the solar atmosphere has been critically re-examined and the conclusion has been reached that its existence in the Sun is by no means proven.[47] Secondly, the radiations emitted by Tc^{98} have been observed in this Laboratory and have been found to consist of a β-ray in coincidence with two γ-rays (Fig. 7). More important, preliminary coincidence rate measurements between the 750 and 600 Kev. γ-rays emitted by a source containing a known number of Tc^{98} atoms gives a half-life value of 1×10^5 years.[48] Even if this value is uncertain to one order of magnitude, it is difficult to see how Tc^{98} can occur in Nature.

Probably it would be difficult, if not impractical, to attempt to establish absolutely the non-occurrence of primordial technetium on the crust of the Earth. All available information at present on the various technetium isotopes is in good accord with the elementary theory of nuclear structure based on the single particle model. It is difficult to see how any long-lived technetium could have been over-looked. However, our understanding of nuclear phenomena is relatively quite new, and the possibility must be admitted that surprises may yet be in store. None-the-less, because there are three technetium isotopes whose ground states are long-lived which may occur as contaminants in terrestrial substances, it is essential that proof be given that any primordial technetium claimed to have been discovered is not Tc^{97g}, Tc^{98g} or Tc^{99g}.

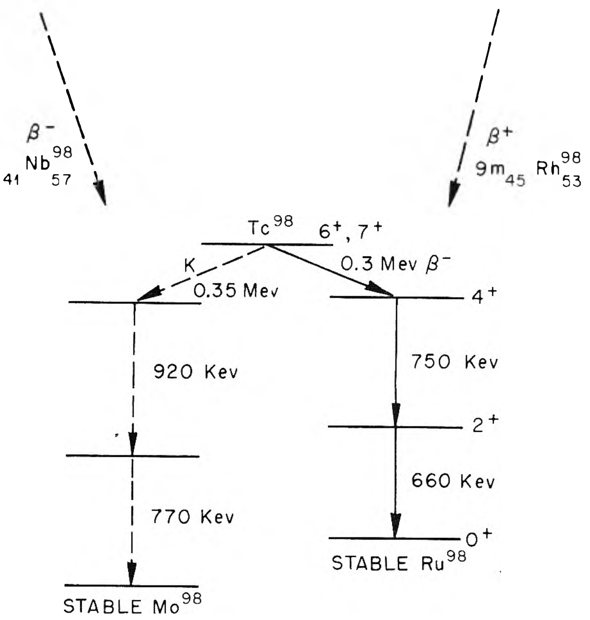

Fig. 7.—Present status of information on the decay of long-lived Tc^{98}.

Acknowledgment.—It is a great pleasure to acknowledge the continuing interest in, and very considerable assistance given to these studies by Dr. Michael Fleischer of the Geochemistry Branch, U. S. Geological Survey, Washington, D. C.

[47] J. L. Greenstein and C. de Jager, *Bull. Astron. Inst. of The Netherlands*, in press.

[48] G. D. O'Kelley, Q. V. Larson and G. E. Boyd, unpublished researches. NOTE ADDED IN PROOF.—Since our initial report, ref. 20, S. Katcoff, *Phys. Rev.*, **99**, 1618 (1955), has described radiations emitted by a long-lived Tc isotope, inferred to be Tc^{98}, which are in agreement with our Fig. 7.

GASEOUS MOLECULES OF GEOCHEMICAL SIGNIFICANCE[1]

BY JOHN L. MARGRAVE

Department of Chemistry, University of Wisconsin, Madison, Wisconsin

Received December 27, 1955

To explain geochemical or astrophysical phenomena one must have a knowledge of the important chemical species at the prevailing conditions of temperature and pressure. From basic thermodynamic principles it can be demonstrated that complex molecules may be important high temperature species. At temperatures below 2000° there is evidence that many gaseous hydroxides exist. Boron forms gaseous hydroxides in significant amounts even at 100–300°. Gaseous gallium nitride has been detected at 900–1000°, and at stellar temperatures (>10,000°K.) gaseous diatomic nitrides probably are important.

When the geochemist tries to account for the distribution of the elements in the sea and in the various parts of the earth, he reverses his thinking to the time of formation and considers the various chemical equilibria which must have been involved. No amount of care or ability in calculation of chemical equilibria can overcome a lack of complete knowledge of the chemical species concerned. It is the purpose of this paper to call attention to some new groups of gaseous molecules, about which little or nothing is known, but which may have played some role in determining the distribution of the elements on the earth and the concentration of certain elements in volcanic areas, and which may aid in explaining the radiation which we now observe from the stars.

Urey[2] has made a detailed study of the formation of the earth's crust in the light of the observed abundances of the elements and has come to the conclusion that temperatures of no more than a few hundred degrees were involved in the formation process. High temperature processes are still of geochemical interest since there were certainly periods in the history of the earth when high temperatures did prevail and, of course, high temperatures still prevail in volcanoes and hot springs, in the inner parts of the earth, and in the stars. For many years it was fairly common to assume that only simple molecules would be of importance at high

[1] Presented at the Geochemistry Symposium of the Physical and Inorganic Division of the American Chemical Society in Minneapolis, September, 1955.

[2] H. C. Urey, *Proc. Roy. Soc. (London)*, **219A**, 281 (1953); *Geochim et Cosmochim. Acta*, **1**, 207 (1951).

temperatures. One can show by a simple thermodynamic argument, however, that in saturated, equilibrium systems, complex molecules can very well be of major significance.[3]

Although Urey[2] has offered strong arguments against gaseous molecules playing an important part in concentration of certain elements at the earth's surface in a high temperature process, and has laid a firm base for water solubility as the concentrating factor, it is of interest that gaseous water can also undergo chemical reaction to form stable gaseous molecules with compounds of Be, B, Al, Si, the alkali metals, and possibly La, Nb, Ta, Mo, W, and other elements, sometimes at relatively low temperatures.[4] That such molecules are of significance in mineral formation, in volcanoes and hot springs, and in certain stellar atmospheres seems a certainty.

Nitrogen is an element which is usually regarded as fairly unreactive. The existence of stable gaseous nitrides, both diatomic and more complex, is of interest, especially in considerations of stellar atmospheres at high temperatures.

Gaseous Hydroxides.—It has been observed that the volatility of a great many metal oxides is enhanced by the presence of water even at low partial pressures. One explanation for this enhanced volatility is the existence of stable gaseous hydroxides or gaseous hydrated oxides.

The direct vaporization of such simple compounds as the alkali metal hydroxides has not been thoroughly studied. There are, however, several references in the literature to gaseous alkali metal hydroxides, especially in high temperature flames.[5] The vaporization process could be by either of two paths

$$2\mathrm{NaOH(s\ or\ l)} = 2\mathrm{NaOH(g)} \qquad (1)$$

$$2\mathrm{NaOH(s\ or\ l)} = \mathrm{Na_2O(s)} + \mathrm{H_2O(g)} \qquad (2)$$

Recent measurements on solid and liquid NaOH by the Knudsen effusion and flow vapor pressure methods have supported the contention that NaOH(g) is the vaporizing molecule.[6]

Solid BeO has a very low vapor pressure in a vacuum or in a non-reactive atmosphere. In the presence of water vapor a considerable increase in the rate of vaporization is observed. The vaporization process has been investigated by Hutchison and Malm,[7] Seifert and Grossweiner,[8] and by Elliott.[4a] Possible vaporization reactions are

$$x\mathrm{BeO(s)} + \mathrm{H_2O(g)} = x\mathrm{BeO{\cdot}H_2O(g)} \qquad (3)$$

$$\mathrm{BeO(s)} + \mathrm{H_2O(g)} = \mathrm{HBeOH(g)} + {}^1/_2\mathrm{O_2(g)} \qquad (4)$$

The latter reaction was suggested by Elliott who found a slight oxygen pressure dependence of weight loss in a flow system.

The vaporization of B_2O_3(s or l) in an inert flow gas (He or N_2) containing various partial pressures of water has been studied over the range 280 to 900°.[9] Possible vaporization reactions include

$$\mathrm{B_2O_3(s\ or\ l)} + 3\mathrm{H_2O(g)} = 2\mathrm{H_3BO_3(g)} \qquad (5)$$

$$\mathrm{B_2O_3(s\ or\ l)} + \mathrm{H_2O(g)} = 2\mathrm{HBO_2(g)} \qquad (6)$$

If the vaporization process is by (5), then a plot of log $P_{\mathrm{H_3BO_3}}$ *vs.* log $P_{\mathrm{H_2O}}$ should be a straight line of slope 3/2. If reaction (6) describes the vaporization, then log $P_{\mathrm{HBO_2}}$ *vs.* log $P_{\mathrm{H_2O}}$ should be a straight line of slope 1/2. Figures 1 and 2 show plots of typical experimental data. The points always fall near a slope 1/2 line and definitely do not favor the 3/2-power dependence on the water pressure. The vaporizing species is apparently HBO_2(g). One point of interest is that even at temperatures as low as 200–300° and at water partial pressures less than 1 atm., gaseous hydroxides of boron exist in appreciable amounts.

Since the hydrated boric oxide molecules are easy to obtain in high concentration, it is of interest to examine the absorption spectra for evidence that might lead to the molecular configuration for HBO_2(g) or H_3BO_3(g). Heated absorption cells containing water and B_2O_3 were examined for ultraviolet, visible and infrared absorption up to 300° and 50 atm. pressure, but no characteristic spectra were found.[10] Visual examination of the interior of the cells showed that boric oxide, originally present as a small sample in a stainless steel boat, was deposited uniformly over the inside of the cell after heating under pressure. An investigation now in progress involves a study of the pressure–temperature behavior of closed systems containing water and boric oxide.

Von Stackelberg, Quatram and Dressel[11] have studied the vaporization of H_3BO_3(s) and HBO_2(s) over a temperature range where they are stable. Their work also favors the existence of H_3BO_3(g) and HBO_2(g) with the more highly hydrated molecule favored at low temperatures. Plots verifying the existence of H_3BO_3(g) and HBO_2(g) are shown in Fig. 3.

Various investigators have reported enhanced volatility of Al_2O_3 under the influence of water vapor. At 1500° there is definite evidence for the transfer of SiO_2 in the presence of small amounts of water. Elliott[4a] has suggested that the gaseous molecule is either $SiO{\cdot}4H_2O$ or $SiO_2{\cdot}3H_2O$, and prefers the former on the basis of a slight oxygen dependence in the vaporization. Hutchison[12] has reported exchange of O^{18} in H_2O–SiO_2 systems at 960°, supporting the idea that some equilibrium reaction is occurring.

Gaseous Nitrides.—Nitrogen is an important constituent of our own atmosphere, yet chemically it is practically inert at ordinary temperatures. Nitrogen is also present in many stellar atmospheres as evidenced by spectra of N_2 and CN, yet this electronegative element is rarely observed in combination as a gaseous nitride. Although nearly

---

[3] L. Brewer, Paper No. 7, in Quill, "Chemistry and Metallurgy of Miscellaneous Materials: Thermodynamics," NNES Vol. IV, 19B, McGraw-Hill Book Co., New York, N. Y., 1950, pp. 261–263.

[4] (a) G. R. B. Elliott, Ph.D. Thesis, University of California, Berkeley, 1952; (b) K. Rankama and T. G. Sahama, "Geochemistry," University of Chicago Press, Chicago, Illinois, 1950.

[5] H. Smith and T. M. Sugden, *Proc. Roy. Soc. (London)*, **211A**, 31, 58 (1951); **219A**, 204 (1953); *Nature*, **171**, 428 (1953).

[6] L. Spinar, S. Suzuki and J. L. Margrave, unpublished work, 1955.

[7] C. A. Hutchinson and J. G. Malm, *J. Am. Chem. Soc.*, **71**, 1338 (1949).

[8] R. L. Seifert and L. I. Grossweiner, *ibid.*, **74**, 2701 (1952).

[9] J. C. Damron and J. L. Margrave, unpublished work, 1955.

[10] R. J. Sime and J. L. Margrave, unpublished work, 1954–1955.

[11] M. von Stackelberg, F. Quatram and J. Dressel, *Z. Elektrochem.*, **43**, 14 (1937).

[12] D. A. Hutchison, *J. Chem. Phys.*, **22**, 758 (1954).

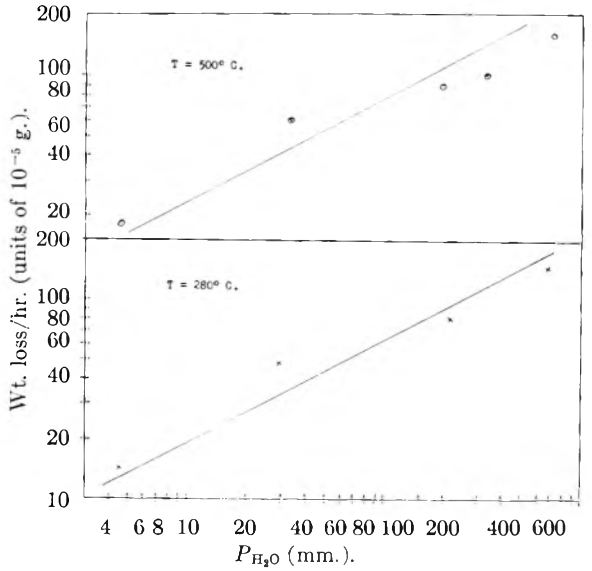

Fig. 1.—The rate of vaporization of B_2O_3 as a function of the partial pressure of water in the flow gas.

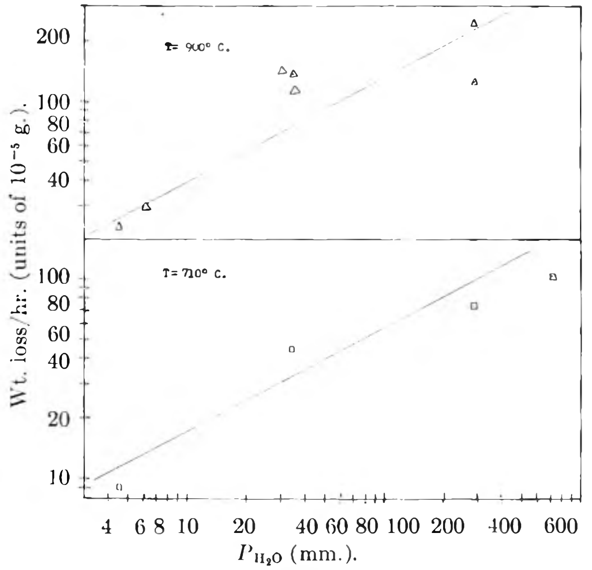

Fig. 2.—The rate of vaporization of B_2O_3 as a function of the partial pressure of water in the flow gas.

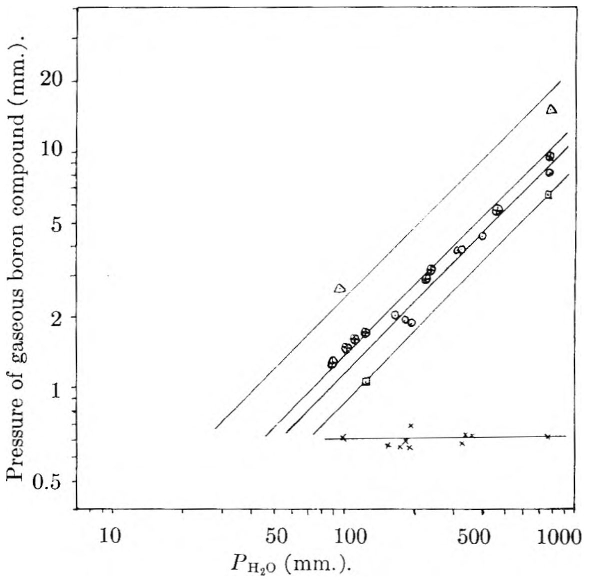

Fig. 3.—Vaporization reactions for $H_3BO_3(s)$ and $HBO_2(s)$[11]: (1) $H_3BO_3(s) = H_3BO_3(g)$; (2) $HBO_2(s) + H_2O(g) = H_3BO_3(g)$; (3) $H_3BO_3(g) = HBO_2(g) + H_2O(g)$. ×, $P_{H_3BO_3(g)}$ over $H_3BO_3(s)$ at various water pressures and 109°; ⊡, $P_{H_3BO_3(g)}$ over $HBO_2(s)$ at various water pressures and 145°; ⊙, $P_{H_3BO_3(g)}$ over $HBO_2(s)$ at various water pressures and 149°; ⊗, $P_{H_3BO_3(g)}$ over $HBO_2(s)$ at various water pressures and 160°; △, $P_{H_3BO_3(g)}$ over $HBO_2(s)$ at various water pressures and 180°. Deviation from the 45°-slope at 180° is attributed to the formation of appreciable $HBO_2(g)$ by dissociation of $H_3BO_3(g)$.

400 gaseous diatomic molecules are known, of which more than 125 are diatomic halides and over 60 are diatomic oxides, only 13 diatomic nitrides have been identified. Only BN(g) comes close to being a gaseous metal nitride. In a survey of the nitrides of the elements, Sime and Margrave[13] found information indicating the probable existence of gaseous gallium nitride. Experimental flow vapor pressure measurements have verified the fact that GaN(s) does vaporize as a complex gaseous nitride around 900–1000°.[14]

Sthapitanonda and Margrave[15] have made calculations based on an ionic model for the gaseous diatomic nitrides and find that nitrides of the metals of Groups I, II and III should be of importance in high nitrogen systems at temperatures of the order of 10,000°K. and higher. These calculations suggest that gaseous nitrides might be important species in stellar atmospheres.

[13] R. J. Sime and J. L. Margrave, "Nitrides of the Elements," to be published.

[14] R. J. Sime and J. L. Margrave, unpublished work, 1955.

[15] P. Sthapitanonda and J. L. Margrave, THIS JOURNAL, **59**, 1231 (1955).

EXPERIMENTAL GEOLOGY

BY GEORGE W. MOREY

Geophysical Laboratory, Carnegie Institution of Washington, Washington, D. C.

Received December 27, 1955

A major concern of geology is to explain the characteristic association of certain minerals in well-known rock types, and the relation of these rock types to each other. From experimentally determined phase-equilibrium diagrams it is shown how by a series of stages of fractional crystallization, many of which result in formation of solid solutions, rocks high in silica, such as granite, can be derived from an initial basic magma low in silica from which orthosilicates such as the olivines are the primary crystallization. This process of separation of chiefly anhydrous minerals results in the accumulation in the magma of volatile constituents, chiefly water, which may result in the building up of pressure, giving rise to a volcanic eruption, or the cooling process may be continuous, with formation of pegmatites, fumaroles, and hot springs.

A major concern of geology is to explain the characteristic association of certain minerals in well-known rock types, and the relation of these rock types to each other. Some rocks are of sedimentary origin, formed by weathering of other rocks and the subsequent consolidation of the sediments. Other rocks, the metamorphic rocks, are formed by the alteration by heat and pressure either of such sediments or of the primary igneous rocks, which are formed by the cooling and crystallization of a molten rock magma. Opinions differ as to the mode of origin of rock magma, but there is little difference of opinion as to the broad relationships of the igneous rocks, which range in composition from highly basic or femic rocks composed chiefly of orthosilicate minerals high in iron and magnesia, to acidic or salic rocks, high in silica and alumina. In the course of solidification of a magma, crystals may settle out from the melt by gravity, or the residual liquid may be squeezed out from the mass of crystals. The liquid may redissolve certain crystals which have separated at an earlier stage in the process of crystallization. Frequently crystals of the earlier crystallizing stages of a solid solution series become coated with crystals of later stages, and the innermost layers of such zoned crystals are effectively removed from the reaction. Examples are known of each of these mechanisms of differentiation.

Over 99% of the earth's crust and hence of any "primordial" magma which may once have existed is composed of ten oxides, which in order of their abundance are: SiO_2, Al_2O_3, Fe_2O_3, FeO, CaO, Na_2O, MgO, K_2O, H_2O and TiO_2. There is much evidence to indicate that the initial magma was basic in composition, containing considerably more than one basic oxide per equivalent of silica. The precipitation series in the crystallization of such a magma follows a pattern determined by the solubilities of the various compounds in the coexisting magma.

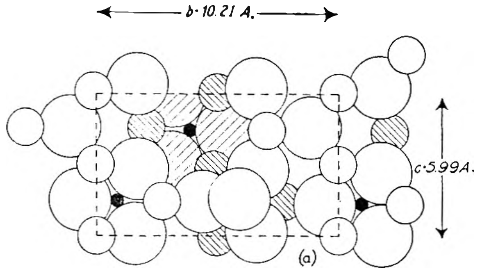

Fig. 1.—The structure of olivine. The large circles are oxygens, the intermediate circles are magnesium, and the small black circles are silicon atoms. After Bragg.

The constitution of such a magma is an unsolved problem. This is not surprising when we consider that the constitution of strong aqueous solutions is still largely a mystery. We do, however, have some definite ideas concerning the molecular arrangements in silicate melts. The fundamental structural unit in all silicates is the positive silicon ion, surrounded by four oxygen atoms in tetrahedral coördination. The Si–O bond is the strongest in silicate structures, and the oxygen atom has the largest radius, so that the manner of arrangement of the skeleton of silicon and oxygen atoms determines the number and position of the basic cations which complete the structure in liquid, glass or crystal. In basic melts there probably is a statistical preponderance of orthosilicate structures in which the SiO_4 groups have no oxygen atoms in common. The structure of olivine[1] is given in Fig. 1. The minerals of the olivine group are of this type, orthosilicates of magnesium, calcium and ferrous iron, of the general formula $RRSiO_4$. These orthosilicate minerals are the first to crystallize from the basic magma, and the heaviest types of silicate rock, formed either by original crystallization in depth or by settling of crystals in a large intrusive mass, are composed principally of orthosilicates. Belonging to this category is peridotite, the characteristic matrix within which diamonds are found in nature. Chromium oxide, as chromite, is another frequent constituent, and the platinum metals are often associated with these heavy rocks.

Sulfides are only slightly soluble in molten silicates; that solubility is greatest in the early-crystallizing magmas containing larger proportions of basic oxides, and it decreases as the temperature is lowered. Sulfides in small quantities are found in most silicate rocks, but only rarely are primary sulfide differentiates in quantity sufficient to be called ores. The nickel–copper ores of the famous Sudbury district may be an example of such a deposit, although there is no unanimity of opinion as to the genesis of these wonderful deposits, which contain, not only nickel and copper, but also gold and the platinum metals. Many authorities consider them to be magmatic segregations of immiscible sulfide ores. If so, they are an example of a process rare in geology, differentiation by separation into two immiscible liquids, a process of frequent application in chemical engineering. Immiscibility in silicate

---

(1) W. L. Bragg, "Atomic Structure of Minerals," Cornell University Press, Ithaca, N. Y., 1937.

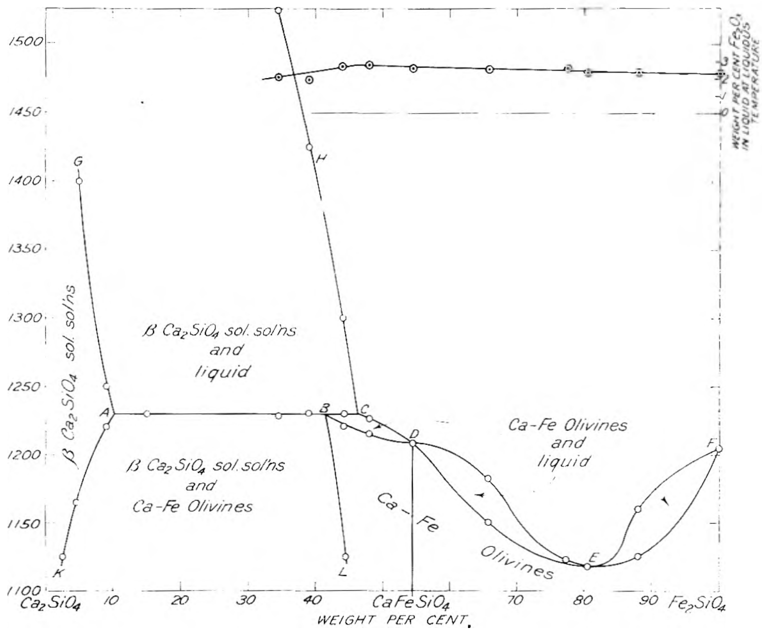

Fig. 2.—The binary system Ca_2SiO_4–Fe_2SiO_4, showing the large area of solid solution in the calcium–iron olivines. The upper right diagram represents the actual amount of Fe_2O_3 in each liquid at the liquidus temperature under the conditions of the experiment. After Bowen, Schairer and Posnjak.

melts has been demonstrated in the laboratory, but all evidence indicates that this plays no part in the formation of silicate rocks. But sulfides and silicates are immiscible, and differentiation by unmixing of sulfide and silicates probably takes place, and it may be more common than is evident from surface indications.

Nearly all the common rock-forming olivines are orthosilicates of magnesium, calcium and ferrous iron. They include forsterite, Mg_2SiO_4; fayalite, Fe_2SiO_4; the olivines, which are an intermediate solid solution between forsterite and fayalite; and monticellite, $[MgCa]_2SiO_4$, a definite magnesium–calcium orthosilicate. The complex nature of these solid solutions[2] is evident from Fig. 2, which shows the calcium–iron olivines forming solid solutions with a minimum melting point. The crystallization of a magma containing an excess of any or all of these basic oxides leads first to the separation of a mineral of the olivine group, but olivines can also crystallize from melts of the metasilicate ratio. This is because of incongruent melting, which causes the orthosilicate field to spread over the metasilicate join. This is well shown in Fig. 3, which represents the phase equilibrium relationships in the ternary system forsterite–diopside ($CaSiO_3 \cdot MgSiO_3$).[3] The metasilicate join is the line from magnesium metasilicate, enstatite, to diopside, and over a large portion of its length olivine is the primary phase. The crystallization path of such a basic magma thus yields a magma from which a metasilicate, a member of the pyroxene solid solution series, crystallizes. A similar relationship is shown in the ternary system MgO–FeO–SiO_2,[4] in which the initial crystallization of olivine brings the residual liquid to the metasilicate field.

Most of the non-aluminous pyroxenes are metasilicates of the same basic oxides, MgO, CaO and FeO. They include enstatite, $MgSiO_3$; bronzite and hypersthene, both mixed metasilicates of magnesium and iron; diopside, $CaMg(SiO_3)_2$; and augite, a complex calcium–magnesium–ferrous iron metasilicate solid solution. These minerals all are characterized by the presence of simple chains of linked tetrahedral groups, with a general structure[5] similar to that shown in Fig. 5. Calcium metasilicate, wollastonite, is a ring polymer, but $CaSiO_3$ enters into solid solution with $MgSiO_3$ and $FeSiO_3$. Many of the aluminous pyroxenes are highly complex solid solutions, and some rocks consist largely of a complex augite, which contains, in addition to $CaMg(SiO_3)$, FeO, Fe_2O_3 and Al_2O_3.

The first crystals which separate from a basic magma usually are of magnetite, sometimes also of spinels, after which comes a major crystallization of the orthosilicate minerals, which removes the excess of bases and gives rise to a basaltic magma from which pyroxenes separate. First the pyroxene minerals are associated with orthosilicates, forming rocks such as the olivine basalts; then the olivines disappear and that important group of minerals known as the feldspars becomes of increasing importance. At the same time the character of the bases is changing. Instead of being dominantly iron and magnesia, they become richer in calcium,

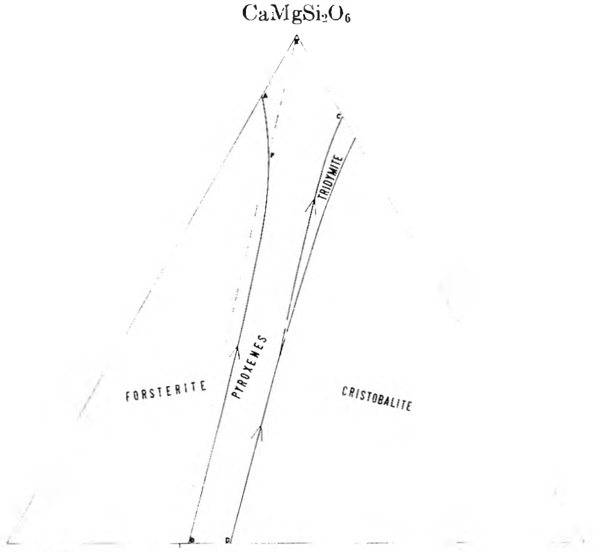

Fig. 3.—The phase equilibrium diagram of the ternary system forsterite Mg_2SiO_4–diopside ($CaMgSi_2O_6$)–silica, showing the field of Mg_2SiO_4 spreading over the metasilicate join $MgSiO_3$–$CaMgSi_2O_6$, and the adjoining field of the monoclinic pyroxene solid solutions. After Bowen.

---

(2) N. L. Bowen, J. F. Schairer and E. Posnjak, *Am. J. Sci.*, **25**, 273 (1933).

(3) N. L. Bowen, *Am. J. Sci.*, **38**, 207 (1914).

(4) N. L. Bowen and J. F. Schairer, *ibid.*, **29**, 151 (1935).

(5) R. W. G. Wyckoff, "The Structure of Crystals," Chemical Catalog Co., New York, N. Y., 1931.

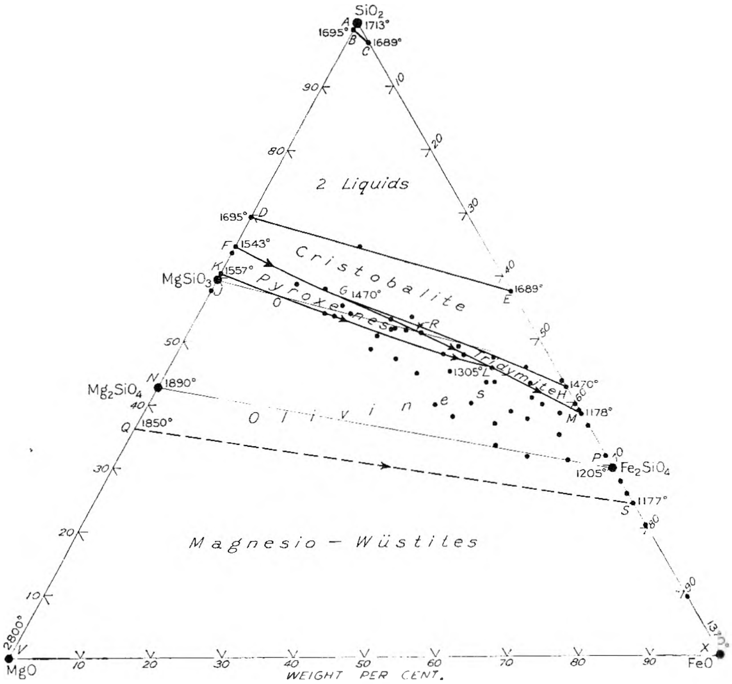

Fig. 4.—The phase equilibrium diagram of the ternary system MgO–FeO–SiO$_2$, showing the fields of stability of the crystalline phases in contact with liquid. The magnesio-wüstites are MgO–FeO solid solutions; the olivines are Mg$_2$SiO$_4$–Fe$_2$SiO$_4$ solid solutions; the pyroxene field also is one of solid solution. After Bowen and Schairer.

and the alkalies, soda and potash, make their appearance in quantity.

The feldspar of basalts is chiefly of the type known as plagioclase, which is the mineralogical name for the continuous series of solid solutions[6] between the two end members, anorthite, CaO·Al$_2$O$_3$·2SiO$_2$, and the much more siliceous soda feldspar, albite, Na$_2$O·Al$_2$O$_3$·6SiO$_2$ (Fig. 6). This solid solution series illustrates an important factor in differentiation. The gradation in composition is continuous, and the course of crystallization leads, not to a eutectic mixture, but to albite itself. Fractional crystallization brings about continuous impoverishment in the lime component, anorthite; continuous enrichment in the soda feldspar, albite. A similar relationship is found when the pyroxene, diopside, Ca·Mg·(SiO$_3$)$_2$ is added (Fig. 7) to the plagioclase feldspars, as is shown in the ternary system[7] albite, Na$_2$O·Al$_2$O$_3$·6SiO$_2$–diopside (MgO·CaO·2SiO$_2$)–anorthite, CaO·Al$_2$O$_3$·2SiO$_2$. The continuous solid solution series persists, and crystallization produces continuous enrichment in albite and impoverishment in anorthite and diopside, or, in chemical terms, enrichment in soda–alumina silicates, impoverishment in magnesia and in both "salic" and "femic" lime. Similar relationships are met with when the alkali is not soda but potash, as is shown in Fig. 8. In the system[8] leucite–anorthite–silica all the major fields sweep down to the field of the potash feldspar, orthoclase, K$_2$O·Al$_2$O$_3$·6SiO$_2$. If the additional component is not the plagioclase feldspar, anorthite, but the pyroxene, diopside, resulting in the system[9] leucite–diopside–silica, the effect is similar, leading to a low temperature residual liquid from which orthoclase crystallizes.

The previous discussion has shown that the process of crystallization differentiation in systems containing magnesia, lime, alumina, silica and either soda or potash leads to a residual liquid rich in the alkaline feldspars, albite and orthoclase, and also necessarily rich in silica. The basic oxides MgO and CaO have been largely eliminated as olivines, pyroxenes or plagioclase feldspars. The ubiquitous iron suffers a similar fate, as is shown in the system[10] nepheline, NaAlSiO$_4$–FeO–SiO$_2$ (Fig. 10). Here the iron-rich melts separate the orthosilicate, fayalite, Fe$_2$SiO$_4$, until low melting eutectics are reached at which orthoclase coexists with melts greatly impoverished in iron oxide, and with either tridymite or nepheline.

No matter what may be the original composition of the magma, all the paths of crystallization enumerated tend toward the same final phases. When both soda and potash are present, as is the case in nature (Fig. 11), this com-

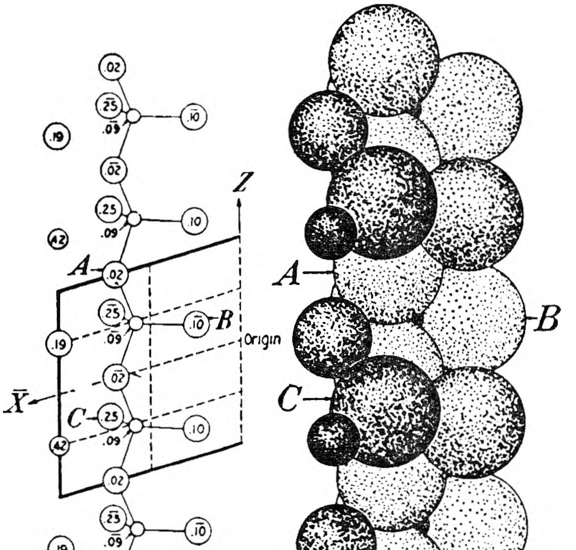

(a) (b)

Fig. 5.—One of the silicate chains in the diopside, CaMgSi$_2$O$_5$, structure, extended through three unit cells. The oxygen atoms are the largest, calcium next, then magnesium, and the silicon atoms hardly show. After Wyckoff.

---

(6) The original study of this system was by Day and Allen (A. L. Day and E. T. Allen, Carnegie Institution of Washington Publ. No. 31, 1905), which was followed by that of Bowen (N. L. Bowen, *Am. J. Sci.*, **35**, 577 (1913)). The present diagram is that of Bowen, corrected for the melting point of albite determined by Greig and Barth (J. W. Greig and Tom. F. W. Barth, *ibid.*, **35A**, 93 (1938)), and including recent unpublished determinations by J. F. Schairer.

(7) N. L. Bowen, *ibid.*, **40**, 161 (1915).

(8) J. F. Schairer and N. L. Bowen, *Bull. Soc. Geol. Finlande*, **20**, 67 (1947).

(9) J. F. Schairer and N. L. Bowen, *Am. J. Sci.*, **35A**, 289 (1938).

(10) N. L. Bowen and J. F. Schairer, *J. Geol.*, **46**, 397 (1938).

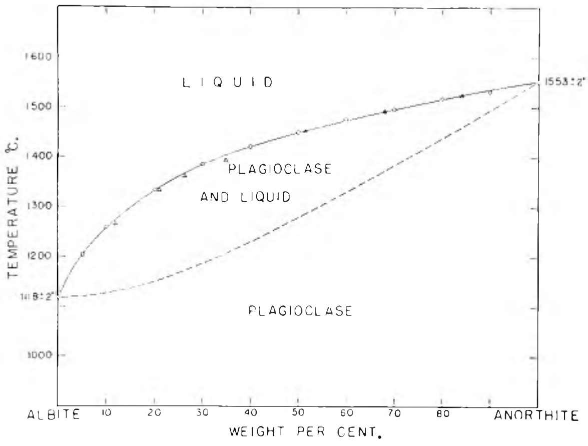

$Na_2O{\cdot}Al_2O_3{\cdot}6SiO_2$ or $NaAlSi_3O_8$ $CaO{\cdot}Al_2O_3{\cdot}2SiO_2$ or $CaAl_2Si_2O_8$

Fig. 6.—Phase equilibrium diagram of the system albite $Na_2O{\cdot}Al_2O_3{\cdot}6SiO_2$–anorthite $CaO{\cdot}Al_2O_3{\cdot}2SiO_2$, showing complete solid solution in the plagioclase feldspars. The points indicated by triangles are by Bowen. Those indicated by circles are by Schairer.

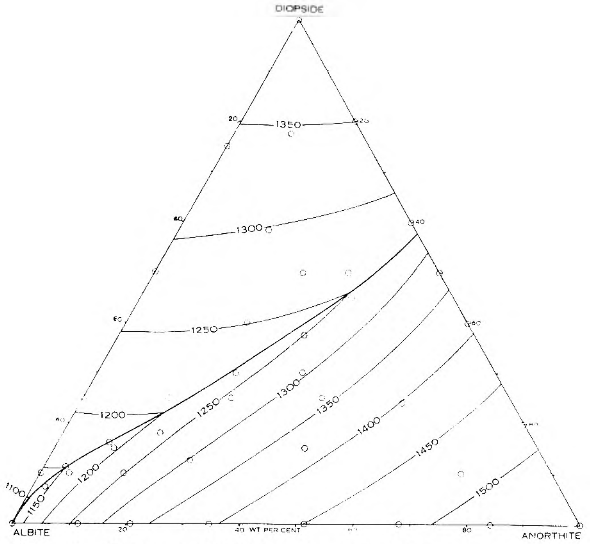

Fig. 7.—Phase equilibrium diagram of the ternary system albite ($Na_2O{\cdot}Al_2O_3{\cdot}6SiO_2$)–diopside ($MgO{\cdot}CaO{\cdot}2SiO_2$)–anorthite ($CaO{\cdot}Al_2O_3{\cdot}2SiO_2$). After Bowen.

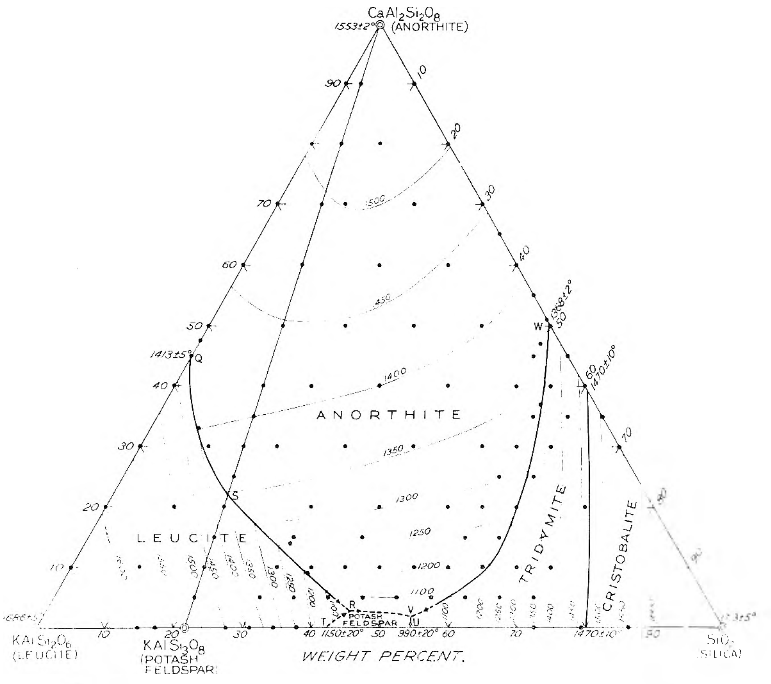

Fig. 8.—Phase equilibrium diagram of the ternary system leucite–anorthite–silica. After Schairer and Bowen.

position may be roughly represented by an area in the system[11] Na_2O–K_2O–Al_2O_3–SiO_2 extending over the minimum in the solid solution series albite–orthoclase, and tending either toward the SiO_2 apex, leading ultimately to the formation of granite, or toward more alkalic rocks, such as the nepheline syenites. This composition region, the sink to which crystallization differentiation brings the mother liquor of a crystallizing magma, has been aptly termed by Bowen "petrogeny's residua system."

The preceding discussion has dealt with dry melts, omitting the influence of water. But water is an essential and important constituent of the rock magma. In the early stages of crystallization its influence is comparatively small. Owing to its low molecular weight small amounts have important effects both in lowering the temperatures at which the various minerals crystallize and in lowering the viscosity. This probably has an important effect in the gravitative separation of heavy minerals. As crystallization differentiation takes its course the water is accumulating. As anhydrous olivines, pyroxenes and plagioclases crystallize out, the mother liquor is being continuously enriched in water. An important effect of this accumulation of water is the building up of pressure.[12] Water is a volatile substance, and to keep it dissolved in the molten rock mass pressure is required, pressure that increases as the mole fraction of the water increases. We thus have a mechanism by which pressure is built up as the result of cooling. As cooling proceeds, the non-volatile basic oxides crystallize out, the mole fraction of the water increases, and as a result the pressure required to hold it in solutions increases. If the crystallization is taking place in depth, under a competent crust, crystallization continues in an orderly manner; the pressure will pass through a maximum, then decrease as temperature falls to that of geyser and hot spring activity. But if the crystallization takes place under a crust not competent to withstand the pressure, when the pressure has reached a limiting value it will force open a vent for itself, giving rise to a volcanic eruption. The phenomenon observed in any particular eruption will depend, in large part at least, on the magnitude of the pressure and on the composition of the non-volatile portions of the

---

(11) J. F. Schairer, *J. Geol.*, **58**, 512 (1950).

(12) G. W. Morey, *J. Wash. Acad. Sci.*, **12**, 219 (1922); *J. Geol.*, **32**, 291 (1923).

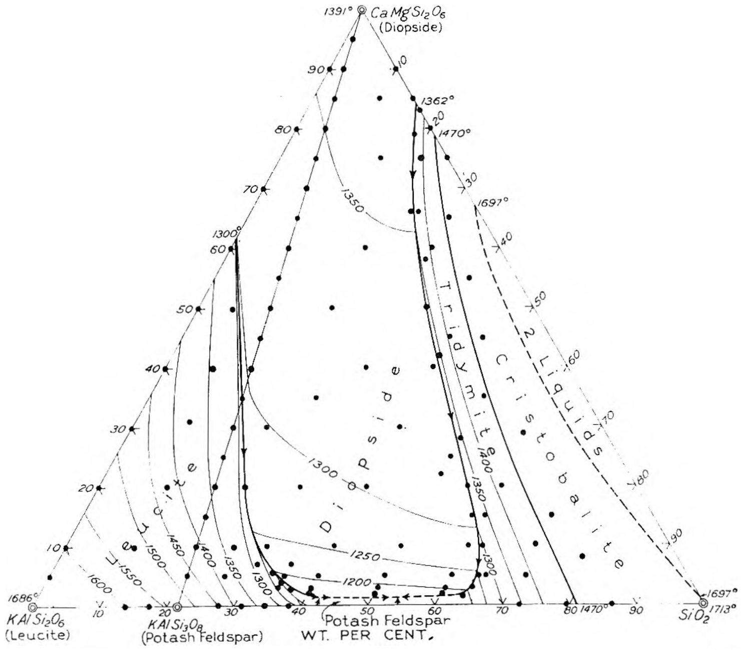

Fig. 9.—Phase equilibrium diagram of the ternary system leucite–diopside–silica. After Schairer and Bowen.

magma, though these factors may not be independent. If the vent is an open one and the lava fairly fluid, enormous pressures will not be developed and the escape of water as steam may be comparatively quiet. This is the case with Kilauea, with a hot, thinly fluid basaltic magma, and the rate of release of steam may be regarded as a measure of the rate of crystallization in the parent body.

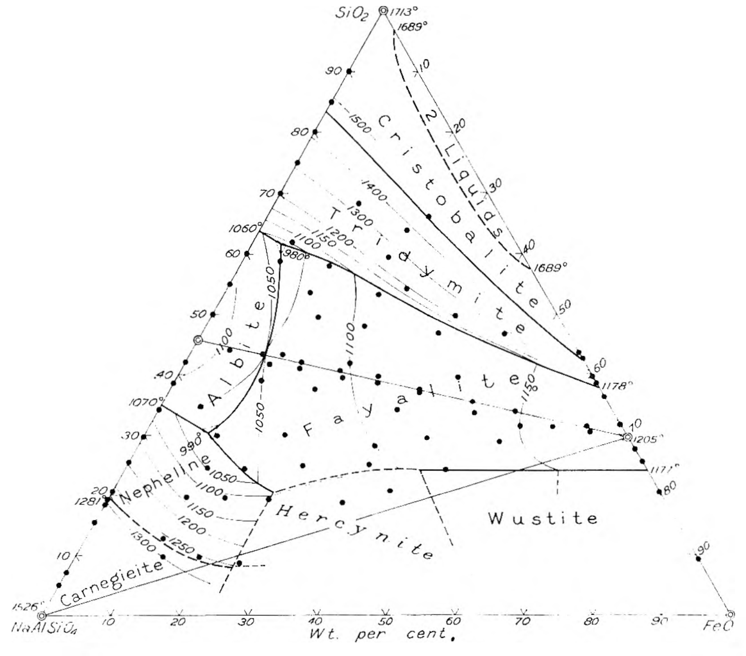

Fig. 10.—Phase equilibrium diagram of the ternary system NaAlSiO$_4$–FeO–SiO$_2$. After Bowen and Schairer.

On the other hand, conditions may be such that a much greater pressure must be developed before the gases are able to force their way to the surface. It may be assumed that eruptions will then take place at less frequent intervals, since more time must elapse for the cooling process which occasions the crystallizations, and that, on account of the greater pressure, the resulting eruptions will tend to be catastrophic. The greatest pressures would be expected to be built up in the late stages in differentiation, when the non-volatile components are present in the proportions of "petrogeny's residua system." We would expect, then, that paroxysmal eruptions would be characterized by the ejection of salic lava. That is known to be the case with the classic eruption of Krakatoa, with the eruption of Martinique, which wiped out the city of Sainte Pierre, and with Mt. Lassen in California. All were catastrophic eruptions following long periods of quiescence, and were characterized by blasts of hot steam and glassy, highly vesiculated salic ejecta.

The magnitude of the pressures involved in such eruptions is not known, but probably the stupendous magnitude of the results is determined not so much by super-pressures but by the great quantity of material available at the prevailing pressure. Certainly the pressures we have attained in the laboratory are adequate. Figure 12 illustrates the build-up of pressure in the system H_2O–$Na_2Si_2O_5$. Sodium disilicate has a retrograde solubility curve, and its solubility in water decreases to essentially zero at the first critical end point, near 374° and 221 bars. But the melting point of sodium disilicate, 874°, is lowered by the presence of water, and as the temperature is lowered the water content increases and so does the pressure exerted by the water. At 600° the pressure is about 650 bars, at 500°, 1200 bars, and at 400°, 2200 bars, or 33,000 pounds per square inch. In other words, if a melt of sodium disilicate containing a small amount of dissolved water is allowed to cool in a closed vessel, the disilicate will crystallize and the water will accumulate and build up a pressure of 33,000 pounds per square inch at 400°. This is above the second critical end point in the system, which will presumably be at an even higher pressure.

These later stages in the crystallization of the igneous rocks are a fascinating study. As the granite crystallizes the water continues to accumulate. Some of it is removed in hydrous minerals such as mica, but that part remaining greatly lowers the viscosity of the magma, producing the coarsely crystalline rock known as granite pegmatite. During the same epoch there is a great tendency for the formation of mineral and ore veins. The pressure is high, and any potential seams or cracks

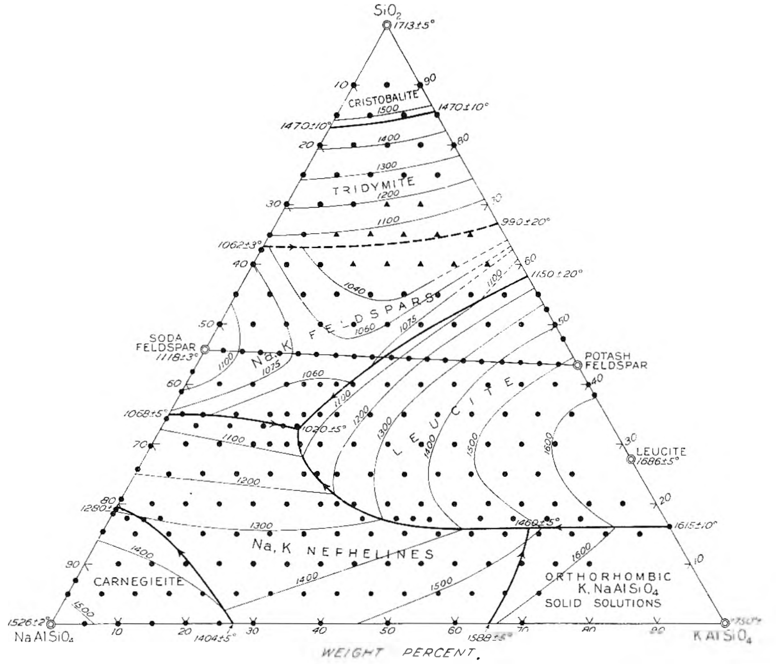

Fig. 11.—Phase equilibrium diagram of the ternary system $NaAlSiO_4$–$KAlSiO_4$–SiO_2. After Schairer.

afford opportunity for a gas phase to form and extend outward as a vein or pneumatolytic deposit. The highly compressed gas is a potent solvent. This is well shown in the curves of Fig. 13, which gives the experimentally determined solubility[13] of quartz in superheated steam at high pressures. These experiments go only to 2000 bars or 30,000 pounds per square inch, but experiments in progress show that the curve at 600° can be extrapolated as a straight line to 45,000 p.s.i. The solubility of germanium oxide in steam is almost twice that of silica. Table I gives the solubilities of sev-

TABLE I

SOLUBILITIES IN SUPERHEATED STEAM AT 500° AND 15,000 P.S.I., GRAMS PER 100 G. H_2O

GeO_2	0.87	Orthoclase	0.076
Na_2SO_4	.43	Fe_2O_3	.009
SiO_2	.26	$BaSO_4$	.004
BeO	.012	$CaSO_4$	.002
$PbSO_4$	.011	NiO	.002
Albite	.077	SnO_2	.0003

eral substances in superheated steam at 500°, 15,000 p.s.i., or 1000 bars. Other salts, such as NaCl and K_2SO_4, are more soluble; indeed, the solubility of K_2SO_4 is so great that we have not found a satisfactory method for its measurement. The solubility of some metallic oxides is increased several fold by the presence in the steam of about 7% of carbon dioxide. An extreme example of solid material dissolved in superheated steam at high pressure was was met with in the system[14] H_2O–Na_2O–SiO_2. At 400° and 2000 bars pressure a gaseous phase in equilibrium with crystalline sodium metasilicate contained 67.4% of H_2O and 32.6% of $Na_2O \cdot SiO_2$, and had a density of 1.35. Gases of this character are potent mineralizers.

The residual liquid in the later stages of pegmatite formation will contain great stores of the rarer components of the original magma. Lithium is too small an ion to fit into a feldspar lattice, and it is characteristically a mineral of the later stages of pegmatite formation. Lithium minerals such as spodumene, petalite and the lithium mica, lepidolite, probably are formed below 500° and sometimes in such spectacular forms as the giant crystals of spodumene at the Etta mine in the Black Hills, many of which are more than 30 feet long. Beryl, a silicate of aluminum and beryllium, the source not only of the gem minerals emerald, aquamarine and golden beryl, but also of the valuable light metal beryllium, is a common mineral of the pegmatites. A crystal of beryl was found in the pegmatites of Albany, Maine, 18 feet long, 4 feet on a side, and weighing 18 tons. The pegmatites are a storehouse of rare minerals, often in large crystals, and often segregated into deposits of exceptional purity.

When an intrusive mass has opportunity to cool completely, the transition from the later stages of pegmatite formation to hot spring and fumarole activity probably is continuous. Here too we find

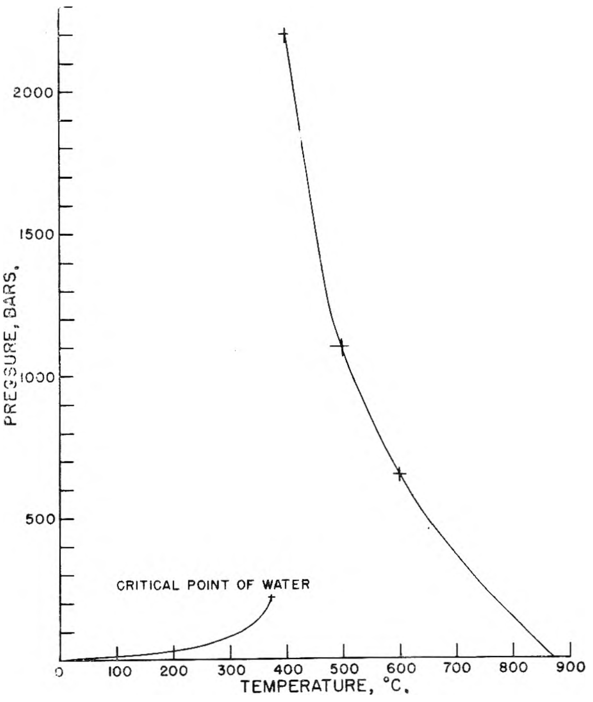

Fig. 12.—Pressure-temperature curve of three-phase equilibrium gas + liquid + solid in the binary system H_2O–$Na_2Si_2O_5$, which is not continuous because of the intersection of the solubility curve with the critical curve. The first critical end point is near the critical point of water; the second critical end point is on the ascending part of the P-T curve, between 374° and 400°. Unpublished results of G. W. Morey.

---

[13] G. W. Morey and J. M. Hesselgesser, *Econ. Geol.*, **46**, 821 (1951).

[14] G. W. Morey and J. M. Hesselgesser, *Am. J. Sci.*, Bowen Vol., 343 (1952).

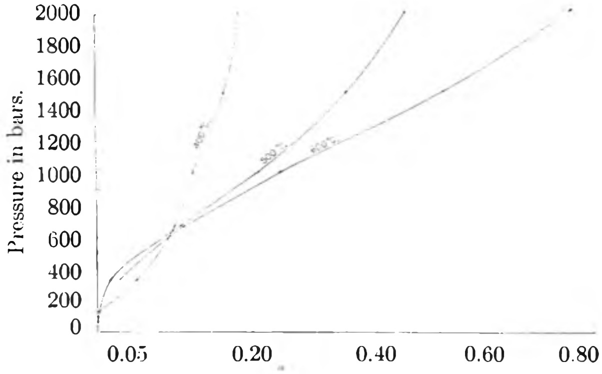

Fig. 13.—The solubility of quartz in superheated steam at high pressures, expressed as weight % of SiO_2 is the condensate. After Morey and Hesselgesser.

important processes of differentiation, which were especially well brought out by Zies[15] in his studies of the fumaroles of the Valley of Ten Thousand Smokes. The Valley contains about 2 cubic miles of rhyolitic pumice, roughly of granitic composition, which was deposited after having been blown through the floor of the Valley. Many fumaroles are located in this area, through which have come great quantities of steam, from which were deposited important quantities of lead, zinc, molybdenum, copper, arsenic, antimony, tin and silver. The acid exhalations of these fumaroles are noteworthy. The concentration of acid in the steam is not great, but the total quantity is enormous. Zies has estimated that in one year the fumaroles of the Valley of Ten Thousand Smokes give off one and a quarter million tons of hydrochloric acid and two hundred thousand tons of hydrofluoric acid. The ultimate destination of these acids is of interest. The sea is an adequate sink for the hydrochloric acid, but not for the hydrofluoric acid. Huge quantities of fluorine are locked up in sedimentary phosphate deposits as the mineral apatite, and such deposits may be the ultimate sink for the huge quantities of hydrofluoric acid given off by volcanic action.

But finally, as the ages go by, the process of magmatic differentiation is complete. From a magma originally basic in composition, first the orthosilicate minerals separate, then the metasilicates and plagioclases crystallize, leading to a magma from which either a nepheline rock, or more commonly a granite, crystallizes. Later is a stage of pegmatite formation, where the influence of the accumulated water has become dominant, and the highly concentrated aqueous solutions contain important quantities of trace elements. But the process is a continuous one, called by chemists fractional crystallization, by geologists, differentiation.

[15] E. G. Zies, *Nat. Geog. Soc., Contributed Tech. Papers*, Katmai Ser., 1, no. 4, 79 pp. (1929); *Chem. Revs.*, **23**, 47 (1938).

EXCHANGE AND ISOMERIZATION OF *trans*-ETHYLENE-d_2 ON NICKEL. KINETIC STUDIES[1]

BY TED B. FLANAGAN AND B. S. RABINOVITCH

Contribution from the Department of Chemistry of the University of Washington, Seattle, Washington

Received September 12, 1955

Activation energies and orders of the pressure dependence of the nickel-catalyzed isomerization and exchange reactions of *trans*-ethylene-d_2 have been determined. The observed activation energies for isomerization are 13.5 and ~6.7 kcal. from 35–105° and 170–195°, respectively; the activation energy for exchange is ≤1.5 kcal. greater for the same temperature intervals. Both reactions proceed by the same mechanism, and their relative rates as well as the small difference in activation energies between isomerization and exchange (and other results) are explained on the basis of an isotope effect in the decomposition of an intermediate ethyl radical. The order of the pressure dependence for both reactions is 0.3 at 53° rising to 1.0 at 170°. The C–H and C–D bond rupture isotope effect has been measured from −78 to 400°. Various mechanisms are discussed.

The mechanism of ethylene hydrogenation and exchange on transition elements is still controversial.[2] Important evidence against a dissociative exchange mechanism[3,4] was the work of Conn and Twigg[5] in which no exchange was found between ethylene-d_0 and ethylene-d_4 on nickel wire. Furthermore, although Beeck's results[4] strongly suggest dissociative adsorption takes place, alternative mechanisms for adsorption (and self-hydrogenation) have been given wherein ethylene does not liberate hydrogen to the catalyst.[6]

Recently, Douglas and Rabinovitch[7] have shown that exchange *does* take place between ethylene-d_0 and ethylene-d_4 on nickel–kieselguhr and on nickel wire; with *trans*-ethylene-d_2, *cis–trans* isomerization was also found. Earlier, Baxendale and Warhurst[8] found a small amount of isomerization of elaidic ester to oleic ester on a platinum black catalyst in the absence of hydrogen, although they attributed this to impurities on the surface. Koizumi[9]

---

[1] Abstracted in part from a thesis submitted by Ted B. Flanagan to the Graduate School in partial fulfillment of the requirements for the degree of Doctor of Philosophy at the University of Washington. Work supported by the Office of Naval Research.

[2] D. D. Eley, *Disc. Faraday Soc.*, No. 8, 99 (1950); G. C. Bond, *Quart. Rev.*, **8**, 279 (1954).

[3] A. Farkas, *Trans. Faraday Soc.*, **35**, 906 (1939).

[4] O. Beeck, *Disc. Faraday Soc.*, No. 8, 118 (1950).

[5] G. K. T. Conn and G. H. Twigg, *Proc. Roy. Soc. (London)*, **A171**, 70 (1939).

[6] D. D. Eley, *Disc. Faraday Soc.*, No. 8, 34 (1950); for further discussion see B. M. W. Trapnell, "Chemisorption," Academic Press, New York, N. Y., 1955, p. 185.

[7] J. E. Douglas and B. S. Rabinovitch, *J. Am. Chem. Soc.*, **74**, 2486 (1952).

[8] J. H. Baxendale and E. Warhurst, *Trans. Faraday Soc.*, **36**, 1186 (1940).

[9] M. Koizumi, *J. Chem. Soc. Japan*, **63**, 1512, 1715 (1942).

showed that ethylene-d_4 and propylene exchanged over nickel powder catalyst at 45°. In all cases where exchange or isomerization of olefins has been observed in the absence of hydrogen, the catalysts have had large surface areas as opposed to the small areas involved where no reaction was found.[5,10]

Very recently, Jenkins and Rideal[11] have presented very strong evidence in favor of dissociative adsorption of ethylene on nickel.

Because of the intimate relation between isomerization, exchange, and hydrogenation reactions of olefins and the fundamental importance of these reactions, a detailed investigation of the kinetics of the exchange and isomerization reactions of pure *trans*-ethylene-d_2 on nickel has been undertaken and is reported here.

Experimental

Reactants.—*trans*-Ethylene-d_2, *cis*-ethylene-d_2 and ethylene-d_4 were prepared as described previously.[7] The *trans*-ethylene-d_2 was 99.3% pure, with ethylene-d_1 as the major impurity. *cis*-Ethylene-d_2 was 98.9% pure, with the remainder ethylene-d_1. Ethylene-d_4 was 97.6%, with 1% ethylene-d_3 and 1.4% ethane-d_6 as the principal impurities. The ethylene-d_0 was Phillips Petroleum Co. research grade, used without further purification. Deuterium (99.5%), obtained on A.E.C. allocation from the Stuart Oxygen Co., was passed over hot platinized asbestos and through liquid nitrogen traps.

Catalysts.—The catalyst for the major portion of the work was a 0.75 mm. "Ballast" Ni wire obtained from the Wilbur Driver Co., stated to be at least 99.7% pure and probably better than 99.9%. A helix of wire 2930 cm. long was wrapped around a sealed off Pyrex tube and fitted snugly inside of another Pyrex tube vessel. The geometric surface area was 730 cm.^{2}. The net volume of the reactor was 33.5 cc. The catalyst was initially activated by oxidation with 10 cm. oxygen at 500° for 15 minutes and then reduction with 30 cm. hydrogen at 330° for two hours, followed by evacuation for at least two hours at 330°; more reproducible results were obtained if the wire was subsequently reactivated merely by reduction and evacuation at 330°. The catalyst was protected at all times from stopcock grease and mercury by a CO_2 trap.

A nickel film was prepared by evaporation of wire (greater than 99.9% pure) onto Pyrex glass at 0°; it had an area of 3400 cm.^{2}. The film was protected by a CO_2 trap.

A few experiments were performed with a Ni-kieselguhr catalyst; this was the same catalyst as was used earlier,[7] and was activated in the same manner, followed by evacuation at 400° for three hours.

Apparatus and Procedure.—A Pyrex glass vacuum apparatus was used; the stopcocks were greased with Apiezon N. The catalyst chamber was heated externally by an electrical furnace and temperature was maintained constant to within one-half degree. Kinetic runs were made in the following way: a sample of *trans*-ethylene-d_2 was exposed to the catalyst for a given time, removed and analyzed for *cis*-ethylene-d_2; a small fraction (approximately 1%) was simultaneously removed for mass-spectral analysis; the remainder of the sample was frozen back into the reactor and reacted for an additional period. Usually six points were obtained in each run. The catalyst chamber was evacuated between runs. A few experiments on mixtures of *trans*-ethylene-d_2 and excess ethylene-d_4 were carried out similarly. Diffusion to the catalyst was never a factor.

The rate of reaction immediately after activation of the catalyst was very fast, as was also the rate of decrease of activity, and the catalyst was partially poisoned or seasoned, *i.e.*, exposed to ethylene-d_2 for a number of hours, usually at 75°, in order to increase reproducibility. Although the activity of the seasoned catalyst decreased further upon long exposure to ethylene, frequently the activity could be maintained constant for a sequence of three, and on some occasions six, runs.

The runs on the determination of the temperature coefficient and the order of the pressure dependence of the rate were always made in series of three; the first and the third experiments were done under the same conditions and only those runs where the activity had not changed appreciably were accepted. This arduous procedure was adopted to eliminate any uncertainty that might attend the otherwise necessary correction of the data to standard catalyst activity, and in fact provided an experimental justification for such a correction. The runs on the temperature coefficient were performed at constant concentration of ethylene in the gas phase.

Analysis.—The conversion to *cis*-ethylene-d_2 was followed by the transmission of the 842 cm.$^{-1}$ band of *cis*-ethylene-d_2 using a Beckman IR-2 spectrophotometer. A calibration curve of per cent. transmission *versus* per cent. *cis*-ethylene-d_2, at a given total pressure, was constructed. As reaction proceeded the analysis became less accurate due to the presence of other isotopic olefins. The effect of the other constituents on the *cis*-analysis was estimated by adding ethylene-d_1 and ethylene-d_0 to *cis-trans*-ethylene-d_2 in relevant amounts (ethylene-d_1 has the largest effect) and obtaining corrected calibration curves. This correction proved negligible in the early stages of the reaction. A calibration curve of *cis* and *trans*-ethylene-d_2 mixtures containing various percentages of added ethylene-d_4 was constructed and used for a few special runs.

Other ethylenic species were analyzed at 70 volts with a model 21-103 Consolidated Mass Spectrometer. The patterns of ethylene-d_0, ethylene-d_1, *cis*-ethylene-d_2, *trans*-ethylene-d_2, *asym*-ethylene-d_2 and ethylene-d_4 were determined using ethylenes available in our laboratory, and that of ethylene-d_3 from the literature.[12] Analysis for *asym*-ethylene-d_2 was made by use of the 16 peak, because the parent peak was interfered with by *cis*- and *trans*-ethylene-d_2. Analysis for *asym*-ethylene was not as accurate as that for the other ethylenes.

Results and Discussion

Possible Effect of Residual Hydrogen Left on the Catalyst from the Activation Procedure.—Experiments were done to assess the influence of residual hydrogen. After reduction with deuterium and evacuation at 330°, an amount of ethylene-d_0 corresponding to one monolayer was added to the catalyst at 100° for a period of time longer than the usual reaction time; negligible ethylene-d_1 was observed while a larger percentage of self-hydrogenation, ethane-d_0, was found, analogous to the earlier result of Douglas and Rabinovitch.[7]

The exchange of *trans*-ethylene-d_2 was also studied on a fresh Ni film on which no H can be present. Complete equilibration was observed in less than one hour at 23° with small amounts of various ethanes also occurring. A lower rate of isomerization and exchange was found at −78°.

Determination of Rate Constants and Time Reaction Order.—Rate constants for isomerization and exchange reactions were calculated from first-order expressions. The equation for isomerization was $dC_c/dt = k_i(C_2^\circ - 2C_3 - 2C_c)$, where C_n refers to an ethylene with n deuterium atoms, C_c refers to *cis*-ethylene-d_2 and C_2° refers to the initial *trans*-ethylene-d_2. This approximate equation is appropriate for small amounts of reaction.[13] For most runs, reaction was allowed to proceed to give finally only around 6–10% total of ethylene-d_1 plus ethylene-d_3 (single step exchange products), and about 8–12% *cis*-ethylene-d_2, de-

---

(10) D. O. Schissler, Ph.D. Thesis, Princeton University, 1951; T. I. Taylor and V. H. Dibeler, THIS JOURNAL, **55**, 1036 (1951).

(11) G. I. Jenkins and E. Rideal, *J. Chem. Soc.*, 2490, 2496 (1955); *cf.* Trapnell (ref. 6).

(12) V. Dibeler, F. Mohler and M. DeHemptinne, *Bull. Nat. Bur. Stds.*, **53**, 107 (1954).

(13) T. B. Flanagan, Thesis, University of Washington, 1955; for the sake of brevity in this paper, reference will sometimes be made to this thesis where the indicated information may be found.

pending upon the temperature; higher exchange products were negligible (indicating that exchange went by a stepwise process). A correction was made for the major source of error in the equation, *i.e.*, *cis*-ethylene-d_2 reaction to give exchange products.

The rate constants for exchange, k_e, were calculated from the simple approximate equation, $d(C_1 + C_3)/dt = k_e(C_2^\circ - (C_1 + C_3))$, which holds for the small percentage reaction employed.[13] Experimentally, ethylene-d_1 and ethylene-d_3 are essentially equal at all times.

Frequently, as the reaction proceeded, the first-order constants for both exchange and isomerization fell somewhat, in a parallel manner. Following a run during which the values of k fell, after evacuation the succeeding run sometimes started off at the original level of catalyst activity. Because of the fall-off present in some runs, average k values were not always satisfactory. Instead, a curve was fitted to the earlier portion of a run and a representative value of k was calculated for a given small percentage reaction where the fall-off, if any, was small. A typical run is shown in Table I. Isomerization was faster than total exchange at all temperatures (−80–100°).

TABLE I

TYPICAL RUN, #66B (75°C., 7.4 CM.)

Time (min.)	E_1 (%)	E_3 (%)	E_c (%)	$k_i \times 10^3$, min.$^{-1}$	$k_e \times 10^3$, min.$^{-1}$	α
13	2.0	1.95	5.5	4.8	3.1	2.69
21	3.1	3.0	7.8	4.4	2.9	2.43
26	3.4	3.6	9.5	4.5	2.9	2.53
31	4.1	4.2	10.7	4.4	2.8	2.49
36	4.3	4.6	11.8	4.2	2.7	2.59
42	5.6	5.2	13.1	4.2	2.6	2.62

In spite of the fall-off in the first-order rate constants observed during some runs, the isomerization and exchange reactions of *trans*-ethylene-d_2 in the absence of hydrogen are believed to be first order. The decline of the rate constants in some instances is quite probably due to some self-poisoning process, because ethylene is known to poison Ni catalysts.[4,11,14] Also, we have found good agreement between theoretical equations, based on first-order elementary reactions, and experimental results for the equilibration of ethylenes.[15]

Pressure Reaction Order.—The order of the pressure dependence, n, was determined from the slope of the plot of log rate *vs.* log pressure at constant catalyst activity. The pressure dependence was studied from 53 to 170° within certain pressure ranges. At reaction pressures lower than 3.7 cm. (75°) it became difficult to analyze for *cis*-ethylene-d_2 and only exchange products were analyzed. The results in Table II are each an average of a number of groups of runs, each group being at constant catalyst activity. The order appeared constant over each pressure range investigated and could be averaged over all groups of runs at a particular temperature since the order appeared to be independent of variation of catalyst activity (two-fold) from one group to another; obviously, correction of the data to a standard catalyst activity would give identical results.

TABLE II

ORDER OF THE PRESSURE DEPENDENCE OF ISOMERIZATION AND EXCHANGE REACTION

Temp. (°C.)	Isomerization "n"	Exchange "n"	Pressure variation (mm.)
53	0.3[a]	0.3[a]	17–68
104	0.4[a]	0.4[a]	20–160
129	0.68	0.57	21–86
152	0.75	0.84	22–90
172	1.0	1.0	24–94

[a] Irreproducibility and experimental error were greatest at low temperatures and the cited value, an average of a limited number of measurements, may contain considerable error.

Within experimental error the pressure dependence order for isomerization is equal to that for exchange at a given temperature; both rise with increase of temperature.

Activation Energies.—Representative k values for isomerization and exchange were evaluated at 7.5% isomerization and 3% ethylene-d_3; if k values calculated at other percentages of reaction than these were used, essentially the same activation energies were obtained.[13] The determination of the activation energies was made in small groups of runs (see Procedure) where each group was at constant catalyst activity. To represent all the data on one Arrhenius plot, the data were corrected to standard catalyst activity. The standard activity toward isomerization was chosen as 7.5% isomerization in 22 minutes for 7.4 cm. of *trans*-ethylene-d_2 at 75°, and that toward exchange was 3% ethylene-d_3 for the same time under the same conditions.

The observed activation energy for isomerization is 13.5 kcal. from 35 to 105°; it then drops continuously, reaching ~6.7 kcal. for the interval 170 to 195°. The observed activation energy for exchange is 15.0 kcal. from 35 to 105; it also decreases reaching ~6.7 kcal. for the interval 170 to 195° (Fig. 1). The average difference, $\Delta E = E_e - E_i$, is 1.5 kcal. for 35–105°, and is also small, but less accurately known, above 105°. These results refer to k values corrected to standard activity at a constant concentration of 2.1×10^{18} molec. cc.$^{-1}$; E values calculated from each group of runs, for which the catalyst activity was constant within a group but differed between groups, were concordant.[13] Correction of the data to a constant catalyst activity thus appears to be a valid procedure here also.

The ratio of *cis*-ethylene-d_2 to ethylene-d_3, at a given percentage reaction, depends only upon the temperature and not on catalyst activity (Table III). In the extreme, results on nickel films, Ni-kieselguhr and a Pd catalyst bear this out, *i.e.*, the ratio of isomerization to exchange at a given percentage reaction was independent of the catalyst.

---

(14) J. R. Anderson and C. Kemball, *Proc. Roy. Soc.* (*London*), **223A**, 361 (1954). Beeck (ref. 4) has found C_4 to C_8 and higher polymers upon hydrogenation of a preadsorbed ethylene layer on a Ni film; we have foud ethane and a very small amount of butene upon addition of what corresponds to a monolayer of ethylene to the Ni wire.

(15) T. B. Flanagan and B. S. Rabinovitch, THIS JOURNAL, **60**, 730 (1956).

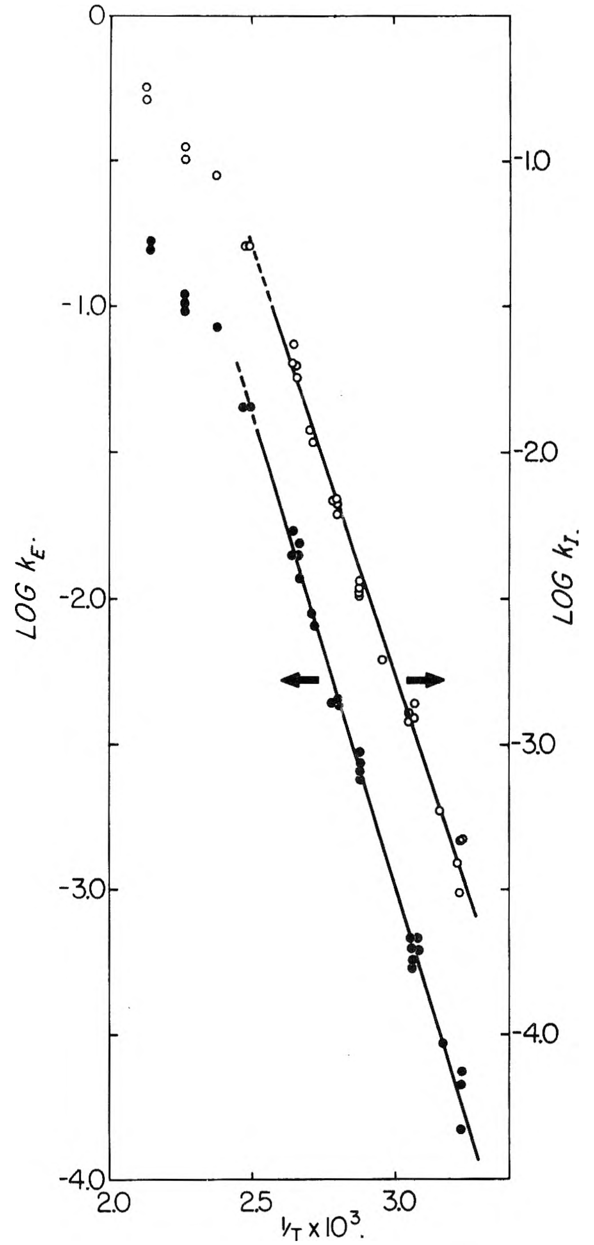

Fig. 1.—Activation energies for the isomerization and exchange of *trans*-ethylene-d_2.

Since the ratio of isomerization to exchange was independent of catalyst activity, ΔE could be calculated directly from all groups of runs by the Arrhenius plot of the ratio of early rates of isomerization and exchange (Fig. 2). ΔE by this method for the region below 105° is 1.1 kcal., in good agreement with the difference between E_e and E_i calculated from the standard activity plot (Fig. 1).

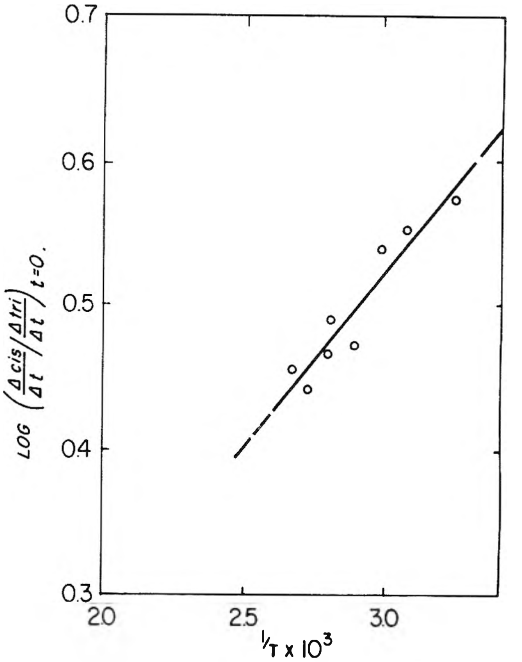

Fig. 2.—ΔE from early rate ratio of isomerization and exchange.

TABLE III

RATIO OF ISOMERIZATION TO EXCHANGE AT VARIOUS TEMPERATURES AND PRESSURES. SOME TYPICAL RESULTS

Temp. (°C.)	Relative cat. activ.	Press. (mm.)	E_c/E_i (at 2% E_3)
54	11.1	6.9	3.30
54	2.2	6.9	3.15
54	0.31	6.9	3.42
54	0.27	3.4	3.40
54	0.27	6.9	3.50
54	0.27	13.8	3.40
75	1.1	7.4	2.80
75	0.81	7.4	2.69
75	0.44	7.4	2.75

In the temperature range 35–105°, the temperature independent factor, *A*, for runs on the seasoned catalyst brought to standard activity is 1.1 × 10^2 sec.$^{-1}$ cm.$^{-2}$ and 16.0 sec.$^{-1}$ cm.$^{-2}$ for total exchange and isomerization, respectively.

Mechanism of the Isomerization and Exchange Reactions.—Since both isomerization and exchange reactions have the same kinetics, *i.e.*, time order, pressure order, similar magnitudes of activation energies (the small difference is discussed later), and variation of these quantities with temperature, no special mechanism can apply for isomerization. It is concluded that both reactions occur by the same mechanism. It is desirable at this point in the presentation of the results to show that the reactions may be assumed to proceed *via* an adsorbed ethyl radical.

By reason of the experimentally observed ratio of isomerization to exchange the following mechanisms cannot, of themselves, account for the results: the Farkas mechanism[3]

$$C_2H_4 \rightleftarrows H_2C{=}\underset{*}{C}H + \underset{*}{H}$$

the Beeck mechanism[4]

$$C_2H_4 \rightleftarrows \underset{*}{H}C{=}\underset{*}{C}H + 2\underset{*}{H}$$

a radical dissociative mechanism

$$C_2H_4 \rightleftarrows \underset{*}{H}\dot{\underset{*}{C}}\text{-}CH_2 + \underset{*}{H}$$

involving a radical postulated as an intermediate in acetylenic hydrogenation[16]; also a disproportiona-

---

(16) J. Sheridan, *J. Chem. Soc.*, 133 (1945).

tion reaction among associatively adsorbed species like, $2H_2\underset{*}{C}{-}\underset{*}{C}H_2 \rightleftarrows \underset{*}{C}_2H_5 + H\underset{*}{C}{=}CH_2$.

On the other hand several mechanisms which proceed with opening of the double bond *via* an adsorbed ethyl radical are consistent with the results. These are the "associative" mechanism (A)[17,18] proceeding through an adsorbed ethyl radical or half-hydrogenated state (h.h.s.)

$$H_2\underset{*}{C}{-}\underset{*}{C}H_2 + \underset{*}{H} \underset{A_r}{\overset{A_f}{\rightleftarrows}} \underset{*}{C_2H_5}$$

and a Rideal mechanism (R)

$$C_2H_4 + \underset{*}{H} \underset{R_r}{\overset{R_f}{\rightleftarrows}} \underset{*}{C_2H_5}$$

for which there has recently been proposed further strong support.[11,19]

In the absence of gas phase hydrogen or deuterium, the H or D pool necessary for these mechanisms must arise from dissociative adsorption. A small amount of $\underset{*}{H}$ or $\underset{*}{D}$ formed by dissociative adsorption can catalyze the entire reaction sequence; removal of H by any process signifies poisoning of the surface and decline in rate.

C–H/C–D Bond Rupture Probabilities in the Half-hydrogenated States.—The ratio of the C–H to C–D bond rupture probabilities, α, for each h.h.s. which arises by addition of an H or D atom to *trans*-ethylene-d_2, $HD\underset{*}{C}{-}CH_2D$ (I) and $HD\underset{*}{C}{-}CHD_2$ (II), is determinable by use of the equations for C_c and C_3 concentrations as a function of time, developed in the following paper,[15] namely

$$C_c = -50e^{-\beta t(\alpha + 1/\alpha + 1)} + 12.5 + 25e^{-\beta t} + 12.5e^{-2\beta t}$$
$$\text{and } C_3 = 25 - 25e^{-2\beta t}$$

from the product analysis at any time. As shown below, α is the same for I and II.

Values of α in a given run are independent of percentage reaction (Table I). The experimental values in Table IV are the average of several runs; for each run, three or more determinations of α were made at different times. An Arrhenius plot for α shows straight line behavior below 160° and the slope gives $E_\alpha = 1.5$ kcal. (Fig. 3).

A frequently used, simple model of the isotope effect for the intramolecular decomposition of h.h.s. I and II may be formulated using equations of Bigeleisen.[20] For h.h.s. I, the reactions are

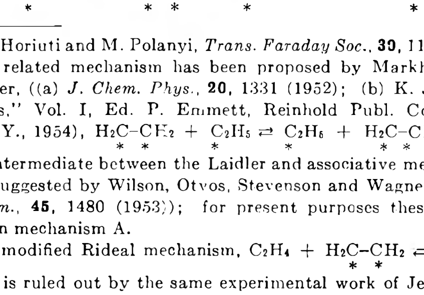

$$\begin{array}{l} D\overset{H}{C}H \xrightarrow{k} D\underset{*}{\overset{H}{C}}{-}\underset{*}{\overset{H}{C}}H + \underset{*}{D} \text{ or } C_2H_3D + \underset{*}{D} \\ \;\;\big| \\ H\underset{*}{C}D \xrightarrow{k'} D\underset{*}{\overset{H}{C}}{-}\underset{*}{\overset{H}{C}}D + \underset{*}{H} \text{ or } C_2H_2D_2 + \underset{*}{D} \end{array}$$

and

$$\alpha = k'/k = \left(\frac{m^*}{m'^*}\right)^{1/2} \frac{u^*_{C-H}\, e^{-u^*_{C-H}/2}\left(1 - e^{-u^*_{C-D}}\right)}{u^*_{C-D}\, e^{-u^*_{C-D}/2}\left(1 - e^{-u^*_{C-H}}\right)}$$

where it is assumed that the transmission coefficients and symmetry numbers cancel, that the force constant of the breaking bond is zero, that the rest of the bonds in the activated complexes are identical, except for an extra C–H bond when a C–D bond breaks and an extra C–D bond when the C–H bond breaks and where only the bond stretching frequencies have been retained. This equation also applies for the isotope effect in the reactions of half-hydrogenated state II, and hence α has the same value for I and II. At low temperatures, E_α should equal ΔE^0, the zero point energy difference for C–H and C–D, 1.14 kcal. Calculated values from the equation are high compared to the experimental values which approach the limiting value 1.36 at 400°. Complication of the model to obtain concordance with the data is not worth while here. Gas phase studies of ethyl radical decomposition are in progress.

Resolution of Total Isomerization into Component Reactions.—The total isomerization at any temperature may be resolved into the contributions from half-hydrogenated states I and II. In the early reaction, ethylene-d_1 arises from I and ethylene-d_3 arises from II. From I, the rates of ethylene-d_1 and *cis*-ethylene-d_2 production are

$$\frac{dC_1}{dt} = k_t(C{-}D)_1(I) = k_t\frac{(I)}{2\alpha + 1}$$
$$\frac{dC_c}{dt} = \frac{k_t}{2}(C{-}H)_1(I) = \frac{k_t\,\alpha(I)}{2\alpha + 1} \quad (1)$$

where k_t is the total specific rate of decomposition of I and $(C{-}H)_1$ and $(C{-}H)_2$ are the fractional probabilities of C–H rupture in I and II, respectively; $(C{-}D)_1$ and $(C{-}D)_2$ are the corresponding quantities for C–D rupture, and the $^1/_2$ factor takes account of re-formation of *trans*-ethylene-d_2. From II

$$\frac{dC_3}{dt} = k_t'(C{-}H)_2(II) = k_t'(\alpha/(2 + \alpha))(II)$$
$$\frac{dC_c}{dt} = \frac{k_t'}{2}(C{-}D)_2(II) = \frac{k_t'(II)}{2 + \alpha} \quad (2)$$

where k_t' is the specific rate of decomposition of II.

From these equations and the relation between k_t and k_t', namely $k_t' = (\alpha + 2)/(2\alpha + 1)k_t$, it is readily shown that the ratio of the concentrations of I and II is α at any temperature; also the isomerization produced from I relative to that from II is α^2. Table IV summarizes the calculations.

Isomerization and Exchange Experiments with Excess Ethylene-d_4.—At small times the normal ratio of $C_c/(C_1 + C_3)$ at any temperature is, from equations 1 and 2, $(\alpha^2 + 1)/2\alpha$—(3); if only I or II were present the ratio would be α or $1/\alpha$, respectively. If the ratio of I/II were changed relative to the normal value, the ratio of isomerization to exchange would shift in the direction indicated. Gaseous H_2 or D_2 was used to alter the normal ratio of I/II. Such experiments gave qualitative agreement with the expected shifts in products, but the experiments were complicated by hydrogenation.

A source of excess $\underset{*}{H}$ or $\underset{*}{D}$ atoms was obtained by

---

(17) J. Horiuti and M. Polanyi, *Trans. Faraday Soc.*, **30**, 1164 (1934).

(18) A related mechanism has been proposed by Markham, Wall and Laidler, ((a) *J. Chem. Phys.*, **20**, 1331 (1952); (b) K. J. Laidler, "Catalysis," Vol. I, Ed. P. Emmett, Reinhold Publ. Corp., New York, N. Y., 1954), $H_2\underset{*}{C}{-}\underset{*}{C}H_2 + \underset{*}{C}_2H_5 \rightleftarrows \underset{*}{C}_2H_6 + H_2\underset{*}{C}{-}\underset{*}{C}H_2$, and a variant, intermediate between the Laidler and associative mechanisms, has been suggested by Wilson, Otvos, Stevenson and Wagner ((c) *Ind. Eng. Chem.*, **45**, 1480 (1953)); for present purposes these may be included in mechanism A.

(19) A modified Rideal mechanism, $C_2H_4 + H_2\underset{*}{C}{-}\underset{*}{C}H_2 \rightleftarrows \underset{*}{C}_2H_6 + H\dot{\underset{*}{C}}{-}\underset{*}{C}H_2$, is ruled out by the same experimental work of Jenkins and Rideal[11] which supports a Rideal type mechanism.

(20) J. Bigeleisen, *J. Chem. Phys.*, **17**, 675 (1949).

addition of ethylene-d_0 or ethylene-d_4. This method was free from the complication of hydrogenation. For swamping concentrations of ethylene-d_4 or ethylene-d_0 with *trans*-ethylene-d_2, only II or I arises. The effect on the products is more dramatic for the case of only II present; *e.g.*, at 90° where $\alpha = 2.4$, $1/\alpha = C_c/C_3$ should be 0.42, compared to the normal ratio 1.42.

In two experiments at 90°, 3.8 cm. of *trans*-ethylene-d_2 and 12.9 cm. of ethylene-d_4 gave (after correction for ethylene-d_3 which arose from ethylene-d_4) an average ratio, $C_c/(C_1 + C_3)$, of 0.60, *i.e.*, approaching the limiting value 0.42. The expected ratio, $C_c/(C_1 + C_3)$, may be calculated: for the ethylene-d_4-*trans*-ethylene-d_2 ratio of 3.4:1 used, assuming the ethylenes are adsorbed in the ratio of their pressures, (I)/(II) is 0.3. The general expression for the ratio, isomerization/exchange, is[13] $(\alpha(\text{I/II}) + 1)/(\text{I/II}) + \alpha)$, which reduces to equation 3 for I/II $= \alpha$ (pure *trans*-ethylene-d_2); for I/II $= 0.3$, isomerization/exchange $= 0.67$ which agrees with the experimental value.

Composition of Observed Activation Energies for Isomerization.—The fact that the ratio I/II varies with temperature should be considered.

Table IV shows that 92.4% isomerization takes place *via* I at 35°. At this temperature, therefore, $\Delta E = E_e - E_i$ should be almost equal to E_α (1.5 kcal.). In general, the value of ΔE at any temperature is[13]

$$\Delta E = \alpha^2/(1 + \alpha^2)E_\alpha - 1/(1 + \alpha^2)E_\alpha = \frac{\alpha^2 - 1}{\alpha^2 + 1}E_\alpha$$

from which $\Delta E = 1.2$ kcal. at 35°, dropping to 0.8 kcal. at 170°. The experimental accuracy was not sufficient to reproduce the fall in ΔE (see earlier Results).

TABLE IV

TEMPERATURE DEPENDENCE OF C-H/C-D RUPTURE RATIO, α, AND RELATED QUANTITIES

Temp. (°C.)	α	Fraction of I = I/(I + II)	Fraction of isomerization from I
−78	15.9	0.94	0.996
−25.5	6.5	.87	.98
0.0	4.9	.83	.96
34.6	3.3	.77	.92
43.0	2.9	.74	.89
53.0	2.8	.74	.89
74.0	2.7	.73	.88
84.0	2.6	.72	.87
104.0	2.4	.71	.85
148.0	1.95	.66	.79
168.0	1.80	.64	.77
195.0	1.77	.64	.76
315.0	1.64	.62	.73
429.0	1.40	.58	.66

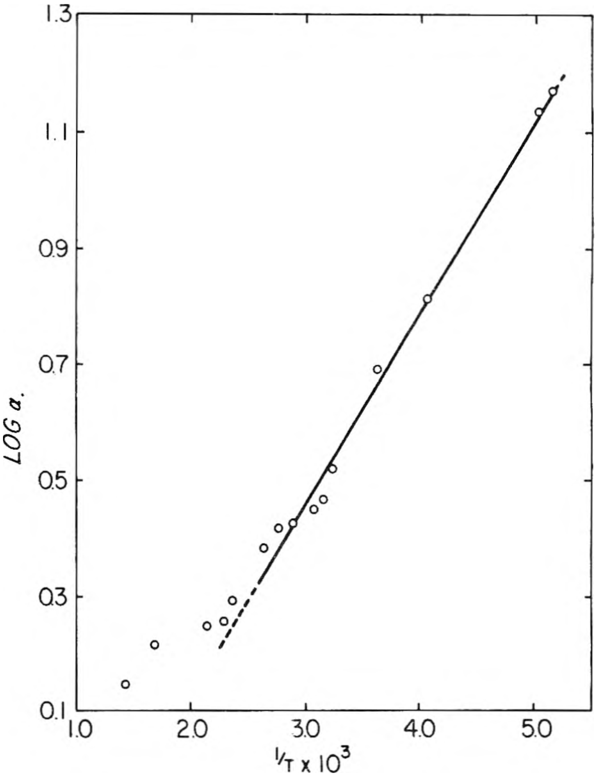

Fig. 3.—Temperature dependence of α.

Conclusions.—For reasonable values of a number of parameters, both the Rideal and associative mechanisms appear to fit the experimental results (pressure order and its variation with temperature, decrease of activation energy with temperature, stepwise nature of the exchange, and the rate of reaction), as shown by absolute rate theory calculations with these mechanisms.[21] The details are not presented; we are unable to distinguish the validity of these mechanisms, and the possibility exists that some or all of the observed temperature variation of parameters may have its origin in a type of experimental artifact, such as changing H atom concentration on the surface due to shift with temperature of the "poisoning" reactions.[11,14] It may be noted that agreement of calculated rates with experiment (calculated for 27°) requires values of θ', H coverage, and θ'', h.h.s. coverage of $\sim 10^{-6}$; there is evidence that these are reasonable magnitudes.[13]

Acknowledgments.—We thank Dr. J. H. Singleton for his kind assistance in the nickel film experiments and for the use of his apparatus; also Professor A. L. Crittenden and Mr. B. J. Nist for some of the mass-spectral analyses and the ONR for their support.

---

(21) Some of the calculations are given in ref. 13.

EXCHANGE AND ISOMERIZATION OF DEUTEROETHYLENES ON NICKEL EQUILIBRATION[1]

BY TED B. FLANAGAN AND B. S. RABINOVITCH

Contribution from the Department of Chemistry of the University of Washington, Seattle, Washington

Received May 23, 1956

The time course of the equilibration of *trans*-ethylene-d_2 and of mixtures of ethylene-d_0 and ethylene-d_4 on nickel wire has been studied. Equations are derived which fit the experimental results. The departure of the equilibrium distribution of products from statistical is examined.

In the preceding paper,[2] the kinetics of the exchange and isomerization of *trans*-ethylene-d_2 on nickel wire were examined in the early stages of reaction, limited essentially to a single exchange step. In the present work, the time course of the equilibration reactions of *trans*-ethylene-d_2 and of mixtures of ethylene-d_0 and ethylene-d_4 is presented.

Experimental

The materials, catalyst and apparatus were the same as previously described.[2] The analytical procedure was also similar except that equilibrated ethylenes were analyzed at low ionizing voltage (11.0 volt) where no breakdown occurred. The sensitivities of the peaks of the isotopic ethylenes were corrected for effusion and other effects by calibration with known *trans*-ethylene-d_2–ethylene-d_0 mixtures.

The experimental procedures for *trans*-ethylene-d_2, and mixtures of ethylene-d_0 with ethylene-d_4, were identical. 7.6 cm. of *trans*-ethylene-d_2, or 3.8 cm. of ethylene-d_0 plus 3.8 cm. of ethylene-d_4, were introduced into the catalyst chamber for a given time interval; the entire sample was then removed for analysis. The sample was transferred to the infrared spectrophotometer for *cis*-ethylene-d_2 analysis and a small fraction was removed for mass-spectral analysis. The rest of the sample was returned to the reactor for a further period of reaction.

Results and Discussion

Figure 1 represents the equilibration of *trans*-ethylene-d_2 at 75° on the nickel wire catalyst. Ethanes or polymers were never observed. The percentages of ethylene-d_1 and ethylene-d_3 were nearly equal throughout, as were ethylene-d_0 and ethylene-d_4. *asym*-Ethylene-d_2, ethylene-d_4 and ethylene-d_0 were formed in significant amounts only after considerable quantities of ethylene-d_1 and ethylene-d_3 were present. Only *cis*-ethylene-d_2 passed through a maximum. Since the catalyst activity decreased progressively with continued exposure to the ethylenes and time could not be used as the abscissa, the percentages of the various ethylenes have been plotted *versus* βt, where β is defined below.

Figure 2 represents the equilibration of ethylene-d_0 and ethylene-d_4 on the Ni wire. Ethylene-d_1 and ethylene-d_0 are omitted for simplicity since they are nearly equal to ethylene-d_3 and ethylene-d_4, respectively. No species pass through a maximum.

Derivation of Equations Describing Equilibration Reactions.—Based either on the Rideal or associative mechanisms,[2] equations may be derived which describe the time course of the reactions. The following scheme is applicable

$$\begin{tikzcd}
C_0 \arrow[r, shift left] & C_1 \arrow[l, shift left] \arrow[r, shift left] \arrow[d, shift left] & C_2 \arrow[l, shift left] \arrow[d, shift left] \\
C_a \arrow[r, shift left] & C_3 \arrow[l, shift left] \arrow[r, shift left] \arrow[u, shift left] & C_4 \arrow[l, shift left] \\
\end{tikzcd}$$

where C_i represents ethylene-d_i, subscript "a" stands for *asymmetric*, and C_2 represents all ethylene-d_2 except C_a. The following simplifications obtain: (1) exchange is stepwise; (2) the rates of addition of H or D to ethylene are not influenced by the isotopic composition of the *non-reacting* end. Then

$$\frac{dC_0}{dt} = k_H(\text{C–D})_1(\text{H})(C_1) - 2k_D(\text{C–H})_1(\text{D})(C_0)$$

$$\frac{dC_1}{dt} = 2k_H(\text{C–D})_1(\text{H})(C_2) + k'_H(\text{C–D})_2(\text{H})(C_a) + 2k_D(\text{C–H})_1(\text{D})(C_0) - [k_D(\text{C–H})_1(\text{D}) + k_H(\text{C–D})_1(\text{H}) + k_D'(\text{C–H})_2(\text{D})](C_1)$$

$$\frac{dC_2}{dt} = k_D(\text{C–H})_1(\text{D})(C_1) + k_H'(\text{C–D})_2(\text{H})(C_3) - [2k_H(\text{C–D})_1(\text{H}) + 2k_D'(\text{C–H})_2(\text{D})](C_2)$$

$$\frac{dC_a}{dt} = k_D'(\text{C–H})_2(\text{D})(C_1) + k_H(\text{C–D})_1(\text{H})(C_3) - [k_H'(\text{C–D})_2(\text{H}) + k_D(\text{C–H})_1(\text{D})](C_a)$$

with similar equations for dC_3/dt and dC_4/dt, and where k_H and k_D are the specific rates of addition of $\underset{*}{\text{H}}$ or $\underset{*}{\text{D}}$ to one end of an appropriate ethylene molecule to give $\text{H}\overset{\text{H}}{\underset{|}{\text{C}}}\text{D}$, and k_H' and k_D' are the corresponding specific rates for formation of $\text{D}\overset{\text{D}}{\underset{|}{\text{C}}}\text{H}$; $(\text{C–D})_1$ and $(\text{C–D})_2$ are the normalized C–D bond rupture probabilities in $\text{H}\overset{\text{D}}{\underset{|}{\text{C}}}\text{H}$ and $\text{D}\overset{\text{D}}{\underset{|}{\text{C}}}\text{H}$, respectively, and $(\text{C–H})_1$ and $(\text{C–H})_2$ are the corresponding C–H bond rupture probabilities. Now the "hydrogen isotope pool" composition is constant with time,[3] and the above equations are effectively first order.

Because of the near equality of C_1 and C_3, and C_0 and C_4 at all times, the rates of formation of C_1 and C_3 and of C_0 and C_4 are equated, and C_4 and C_3 are replaced by C_0 and C_1.[4] Then $k_H(\text{C–D})_1(\text{H}) = k_D'\cdot$

---

[1] Abstracted from part of a thesis submitted by T. B. Flanagan to the Graduate School in partial fulfillment of the requirements for the degree of Doctor of Philosophy at the University of Washington. Work supported by the Office of Naval Research.

[2] T. B. Flanagan and B. S. Rabinovitch, THIS JOURNAL, **60**, 724 (1956).

[3] This may readily be shown by solving the *a* and *b* relations below, *i.e.*

$$\frac{\text{H}}{\text{D}} = \frac{k_D'(\text{C–H})_2}{k_H(\text{C–H})_1} = \frac{k_D(\text{C–D})_1}{k_H'(\text{C–D})_2}$$

[4] Because of the different thermodynamic stabilities of the isotopic ethylenes this assumption is not strictly true; any other assumption would enormously complicate the equations. In the initial stages of reaction, because the amount of material on the surface is negligible, the amounts and rates of formation of ethylene-d_1 and ethylene-d_3 are identical. Throughout the course of the reaction, the requirement of H and D mass balance which is imposed on the system ensures that the amounts and rates of formation C_1 and C_2, and C_0 and C_4 are very nearly identical (Fig. 1).

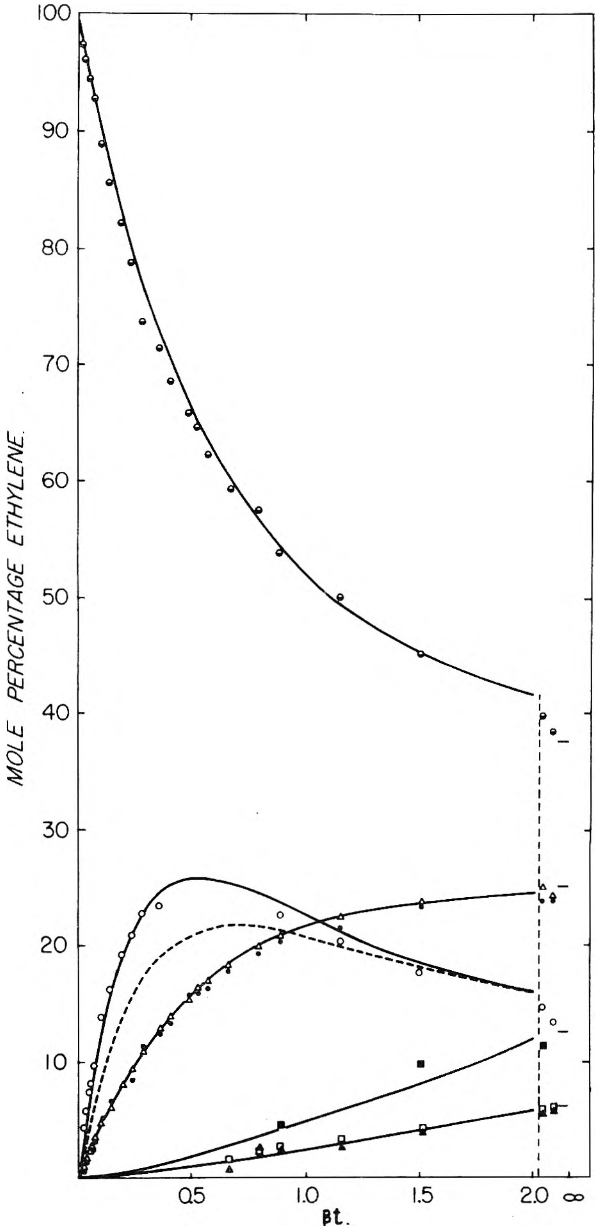

Fig. 1.—Equilibration of *trans*-ethylene-d_2 at 7.4 cm. Hg and 75°. The solid lines represent calculated percentages: ◒, total $C_2D_2H_2$; ○, *cis*-$C_2D_2H_2$; △, C_2D_3H; ●, C_2H_3D; ■, *asym.*-$C_2D_2H_2$; ▲, C_2H_4; □, C_2D_4.

$(C–H)_2(D) = a$ and $k_D(C–H)_1(D) = k_H'(C–D)_2(H) = b$. It was shown[2] that in any half-hydrogenated state, for each C–H and C–D bond

$$\alpha = \frac{\text{prob. of C–H rupture}}{\text{prob. of C–D rupture}} = \frac{(C–H)_1}{2(C–D)_1} = \frac{2(C–H)_2}{(C–D)_2}$$

Re-define $(C–H)_1 = \dfrac{2\alpha}{1+2\alpha}$, $(C–D)_1 = 1/(1 + 2\alpha)$, $(C–H_2) = \alpha/(2 + \alpha)$ and $(C–D)_2 = 2/(2 + \alpha)$. Upon substitution of a and b into the differential equations

$$\frac{dC_1}{dt} = 2a(C_2) + 2b(C_0) + b(C_a) - (2a + b)(C_1)$$

$$\frac{dC_2}{dt} = 2b(C_1) - 4a(C_2)$$

$$\frac{dC_0}{dt} = a(C_1) - 2b(C_0);\quad \frac{dC_a}{dt} = 2a(C_1) - 2b(C_a)$$

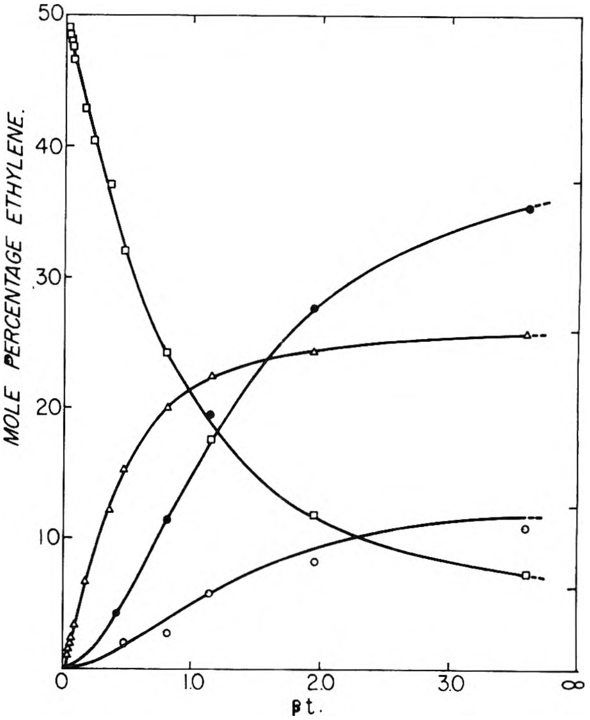

Fig. 2.—Equilibration of 3.8 cm. of ethylene-d_0 and 3.8 cm. of ethylene-d_4 at 153°. The solid lines represent calculated percentages: □, C_2D_4; △, C_2D_3H; ●, total $C_2D_2H_2$; ○, *cis*-$C_2D_2H_2$.

This set of equations may be solved by the method of Matsen and Franklin.[5] The final solutions are

$$\begin{aligned} C_1 &= 25 - 25e^{-2\beta t} \\ C_2 &= 25 + 50e^{-\beta t} + 25e^{-2\beta t} \\ C_0 &= 6.25 - 12.5e^{-\beta t} + 6.25e^{-2\beta t} \\ C_a &= 12.5 - 25e^{-\beta t} + 12.5e^{-2\beta t} \end{aligned} \qquad (1)$$

where $\beta = k_H(H)\,4/(1 - 2a) = 2a + b$. The rate of formation of *cis*-ethylene-d_2, C_c, is

$$\begin{aligned} \frac{dC_c}{dt} = {} & k_H(C–H)_1(H)(C_2 - C_c) + \\ & k_D'(C–D)_2(D)(C_2 - C_c) - 2k_H(C–D)_1(H)(C_c) - \\ & 2k_D'(C–H)_2(D)(C_c) - k_H(C–H)_1(H)(C_c) - \\ & k_D'(C–D)_2(D)(C_c) + \frac{k_D}{2}(C–H)_1(D)(C_1) + \\ & \frac{k_H'}{2}(C–D)_2(H)(C_3) \end{aligned}$$

The probability of *cis*-ethylene-d_2 formation from the half-hydrogenated states $HDC–\underset{*}{C}H_2D$ and $HDC–\underset{*}{C}HD_2$, on removal of H or D, respectively, is equal to that of *trans*-ethylene-d_2.[6] Using the relations

$$k_H(H)(C–H)_1 = \frac{b(H)k_H}{(D)k_D}$$

and

$$k_D'(D)(C–D)_2 = b\,\frac{(D)k_D'}{(H)k_H'}$$

there is obtained

$$\frac{dC_c}{dt} = b(x)(C_2) - 2b(x)(C_c) - 4a(C_c) + b(C_1)$$

---

(5) F. A. Matsen and J. L. Franklin, *J. Am. Chem. Soc.*, **72**, 3334 (1950).

(6) J. E. Douglas, B. S. Rabinovitch and F. S. Looney, *J. Chem. Phys.*, **23**, 315 (1955).

where

$$x = \frac{k_H(H)}{k_D(D)} + \frac{k_D'(D)}{k_H'(H)} = \alpha + \frac{1}{\alpha}$$

since it may be shown that $\alpha = k_H(H)/k_D(D)$ and $k_H' = [(2 + \alpha)/(2\alpha + 1)]k_H$, $k_D' = [(2 + \alpha)/(2\alpha + 1)]k_D$. Substituting the values of C_1 and C_2 and solving

$$C_c = -50e^{-\beta(\alpha + 1/\alpha + 1)t} + 12.5 + 25e^{-\beta t} + 12.5e^{-2\beta t}$$

α may be evaluated by measurement of *cis*-ethylene-d_2 at time, t.

The same ethylenic inter-reactions occur for the case of ethylene-d_0 and ethylene-d_4. The solutions of the appropriate equations are

$$C_1 = 25 - 25e^{-2\beta t};\quad C_2 = 2C_c = 25 - 50e^{-\beta t} + 25e^{-2\beta t}$$
$$C_0 = 6.25 + 37.5e^{-\beta t} + 6.25e^{-2\beta t}$$
$$C_a = 12.5 - 25e^{-\beta t} + 12.5e^{-2\beta t} \qquad (2)$$

TABLE I

EQUILIBRIUM CONSTANTS (200°) FOR ETHYLENE INTERREACTIONS

	Classical	Quantum	Experimental
K_a	2.67	2.47	2.50
K_b	2.25	2.25	2.24
K_c	2.67	2.65	2.62

For *trans*-ethylene-d_2, excellent agreement is obtained between experimental and calculated results from equations 1 for all species, except *cis*-ethylene-d_2 in the later stages of reaction where the analytical corrections due to the presence of other isotopic ethylenes apparently become less accurate (Fig. 1). A value of $\alpha = 2.7$[2] was used for the entire reaction (only *cis*-ethylene-d_2 formation depends upon α). If the C–H rupture probability were assumed to equal that of C–D the same calculated curves result for all species, except for *cis*-ethylene-d_2 which would then be represented by the dotted line. Similar agreement is obtained between equations 2 and the experimental results (Fig. 2).

Equilibrium Constants.—The experimental equilibrium percentages of products from *trans*-ethylene-d_2 at 200° were C_0 = 6.4 (6.25), C_1 = 24.5 (25.0), $C_2 + C_a$ = 37.4 (37.5), C_3 = 25.5 (25.0), C_4 = 6.5 (6.25); numbers in brackets are statistical percentages calculated from random shuffling of H and D atoms. The results show that the assumption[4] used in equations 2 and 3 is justified within experimental error. These values are not sufficiently accurate to determine precise equilibrium constants for the reactions

$$C_2H_4 + C_2D_2H_2 = 2C_2H_3D \qquad (a)$$
$$C_2H_3D + C_2D_3H = 2C_2H_2D_2 \qquad (b)$$
$$C_2H_2D_2 + C_2D_4 = 2C_2HD_3 \qquad (c)$$

The experimental equilibrium constants together with classical and quantum mechanical constants are shown in Table I. The quantum mechanical constants have been calculated using frequencies tabulated by Crawford, Lancaster and Inskeep[7] and, in the calculations of ΔE^0, the anharmonicity correction for the C–H and C–D stretches as given by Arnett and Crawford.[8] Small changes in the observed equilibrium percentages of the ethylenes result in large changes in the equilibrium constants. Kemball[9] also found with methane that the experimental measurements do not give accurate values for the equilibrium constants.

---

[7] B. L. Crawford, J. E. Lancaster and R. G. Inskeep, *J. Chem Phys.*, **21**, 678 (1953).

[8] R. L. Arnett and B. L. Crawford, *ibid.*, **18**, 118 (1950).

[9] C. Kemball, *Proc. Roy. Soc.* (*London*), **207A**, 539 (1951).

XII. AN INVESTIGATION OF METAL-AMMONIA SYSTEMS BY MEANS OF THEIR VAPOR PRESSURES

BY PHILIP R. MARSHALL AND HERSCHEL HUNT

A Contribution from the Department of Chemistry, Purdue University, Lafayette, Indiana

Received July 11, 1955

The vapor pressures of calcium–, strontium–, barium–, lithium– and sodium–ammonia systems have been determined as a function of concentration and temperature. The compounds of calcium, strontium and barium in equilibrium with the metal were shown to contain non-integral values of the ammonia to metal ratios. These values are 5.67, 4.89 and 7.49, respectively, at −63.8°. The activities of the ammonia and the relative activity coefficients of the metals have been calculated for the lithium and sodium solutions and compared to each other and to the corresponding values for potassium and cesium solutions calculated from literature data. In addition, the relative lowering of the fugacity was determined for each of the alkali metal solutions and compared to each other and to the ideal curves for 1–1 electrolytes and non-electrolytes. The results were interpreted as being inconsistent with the uni-univalent electrolytic hypothesis generally given for more dilute solutions.

Introduction

The nature of the solute and the character of the solid separating from metallic solutions in liquid ammonia have not been established to everyone's satisfaction. There is general agreement that the alkaline earth metals form compounds with the formula $M(NH_3)_6$ but the existence of alkali metal compounds is disputed.

A region of two liquid phases has been reported for sodium[1] and lithium[2] solutions. Kraus has presented a vapor *vs.* concentration curve for calcium which showed a similar two liquid phase region along with plateaus for the saturated solution and compound.[3] However, the curves for the vapor pressures of the alkaline earth metals as

---

[1] C. A. Kraus and W. W. Lucasse, *J. Am. Chem. Soc.*, **44**, 1941 (1922).

[2] O. Ruff and J. Zedner, *Ber.*, **41**, 1948 (1908).

[3] C. A. Kraus, *J. Am. Chem. Soc.*, **30**, 653 (1908).

determined by Biltz and Huttig[4] do not show even one plateau.[4]

The determinations of the relative activities of lithium and potassium solutions as determined by Johnson and Meyer[5] were limited by the fact that the vapor pressures had been determined only in concentrated solutions.

Accordingly, we proposed to determine vapor pressure *vs.* concentration curves for calcium, strontium and barium solutions in order to learn more about the two liquid phase and compound formation in these systems. In addition, the determination of the vapor pressures of more dilute alkali metal solutions will further the knowledge of relative activities in these unique solutions.

Experimental Procedure

The equilibrium pressures of the metal–ammonia systems were determined in a vacuum line consisting of a reaction tube, ammonia gas measuring bulb, calibrated standard bulb (each with a mercury manometer) and a liquid ammonia reservoir bulb. A McLeod gage in the system indicated that a vacuum of better than 10^{-6} mm. of mercury could be attained.

Ammonia was distilled from a sodium solution in a small steel cylinder to the line storage bulb which also contained sodium. It was distilled from this to the gas measuring bulb and then transferred to the reaction tube through sintered glass mercury valves.

TABLE I

THE VAPOR PRESSURES OF METAL–AMMONIA SYSTEMS AT −63.8°[a] AS A FUNCTION OF CONCENTRATION

Series	$\frac{\text{Moles NH}_3}{\text{Moles Ca}}$	p, cm.	Series	$\frac{\text{Moles NH}_3}{\text{mole Ca}}$	p, cm.
		A. Calcium–Ammonia			
A	27.6	12.755	A	8.79	8.890
A	25.0	12.700	A	7.86	8.815
A	22.9	12.540	A	6.62	7.440
A	18.9	12.115	A	6.26	2.015
A	18.0	11.945	A	5.91	0.325
A	16.6	11.600	A	5.82	.200
A	15.3	11.270	A	5.73	.075
A	14.4	10.845			
A	13.2	10.605			
A	12.1	10.450			
A	11.2	9.630	A	2.78	0.045
A	10.03	9.165			
		B. Strontium–Ammonia			
	$\frac{\text{Moles NH}_3}{\text{moles Sr}}$			$\frac{\text{Moles NH}_3}{\text{mole Sr}}$	
A	52.7	12.165	C	5.23	0.935
A	46.5	12.045	A	5.07	.190
A	36.1	11.816	A	5.06	.195
A	33.5	11.785	B	5.04	.205
A	25.9	11.510	C	5.02	.295
A	17.3	11.440	D	4.95	.150
A	14.4	11.535	A	4.92	.065
A	8.44	9.235	B	4.91	.060
A	8.37	9.320	C	4.88	.095
B	6.54	9.340	D	4.86	.055
A	6.37	6.880	A	4.79	.055
D	5.69	4.510	C	4.79	.055
A	5.50	3.810	C	4.76	.055
A	55.32	1.005	A	4.63	.055
B	5.30	.0665	C	4.54	.055
D	5.30	.785	D	3.65	.055
A	5.23	.525	D	1.35	.055
B	5.23	.440			
		C. Barium–Ammonia			
	$\frac{\text{Moles NH}_3}{\text{mole Ba}}$			$\frac{\text{Moles NH}_3}{\text{mole Ba}}$	
A	39.9	12.765	A	8.81	5.575
A	37.0	12.730	A	8.65	5.380
A	33.5	12.555	A	8.45	4.560
A	30.2	12.535	A	8.27	3.600
A	23.1	12.470	B	8.24	3.400
A	19.7	12.060	A	8.06	2.180
A	17.2	11.650	A	7.94	1.340
A	15.9	11.195	B	7.93	0.890
A	15.0	10.875	A	7.85	0.665
A	13.5	10.150	A	7.71	.210
A	12.2	9.305	C	7.57	.235
A	11.1	8.770	B	7.55	.070
A	10.6	8.775	A	7.55	.065
A	9.79	8.780	C	7.47	.090
A	9.60	8.450	A	7.34	.020
A	9.44	7.490	A	7.26	.020
A	8.98	5.570	A	7.22	.020
		D. Lithium–Ammonia			
	$\frac{\text{Moles NH}_3}{\text{mole Li}}$			$\frac{\text{Moles NH}_3}{\text{mole Li}}$	
A	57.1	12.635	A	13.2	12.385
A	53.2	12.590	A	8.36	11.710
A	50.3	12.545	A	5.33	8.390
A	47.2	12.495	A	3.94	1.565
A	43.7	12.450	A	3.79	1.165
A	40.2	12.470	A	3.53	0.005
A	36.6	12.435	A	2.67	.020
A	31.9	12.495	A	2.07	.005
A	27.6	12.480	A	1.68	.010
A	22.7	12.440	A	1.50	.005
A	18.2	12.450	A	1.41	.010
		E. Sodium–Ammonia			
	$\frac{\text{Moles NH}_3}{\text{mole Na}}$			$\frac{\text{Moles NH}_3}{\text{mole Na}}$	
A	74.4	12.685	A	12.4	12.625
A	73.0	12.645	A	8.66	12.155
A	70.5	12.625	A	7.03	10.800
A	66.4	12.630	A	6.24	9.505
A	61.7	12.625	A	5.85	8.540
A	52.6	12.635	A	5.51	7.660
A	42.5	12.640	A	5.30	6.625
A	30.4	12.645	A	4.70	6.340
A	19.7	12.635	A	2.73	6.335

[a] The vapor pressure of pure ammonia indicated a temperature of −63.77 ± 0.02°.

In all calculations of the amount of ammonia in the measuring bulb and reaction tube the following procedure was employed: the pressure differential in the manometers was determined by means of a cathetometer having a precision of 0.005 cm.; the temperature was read to 0.02°, the observed mercury heights were corrected for the shape of the menisci and the pressure corrected to 0°, sea level and 0° latitude. The moles of ammonia present were then calculated by means of the van der Waals equation.

In making trial runs with sodium it was observed that a small amount of mercury from the manometer and mercury valve condensed on the sodium. To eliminate this source of error, traps were placed between the reaction tube and any source of mercury vapor. Prior to each run a small amount of sodium was distilled into each trap. Over a period of five days, no mercury was found to condense in the reaction tube although some was found in the traps.

In the case of runs with sodium, a side tube containing the metal was sealed to the bottom of the reaction tube,

---

(4) W. Biltz and G. F. Huttig, *Z. anorg. Chem.*, **114**, 241 (1920).

(5) W. C. Johnson and A. W. Meyer, *Chem. Revs.*, **8**, 273 (1931).

the vacuum line was exhausted, the sodium distilled into the reaction tube and the side tube sealed off. For calcium, strontium, barium and lithium the vacuum line was filled with carbon dioxide and the reaction tube removed. The openings to the line and reaction tube were stoppered and the latter placed in a dry box with a carbon dioxide atmosphere. The metal to be used was freshly cleaned, placed in a weighing bottle and weighed under a carbon dioxide atmosphere. The bottle was returned to the dry box and a small amount of the metal transferred to the reaction tube. The latter was attached to the vacuum line and the system evacuated. The bottle was reweighed and the amount of metal used obtained by difference.

In most runs a large measured amount of ammonia was condensed on the metal, the equilibrium pressures of the resulting dilute solutions determined and then small amounts of ammonia were removed to the gas measuring bulb. The pressures were then determined again. This process was repeated until nearly all of the ammonia was removed. In this way the pressures were approached "from below." In some instances a small amount of ammonia was added to the system and the pressures determined "from above." The former method is believed to yield more accurate results, at least in the metals.

TABLE II

THE VAPOR PRESSURES OF METAL–AMMONIA SYSTEMS AT $-45.3°$[a] AS A FUNCTION OF CONCENTRATION

A. Calcium–Ammonia

Series	$\frac{\text{Moles NH}_3}{\text{mole Ca}}$	p, cm.	Series	$\frac{\text{Moles NH}_3}{\text{mole Ca}}$	p, cm.
B	19.1	38.825	B	6.54	11.025
B	15.8	35.215	B	6.16	2.365
B	13.5	33.005	B	5.94	0.740
B	12.1	31.405	C	5.87	0.430
B	10.9	28.980	B	5.84	0.345
B	9.48	25.965	C	5.74	0.150
B	8.00	25.150	C	2.15	0.295
B	7.17	22.515			

B. Strontium–Ammonia

	$\frac{\text{Moles NH}_3}{\text{mole Sr}}$			$\frac{\text{Moles NH}_3}{\text{mole Sr}}$	
B	5.18	1.900	A	4.57	0.940
A	5.14	3.460	B	4.52	0.175
B	4.89	0.475	C	3.74	0.425
B	4.82	0.175	B	3.69	0.950
B	4.72	0.175	C	1.23	0.430

C. Barium–Ammonia

	$\frac{\text{Moles NH}_3}{\text{mole Ba}}$			$\frac{\text{Moles NH}_3}{\text{mole Ba}}$	
A	23.3	40.215	A	8.62	15.565
A	17.4	35.875	A	8.26	10.115
A	12.1	27.945	A	7.99	4.940
A	10.7	25.225	A	7.74	1.000
A	plateau	24.995	B	7.58	1.960
A	9.80	24.775	A	7.55	0.260
A	9.34	21.170	B	7.53	0.410
A	9.10	17.855	A	6.93	0.265
A	plateau	17.330	C	4.29	0.295
A	8.78	16.810			

D. Lithium–Ammonia

	$\frac{\text{Moles NH}_3}{\text{mole Li}}$	p, cm. of Hg	Series	$\frac{\text{Moles NH}_3}{\text{mole Li}}$	p, cm. of Hg
C	685	39.980	A	44.4	39.280
C	555	39.950	B	31.4	39.145
C	429	39.935	A	26.0	39.090
C	301	39.900	A	15.4	38.585
C	236	39.870	C	12.1	38.155
C	166	39.835	A	10.7	37.275
B	153	39.850	A	7.70	33.855
B	145	39.960	A	5.78	26.855
B	140	39.845	B	4.53	14.840
B	139	39.850	A	4.27	11.360
B	132	39.745	C	4.45	8.480
B	124	39.690	A	3.89	1.585
C	90.4	39.640	..	3.78	0.055
B	73.4	39.570	A	2.90	0.050
C	47.0	39.330	A	1.53	0.055

E. Sodium–Ammonia

	$\frac{\text{Moles NH}_3}{\text{mole Na}}$			$\frac{\text{Moles NH}_3}{\text{mole Na}}$	
C	694	39.985	A	40.7	39.510
C	617	39.970	B	35.5	39.455
C	533	39.955	C	35.4	39.450
C	466	39.945	A	32.3	39.525
C	395	39.930	B	28.7	39.445
C	326	39.910	A	24.3	39.450
C	255	39.890	B	21.4	39.455
C	189	39.855	A	17.1	39.360
B	163	39.845	B	12.2	38.860
B	145	39.810	A	9.09	37.040
C	135	39.780	B	7.60	33.070
B	125	39.770	A	6.65	29.535
B	103	39.745	C	6.28	27.010
B	84.0	36.690	A	5.86	24.510
C	79.1	39.645	B	5.64	22.725
A	64.3	39.610	A	5.43	20.670
B	63.2	39.590	..	5.38	20.010
A	60.1	39.575	C	5.31	20.755
A	55.0	39.540	A	3.86	20.010
A	48.3	39.535	A	1.82	20.015
B	46.2	39.510			

[a] The vapor pressures of pure ammonia indicated temperature of $-45.30 \pm 0.02°$ for the alkaline earth metals, $-45.39°$ for lithium and $-45.41°$ for sodium.

The constant temperature baths which were placed about the reaction tube consisted of slush baths of chloroform, chlorobenzene, carbon tetrachloride and ice contained in narrow mouthed dewar flasks. The temperatures at which measurements were made were determined either by a calibrated mercury thermometer or from the vapor pressures of pure ammonia using the values of Henning and Stock.[6] The temperature variation during any given run at no time exceeded $-0.02°$ as determined by the pressure of pure ammonia immersed in the constant temperature bath. In most cases it was considerably less than this value.

The criterion of equilibrium was that the pressure of the reaction tube manometer did not change over a period of 20 to 30 minutes. In the concentrated regions where equilibrium was reached more slowly this period was extended to an hour or more, in some cases as much as three or four hours being allowed. The equilibrium pressures for the compounds in the case of the alkaline earth metals and of the saturated solutions for the alkali metals were obtained by independent determinations. From four to nine hours were allowed for equilibrium to be attained in each case. After the system had reached equilibrium the pressure was determined, the ammonia frozen out with liquid nitrogen and the final pressure obtained. The difference between the initial and final pressures was taken to be the equilibrium vapor pressure of ammonia for the system.

Stirring was not necessary in the case of the alkaline earth metal solutions and hence was not used, since only the solid and gas phases were present for many points. However, for the alkali metals a stirrer was quite essential, especially in the concentrated regions. Therefore, a glass stirrer containing an enclosed iron rod and activated by a solenoid was used for the lithium and sodium solutions.

In most of the solutions amide formation was observed. The amount of amide formed was determined for each reading of each run in the following manner. Following the determination of the equilibrium pressure for a given con-

---

(6) F. Henning and A. Stock, *Z. Physik*, **4**, 227 (1921).

TABLE III

EQUILIBRIUM PRESSURES FOR THREE PHASE METAL–AMMONIA SYSTEMS AT VARYING TEMPERATURES

Phases present	T, ° C.	Equilibrium pressures in cm.						Pressure of pure ammonia[b]	
		Calcium	Strontium	Barium	Lithium	Sodium	Potassium[a]	T, ° C.	p
Metal, compound, vapor	−63.8	0.030	0.050	0.030	...	...	...	−63.77	12.795
	−45.4[c]	0.180	0.310	0.265	...	...	...	−45.40	40.060
	−22.9	1.245	1.905	2.385	...	...	...	−22.90	125.51
	0.0	4.595	...	...	...	...	...	0.0	322.1
Metal or compound, saturated soln., vapor	−63.8	7.440	9.330	5.575	0.005	6.335	2.66	21.3	673.3
	−45.4[c]	25.15	...	17.330	0.055	20.010	8.44		
	−22.9	...	...	...	0.760	63.750	27.5		
	0.0	...	...	...	3.285	169.725	75.0		
	21.3	...	...	...	10.390	...	...		
Two liquid phases, vapor	−63.8	10.605	11.50	8.775	12.450	12.630	...		
	−45.4[c]	33.00	...	24.995	39.090	39.450	...		

[a] Potassium pressures calculated from the data of Johnson and Meyer[8] using the Clausius–Clapeyron equation. [b] Pressures from Henning and Stock[6] and the "Handbook of Chemistry and Physics." [c] The temperature for calcium, strontium and barium was −45.3°.

centration and the subsequent removal of ammonia, the ammonia in the measuring bulb was frozen out with liquid nitrogen. The observed pressure of hydrogen was used to calculate the amount of amide present in the reaction tube. For each point, then, the amount of metal was corrected for amide formation. The amount of ammonia in solution was corrected for amide formation and for the ammonia present in the gas phase. In most cases the hydrogen pressure was well under 0.05 cm. and in no case did it exceed 0.20 cm.

For all metals except sodium the metal was weighed prior to a run. The amount of metal was determined by titration following a run. In the alkaline earth runs the metals were allowed to react completely with the ammonia and the resulting amount of hydrogen determined. The amount of metal by weight and titration agreed quite closely but that determined by amide formation was lower in some cases. This was believed due to oxide or nitride formation during the transfer of the metal to the reaction tube and before the system was entirely evacuated. A slight darkening of the metal surface supported this hypothesis. The determination by amide formation was given maximum weight in such cases. The largest discrepancy observed was 3.8% and all others were about 1% or less.

In the lithium and sodium solutions the amount of metal was determined by adjusting the number of moles until the pressure–concentration curve intersected the constant pressure line at the ammonia–metal ratio obtained from the literature. For lithium these values are 3.81 at −63.8° and 3.78 at −45°. They were obtained from the work of Johnson and Piskur.[7] The sodium values were obtained by combining the data of Kraus and others at various temperatures given in a review article by Johnson and Meyer.[5] The values are 5.26 at −63.8° and 5.38 at −45.4°.

In separate determinations hydrogen was found to be insoluble in both pure ammonia and metal–ammonia solutions. In addition it was observed that a relatively large amount of amide adsorbed only a negligible quantity of ammonia even at high pressures. The amides were found to be essentially insoluble in liquid ammonia.

The ammonia used was the commercial anhydrous product and, as described previously, was twice distilled from a sodium solution before being used.

The lithium and barium were "99 + %" pure whereas the sodium and strontium contained less than 0.1% impurities, principally the other alkali and alkaline earth metals. The calcium contained an appreciable amount of calcium oxide. Assuming all of the uncombined metal present to be calcium, the commercial "turnings" were found to be 96.8% metallic calcium by reaction with water and a determination of the volume of the resulting hydrogen. This value was used in the calcium runs and agreed closely with the value found by amide formation. All of the metals contained a negligible amount of iron.

Results

The results of the vapor pressure measurements are given in Table I, II and III and plotted in Figs. 1 and 2. In Figs. 1 and 2 are shown also the calculated pressure values for potassium in the concentrated region (from the data of Johnson and Meyer[8] using the Clausius–Clapeyron equation) and the estimated pressure of a saturated cesium solution (from the data of Hodgins[9]). All plateaus shown in the curves obtained from this work were further verified by observing the regions in which repeated withdrawals of small amounts of ammonia did not change the solution pressure.

Compound Formation.—The number of moles of ammonia per mole of metal, for the solids in equilibrium with the metal for calcium, strontium and barium, were found to be 5.67, 4.87 and 7.49, respectively, at −63.8° and, in the same order, 5.79, 4.92 and 7.55 at −45.3°. It may easily be seen that these values are neither integral nor is the nearest integral value for any metal the same as that for any other metal. It is evident that the results for strontium and barium are not in agreement with the findings of Roederer,[10] and Mentrel[11] or Biltz and Huttig.[4] However, the values for calcium are in very good agreement with the findings of Kraus who obtained a ratio of 5.90 at −33°.[1]

Phase Separation.—A region of two liquid phases was found for solutions of all of these metals. The presence of an upper consolute temperature was indicated in each case by the decrease in length of the plateau with increasing temperature. (No runs were made on dilute strontium solutions at −45.3° because of their instability at this temperature.)

Relative Activity Coefficients.—Although the vapor pressures of these solutions are not sufficiently accurate in the dilute regions for absolute activities to be obtained reasonably good values of the relative activity coefficients, $k\gamma$, may be calculated. The values of $k\gamma$ for the metals were determined by means of the Gibbs–Duhem equation using the method of Lewis and Randall.[12]

For purposes of comparison the pressure–concentration curves for potassium at −50.4° and for

---

[7] W. C. Johnson and M. M. Piskur, THIS JOURNAL, **37**, 93 (1933).

[8] W. C. Johnson and A. W. Meyer, *ibid.*, **33**, 1922 (1929).

[9] J. W. Hodgins, *Can. J. Res.*, **278**, 861 (1949).

[10] G. Roederer, *Compt. rend.*, **140**, 1252 (1905).

[11] Mentrel, *ibid.*, **135**, 740 (1902).

[12] G. N. Lewis and M. Randall, "Thermodynamics and the Free Energy of Chemical Substances," McGraw-Hill Book Co., New York, N. Y., 1923, pp. 273–278.

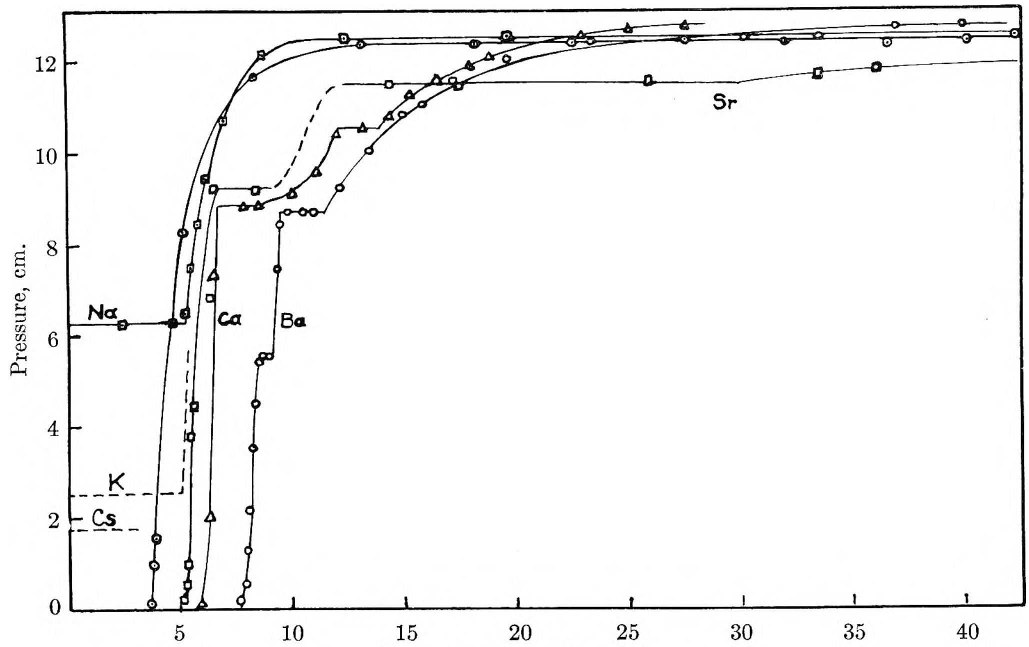

Fig. 1.—Vapor pressures of metal–ammonia systems at −63.8°: △, Ca; □, Sr; ○, Ba; ⊙, Li; ⊡, Na.

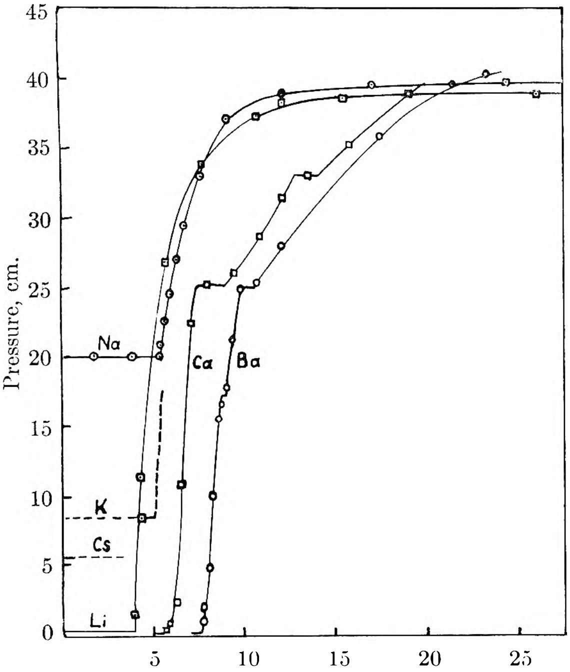

Fig. 2.—Vapor pressures of metal ammonia systems at −45.3° for Ca and Ba and −45.4° for Li and Na: □, Ca; ○, Ba; ⊡, Li; ⊙, Na.

cesium at −50.0° were plotted from the literature values and $k\gamma$ calculated as above. Although the curve for cesium was observed to bend decidedly toward the pressure axis at high concentrations none of the curves for the other metals, either in this or previous work, were found to do so. From the description given for the cesium determinations it appears that only one run was made and that all points were obtained "from above," *i.e.*, by adding ammonia. The author waited "a few minutes" for pressure equilibrium to be attained. Such a procedure has been found to give erroneous results for the other metal solutions, at least in the concentrated region. Assuming that true equilibrium had not been reached and that the cesium curve has the same form as the other alkali metals, an extrapolated curve was drawn. It will be referred to as cesium*.

As may be seen from Table IV, the values of $k\gamma$ for sodium and lithium were determined relative to a one molal solution. For potassium and cesium the reference point is 4.89 molal, the most dilute solution for which pressures of potassium solutions are known, but −0.52 has been added to each log $k\gamma$ value so that these curves will intersect the sodium curve at m = 4.89. When −0.32 is added to each log $k\gamma$ value for lithium the curve for that metal also intersects the others at m = 4.89 as is shown by the lithium curve in Fig. 3.

TABLE IV

COMPARISON OF LOG $k\gamma$ VALUES FOR THE ALKALI METALS IN METAL–AMMONIA SOLUTIONS

		Log $k\gamma$				
m	$m^{1/2}$	Li	Na	K	Cs	Cs*
0.20	0.45	0.08	0.24	..	..	..
0.50	0.71	0.05	0.14	..	..	..
1.00	1.00	0.00	0.00	..	..	..
2.00	1.41	−0.07	−0.22	..	..	..
3.00	1.73	−0.31	−0.42	..	..	..
4.89	2.21	−0.20	−0.52	−0.52	−0.52	−0.52
6.00	2.45	−0.13	−0.44	−0.20	−0.24	−0.24
8.00	2.83	0.07	−0.06	0.57	0.40	0.40
10.00	3.16	0.41	0.54	1.77	1.24	1.24
10.91	3.30	0.76	1.06	2.43	1.76	1.76
11.63	3.42	1.19	..	3.29	2.06	2.09
14.36	3.79	3.28	..	..	2.72	3.62
15.53	3.94	11.2	..	..	2.88	..
25.09	5.01	..	..	..	3.23	..

It should be noted here that in a region of two liquid phases the value of $k\gamma$ is actually an apparent relative activity coefficient being the weighted average of the coefficients in the two phases.

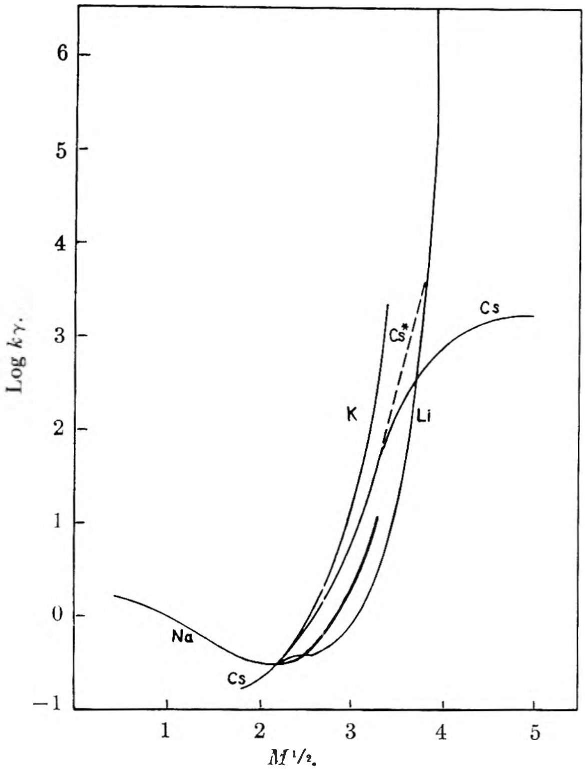

Fig. 3.—The relative activity coefficients of the alkali metals in liquid ammonia.

Although there may be a small change in γ between -45.4 and $-50.0°$ or $-50.4°$ the effect on log $k\gamma$ will be negligible for such a small temperature change.

The Fractional Lowering of the Fugacity.—In Fig. 4 are plotted the values for the fractional lowering of the fugacity for these metal solutions and also for ideal solutions of 1–1 electrolytes and non-electrolytes. For purposes of comparison the curve for an aqueous solution of sodium chloride at 25° is also included. This curve was calculated from Robinson's data given in Harned and Owen.[13]

Discussion

As has already been noted, many of the results found here are in disagreement with the current theories for these solutions and compounds. Whereas the pressure–concentration curves establish the presence of a region of two liquid phases for all of these metal solutions the curves also show that the alkaline earth metals do not form the hexammoniate compounds long ascribed to them.

From Figs. 1 and 2 it is also apparent that there is not a vertical line connecting the compound with the saturated solutions for the alkaline earths. In the region between the compound dissociation pressure and the saturated solution pressure it appears that these solids are adding as much as a mole of ammonia per mole of metal before any solution is formed. This phenomenon may be due either to the formation of a solid solution or to the adsorption of gaseous ammonia on the surface of the compound.

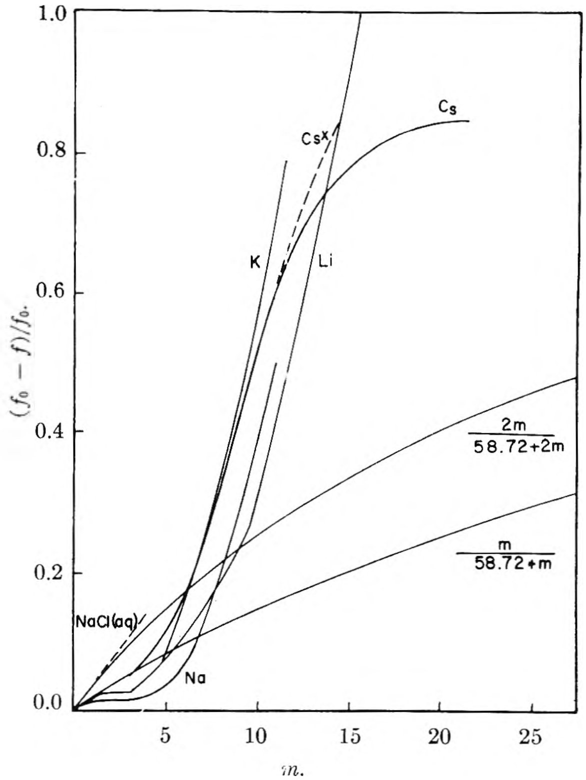

Fig. 4.—The fractional lowering of the fugacity, $(f_0 - f)/f_0$ as a function of the molality for solutions of alkali metals in liquid ammonia.

The most logical explanation for the observed behavior of these systems, which presents itself to the authors, is a non-stoichiometric interstitial type of compound in an expanded metal lattice.

These solutions have been described as being 1–1 electrolytes, at least in the dilute region. However, any equilibrium, as for example the ionization of Na to give Na^+ and e^-, which occurs in dilute solutions must also be present in concentrated solutions. Any observed deviations from the expected behavior are usually explained in terms of other equilibria set up in the same solution. Hence, many writers have used electron pairing, metal ion pairing, solvation, etc., in an attempt to derive a suitable theory. This is similar to aqueous solutions of the alkali chlorides, bromides, acetates, etc., in which double and triple ions, hydration, etc., are used to explain the observed behavior.

In such uni-univalent solutions certain characteristics have been observed. For example, when log $k\gamma$ is plotted against $m^{1/2}$ for the alkali chlorides and k chosen so that the curves intersect at $m^{1/2} = 1.00$ it is found that, to the right of the intersection, the order is Li > Na > K > Rb > Cs and to the left this order is reversed. The bromides and iodides are similar but for the acetates, hydroxides and fluorides the above order is exactly reversed. It should be emphasized that no cases of partial reversal have ever been found.[14]

The curves in Figs. 3 and 4 seem to indicate that these solutions display some deviation from normal 1–1 electrolytic behavior. The log $k\gamma$ curves differ from the prescribed behavior in that they cross at

---

(13) H. S. Harned and B. B. Owen, "The Physical Chemistry of Electrolytic Solutions," Reinhold Publ. Corp., New York, N. Y., 1950, p. 289.

(14) H. S. Harned and B. B. Owen, ref. 13, p. 385, 562–563.

other than the reference point and a partial reversal is found. In addition, consider the fugacity lowering curves in the concentrated region. Neglecting the cesium curve, whose behavior is practically impossible to explain, it is found that the order, at concentrations above $m^{1/2} = 2.55$, is K > Na > Li. Since the anions are considered to be identical in these solutions they cannot cause the observed differences. However, it is also impossible to attribute these differences to the cations present since this is in direct contradiction to the accepted theory that the amount of solvation is greater the less the size of the cation. The degrees of ionization and polymerization for lithium and sodium as indicated by the curves in the dilute solutions also point to an order in the concentrated region which is opposite to that observed. Such behavior would seem to indicate that these solutions should not be regarded as simple ionic solutions in either the concentrated or dilute regions.

INTERACTION OF CHROMIUM(VI) ANIONS WITH CHROMIUM METAL SURFACES[1,2]

By SHERMAN KOTTLE AND L. O. MORGAN

Contribution from the Department of Chemistry, The University of Texas, Austin, Texas

Received July 15, 1955

Experiments were carried out in which electrode potential changes were correlated with adsorption of chromium(VI) anions on a chromium metal surface. Three classes of chromium metal surfaces were recognized: (1) active, such as those obtained upon removal of metal from a typical plating bath without subsequent treatment, (2) passive, produced by treatment of active metal with boiling nitric acid, and (3) etched, produced from either active or passive metal by treatment with hydrochloric acid. Etched chromium was similar to reactive chromium with respect to potential behavior, but differed markedly with both reactive and passive metal in its very much larger apparent surface area. Calculations based upon the observed electrode potential change and the number of adsorbed anions led to a value of 1.40 debye for the electric moment of each adsorbed ion.

Corrosion inhibition of iron by chromate, molybdate and tungstate ions has been studied by Robertson[3] who concluded that those ions were chemisorbed at the metal surface. His conclusions were based on the great similarity in the over-all behavior of the three ions despite large differences in oxidation potential. Thus, the proposal that a mixed iron–chromium oxide film is formed[4] does not logically extend to a consideration of tungstate and molybdate reactions because of their very low oxidation potentials. Uhlig and Geary[5] measured electrode potentials of iron immersed in chromate solutions of various concentrations and were able to correlate changes in potential with the supposed adsorption of chromate ions upon the assumption that adsorption followed a typical Langmuir isotherm. Using radioactive chromium Powers and Hackerman[6] demonstrated the uptake of chromium from chromate solutions on chromium surfaces and their results followed a pattern predictable on the basis of irreversible adsorption. After due consideration of changes in ionic species in solution the results were compatible with a simple monolayer isotherm.

It seems virtually certain that the primary process at both iron and chromium surfaces in chromate solutions is one of adsorption and that such adsorption is capable of inhibiting oxidation reactions at those surfaces although it is possible that in many cases further reaction to form oxide films may occur and the coatings thus formed are capable of preventing corrosion. It is our purpose in this paper to demonstrate directly the correspondence between chromate adsorption and electrode potential change at the chromium metal surface.

Preparation of Solutions.—The radioisotope chiefly used was chromium-51, obtained by neutron irradiation of chromium metal at the Oak Ridge National Laboratory, Oak Ridge, Tennessee. One-gram pieces of electrolytically prepared chromium were irradiated for one month (about one half-life). Chromium(VI) solutions were prepared by electrolysis with radioactive chromium as the anode and a platinum wire as the cathode. When the solutions were to be of a concentration less than 10^{-5} *M*, distilled water was used as the electrolyte, with an anode current density of less than ten microamperes per cm.^{2} Those solutions contained essentially pure hydrogen chromate and were completely free of chromium(III) ions.

Solutions of greater concentration were made by diluting a 0.01 *M* chromic acid stock solution prepared as follows. Chromium was electrolyzed in *p*H 11 to 12 sodium hydroxide solution at approximately one milliampere per cm.^{2}. The resulting solution, containing sodium chromate and sodium chromite, was washed and treated with concentrated (30%) hydrogen peroxide. Excess peroxide was decomposed by contact with a piece of platinum foil, and the solution was purified by passing it through a column, 2.5 cm. diameter and 50 cm. long, of Dowex-50 (sulfonic acid ion-exchange resin) in the hydrogen form.

For solutions which were not radioactive a "dead stop" potentiometric titration method was used in which chromium(VI) was reduced to chromium(III) with ferrous sulfate. In order to conserve radioactive chromium solutions, chromium(VI) concentrations were determined colorimetrically in those cases. Solutions were compared with known standards with a Rubicon "Evelyn" colorimeter using light of 380 mμ wave length.

Preparation of Chromium Samples.—Experiments were done using chromium discs 2 cm. diameter and 0.05–0.15 mm. thick. Electrical leads, disc edges and the reverse sides of electrodes were coated with ceresin wax in order to define the conducting surface. It was determined by coprecipitation experiments that chromium(VI) was not re-

---

[1] Taken from the dissertation submitted to the Graduate School of the University of Texas by Sherman Kottle in partial fulfillment of the requirements for the degree of Doctor of Philosophy, 1954.

[2] This work was supported financially by the Office of Naval Research under contract No. Nonr 375, Task Order 04.

[3] W. D. Robertson, *J. Electrochem. Soc.*, **98**, 94 (1951).

[4] U. R. Evans, *J. Chem. Soc.*, 1020 (1927); T. P. Hoar and U. R. Evans, *ibid.*, 2476 (1932); J. Mayne and M. Pryor, *ibid.*, 1831 (1949); U. R. Evans and J. Stockdale, *ibid.*, 2651 (1929).

[5] H. H. Uhlig and A. Geary, *J. Electrochem. Soc.*, **101**, 215 (1954).

[6] R. A. Powers and N. Hackerman, THIS JOURNAL, **57**, 139 (1953).

duced by the wax under conditions similar to those used in the electrical measurement experiments.

Chromium metal was prepared by electrodeposition from a standard plating bath.[7] Three pretreatment procedures were used in the preparation of samples. (1) Chromium plates were removed from the plating bath, rinsed with distilled water, treated with cold dilute nitric acid to remove the copper basis metal, and again rinsed with distilled water. (2) The metal was removed from the plating bath, treated with boiling concentrated nitric acid, and rinsed with distilled water. (3) Chromium metal prepared in either of the preceding ways was treated with hydrochloric acid (1:1) until hydrogen was evolved uniformly from the surface, and rinsed with distilled water. The first of these produced a surface which was distinctively different from the passive surface produced by the second procedure—measured electrode potentials were considerably more anodic, or active, and the rates of adsorption were subsequently found to be quite different in the two cases. For the sake of brevity metal of the first kind will be called "reactive" and of the second kind, "passive." The third pretreatment process led to a very reactive chromium surface which we shall call "etched."

Measurement of Adsorption.—Chromium uptake was determined by measurement of the radioactivity of chromium-51, which decays with the emission of vanadium X-rays, low energy electrons, and 0.32 Mev. γ-rays.[8] Measurements were done with a scintillation counter comprising a 25 cm. diameter, thallium-activated, sodium iodide crystal optically coupled to an RCA 5819 multiplier phototube. Electrical pulses from the phototube were amplified and counted in the usual manner.[9]

Measurement of Electrode Potentials.—Cells used in the measurement of the potentials of chromium immersed in chromate solutions were 50-ml. Pyrex beakers, fitted with holders for a saturated calomel electrode, or solution bridge and a chromium coupon. All measurements were made with the cells open to the atmosphere. A self-contained Rubicon portable potentiometer[10] was used to obtain potential data. Because the calomel electrodes slowly leaked potassium chloride, they were separated from the experimental solutions by a bridge constructed of 2 mm. capillary tubing filled with cell electrolyte. The bridge ended in a tubulus which could be placed in contact with a chromium electrode. It was possible to avoid chloride contamination of the bulk solution by occasionally discarding the bridge contents.

Adsorption Experiments.—Amounts of adsorbed chromium(VI) and rates of adsorption were determined in 3.3 $\times$ 10^{-4} M radioactive chromic acid solutions. This concentration was sufficiently great that the surfaces could be considered to be saturated upon attainment of constant values. At intervals the metal samples were withdrawn, washed thoroughly with distilled water and counted. The counting data were corrected for radioactive decay and amounts of chromium were calculated on the basis of comparison of observed counting rates with those of standard samples. Both rates of adsorption and total amounts varied widely depending upon the pretreatment of the metal. An example is illustrated in Fig. 1. The bottom curve was obtained with passive chromium, the top curve, with the same coupon after treatment with dilute hydrochloric acid to produce reactive chromium, and the bottom curve was obtained once more with the same coupon after treatment with boiling concentrated nitric acid, which served to remove radioactivity from the surface and to repassivate the chromium.

Time–adsorption curves for passive chromium are illustrated in Fig. 2. It will be seen that a marked change in slope occurred at 20–30 min. as shown in the bottom curve. Another change at a relatively much longer time may be seen in the upper curve. In solutions containing 3.3 $\times$ 10^{-4} M chromic acid, the second change occurred approximately 60 times later than the first. Subsequent pick-up

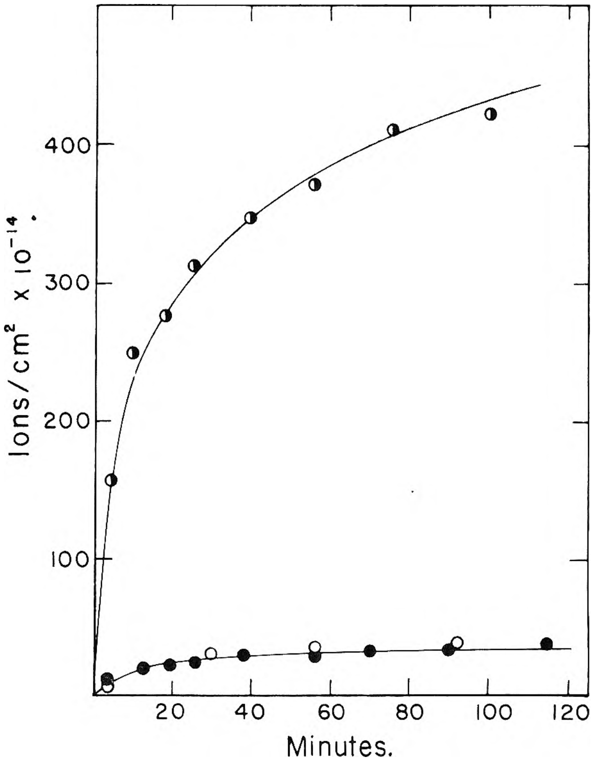

Fig. 1.—Adsorption as a function of time; chromium in 3.3 $\times$ 10^{-4} M chromic acid solution: O, passive; ◑, etched; ●, re-passivated.

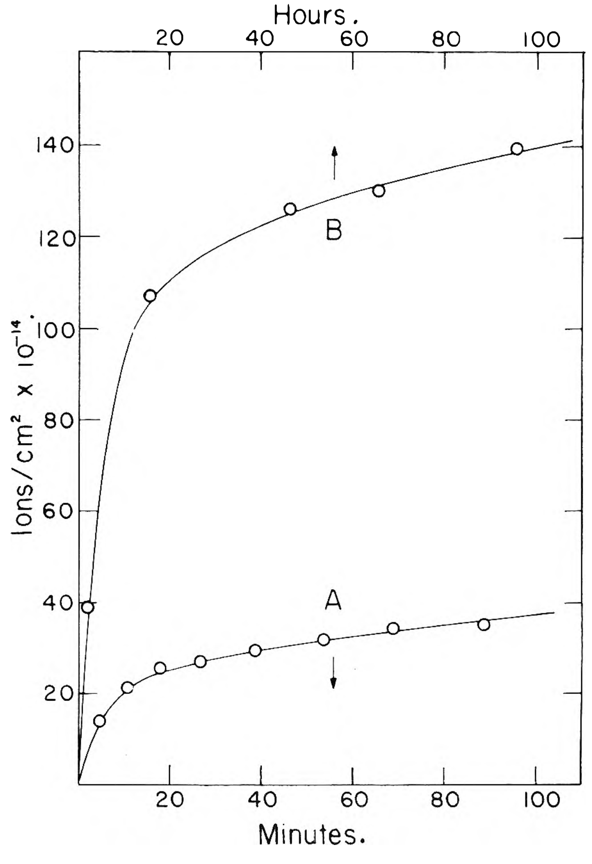

Fig. 2.—Adsorption as a function of time; passive chromium in 3.3 $\times$ 10^{-4} M chromic acid solution: A, abscissa in minutes; B, abscissa in hours.

---

[7] George Dubpernell, "Chromium Plating," "Modern Electroplating," The Electrochemical Society, 1942, pp. 117-143.

[8] U. S. Department of Commerce, National Bureau of Standards Circular No. 499, 1950, p. 47.

[9] W. C. Elmore and M. Sands, "Electronics," McGraw-Hill Book Co., Inc., New York, N. Y., 1949.

[10] In a few cases it was necessary to use an auxiliary, high-sensitivity galvanometer because of high solution resistances.

was very slow. The amount of adsorbed material continued to increase, more and more slowly, until the rate of uptake was less than the errors in observation. At maximum deposition, there was no discernible change in the microscopic appearance of the metal surface.

The same type of measurement carried out using unetched, reactive samples, yielded curves similar to those of Fig. 2 with the exception that the changes in slope occurred much sooner and were more abrupt. Time–adsorption curves obtained for etched chromium exhibited essentially the same characteristics but the total amounts of adsorption were of the order of 10 times greater. At low microscope magnifications an extensive crack system was visible in samples used for those experiments, which was in all respects similar to those observed by Hackerman and Marshall.[11] After long exposure to chromium(VI) solutions, corrosion began to occur on etched surfaces. Viewed under the microscope, reduction products could be seen accumulating at crack intersections. The deposits were not removed by flowing distilled water, but were soluble in concentrated nitric acid.

Because there was no completely reliable information on the true area of the chromium surfaces, it was convenient to assume that a close-packed layer was formed in each case, and to speak of the apparent "roughness" for each mode of deposition and each type of pretreatment. If an area of 25 Å.^{2} was assumed for each adsorbed ion, there were 4 × 10^{-14} per cm.^{2} in a monolayer. On that basis the general characteristics observed in time–adsorption curves obtained for the various surfaces may be summarized as follows

Passive	Time	Roughness factor
First change in slope	20–30 min.	5–7
Second change in slope	20–30 hr.	25–30
Max. adsorption	250 hr.	75–80
Reactive		
First change in slope	5–10 min.	5–6
Second change in slope	2–3 hr.	20–25
Max. adsorption	250 hr.	80–100
Etched		
First change in slope	20–30 min.	75–80
Second change in slope	80–100 hr.	225–250
Max. adsorption	None	

Potential Measurements.—With no externally applied current flowing, the potential of chromium in solutions of salts of chromic acid became more cathodic (positive with respect to the reference electrode) with increasing concentration. There were usually pronounced "memory" effects in measurement when a single coupon was transferred from solution of one concentration to one of another. After a series of potential measurements solutions of successively greater concentration, the coupon was placed again in the most dilute solution. Invariably coupons exhibited the same potential in solutions of lower chromate concentration as they did in the most concentrated.

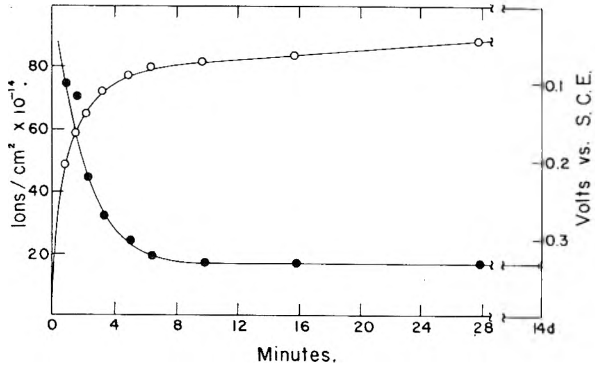

Fig. 3.—Adsorption and electrode potential as a function of time for etched chromium metal in 10^{-3} *M* chromic acid solution: ○, adsorption values; ●, electrode potentials.

Three types of chromium plate were used in the potential experiments: those termed semi-bright reactive[12] (as contrasted with mirror-finish plates), dull reactive, and etched.

There was usually an abrupt change in the rate of adsorption at the same time that potential equilibrium was reached. Data represented in Fig. 3 which were obtained with etched chromium show that after about eight minutes immersion in 10^{-3} *M* chromic acid solution, the potential of the chromium became essentially constant, while the adsorption curve approached linearity. When the potential change was plotted as a function of the amount of adsorption at the same time, there was a linear region over an interval of several hundred millivolts. For example, the data of Fig. 3 yielded the curve of Fig. 4 when plotted in that manner.

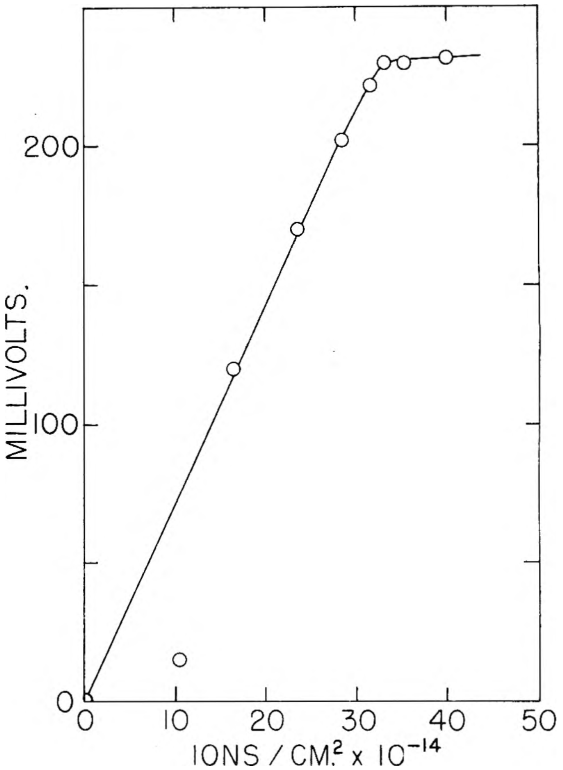

Fig. 4.—Potential change as a function of adsorption upon immersion of etched chromium metal in chromic acid solution.

Below *p*H 7 there was no concentration dependence of the slopes of potential–adsorption curves over the range 10^{-5} to 10^{-3} *M* chromic acid. In basic solutions a straight line potential-pickup relation usually appeared, but with a much greater slope. Data were obtained with difficulty; carbon dioxide, which changed the basicity, could not be completely excluded because it was necessary to open the system for each adsorption measurement.

Slope of the potential-adsorption plots varied according to the type of chromium used. In units of millivolts per ion-cm.^{2}, the slopes were: semi-bright, 2.12 × 10^{-13}; dull, 1.67 × 10^{-13}; etched, 0.70 × 10^{-13}. Apparent areas were used in calculating the values given.

In contrast with both active and etched chromium metal, the passive metal did not exhibit linear potential change with adsorption, any changes being irregular and very nearly negligible compared to the changes observed with corresponding adsorption for the other plates. Recalling the time–adsorption data of the preceding section, reactive metal behaved similarly to passive metal with regard to total adsorption while both active and etched metal exhibited linear potential-adsorption relations, each achieving a final, steady state potential, of about −0.3 volt (*vs.* S. C. E.). At that potential the active metal became essentially unreactive and the etched metal did not.

Electric Moment Calculations.—Data were treated in terms of the resultant total moment and an effective single

---

[11] N. Hackerman and D. I. Marshall, *Trans. Electrochem. Soc.*, **89**, 195 (1946).

[12] Betty Pegues, M.A. Thesis, The University of Texas, 1951.

ionic moment was calculated from the amount of adsorbate present, using the equation for a plane parallel condenser

$$\Delta E = \frac{4\pi N\rho}{D}$$

in which ΔE is the change in potential, N, the number of adsorbed ions per cm.², D the dielectric constant, and ρ, the dipole moment; D was assumed to be 1. Because the adsorption data were based on unit projected area, the values so obtained were assumed to be too small by the value of the roughness factor for each surface used. Using values obtained by Pegues[12] for the roughness values of the different types of chromium—semi-bright, 25; dull, 32; etched, 67 to 79—the moments were found to be 1.40, 1.41, 1.39 debye, respectively.

The linear relationship existing between adsorption of chromium(VI) anions and the observed change in electrode potential of the surface was obtained over the first portion of adsorption curve for reactive and for etched chromium. If all of the surfaces had the same roughness the slopes of the adsorption–potential curves obtained for each would have been the same. Because the surfaces were not equivalent and exhibited roughness depending upon the conditions of deposition and type of pretreatment the net effective moment of the adsorbed ions varied in the several experiments. The effective moment of each ion was the component of the total moment normal to the projected surface. It was to be expected, therefore, that the greater the roughness of the surface the smaller was the effective moment exhibited by each adsorbed ion. Correction for the predicted roughnesses of these separate surfaces did, in fact, lead to a constant value for the total electric moment per adsorbed ion of 1.40×10^{-18} e.s.u.

Reactive and passive chromium differed from each other with respect to the rate of adsorption and the electrical behavior upon the adsorption of the chromium(VI) anions. The two types of surface were the same with respect to the total amount of chromium adsorbed. It is apparent that the nitric acid passivation of the metal polarized it to about the same extent as did adsorption of chromate ions. We suggest that the passive surface was covered with a layer of polar molecules, which were replaced only slowly by chromium(VI) anions, and that reactive surfaces contained a layer of chemisorbed non-polar oxygen atoms which were replaced more rapidly upon immersion in chromium(VI) solutions. In each the total surface eventually covered by chromate ions was the same.

The total area exhibited by etched chromium was much greater than in either of the other two cases. The roughness factor of 75 suggests that an extensive interstitial crack system was made available to the solution, probably through dissolution of chromium(III) oxide[13] with hydrochloric acid, so that areas normally blocked off became available to adsorption. Pick-up of radioactive chromium continued at a slower rate after the etched surface was covered with a monolayer of adsorbed ions. The additional pick-up was apparently associated with reduction of chromium(VI) and the formation of oxides.[14] Those conclusions were suggested by the formation of visible deposits at the crack intersections upon long immersion of the etched chromium metal.

---

(13) J. B. Cohen, *Trans. Electrochem. Soc.*, **86**, 441 (1944).

(14) Oxidation-reduction occurring under these circumstances may be attributed to local cells set up as a result of depletion of dissolved oxygen at the bottoms of the cracks or through establishment of concentration gradients within the cracks. Further consideration of the effect was not within the scope of this work.

THE CELLULOSE–WATER–SALT SYSTEM

By S. M. Neale and G. R. Williamson

Faculty of Technology, University of Manchester, Manchester, England

Received August 17, 1955

The specific volume of cellulose in aqueous solutions of various inorganic and organic salts has been measured. The specific volume of cellulose in sodium chloride and in potassium chloride solutions passes through a maximum with increasing solute concentration. A qualitative explanation is offered on the basis of a cellulose–salt linkage. The conditions for the validity of specific volume measurements for the determination of "bound water" in cellulose are also considered. The absorption of water from unsaturated vapor by cellophane sheets at 25 and 40° impregnated with sodium chloride and potassium chloride, has been studied. Analysis of the isotherms shows that the water uptake of the cellulose–salt system is governed by the quantity of solute directly adsorbed onto the cellulose surface, and is virtually independent of the presence of excess macrocrystalline salt. It is suggested that at low humidities the water molecules are in competition with the salt ions for the active sites on the cellulose surface, and the adsorption of water is then reduced owing to the presence of the salt. At a fairly critical activity of water in the system, the adsorbed salt is displaced from the cellulose surface, and both cellulose and salt then absorb water, so that the absorption at the higher humidities is greater than in the case of cellulose alone.

Part I. The Specific Volume of Cellulose in Aqueous Solutions

Introduction

Various methods have been used during the last century in attempts to obtain accurate and reproducible results for the specific volumes of cellulose in a variety of media, but it was not until 1927 that the first reliable data were published. In this year Davidson[1] (1927) determined the specific volume of cotton and regenerated cellulose in water, toluene and helium gas, and found in every case the specific volume in helium was about 1% lower, and the water value 3–5% lower, than the value obtained in toluene.

The variation of the specific volume of a colloid with the liquid immersion medium used in the determination is well known and has been attributed to two factors: (1) a compression of the liquid at the surface of the colloid; (2) A varying degree of

---

(1) G. F. Davidson, *J. Text. Inst.*, **18**, T.175 (1927).

accessibility of the small pores and voids within the colloid to the liquid medium .

The latter factor may be considered to be mainly dependent on the size and shape of the liquid molecule.

During the swelling of many colloidal materials in liquids, the apparent volume of the colloid increases, but the total volume of the colloid plus imbibed liquid is usually less than the sum of the volumes occupied by the separate constituents.

X-Ray measurements show that there is no change in the crystal lattice of cellulose when swollen in water. The volume changes, therefore, must occur in the amorphous regions of the cellulose structure.

From the specific volume data available it appears that the water imbibed by cellulose undergoes a contraction, and this is believed to be due to a compression of the adsorbed water, caused by orientation and packing of the water molecules on the cellulose surface.

Katz[2] (1934) and Stamm and Loughborough[3] (1935) determined the initial entropy of swelling for a number of different cellulosic materials. The value 0.3 to 0.35 cal./g. of water adsorbed by an infinite amount of the swelling material, was, as Katz pointed out, the same as that obtained when water is frozen. The initially adsorbed water may therefore be oriented to give a structure similar to that of ice.

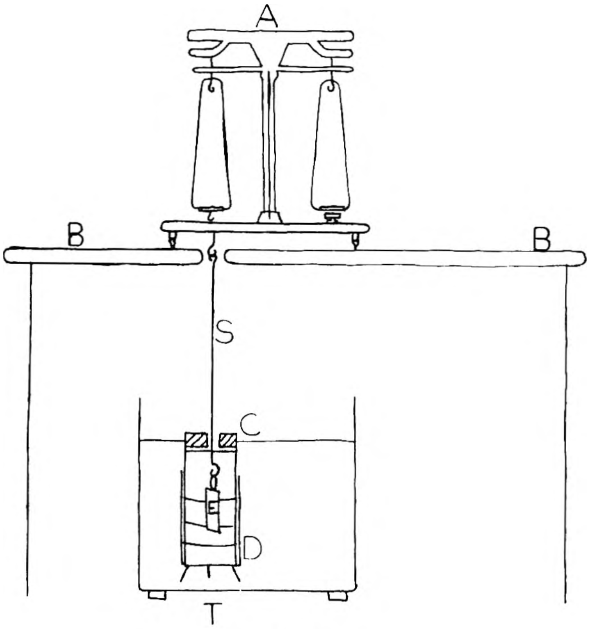

Fig. 1.

From specific volume measurements of cellulose and other colloids in water, and from the heat of adsorption of water, various workers, Harkins and Ewing[4] (1921), Lamb and Coolidge[5] (1920), Davidson[1] (1927) and Hailwood and Horrabin[6] (1945), have estimated the compression forces existing in the colloid–water system for the initially adsorbed water. For the cellulose–water system the value is about 2000 atmospheres. If such compressive forces really exist in the cellulose–water system, then it is not unreasonable to presume that the adsorbed water layer may exhibit anomalous properties.

It has been shown that this water layer (usually termed "bound water") because of the tenacity with which it is attached to the cellulose structure, is no longer capable of acting as a solvent, nor can it be frozen, or removed from the cellulose under high pressure.

Many methods have been adopted for the estimation of the "bound water" content of various colloids, based on the above properties. and recently a method suggested by Hermans[7] (1946) attracted interest. This involved the determination of the specific volume of cellulose in various aqueous media.

From these data Hermans proposed the existence of two hydrates for cellulose $C_6H_{10}O_5\cdot{}^1/_3H_2O$ and $C_6H_{10}\rightarrow O_5\cdot{}^4/_3\ H_2O$.

It appears from previous work that addition of a solute to water generally causes an increase in the apparent specific volume of immersed cellulose. The present authors, after an examination of the theoretical considerations underlying the calculation of the "bound water" in the method adopted by Hermans[7] (1946) and in conjunction with the data obtained by Farrar and Neale[8] (1952) on the distribution of solute in the cellulose–aqueous solution system, decided to re-examine the specific volume of cellulose in aqueous inorganic and organic salt solutions.

Experimental Method

Examination of the literature showed that pycnometer and dilatometer methods were incapable of yielding reproducible results to the third or even the second decimal place in the specific volume value for cellulose.

In a specific volume measurement with a porous solid it is essential to remove all traces of occluded air from the sample. In the present experiments the weight ratio of cellulose to solute must be kept low in order to avoid appreciable exhaustion of the solution by preferential adsorption of the salt by cellulose.

After preliminary experiments with the totally submerged float method of Lamb and Lee[9] (1913), as modified by Mahtre and Preston[10] (1949), the final method chosen was that of the "hydrostatic balance." This method has been used extensively for accurate density determinations (see for example, Kahlbaum[11] (1904), Davidson[1] (1927), Hermans[7] (1946)). It is based on the principle of Archimedes and involves weighing the sample in two media of known density.

The design of the apparatus used follows closely that of Osborne, McKelvey and Bearce[12] (1913) and is shown diagrammatically in Fig. 1. The balance used was an Oertling Analytical balance, maximum load 200 g., sensitivity

---

(2) J. R. Katz, "X-Ray Spectrography of Swelling," General Session of Am. Chem. Soc., 1934.

(3) A. J. Stamm and W. K. Loughborough, This Journal, **39**, 121 (1935).

(4) W. D. Harkins and D. T. Ewing, *J. Am. Chem. Soc.*, **43**, 1787 (1921).

(5) A. B. Lamb and A. S. Coolidge, *ibid.*, **42**, 1146 (1920).

(6) A. J. Hailwood and S. Horrabin, *General Disc. Faraday Soc.*, **XLIIB**, 84 (1946).

(7) P. H. Hermans, "Contribution to the Physics of Cellulose Fibres," Elsevier Co., Inc., Amsterdam, 1946, p. 103.

(8) J. Farrar and S. M. Neale, *J. Colloid Sci.*, **7**, 186 (1952).

(9) A. B. Lamb and R. E. Lee, *J. Am. Chem. Soc.*, **35**, 1606 (1913).

(10) S. H. Mahtre and J. M. Preston, *J. Text. Inst.*, **40**, T.831 (1949).

(11) G. W. A. Kohlrausch, *J. chim. phys.*, **2**, 537 (1904).

(12) N. S. Osborne, E. C. McKelvey and H. W. Bearce, Dept. Comm., Bull. Bureau of Standards, 9, No. 3 (1913).

about 4 divisions/mg. In order to eliminate undue fatigue during the determination of the rest point and the sensitivity, an optical lever was used.

The most troublesome feature of this method is the effect of surface tension upon the platinum suspension wire (S), and in order to weigh by the method of swings this effect must be reduced as far as possible. This was achieved by coating the wire electrolytically with platinum black in this region, and subsequently converting this to platinum grey, following the method due to Kohlrausch[13] (1895).

The immersion vessel *C* consisted of a large cylindrical flat-bottomed vessel, capacity 850 cc. The suspension wire passed through a central hole (minimum diameter 2 cm.) and the vessel was repeatedly evacuated *via* a splash trap over a period of one hour to remove all traces of occluded air from the sample.

The sample consisted of viscose sheet (cellophane "300") manufactured by du Pont, Ltd. The material was cut into strips 4 × 16 cm., and 15 such strips were threaded together using a small length of standard bleached cotton to form a U-shaped sample of about 4 g. weight, in such a manner that each strip hung separately from its neighbor at the bend in the U-formation. This prevented air from becoming mechanically trapped during de-aeration, and bubbles of air could be induced to escape by manually tilting the sample whilst under vacuum.

It was necessary to condition the sample before commencing measurements of any kind, in order to remove zinc and calcium ions present, and the plasticizer—glycerol. To remove the latter the sample was washed with several liters of distilled water over a period of four days. It was then soaked in several 2-l. portions of *N*/1000 acetic acid for two days more to remove the cations present, and the dilute acid was then removed by repeatedly washing with distilled water until the washings were neutral.

It was necessary to determine the specific volume of cellulose in air-free distilled water, and then to proceed to the determination of the specific volume in the various aqueous salt solutions.

Procedure.—After suspending and de-aerating the sample, the vacuum was released, and the immersion vessel C and contents transferred to support D within the thermostat T (Fig. 1), accurately controlled to 25 ± 0.005°.

When temperature equilibrium was established, weighing operations were commenced. To determine the specific volume in water two operations were necessary, giving the following values: $W_1{}^1$ = weight of suspension and sample in water; $W_2{}^1$ = weight of suspension in water. Weighing was carried out using the method of swings and at each weighing the sensitivity of the balance was determined. The sensitivity changed slightly at the various stages but was of the order of 1.5 to 2.5 divisions/mg.; any abrupt change indicated the need for replating the wire.

After $W_1{}^1$, the sample was detached and allowed to fall to the bottom of the flotation vessel. After $W_2{}^1$, the system was withdrawn from the thermostat and the sample removed and dried to constant weight at 110°. After making allowance for the residual moisture at this temperature, using the data of Davidson and Shorter[14] (1930), the dry weight of the sample *in vacuo* was obtained. Assuming the density of air-free distilled water to be 0.99707 g./ml. at 25°, the specific volume of cellulose was calculated from equation 1

$$S_w = \frac{C - (W_1{}^1 - W_2{}^1)k}{Cd_w} \qquad (1)$$

where

S_w = specific vol. of cellulose in water
C = dry wt. of sample *in vacuo*
d_w = density of water in g./ml.
$W_1{}^1$, $W_2{}^1$ = as previously defined
k = correction factor for converting $W_1{}^1$ and $W_2{}^1$ to weights *in vacuo*

The following results were obtained for the specific volume of cellulose in water in ml./g. at 25°: (1) 0.62028; (2) 0.62022; (3) 0.62038; (4) 0.62029; (5) 0.62027. A mean value of 0.62027 ml./g. was taken.

When the specific volume of cellulose was to be determined in a solution, the following procedure was adopted. The value of the specific volume in water was assumed to be 0.62027 ml./g. The sample was first weighed in water as described, and by application of equation 1, inserting S_w = 0.62027 and the values of $W_1{}^1 - W_2{}^1$, the dry weight *in vacuo* (*C*) was calculated. In this way the necessity of actually drying each sample was avoided.

The sample was then transferred to the requisite salt solution and allowed to stand in this solution in the immersion vessel at least 24 hours. The sample was then de-aerated and, after thermostatting, weighing operations were commenced as before. The following weights were obtained

W_1 = wt. of sample and suspension in aq. soln.
W_2 = wt. of suspension in aq. soln.
W_3 = wt. of suspension + platinum hook + glass bulb = in aq. soln.
W_4 = wt. of suspension in aq. soln.

(*Note* W_2 and W_4 are not the same due to a difference in the depth of immersion of the suspension wire).

To determine the density d_l of the aqueous salt solution a small sealed glass bulb weighted with lead shot, whose overall density had been determined by weighing in air and water, was attached and weighed in the solution.

Hence, knowing the dry weight of the sample, and the density of the solution, the specific volume S_s of cellulose in the particular concentration of solution given by d_l could be calculated.

Experimental Results

TABLE I

SPECIFIC VOLUME OF CELLULOSE IN AQUEOUS SOLUTIONS OF AMMONIUM CHLORIDE AT 25°

Specific vol., ml./g.	Density of soln., g./ml.	Concn. (wt. %)	Molality
0.62027	0.99707	0.0	0.0
.62174	1.01763	6.90	1.385
.62245	1.02987	11.00	2.310
.62285	1.03894	14.25	3.106
.62269	1.04794	17.60	3.992
.62240	1.06706	24.40	6.033

TABLE II

SPECIFIC VOLUME OF CELLULOSE IN AQUEOUS SOLUTIONS OF SODIUM CHLORIDE AT 25°

0.62027	0.99707	0.0	0.0
.62385	1.02292	3.60	0.638
.62527	1.04096	6.10	1.110
.62572	1.05208	7.60	1.406
.62624	1.08004	11.48	2.261
.62658	1.10529	14.85	2.981
.62667	1.12925	18.00	3.760
.62618	1.16993	23.10	5.135
.62559	1.19376	26.00	6.006

TABLE III

SPECIFIC VOLUME OF CELLULOSE IN AQUEOUS SOLUTIONS OF POTASSIUM CHLORIDE AT 25°

0.62027	0.99707	0.0	0.0
.62229	1.02467	4.30	0.603
.62269	1.05028	8.25	1.206
.62293	1.07305	11.70	1.777
.62313	1.09534	15.00	2.367
.62311	1.11768	18.15	2.975
.62304	1.13674	20.80	3.523
.62277	1.16563	24.80	4.424

---

[13] F. Kohlrausch, *Wied. Ann.*, **56**, 184 (1895).

[14] G. F. Davidson and S. A. Shorter, *J. Text. Inst.*, **21**, T.165 (1930).

Table IV

Specific Volume of Cellulose in Aqueous Solutions of Ammonium Nitrate at 25°

0.62027	0.99707	0.0	0.0
.62161	1.01819	5.20	0.686
.62278	1.04460	11.40	1.608
.62377	1.06360	16.20	2.416
.62468	1.08443	21.10	3.343
.62578	1.09811	24.40	4.034
.62786	1.12421	30.60	5.512
.62947	1.14323	35.20	6.790
.63033	1.15570	38.20	7.727
.63283	1.19862	48.20	11.630
.63357	1.20236	49.30	12.155
.63479	1.23947	58.90	17.910
.63532	1.25277	61.30	19.799
.63575	1.26852	65.10	23.316

Table V

Specific Volume of Cellulose in Aqueous Solutions of Potassium Nitrate at 25°

0.62027	0.99707	0.0	0.0
.62110	1.02461	4.30	0.445
.62360	1.07181	11.40	1.274
.62525	1.11159	17.20	2.057
.62658	1.13690	20.95	2.624
.62900	1.18320	28.00	3.850

Table VI

Specific Volume of Cellulose in Aqueous Solutions of Hexamine at 25°

0.61927	0.99707	0.0	0.0
.62011	1.01899	9.82	0.77
.62039	1.02883	14.52	1.21
.62064	1.03639	17.37	1.50

Table VII

Specific Volume of Cellulose in Aqueous Solutions of Urea at 25°

0.61927	0.99707	0.0	0.0
.61574	1.03263	13.00	2.50
.61577	1.03467	13.80	2.68
.61952	1.04531	17.60	3.46
.62557	1.04676	18.12	3.70
.61844	1.04706	18.25	3.73
.61826	1.04718	18.35	3.75

Table VIII

Specific Volume of Cellulose in Aqueous Solutions of Mannitol at 25°

0.61927	0.99707	0.0	0.0
.62252	1.01449	4.81	0.28
.62461	1.02908	8.75	0.53
.62498	1.03175	9.52	0.58
.62733	1.04784	13.61	0.86
.62744	1.04842	13.78	0.88

Discussion of Results

The specific volume of cellulose in helium gas is 0.640 cc./g. (Davidson[1] 1927) and in liquid water about 0.620 cc./g.; in the salt solution investigated the value falls between these two limits.

It has been suggested from evidence provided by many investigators, that the difference in specific volume of cellulose in helium gas and in water is due to compression of the water molecules on the cellulose surface, on the assumption that cellulose does not adsorb helium gas. It would thus appear that the salts exert a "decompressing" effect upon the adsorbed water layer.

It will be seen from the plot of specific volume against concentration for ammonium, sodium and potassium chlorides (Fig. 2) that the specific volume of cellulose passes through a maximum. A smooth curve was not obtained with lithium chloride solutions, presumably owing to the effective swelling powers of this salt on cellulose.

In order to account for this maximum the following tentative theory is proposed.

If we assume that water molecules are attached to the cellulose surface by hydrogen bonds with the hydroxyl groups of the cellulose, leading to the "close packed" or compression effect, then addition of salt ions provides polar centers which tend to disorganize the adsorbed water layer, causing a decompressing effect. The specific volume of cellulose, therefore, increases with increasing salt concentration.

The hydration sheath of, say, the potassium ion, is undergoing a continual and rapid interchange with the "free" water molecules present in the solution. Continual addition of salt will increase the ratio salt moles/water moles; *e.g.*, at 16% by weight in a solution of potassium chloride this ratio has the value of 1/23.2.

However, since both the cation and anion are capable of hydration, and as they are approximately the same size in this case, we may assume equal hydration of each ion, then the above ratio expressed in

$$\frac{\text{g. ions of salt}}{\text{g. mol. of water}} = \frac{1}{11.6}$$

If further salt is added to the solution, the activity of the water present may be so reduced as to be unable to satisfy the hydration requirements of the salt ions. Further addition of salt may then result in a direct linkage of the salt ions with the cellulose hydroxyl groups, and the specific volume of the cellulose decreases once more.

From purely geometrical considerations we can calculate the number of water molecules which can be packed around each ion, assuming that the effective radii of ions and of water molecule are as calculated by Goldschmidt[15] (1929). Calculation of the ratio of g. molecules of water to g. ions of cation at the concentration of maximum specific volume, assuming equal hydration of anion and cation in all cases, gives the following values

Ion	Radius, Å.	"Geometrical" no. of H_2O molecules
NH_4^+	1.42	12.0
Na^+	0.95	7.5
K^+	1.33	12.0
H_2O (mol.)	1.38	12.0

Salt	Concn. (wt. %)	Hydration ratio
NH_4Cl	14.3	8.9
NaCl	18.0	7.5
KCl	16.0	11.6

---

(15) V. M. Goldschmidt, *Trans. Faraday Soc.*, **25**, 253 (1929).

Although secondary hydration sheaths have been ignored, and equal hydration values for cation and anion have been assumed, agreement with the two alkali chlorides is excellent.

With the nitrates of ammonium and potassium, the specific volume does not pass through a maximum but rises almost linearly from zero concentration to the maximum concentration of the salt. This indicates that the activity of water in the ternary system nitrate–water–cellulose is not reduced sufficiently before the maximum solubility of the salt is reached at 25° for linkage to occur between the salt and cellulose.

Measurements were also carried out with a cellophane manufactured by the British Cellophane Company, using three organic substances as solute, *viz.*, hexamine, urea and mannitol.

This cellophane gave a slightly lower value for the specific volume in water, 0.61927 ml./g.

Hexamine provides a large non-polar molecule which by virtue of its chemical constitution should have little effect on the adsorbed water molecules on the cellulose surface. This is adequately confirmed by the fact that even though the solute concentration (molality) is of the same order of magnitude as other solutes used, there is little change in the specific volume of the cellulose.

Urea proved to be anomalous as this was the only solute used which yielded a minimum and a maximum in the specific volume for cellulose, and gave values lower than the specific volume of cellulose in water.

Mannitol was used as a substance providing a similar structure to the monomer unit in cellulose. A disaccharide was not used, because hydrolysis of the molecule to a monosaccharide catalyzed by the hydrogen ions of the carboxyl groups within the viscose sheet has been shown to occur by Heymann and McKillop[16] (1941). From previous considerations, because mannitol is capable of bonding large quantities of water by means of hydrogen bond formation, it should be capable of removing (or "decompressing") the adsorbed water layer on cellulose to a considerable extent, and results show that this occurs. The plot of specific volume *vs.* molality is linear (see Fig. 2) and this solute yields the highest specific volume for a given molality. It is also apparent that over the concentration range used, bonding with the cellulose structure has not occurred.

Specific volume measurements have been used for the determination of "bound" water in cellulose, by various authors.

Theoretical considerations leading to the calculation of "bound" water from such measurements demand that the concentration of the internal solution within the cellulose phase, and the external solution shall be the same. If this is not the case, then a correction must be applied to allow for the change in buoyancy brought about by the inequality of concentration.

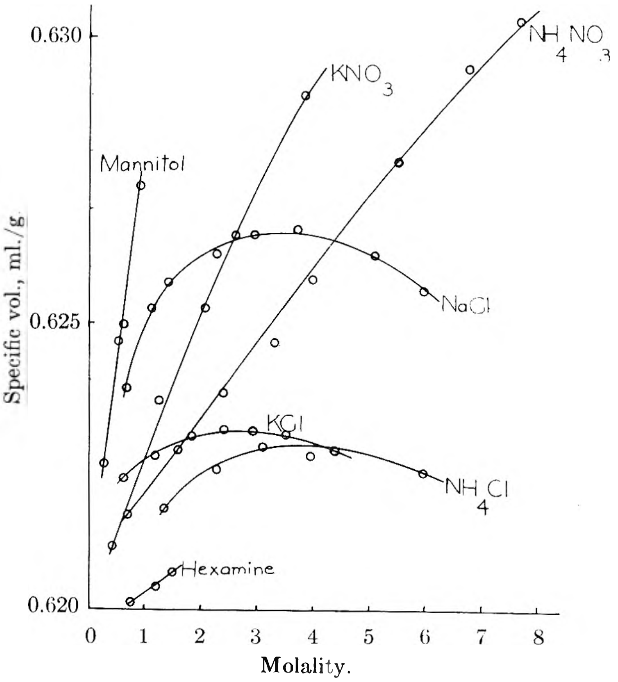

Fig. 2.

From preliminary measurements made by the authors, and by Farrar and Neale[8] (1952) by a direct analysis of the "internal" and "external" solution phases, it has been shown that a small preferential absorption of solute occurs from solution of the alkali chlorides, and consequently, if these solutes are used for "bound" water determinations, negative values should be obtained (see also Farrar, Neale and Williamson[17] (1951)).

It is also necessary that the solute used (often termed "reference" or "auxiliary" substance) shall be completely inert to the cellulose structure. From the few substances investigated, this does not appear to be a very common occurrence, and the reference substance must be chosen very carefully if the results for the "bound" water in cellulose are to have any significance.

Part II. (a) The Absorption of Water by Cellulose in the Presence of Inorganic Salts

Introduction

It has been shown by Farrar and Neale[8] (1952) that the ions of simple inorganic salts may be positively adsorbed from aqueous solution by cellulose. On account of the more or less evenly competitive forces of interaction between ion–water on the one hand and ion–cellulose on the other, such adsorption is not very pronounced. It was shown, however, that if water is replaced by some less polar solvent, very marked adsorption effects appear.

In order to arrive at a full understanding of energy relationships in such a system, it must also be necessary to take into account the solvent–cellulose interaction in the presence of salt ions.

The results obtained by Farrar and Neale[8] (1952) as well as those reported in Part I of the present paper are, in this respect, of limited value, since such experiments could not be carried out at a humidity below that of the saturated salt solution.

---

[16] E. Heymann and G. C. McKillop, THIS JOURNAL, **45**, 195 (1941).

[17] J. Farrar, S. M. Neale and G. R. Williamson, *Nature*, **167**, 524 (1951).

In the present work the adsorption of water from unsaturated vapor is used as the criterion, and measurements of adsorption have been made at varying pressures and temperatures.

The Apparatus and Experimental Method

The method used in measuring the adsorption of water by salt-impregnated cellulose was adapted from that first given by McBain and Bakr[18] (1926), who measured the adsorption of gases on charcoal using a quartz helical-spring.

A number of springs were made using a lathe developed by the British Rayon Research Association, but the greater part of the investigation was carried out using springs of the following specification supplied by the kindness of the Atomic Energy Establishment at Harwell.

Specification.—Extension = 11 cm./g.; fiber thickness = 0.023 cm.; coil diameter = 2.0 cm.; no. of coils/cm. = 10; unloaded length = *ca.* 5.8 cm.; average maximum load carried = 130 mg. Each spring was suspended in a glass tube from a glass bulb which rested on four indentations in the wall of the tube, and the salt-impregnated cellulose sample was hung from the spring using a small piece of platinum wire. The glass tube was fitted with a standard male glass joint and six of these tubes were connected to a manifold connected to a high vacuum pumping unit, capable of reducing the pressure in the system to about 10^{-5} mm.

It has been very adequately illustrated by Neiman and Kargin[19] (1939) that in experiments where adsorption of water by cellulose is occurring, the process is 100 to 1500 times more rapid in the absence of air.

In order to maintain a constant and known humidity within the system, sulfuric acid–water mixtures were used, the whole of the apparatus, except the pumping unit, being enclosed in an air thermostat maintained either at 25° or at 40 ± 0.3°.

The sulfuric acid–water mixture (of approximately known strength) was contained in a small detachable trap at the end of the manifold. The strength of the acid was determined by titration with standard alkali at the end of the experiment, and the corresponding humidity obtained from the tables in Perry's Handbook[20] (1949).

The use of a manometer filled with Apiezon oil proved unsuccessful for the direct measurement of the relative humidity, especially at the higher values, due presumably to absorption of water vapor by the oil.

The cellulose sample consisted of sheet cellophane (du Pont "300"), washed free from plasticizer (glycerol) with distilled water, then treated with very dilute acetic acid solution, and subsequently washed with distilled water until the washings were neutral, to remove any calcium or zinc ions remaining from the manufacturing process.

The sample was allowed to dry in the air and was hung by means of a small piece of fine platinum wire (whose weight was subsequently determined) on one of the calibrated springs. The sample was then dried under vacuum at 10^{-5} mm. pressure until a constant length of the spring was obtained (this operation normally took about 24 pumping hours). The sample was carefully removed, the platinum wire cut off and weighed, and the cellulose sample soaked in the requisite salt solution for about 12 hours. The cellulose was removed from the solution, blotted with sheet filter paper to remove excess surface liquid, and the weight of the dry salt-impregnated sample determined by again suspending from the spiral spring and drying under vacuum as before.

The samples were then exposed to the sulfuric acid–water mixture (which was degassed by the usual method of repeated freezing and pumping), and the equilibrium water regain measured by the determination of the spring length using a cathetometer accurate within 0.01 mm.

Equilibrium was attained within 24 hours.

Measurements could be taken much more rapidly than in other methods (see, for example, Urquhart and Eckersall[21] (1932)) where larger samples of cellulose are required.

Experimental Results

It was first necessary to show that the apparatus and the technique were capable of giving satisfactory and reproducible results, and so the adsorption isotherm of water vapor on cellulose alone was determined at 25° and the results compared with the values of Urquhart and Eckersall[21] (1932). Agreement was good, allowing for the fact that different samples of regenerated cellulose were used in the two sets of experiments, and it was found that the isotherm was accurately reproducible. The adsorption isotherms of cellulose in the presence of various quantities of sodium chloride and potassium chloride, were then measured at 25 and 40°. The values are recorded in Tables X and XII, expressed as moles H_2O absorbed per mole $C_6H_{10}O_5$.

The humidity range was restricted to the relative humidity of the corresponding saturated solution of the salt at the same temperature, since at this humidity the salt commences to dissolve and there was a danger of salt solution dripping off the sample and thus invalidating the adsorption measurements. These values are approximately

NaCl = 85.7% r.h.
KCl = 76.0% r.h.

Several of the isotherms were repeated, and it was found that the results were reproducible within the error of measurement (about ±0.009 mole water/mole $C_6H_{10}O_5$).

All determinations were for sorption of water vapor only, as the design of the apparatus did not permit desorption measurements to be made with convenience.

Owing to the fact that the differences in the regain at the lower humidities between the various cellulose–salt systems are rather small, and as all isotherms recorded follow very similar paths, it is not feasible to represent all the isotherms on one graph. In Figs. 3, 4, 5 and 6 the differences themselves, that is to say, the values of the quantity regain cellulose–salt minus regain cellulose, are plotted against the r.h. for NaCl and KCl at 25° and at 40°.

The two systems cellulose–sodium chloride and cellulose–potassium chloride will now be examined in the light of the information obtained.

The Cellulose–Sodium Chloride System.—An examination of the results for the various salt concentrations shows that the absorption of water is almost independent of the quantity of the salt present, within the humidity range 0–50%.

Where the curves in Figs. 3 and 4 cut the horizontal axis, the two systems, cellulose–sodium chloride and cellulose alone, have the same moisture regain, *i.e.*, $\Delta W = 0$. This point is attained by all the systems examined (except for the very small salt concentrations) both at 25 and 40°, at a moisture regain of 0.5 to 0.6 mole water/mole $C_6H_{10}O_5$. This corresponds to a relative humidity of 25–30%; beyond this value ΔW is positive, and this means, if we assume the cellulose is absorbing water to the

---

[18] J. W. McBain and A. M. Bakr, *J. Am. Chem. Soc.*, **48**, 690 (1926).

[19] R. S. Neimann and V. A. Kargin, *Promyshlennosti Organischeskoi Khimii*, **6**, 628 (1939).

[20] J. H. Perry, "Chemical Engineers' Handbook," McGraw-Hill Book Co., 3rd Ed., 1950, p. 168.

[21] A. R. Urquhart and N. Eckersall, *Shirley Inst. Mem.*, **11**, 75 (1932).

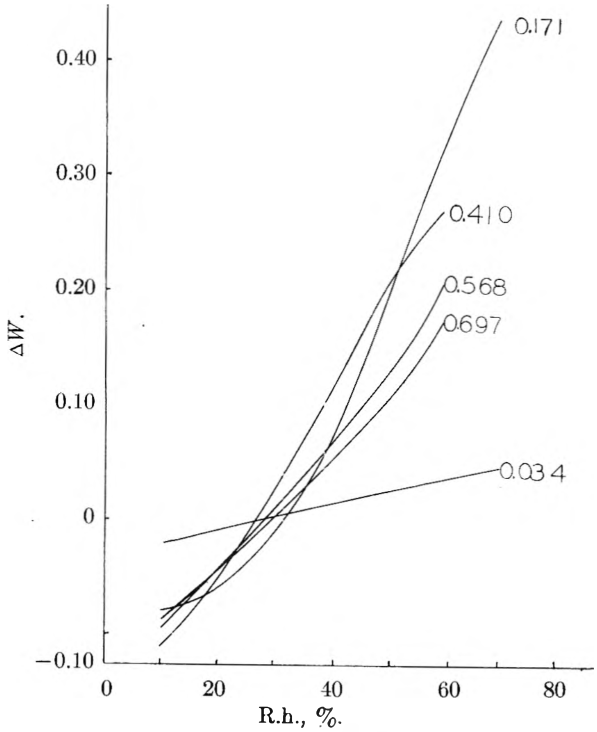

Fig. 3.—NaCl at 25°: figures indicate proportion of salt in moles/mole $C_6H_{10}O_5$.

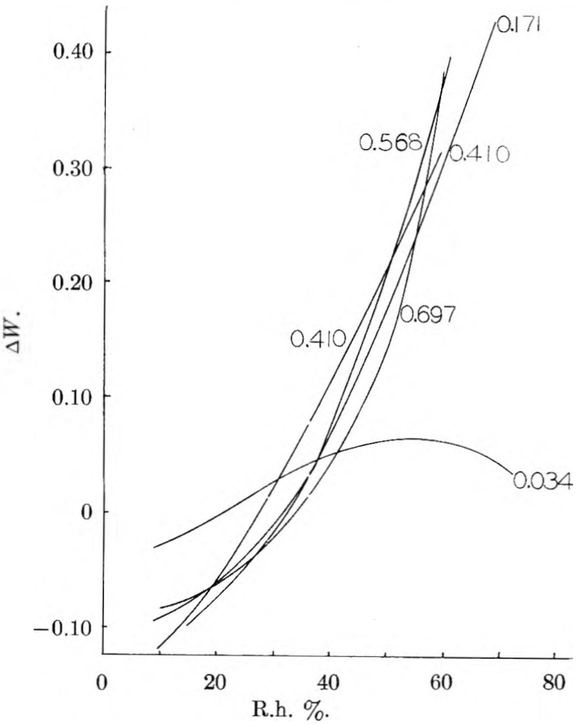

Fig. 4.—NaCl at 40°.

same extent as when in the free condition, that sodium chloride is absorbing water at relative humidities well below that corresponding to the saturated solution of the salt at the same temperature.

The Cellulose–Potassium Chloride System.—This system shows a similar behavior to that just outlined for sodium chloride. The point at which $\Delta W = 0$, however, appears to vary with temperature and gives the values: at 25°, 1.0 moles water/mole $C_6H_{10}O_5$; at 40°, 0.65 moles water/mole $C_6H_{10}O_5$, corresponding to 48–53% and 30–40% relative humidity, respectively.

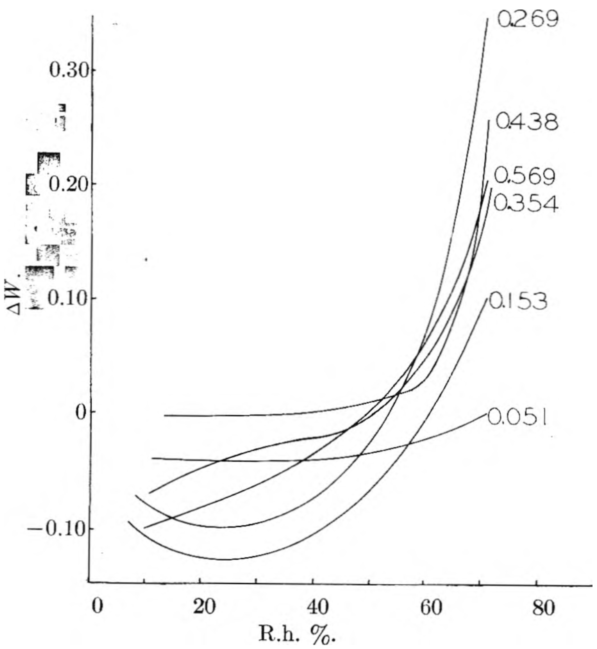

Fig. 5.—KCl at 25°.

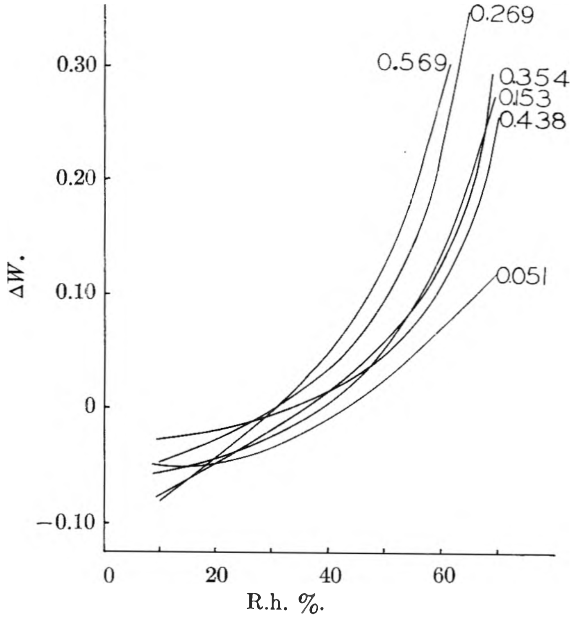

Fig. 6.—KCl at 40°.

Discussion of the Results

A striking feature in the behavior of the cellulose–alkali chloride systems, not previously observed (see O'Sullivan[22] (1947)) is the depression of the moisture regain by the salt present when the relative humidity is low. The regain is less than for cellulose alone at the same humidity by an approximately constant amount. This suggests that a constant amount of the salt present is adsorbed in competition with water in this particular humidity range.

(22) J. B. O'Sullivan, *J. Text. Inst.*, **38**, T.271 (1947).

TABLE IX

THE SORPTION OF WATER W (MOLES WATER/MOLE $C_6H_{10}O_5$) BY DU PONT CELLOPHANE "300" AT 25 AND 40°

R.h. (%)	Experimental values W	R.h. (%)	Interpolated values W	R.h. (%)	Experimental values W	R.h. (%)	Interpolated values W
25°				40°			
7.3	0.277	10	0.327	8.4	0.252	10	0.277
14.5	.392	20	.479	15.6	.360	20	.423
21.0	.495	30	.618	21.5	.441	30	.558
30.6	.693	40	.764	28.0	.536	40	.690
38.0	.729	50	.931	38.5	.671	50	.844
53.4	1.002	60	1.118	54.0	.918	60	1.035
62.4	1.161	70	1.379	60.7	1.053	70	1.272
75.7	1.616	75	1.589	70.4	1.278	75	1.485
				76.3	1.485		
				87.0	2.070		

TABLE X

THE SORPTION OF WATER W (MOLES WATER/MOLE $C_6H_{10}O_5$) BY DU PONT CELLOPHANE CONTAINING SODIUM CHLORIDE (MOLES/MOLE $C_6H_{10}O_5$) AT 25 AND 40°

NaCl concn., moles/mole R.h. (%)	R.h. (%)	0.034	0.171	0.410	0.568	0.697
		Experimental values, W				
		20°				
6.3	7.3	0.225	0.182	0.152	0.167	0.193
13.0	14.5	.360	.326	.298	.329	.338
19.4	21.0	.453	.430	.438	.446	.456
26.5	30.8	.563	.617	.666	.636	.636
34.0	38.0	.689	.778	.827	.786	.727
51.0	53.4	.981	1.224	1.219	1.136	1.148
60.3	62.4	1.148	1.526	1.444	1.397	1.341
69.0	75.7	1.382	2.133	...	...	...
		40°				
7.2	8.1	0.194	0.158	0.121	0.126	0.149
14.0	15.6	.326	.285	.283	.271	.284
20.0	21.5	.428	.378	.392	.381	.360
26.0	28.0	.518	.513	.534	.536	.495
36.5	38.5	.688	.738	.778	.751	.707
50.3	54.0	.918	1.155	1.121	1.193	1.116
56.5	60.7	1.016	1.350	...	1.440	1.418
62.8	70.4	1.165	1.737	...	...	...
69.0	...	1.290	...	...	...	...

TABLE XI

THE SORPTION OF WATER BY DU PONT CELLOPHANE CONTAINING SODIUM CHLORIDE (MOLES/MOLE $C_6H_{10}O_5$) AT 25 AND 40°

NaCl concn., moles/mole R.h. (%)	0.034	0.171	0.410	0.568	0.697
	Interpolated values of ΔW				
	25°				
10	−0.021	−0.080	−0.114	−0.093	−0.123
20	− .011	− .060	− .049	− .042	− .041
30	+ .002	− .008	+ .024	+ .009	− .002
40	+ .017	+ .073	+ .109	+ .064	+ .052
50	+ .029	+ .190	+ .210	+ .129	+ .133
60	+ .037	+ .330	+ .266	+ .207	+ .172
70	+ .048	+ .437	...	...	...
	40°				
10	−0.027	−0.088	−0.118	−0.117	−0.086
20	.000	− .063	− .055	− .074	− .063
30	+ .023	− .011	+ .023	− .020	− .023
40	+ .050	+ .068	+ .109	+ .072	+ .039
50	+ .065	+ .184	+ .200	+ .209	+ .141
60	+ .067	+ .304	+ .320	+ .376	+ .395
70	+ .045	+ .440	...	...	...

TABLE XII

THE SORPTION OF WATER W (MOLES WATER/MOLE $C_6H_{10}O_5$) BY DU PONT CELLOPHANE CONTAINING POTASSIUM CHLORIDE (MOLES/MOLE $C_6H_{10}O_5$) AT 25 AND 40°

KCl concn., moles/mole R.h. (%)	0.051	0.153	0.269	0.354	0.438	0.569
	Experimental values, W					
	25°					
6.7	0.207	0.165	0.194	0.207	0.268	0.171
13.6	.338	.264	.288	.319	.383	.279
20.8	.365	.356	.389	.442	.495	.410
39.8	.729	.666	.682	.747	.770	.738
46.1	.825	.774	.811	.851	.873	.864
63.5	1.181	1.247	1.382	1.280	1.287	1.300
75.3	1.648	1.706	2.090	1.990	1.985	2.192
	40°					
7.0	0.157	0.165	0.189	0.140	0.187	0.144
15.0	.303	.302	.338	.293	.332	.290
20.3	.387	.383	.411	.383	.428	383
38.0	.646	.654	.698	.666	.673	.698
54.0	.995	1.004	1.058	.981	.969	1.083
64.7	1.278	1.337	1.476	1.395	1.270	1.440
76.5	...	1.814	2.370	2.394	2 586	2.530

A similar observation has been made by Kanamaru and Nakamura[23] (1937) who found that there was a decrease in hygroscopicity of cellulose in the presence of aluminum chloride (or in effect aluminum hydroxide).

Beyond the humidity ranges mentioned above, the moisture regains for the cellulose–salt system are higher than for cellulose at the same humidity, and this may be explained by assuming that hydration of the dispersed salt ions present is occurring at these humidities.

The effect of the salt on the hygroscopic power of cellulose might be explained as shown in Fig. 7. In this figure, at low humidities (stage I) the salt ions are depicted as being bound to the cellulose hydroxyl groups by ion–dipole interaction, and therefore occupy sites to the exclusion of entering water molecules. When the pressure of water vapor is below a certain critical value this condition persists (stage II). Above a certain humidity value, however, the salt ion–cellulose attachment begins to break down in favor of cellulose–water and salt–water attachments, as shown in stage III.

The cellulose–water attachment is presumably a hydroxyl bond, whereas the salt ions are hydrated more or less in the same way as when dispersed in aqueous solution. This hydration occurs below the critical humidity associated with hydration of the macrocrystalline salt (85.7% r.h. for NaCl and 76.0% r.h. for KCl) because in the present system the salt ions are already dispersed on account of their attachment to the cellulose hydroxyl groups.

This is in agreement with conclusions reached from the specific volume measurements described in the first part of this paper.

It will be recalled that when the salt concentra-

---

[23] K. Kanamaru and T. Nakamura, *Kolloidzschr.*, **78**, 83 (1937).

TABLE XIII

SORPTION OF WATER BY DU PONT CELLOPHANE CONTAINING POTASSIUM CHLORIDE (MOLES/MOLE $C_6H_{10}O_5$) AT 25 AND 40°

KCl concn., moles/mole R.h. (%)	0.051	0.153	0.269	0.354	0.438	0.569
			Interpolated values of ΔW			
			25°			
10	−0.037	−0.107	−0.084	−0.068	0.000	−0.098
20	− .041	− .129	− .096	− .047	− .001	− .085
30	− .038	− .199	− .092	− .028	+ .002	− .053
40	− .035	− .098	− .071	− .014	+ .006	− .019
50	− .030	− .072	− .025	− .007	+ .014	+ .005
60	− .020	+ .019	+ .104	+ .048	+ .057	+ .074
70	+ .003	+ .109	+ .354	+ .208	+ .265	+ .210
			40°			
10	−0.050	−0.052	−0.034	−0.078	−0.027	−0.079
20	− .043	− .046	− .014	− .043	− .015	− .050
30	− .033	− .023	− .000	− .014	.000	− .007
40	− .002	+ .005	+ .039	+ .012	+ .016	+ .055
50	+ .050	+ .052	+ .096	+ .044	+ .045	+ .134
60	+ .116	+ .176	+ .221	+ .136	+ .079	+ .235
70	+ .121	+ .276	+ .508	+ .465	+ .258	+ .411

tion is continually increased in the cellulose salt-water system and the amount of water present becomes insufficient fully to satisfy the salt hydration requirements, bonding occurs between the salt and the cellulose structures.

Since it is only the salt present which is directly adsorbed which is displaced, this condition should be dependent on the surface area of the cellulose, and not on the quantity of salt present. This has been shown experimentally, the humidity at which $\Delta W = 0$, being virtually independent of the salt content.

(b) The Sorption of Water by Dyed Cellulose

Experiments on Dyed Cellulose.—Following the experimental evidence obtained on the adsorption of water by cellulose containing salt, the general conclusions drawn suggest that the salt ions occupy active sites in the cellulose structure, and are then gradually displaced by water, and finally hydrated.

It seemed that one might expect a similar sort of behavior with dyed cellulose, and as there has been a considerable amount of conjecture regarding the general arrangement of the adsorbed dye molecule on the cellulose structure, an analysis of the water adsorption isotherms on dyed cellulose might give information on this problem.

The quantity of dye present in the cellulose sample was measured by two methods (a) from the increase in weight of the sample after dyeing and (b) by removal of the dye from the sample using aqueous pyridine, and a colorimetric determination of the dye concentration of the resulting solution. Agreement between the two methods was good.

The dye used was Chlorazol Sky Blue FF (Colour Index 518) and dyeing of the cellulose was carried out at 90–95°, using a dye-bath concentration of 0.05 g./l.; the take up of dye was varied by adding different quantities of sodium chloride (5, 12.0 and 35 g./l.) to the dye solution.

The dyed sample was freed from salt by washing with copious quantities of cold distilled water until the washings gave no test with silver nitrate.

It was also necessary to determine the adsorption isotherm of an undyed sample of cellulose which had undergone the same "heat" treatment as the dyed

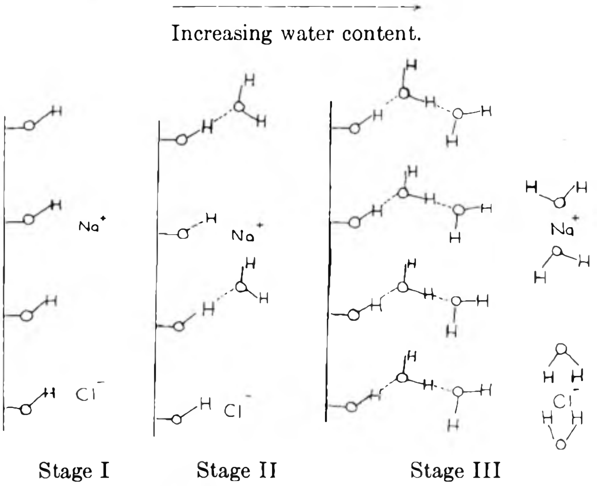

Fig. 7.—Schematic representation of changes occurring during the sorption of water by salt impregnated cellulose: I, dry cellulose containing salt; II, ΔW negative, quantity of water present smaller than that required to form a monolayer; III, ΔW positive, multimolecular layers of water formed, salt displaced and hydrated.

TABLE XIV

THE SORPTION OF WATER W (MOLES WATER/MOLE $C_6H_{10}O_5$) BY UNDYED DU PONT CELLOPHANE AT 25 AND 40°

R.h. (%)	Experimental values W	R.h. (%)	Interpolated values W	R.h. (%)	Experimental values W	R.h. (%)	Interpolated values W
	25°				40°		
7.3	0.277	10	0.327	8.4	0.252	10	0.277
14.5	.392	20	.479	15.6	.360	20	.423
21.0	.495	30	.618	21.5	.441	30	.558
30.6	.693	40	.764	28.0	.536	40	.690
38.0	.729	50	.931	38.5	.671	50	.844
53.4	1.002	60	1.118	54.0	.918	60	1.035
62.4	1.161	70	1.379	60.7	1.053	70	1.272
75.7	1.616	75	1.589	70.4	1.278	75	1.485
				76.3	1.485		
				87.0	2.070		

TABLE XV

THE SORPTION OF WATER W (MOLES WATER/MOLE $C_6H_{10}O_5$) BY DYED DU PONT CELLOPHANE AT 25 AND 40°

% dye in sample R.h. (%)	0	1.09	1.68	3.42
	Experimental values W			
		25°		
6.8		0.240	0.235	0.248
14.7		.409	.388	.400
18.6		.478	.456	.468
25.6		.576	.566	.567
33.8		.703	.692	.694
43.4		.842	.828	.828
52.3		.974	.964	.972
61.0		1.132	1.098	1.121
67.4		1.279	1.240	1.260
73.2		1.470	1.450	1.445
85.0		2.070	2.030	2.103
		40°		
8.0		0.231	0.203	0.196
13.9		.343	.311	.311
20.0		.442	.401	.405
26.5		.540	.486	.500
34.4		.648	.622	.617
45.6		.815	.784	.804
52.8		.936	.890	.925
60.3		1.062	1.018	1.045
73.8		1.410	1.365	1.365
84.8		1.910	1.922	1.980
	Interpolated values W			
		25°		
10	0.327	0.317	0.302	0.315
20	.479	.491	.482	.486
30	.618	.645	.635	.642
40	.764	.792	.783	.784
50	.931	.951	.927	.932
60	1.118	1.120	1.081	1.100
70	1.379	1.355	1.323	1.335
75	1.589	1.537	1.521	1.521
		40°		
10	0.277	0.274	0.249	0.235
20	.423	.441	.407	.410
30	.558	.588	.558	.560
40	.690	.731	.702	.711
50	.844	.887	.846	.869
60	1.035	1.058	1.012	1.038
70	1.272	1.287	1.232	1.245
75	1.485	1.454	1.409	1.413

samples, *i.e.*, heated in water at 90–95° for two hours.

The adsorption of water vapor by this sample differed slightly from that of cellophane sheet which had not been heated in water.

Water adsorption isotherms on three dyed samples were determined at 25 and 40°. The values obtained are given in Tables XIV and XV.

It appears that there is no very marked difference in hygroscopicity between dyed and undyed cellulose.

ION-EXCHANGE MEMBRANES. II. ION TRANSFER RATES[1]

BY R. J. STEWART AND W. F. GRAYDON

Department of Chemical Engineering, University of Toronto, Toronto, Canada

Received August 23, 1955

The rates of cation transfer for the sodium–hydrogen, and the calcium–hydrogen exchange across various polystyrenesulfonic acid membranes have been measured. Anion transfer rates for the chloride ion have also been estimated. In all determinations the interdiffusion rates were measured directly using a modified diaphragm diffusion cell. The results are discussed in terms of the relative contribution of membrane resistance and liquid–film resistance to ion transfer. Cation diffusion coefficients are correlated empirically with membrane characteristics. Anion transfer rates are considered in terms of the Donnan membrane equilibrium and membrane potentials.

Introduction

The membranes described in this report were prepared by the copolymerization of the propyl ester of *p*-styrenesulfonic acid with divinylbenzene and the subsequent hydrolysis of the polymer to produce polystyrenesulfonic acid. This method permitted the preparation of membranes of various capacities with the sulfonate groups distributed throughout the bulk of the membrane. The method of preparation also permitted independent variation of the divinylbenzene content of the membrane.

Previous determinations of ion-diffusion coefficients in ion-exchange materials have been made by the radiotracer spread method, by the electrical conductance method, and by radiotracer exchange methods.[2-5] These methods in general yield self-diffusion coefficients rather than the more useful interdiffusion coefficients. The method of calculation of interdiffusion coefficients from self-diffusion coefficients is not immediately obvious.[4] By contrast, the ion-exchange diaphragm cell method used in this work yields values of interdiffusion coefficients directly. In addition the ion-transfer rates may be measured by simple solution analysis. The values of interdiffusion coefficients may be obtained from the analytical data without curve fitting.

---

(1) This report is abstracted from the thesis of R. J. Stewart submitted for the degree of Master of Applied Science, University of Toronto, September, 1953.

(2) G. E. Boyd, W. Adamson and L. S. Myers, *J. Am. Chem. Soc.*, **69**, 2836 (1947).

(3) G. E. Boyd, B. A. Soldano and O. D. Bonner, THIS JOURNAL, **58**, 456 (1954).

(4) K. S. Spiegler and C. D. Coryell, *ibid.*, **57**, 687 (1953).

(5) M. Tetenbaum and H. P. Gregor, *ibid.*, **58**, 1156 (1954).

Experimental

Membranes.—The membranes used in this work were prepared by the methods described previously.[6,7] The membrane characteristics of capacity, nominal cross-linking and moisture content have been given.[7] The same membranes as described[7] have been used in this work and are designated in the same way by two digits each, the second of which designates in each case the mole per cent. divinylbenzene used in the preparation of the membrane. The first digit represents the exchange capacity of each membrane to the nearest integer.

Cation Diffusion Measurements.—The diffusion cell was a double-ended glass or Lucite cell consisting of two stoppered compartments, each of 11.5 ml. volume, separated by an ion-exchange membrane. The membrane was supported between two gaskets of 2.00 cm. internal diameter. The two flanged halves of the cell were bolted together. By means of a pipet 10-ml. portions of 0.1 N sodium nitrate and 0.1 N hydrochloric acid were placed in the cell compartments. The stoppered cell was then shaken mechanically at a measured rate in an air thermostat at 25 ± 1°. After 15 minutes, the solutions were removed and analyzed by acidimetric titration. This procedure was repeated until agreement between consecutive runs was obtained. The data for the initial runs were discarded. The same procedure was then repeated for various shaking rates and time intervals. Calcium–hydrogen interdiffusion data were obtained in a similar fashion using 0.1 N (0.05 M) calcium nitrate solution and 0.1 N hydrochloric acid solution.

Anion Diffusion Measurements.—The procedure used was similar to that described above except that all runs were for a shaking time of one hour. At the end of each run the nitrate solution was analyzed for chloride by potentiometric titration.

Results and Discussion

The data which have been obtained for the transfer of hydrogen ion to the sodium nitrate solution during a 15-minute interval as a function of the shaking rate are given in Fig. 1. The plots for various membranes are similar in shape. All show a region at low shaking rates which is characterized by an increasing rate of ion transfer, and a region at higher shaking rates for which the ion-transfer rate is independent of the shaking rate. This independence of shaking rate has been checked for several membranes up to 750 oscillations per minute and the rate of ion transfer has been found to be constant within a few per cent. The assumption may be made that at high shaking rates the resistance to ion transfer in the liquid is negligible and that at low shaking rates, below the break in each plot, the ion-transfer rate is determined by both liquid film and membrane resistances. That this assumption is consistent with the data obtained is illustrated by the calculation below.

A sufficient approximation may be obtained for the interdiffusion coefficient across the membrane at high shaking rates using the unintegrated diffusion equation

$$D_M = \frac{V \Delta C_1 L_M}{A C_{1t} \Delta t} \tag{1}$$

where

A = gross surface area of the membrane (3.14 cm.^{2})
V = vol. of soln. on either side of the membrane (10 cc.)
L_M = thickness of membrane as measured by micrometer in cm.
Δt = shaking time (900 sec.)
ΔC_1 = change in concn. of either ion species on either side of the membrane during the shaking time interval
C_{1t} = concn. of either ion species at the conclusion of the run in the compartment soln. more concd. with respect to that species. This quantity is the av. concn. difference across the membrane during a run
D_M = apparent interdiffusion coefficient for sodium-hydrogen ions across the membrane. The term "apparent" is used because this value is based on the concn. gradient between the liquids at the membrane interfaces rather than the gradient in the membrane

By means of equation 1 values of D_M may be estimated for each membrane from the observed flux at high shaking rates. These values of D_M permit an estimation of the concentration difference across the assumed liquid films at low shaking rates.

$$\Delta C_L = \frac{C_{1t}}{2} - \frac{L_M V \Delta C_1}{2 D_M A \Delta t} \tag{2}$$

where ΔC_L represents the average concentration difference across either of the two liquid films at the membrane surface. Thus the thickness of the liquid film layer may be estimated.

$$L_L = \frac{D_L}{2}\left(\frac{A \Delta t C_{1t}}{V \Delta C_1} - \frac{L_M}{D_M}\right) \tag{3}$$

where

L_L = liquid film thickness in cm.
D_L = interdiffusion coefficient in water, estimated as 2.4 × 10^{-5} cm.^{2}/sec.

The values for the liquid layer thickness and the concentration gradient difference for various membranes and various shaking rates are given in Fig. 2 and Table I.

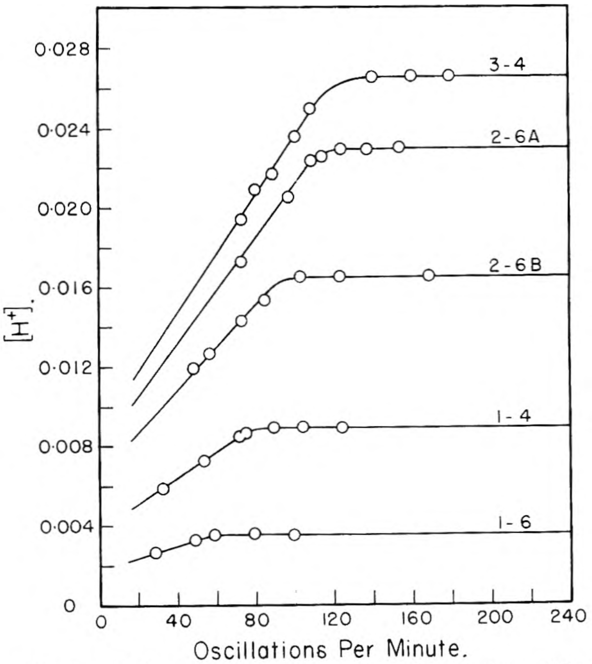

Fig. 1.—Cation transfer at various shaking rates. [H$^+$] is the acid concentration in the solution originally 0.1 N NaNO$_3$ after a 15-min. shaking time; 25.0°; acid solution 0.1 N HCl.

It may be noted that the liquid film thickness calculated is independent of the membrane and the flux and is determined by the shaking rate. The

---

[6] I. H. Spinner, J. Ciric and W. F. Graydon, *Can. J. Chem.*, **32**, 143 (1954).

[7] W. F. Graydon and R. J. Stewart, THIS JOURNAL, **59**, 86 (1955).

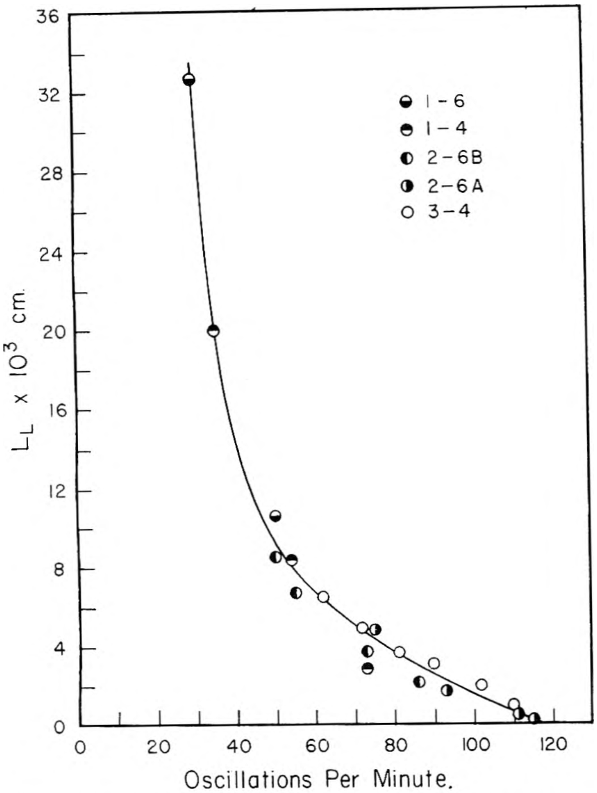

Fig. 2.—Liquid layer thickness at various shaking rates.

values obtained indicate that a hydrodynamic limit is being approached but that it is by no means attained at a shaking rate of 110 oscillations per minute. The values of ΔC_L are of more direct interest. These values are dependent on flux as well as liquid-film thickness. The observed flux is expected to be essentially independent of shaking rate when the value of ΔC_L becomes small relative to the over-all concentration difference. Thus the break in plot on Fig. 1 occurs at a higher shaking rate the greater D_M. In Table I it may be seen, for example, that ΔC_L is small for the 1–6 membrane relative to the 2–6B membrane at the shaking rate of 50 o.p.m. although the liquid film thickness has been assumed the same in both cases.

TABLE I

LIQUID FILM CONCENTRATION DECREASE

Shaking rate min.$^{-1}$	ΔC_L, moles/l. 1–6	1–4	2–6B	2–6A	3–4
30	0.0135				
35		0.0176			
50	0.0053		0.0152		
55		0.0092	.0127		
73		0.0033	.0079	0.0124	0.0141
86			.0048		
92				0.0053	0.0099
110				0.0014	0.0038

All of the measurements of interdiffusion coefficients reported below were obtained at shaking rates greater than 160 o.p.m. Each diffusion coefficient is the average of the values obtained for five or six runs of different duration up to one hour.

The data were evaluated using the integrated form of the diffusion equation given by Gordon.[8]

$$\ln \frac{\Delta C_t}{\Delta C_0} = -kt \qquad (4)$$

where

ΔC_0 = initial concn. difference between the 2 bulk soln. at time zero

ΔC_t = final concn. difference between the 2 bulk soln. at time t

k = constant containing the diffusion coefficient and terms describing the geometry of the cell as shown in eq. 5

The linearity of the plots as shown in Fig. 3 indicates the adherence of the data obtained to an equation of the form of equation 4. The constant k in equation 4 has been analyzed according to equation 5[8]

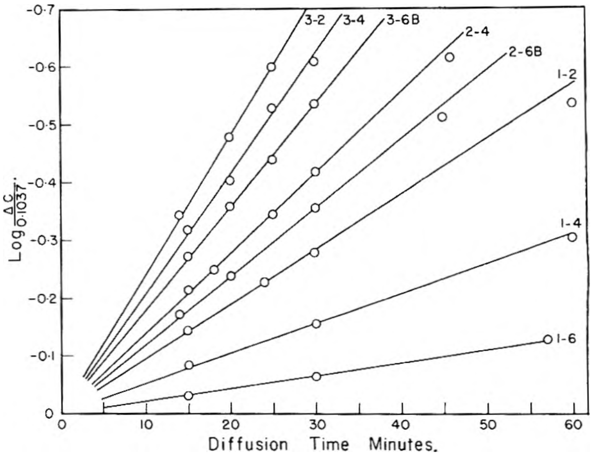

Fig. 3.—Sodium–hydrogen interdiffusion across various membranes; 25°; approximately 0.1 N solution concentrations.

$$k = 2D_M A/VL_M \qquad (5)$$

where the symbols have the same significance as previously. This integrated equation has been used to calculate the values of apparent membrane interdiffusion coefficients as given in Table II. These values are integral diffusion coefficients.

Although it might be expected that the diffusion coefficients would be dependent on the ion composition of the membrane, the linearity of the plots in Fig. 3 indicates that this dependence is small over most of the range studied. Differential diffusion coefficients measured in this Laboratory indicate that composition dependence is small for the sodium–hydrogen interdiffusion over this range but may be appreciable for systems involving large ions.

The values for anion diffusion coefficient listed in Table II have been calculated directly from the chloride-ion flux and the concentration difference which was assumed to be a constant, 0.1037 mole/l. These values may be expected to be somewhat high because the bi-ionic potential gradient has been neglected. At any rate the values are indicative only because of the very small anion flux. After one hour chloride concentrations of the order of 10^{-4} N were found in the nitrate solution.

[8] A. R. Gordon, *Ann. N. Y. Acad. Sci.*, **46**, [5] 285 (1945).

TABLE II

APPARENT MEMBRANE INTERDIFFUSION COEFFICIENTS[a]

25.0°, solution concentrations 0.1 N

Membrane no.	$D_{Na^+-H^+}$, cm.²/sec. × 10⁵	D_{Cl^-}, cm.²/sec. × 10⁸	$D_{Ca^{++}-H^+}$, cm.²/sec. × 10⁶
1–6	0.46	0.88	
1–4	0.97	1.8	
1–2	2.9	22	
2–6A	3.8	8.3	1.9
2–6B	3.1		
2–4	4.1	18	2.3
2–2	6.1	57	
3–6A	6.3	16	3.6
3–6B	5.8	16	
3–4	6.5	50	4.6
3–2	7.4	215	

[a] The word "apparent" is used since these values are calculated on the basis of the liquid concentrations rather than membrane concentrations.

The values of apparent diffusion coefficients as given in Table II are derived directly from the analytical data and are subject to no assumptions as to the diffusion mechanism in the membrane. These values are not comparable to membrane self-diffusion coefficients. Values that are more nearly comparable may be obtained by assuming that the effective concentration gradient is the concentration gradient for the ion species in the membrane. Because of the high effective concentration in the membrane this concentration gradient may be of the order of 20 to 30 times the gradient between the two solutions. The method of estimating the gradient in the membrane is also a matter for speculation. However, without regard to the precise method of computation it is apparent that the concentration gradient in the membrane will be relatively insensitive to external solution concentrations. The data given in Table III illustrate this effect.

TABLE III

CORRECTED DIFFUSION COEFFICIENTS FOR A 2–6 MEMBRANE, 25.0°

Soln. concn. total, moles/l.	Membrane concn., meq./g. water	Apparent $D_{Na^+-H^+}$ cm.²/sec.	Cor. membrane interdiffusion coefficients, cm.²/sec.
0.10	3.70	3.3×10^{-5}	8.9×10^{-7}
0.30	4.02	1.2×10^{-5}	9.0×10^{-7}
0.50	4.35	0.78×10^{-5}	9.0×10^{-7}

It will be noted that the apparent diffusion coefficients show a considerable dependence on solution normality indicating that the flux is essentially independent of the external solution concentration. However, if these apparent diffusion coefficients are multiplied by the ratio of the solution concentration to the membrane concentration, the products, which may be considered as membrane interdiffusion coefficients, are quite independent of external solution concentration and are of the same order of magnitude as reported self-diffusion coefficients for polystyrenesulfonic acid resins. For example, Boyd, Soldano and Bonner give a value of 8.44×10^{-7} cm.²/sec. for the self-diffusion of sodium in a resin of capacity 1.91 meq./g. and 8.6% D.V.B.

In Table IV are listed the ratios of the interdiffusion coefficients for sodium–hydrogen to those for chloride. These values have been compared to the values estimated on the basis of an ideal Donnan equilibrium. Assuming that activity coefficients are unity and solution mobility ratios for the sodium and chloride ions we would expect

$$[\mathrm{Cl}^-]\mathrm{m} = \frac{[\mathrm{NaCl}]^2\mathrm{s}}{[\mathrm{RSO_3}^-]_\mathrm{m}}$$

$$\frac{[\mathrm{Na}^+]\mathrm{m}}{[\mathrm{Cl}^-]\mathrm{m}} = \frac{[\mathrm{RSO_3}^-]^2{}_\mathrm{m}}{[\mathrm{NaCl}]^2\mathrm{s}}$$

$$\frac{D_{\mathrm{Na}^+}}{D_{\mathrm{Cl}^-}} = \frac{[\mathrm{RSO_3}^-]^2}{[\mathrm{NaCl}]^2{}_\mathrm{s}} \times \frac{1.35}{2.03}$$

where [ ] indicates concentration in gram ions or gram moles per liter and subscripts m and s refer to membrane and solution, respectively.

The values calculated for this expression are given in Table IV. The agreement in general is within the limits of error of the chloride analyses. However, for the 3–4 and the 3–2 membranes the deviations are very large. For these membranes a gross mechanical leak may be suspected.

TABLE IV

RELATIVE ANION–CATION DIFFUSIVITIES

Membrane no.	Membrane concn. $[\mathrm{RSO_3}^-]$, meq./g. water	$\left(\frac{D_{Na^+}}{D_{Cl^-}}\right)_{\text{calcd}}$	$\left(\frac{D_{Na^+-H^+}}{D_{Cl^-}}\right)_{\text{obsd}}$
1–6	3.33	740	522
1–4	3.16	670	540
1–2	1.90	243	132
2–6A	3.20	692	460
2–4	2.65	471	233
2–2	1.58	168	106
3–6A	3.01	610	403
3–6B	3.11	654	374
3–4	2.17	315	77
3–2	1.37	126	35

The data given in Table IV are also of interest in connection with the interpretation of membrane potentials. The values of diffusion coefficients are not completely suitable for the estimation of

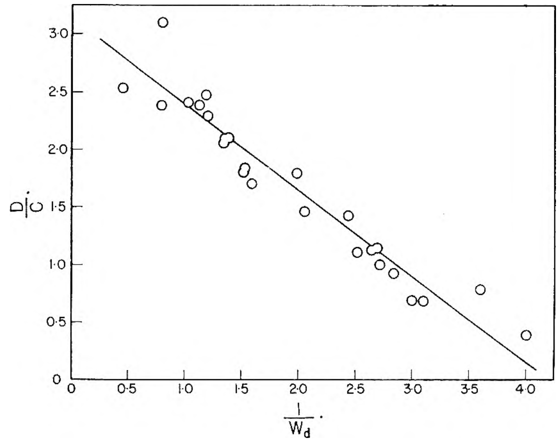

Fig. 4.—Empirical correlation of interdiffusion coefficients. D is interdiffusion coefficient for sodium–hydrogen ions in cm.²/sec.; 25.0°; solution concentration approximately 0.1 N. C is membrane capacity in meq./g. dry hydrogen form. W_d is the moisture content of the membrane expressed as grams of water per gram of dry hydrogen resin.

sodium chloride membrane transport numbers because of the simultaneous hydrogen-ion diffusion. However, this error will be less in the diffusion coefficient ratio than in the individual values, and in any case should be less than a factor of two. On the basis of the diffusion coefficient ratios in Table IV, membrane chloride transport numbers may be estimated to be between 0.002 and 0.004 for the six membranes of lowest chloride-ion transfer. Membrane potentials for these membranes[7] show considerably larger deviations from ideality than would be expected for anion transport numbers of this order. Thus the ion-transfer rate data provide confirmation for the previous conclusion[7] that the transfer of water electroösmotically is a major factor in the deviation of membrane potentials from ideal values.

Since it is difficult to prepare a membrane of precisely a given capacity or cross-linking, membranes cannot be reproduced identically. For this reason, it is of considerable usefulness in the routine preparation of ion-exchange membranes to have an empirical correlation of the experimental data. Preferably such a correlation should involve only quantities which may be measured with some precision. The sodium–hydrogen ion-transfer rates may be correlated empirically as shown in Fig. 4. The experimental points have been obtained by a number of workers in this Laboratory using membranes prepared from different batches of ester monomer and divinylbenzene. The membranes used were of capacity between one and three milliequivalents per gram, and between 2 and 12 mole % divinylbenzene.

Acknowledgment.—The authors are indebted to the National Research Council, Ottawa, and to the Advisory Committee on Scientific Research, University of Toronto, for financial support.

THE ACTIVITY COEFFICIENTS OF HYDROCHLORIC ACID IN METHANOL–WATER MIXTURES

By I. T. Oiwa

Department of Chemistry, Faculty of Science, Tohoku University, Sendai, Japan

Received August 30, 1955

Electromotive force measurements were made on cells: H_2(1 atm.)/HCl(m), $X\%$ CH_3OH, $Y\%$ H_2O/AgCl–Ag over the molalities of hydrochloric acid from 1×10^{-3} to 0.1, at 25° and methanol contents of 0, 20, 40, 60, 80 and 90 in weight per cent. From the data obtained, standard potentials of silver–silver chloride electrode and ion-size parameters, 5.6, 4.6, 4.3, 4.3, 5.3 and 5.5 Å., respectively, in these solvents are determined. The activity coefficients of hydrochloric acid, which are referred to unity at infinite dilution in pure water, are calculated. Further, for the free energy change of the reaction transferring hydrochloric acid of unit activity from aqueous solution to the methanol–water mixture, equations are introduced which consider the change of ionic solvation and proton transfer from water to methanol molecule over the electrostatic energy change. These equations elucidate the experimental results. The proton transfer is accompanied by an increase of free energy of 0.0834 e.v. per mole of hydrochloric acid.

I. Introduction

It seems desirable, in elucidating the various experimental results of non-aqueous solution of electrolytes to determine the activity of strong electrolytes in non-aqueous solution with the same scale as that in aqueous solution.

In this study electromotive forces of the reversible cells

$$H_2(1\text{ atm.})/HCl(m),\ X\%\ CH_3OH,\ Y\%\ H_2O/AgCl\text{–}Ag \qquad (1)$$

were measured, and the standard potentials of the silver–silver chloride electrode were calculated.

The activity coefficients of hydrochloric acid of concentration C, designated by f, in any methanol–water medium, are given by the relation

$$f = yf_c \qquad (2)$$

where y is the activity coefficient of the acid at zero concentration in the non-aqueous solvent referred to unity at the standard state (aqueous solution at infinite dilution) and f_c is that at concentration C referred to unity at the reference state (each particular solution at infinite dilution), were determined.[1]

The free energy change $G(C)$ at the time of transferring 1 mole of free ion of vapor phase into a solution of concentration C is shown by the equation[2]

$$G(C) = G_s^0 + G_{i,s}(C) + G_i(C) \qquad (3)$$

where G_s^0 and $G_{i,s}$ are the free energy changes of the interaction between the ion and the solvent, and G_i, that between ions. $G_{i,s}$ is a portion of G_s, which changes with concentration by ionic atmosphere. G_i and $G_{i,s}$ become zero at infinite dilution. Therefore, G_s^0 shows the ionic state of each solution at infinite dilution. Correlations of G_s^0 with the properties of the solvent are examined.

II. Experimental

Material Used.—Methanol, Extra Pure Grade Reagent of the Wako Pure Chemical Industries (d_{20} = 0.7916, n^{18}_D 1.330) was distilled. The amount of aldehydes was determined as less than 10^{-5} mole/l. by the polarographic method. Distilled water passed through a column of ion-exchange resin ($\kappa < 1 \times 10^{-6}$ ohm^{-1} cm.$^{-1}$) was used. Hydrochloric acid, Special Reagent Grade of Mitsubishi Chemical Industries, was distilled twice at a constant pressure. The concentration was calculated from the Foulk table[3] and also determined by the gravimetric method; the results agreed with an accuracy of 0.01%.

Cell Solutions.—An aqueous stock solution of hydrochloric acid of one molal concentration was prepared and

---

(1) I. T. Oiwa, *J. Chem. Soc. Japan*, **75**, 1047 (1954).

(2) *Cf.* R. H. Fowler and E. A. Guggenheim, "Statistical Thermodynamics," Cambridge University Press, 1939, p. 383.

(3) C. W. Foulk and M. Hollingsworth, *J. Am. Chem. Soc.*, **45**, 1220 (1923).

diluted by weight to the desired concentrations of the cell solution. The molality of hydrochloric acid in the cell solution, m, ranged from 1×10^{-3} to 0.1 mole of hydrochloric acid per 1000 g. of the methanol–water mixture, and the methanol contents, X, were varied to 0, 20, 40, 60, 80 and 90 in weight per cent.

Silver–Silver Chloride Electrodes.—A mixture of 10% silver perchlorate and 90% silver oxide was made into a paste with water, painted on a platinum spiral fused in a glass tube, heated at 550° for 20 minutes, and allowed to stand in the cell solution for 24 hours.[4] Electrodes whose potentials agreed within ±0.05 mv. in methanol–water media (±0.01 mv. in aqueous media) were used for the measurement.

Hydrogen Electrodes.—A platinized platinum strip of 1 cm. × 2.5 cm. was used with the platinum black made as thin as possible.

The Cells.—H-type cells with a vacuum cock between the two electrodes, attached with two Linhart-type saturator tubes,[5] were employed. The cells were immersed in 1% carbon tetrachloride solution of Dow-Corning No. 200 silicone fluid, drained, and heated at 300° for one hour.

Measurement of Electromotive Force.—At least two measurements were made with every solution. The electromotive force reached the equilibrium 1–2 hours after passage of hydrogen was started, and it showed a definite value for at least 12 hours, with a variation of less than ±0.1 mv.

Density of the Solvent.—An Ostwald-Sprengel type pycnometer of 25-ml. capacity was used for the measurement.

All measurements were carried out at 25.00°.

The density (d_0), dielectric constant[6] (D) and total vapor pressure[7] (P), of the solvents are shown in Table I (N is the mole fraction of methanol).

TABLE I

PROPERTIES OF THE SOLVENT (25.00°)

Wt. % MeOH	N	d_0	D[a]	P,[b] mm.	p_w, mm.
0	0.0000	0.9971	78.48	23.76	23.76
10	.0588	.9799	74.18	33.7	22.4
20	.1232	.9645	69.99	43.8	21.0
40	.2725	.9319	60.94	63.1	18.1
60	.4574	.8914	51.67	80.2	14.6
80	.6941	.8425	42.60	99.7	9.5
90	.8350	.8156	37.91	111.8	4.7
94.2	.9013	....	35.76	117.8	2.96
100	1.0000	.7864	32.66	126.6	0

[a] Ref. 6. [b] Interpolated the data of ref. 7.

III. Results

Table II gives the observed values of the electromotive force of the cells, E, corrected for the hydrogen pressure to one atmosphere. The values are taken as positive when the positive charge moved from left to right.

TABLE II

ELECTROMOTIVE FORCE OF THE CELLS (1)

Aq.		20%		40%		60%		80%		90%	
m	E, v.	m	E, v.	m	E, v.	m	E, v.	m	E, v.	m	E, v.
0.000991	0.57935	0.001142	0.5597	0.000991	0.5551	0.000991	0.5404	0.000991	0.5088[a]	0.001267	0.4626
.001982	.54443	.001798	.5370	.001982	.5202	.001982	.5059[a]	.001982	.4746[a]	.001889	.4423
.005011	.49806	.005027	.4861	.005300	.4720	.005535	.4556	.005011	.4301	.004759	.3977
.010024	.46378	.01042	.4502	.010024	.4408	.009332	.4310	.010024	.3977	.01012	.3632
.02004	.42988	.01938	.3202	.02000	.4076	.02316	.3868	.02344	.3583	.02065	.3306
.02636	.41651	.04894	.3757	.02138	.4056	.02991	.3765	.05318	.3214	.04172	.2997
.05021	.38530	.10202	.3407	.05000	.3645	.05825	.3462	.08902	.2987	.05417	.2881
.10284	.35076			.09953	.3333	.06283	.3428			.07252	.2757
						.10310	.3203			.09404	.2642

[a] A. Amano, unpublished data.

IV. Standard Potentials of the Silver–Silver Chloride Electrode

The standard potential, $E_{\mathrm{m}}^{\circ *}$, of the silver–silver chloride electrode is determined by using the function E' of the equation,[2,8a]

$$E' = E + 2k \log m - 2kS_{(\mathrm{f})}\sqrt{C}/(1 + A'\sqrt{C}) - 2k \log(1 + 0.002M_{\mathrm{XY}}m) = E_{\mathrm{m}}{}^{\circ *} + E_{\mathrm{ext}} - 2kBC \quad (4)$$

where E is the electromotive force of the cell (1), $S_{(\mathrm{f})}$ and A' are Debye–Hückel constants, k is given by 2.3026 RT/F, C is the molarity of hydrochloric acid, M_{XY} is the mean molecular weight of the solvent, and B is the salting-out coefficient. These constants were calculated by using the values given in Table I, and are given in Table III.

TABLE III

CONSTANTS OF EQUATION 4

Wt. % MeOH	M_{XY}	$S_{(\mathrm{f})}$	$A'/\mathring{a}$	$\mathring{a}$, Å.
0	18.016	0.5065	0.3288	5.60
20	19.75	.6017	.3418	4.60
40	21.84	.7405	.3731	4.30
60	24.43	.9484	.4052	4.30
80	27.72	1.2672	.4463	5.30
90	29.73	1.5092	.4731	5.50
100	32.04	1.8876	.5098	4.00

$2k = 2 \times 2.3026RT/F = 0.11832.$

A' is a constant which depends on the ion-size parameter, $\mathring{a}$. In the present calculation the value of $\mathring{a}$ in each solvent was evaluated so as to make the value of $E' - E_{\mathrm{ext}}$ as constant as possible, when the salting-out term in eq. 4 was not taken into consideration. The calculated values of $\mathring{a}$ in various media are indicated in the 5th column of Table III. Variation of $\mathring{a}$ with varied content of methanol will be discussed later.

In the range of electrolyte concentrations used in the present experiments, E_{ext} was found to be less than 0.1 mv. when the solutions contained less than 60% methanol. In order to advance the present discussions, the values of $E' - E_{\mathrm{ext}}$ of pure methanol were calculated using the constants listed in Table III and the values of electromotive force measured by Nonhebel and Hartley.[9] As the ratio of methanol increases, the electromotive force of the cell containing the smallest concentration of hydrochloric acid ($m < 0.005$) becomes fairly low. This is assumed, as pointed out by Grunwald,[10] to be due to the reduction of silver chloride by hydrogen dur-

---

(4) F. Ishikawa and M. Matsuo, *Sci. Rept. Tohoku Univ. Ser. I*, **33** 228 (1949); I. T. Oiwa, *ibid.*, **37**, 34 (1953).

(5) G. A. Linhart, *J. Am. Chem. Soc.* **41**, 1175 (1919).

(6) P. S. Albright and L. J. Gosting, *ibid.*, **68**, 1061 (1946).

(7) J. A. V. Butler, D. W. Thomson and W. H. Maclennan, *J. Chem. Soc.*, 674 (1933).

(8) H. S. Harned and B. B. Owen, "The Physical Chemistry of Electrolytic Solutions," Reinhold Publ. Corp., New York, N. Y., 2nd Ed., 1950, (a) p. 332, (b) p. 346, (c) pp. 122, 190 (d) p. 338, (e) p. 337.

(9) G. Nonhebel and H. Hartley, *Phil. Mag.*, **50**, 729 (1925).

(10) E. Grunwald, *J. Am. Chem. Soc.*, **76**, 3855 (1954).

ing the measurement which, in turn, increases the concentration of hydrochloric acid. This change in concentration considerably affected the electromotive force measurements in smaller concentrations of hydrochloric acid. The most probable values of $E^{\circ}_{\mathrm{m}}{}^{*}$ obtained by averaging the foregoing are listed in Table IV.

Table IV

Standard Potential of the Silver–Silver Chloride Electrode

Wt. % MeOH	$E^{\circ}_{\mathrm{m}}{}^{*}$, v.	$E^{\circ}_{\mathrm{c}}{}^{*}$, v.	$E^{\circ}_{\mathrm{N}}{}^{*}$, v.
0	0.22216	0.22201	0.01578
10[a]	.2155	.2145	.0114
20	.2094	.2076	.0077
40	.1968	.1932	.0003
60	.1818	.1759	− .0089
80	.1492	.1404	− .0350
90	.1135	.1030	− .0672
94.2[b]	.0841	...	− .0950
100	− .0099	− .0223	− .1867

[a] Ref. (11). [b] B. E. Conway, "Electrochemical Data," Elsevier Publishing Co., Houston, Texas, 1952.

The standard potentials of the molarity and mole fraction unit are calculated by

$$E_{\mathrm{c}}{}^{*} = E^{\circ *} + 0.11832 \log d_0 \qquad (5)$$

and

$$E^{\circ}_{\mathrm{N}}{}^{*} = E^{\circ}_{\mathrm{m}}{}^{*} - 0.11832 \log (1000/M_{\mathrm{XY}}) \qquad (6)$$

The results are shown in the 3rd and 4th columns of Table IV.

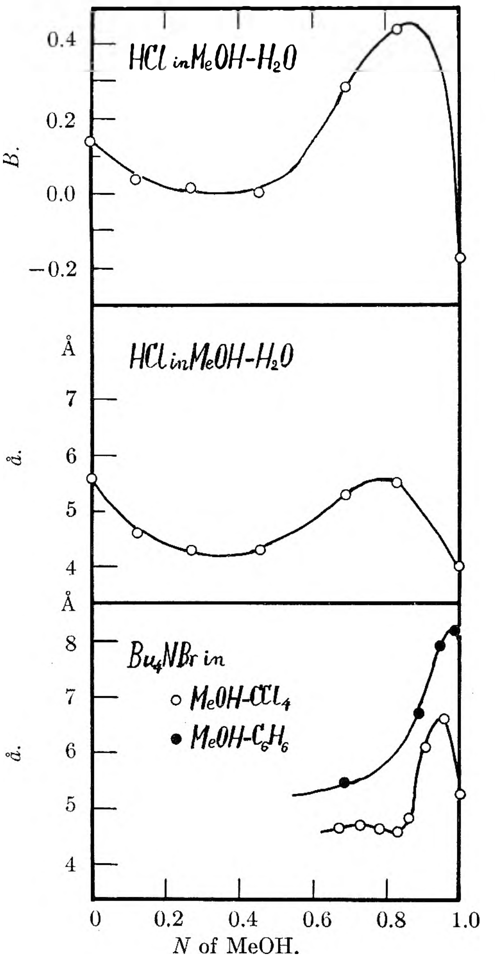

Fig. 1.—Top curve, salting-out coefficients of HCl in MeOH–H$_2$O; middle curve, ion-size parameters of HCl in MeOH–H$_2$O; bottom curves (ref. 20), ion-size parameters of Bu$_4$NBr in MeOH–CCl$_4$ and MeOH–C$_6$H$_6$ (solid).

In order to consider the change of $\mathring{a}$ with the solvent composition, B was calculated from eq. 4 setting $\mathring{a}$ to 4.3 Å., a value adopted by Harned and others[8b,11] for aqueous 10 and 20% methanol solutions. These are plotted against mole fraction of methanol as shown in Fig. 1, which indicates that the change of B with change of methanol content is similar to that of $\mathring{a}$ when the latter was calculated assuming B equal to zero. This seems to be natural, because the greater the solvation (coördination) sphere, the greater is the salting-out effect.

In this system, the hydration takes place most completely in the aqueous solution in which $\mathring{a}$ is the maximum and B is also large. When alcohol is added to the aqueous solution, the water molecule undergoes preferential solvation which, in turn, makes the ratio of alcohol to water outside the ionic solvation sphere greater than that of pure solvent, resulting in a low dielectric constant of the bulk solution, and giving B a positive value. As the ratio of alcohol to water increases, the activity of water becomes smaller, and B decreases gradually. The foregoing facts agree with the findings of Bockris and others,[12] who reported that the minimum of the salting-out effect appeared in a 58% methanol solution. In 80 and 90% methanol solutions, both $\mathring{a}$ and B become extremely large. This may be explained in terms of alcoholation; in the presence of a water molecule, breaking of the polymer chain structure of alcohol takes place to form the reactive monomer.[13] In 100% methanol alcoholation alone occurs, but the ion–dipole force is not so great (as in the case of water) that alcohol is naturally expelled out of the ions; thus ionic association can be assumed to occur. The value of $\mathring{a}$ was calculated to be 4.00 Å., which is extremely smaller than 5.60 Å. in water. It should be mentioned here that the above value (4.00 Å.) is much smaller than the value of 5.00 Å. which was obtained by Marshall and Grunwald[14] for $\mathring{a}$ of hydrochloric acid in 100% methanol. This variance probably arose from the fact that in the present experiments the degree of association was not used as an independent variable in applying the Debye–Hückel equation for the activity coefficient of hydrochloric acid and that $\mathring{a}$ was obtained as the mean value of the total ions, including the associated ions.

The propriety of this value of $\mathring{a}$ = 4.00 Å. may be interpreted as follows. According to the theory of ionic association of Bjerrum,[8c,15] the relation between the association constant, $1/K$, and $\mathring{a}$ of the acid in the solvent of dielectric constant D will be given by

$$K^{-1} = \frac{4\pi N}{1000}\left(\frac{e^2}{DkT}\right)^3 Q(b)$$

---

(11) H. S. Harned and H. C. Thomas, *J. Am. Chem. Soc.*, **57**, 1666 (1935); **58**, 761 (1936).

(12) J. O'M. Bockris and H. Egan, *Trans. Faraday Soc.*, **44**, 151 (1948).

(13) R. Mecke, *Disc. Faraday Soc.*, **9**, 161 (1950).

(14) H. P. Marshall and E. Grunwald, *J. Chem. Phys.*, **21**, 2143 (1954). They obtained the value of $\mathring{a}$ = 3.60 Å. for ethanol.

(15) F. M. Fuoss and R. M. Sadek, *J. Electrochem. Soc.*, **99**, 483 (1952).

TABLE V

ACTIVITY COEFFICIENT, γ, OF HYDROCHLORIC ACID

		Wt. % MeOH					
m	Aq.	20	40	60	80	90	Methanol
0.001	0.9665	0.961	0.953	0.942	0.924	0.914	0.897
.002	.9532	.946	.933	.921	.896	.880	.857
.005	.9298	.915	.896	.879	.843	.826	.782
.01	.9053	.886	.864	.835	.790	.767	.713
.02	.8758	.851	.821	.786	.740	.710	.629
.03	.8582	.830	.791	.756	.709	.670	.582
.05	.8324	.801	.755	.712	.664	.622	.520
.07	.8139	.782	.734	.684	.634	.590	.481
.1	.7964	.762	.708	.658	.602	.563	.447

TABLE VI

					Aq. soln. side		Alc. soln. side		
Wt. % MeOH	log y_m	$\Delta G^\circ = E^\circ_N{}' - E^\circ_N{}^*$, ev.	log y_n	$\Delta G^\circ_{\text{elect.}}$, ev.	$\Delta G^\circ_{\text{solv.}}$, eq. (12), ev.	ΔG°, ev.	$\Delta G^\circ_{\text{solv.}}$, eq. (14), ev.	$\Delta G^\circ_{\text{p.t.}}$, eq. (17), ev.	ΔG°, ev.
0	0.0000	0.0000	0.0000	(0.0000)	(0.0000)	(0.0000)	...	...	...
10	.0566	.0044	.0372	.0049	− .0015	.0034	...	...	...
20	.1073	.0080	.0676	.0103	− .0032	.0071	...	...	...
40	.2138	.0154	.1302	.0244	− .0070	.0174	...	...	...
60	.3406	.0246	.2079	.0440	− .0125	.0315	−0.0169	0.0026	0.0297
80	.6161	.0507	.4285	.0714	− .0236	.0478	− .0087	.0054	.0691
90	.9178	.0829	.7006	.0908	− .0416	.0492	− .0043	.0119	.0983
94.2	1.1663	.1107	.9356	.1013	...	...	− .0025	.0184	0.1172
100	1.9608	.2024	1.7106	.1190	...	....	(.000C)	(.0834)	(.2024)

or

$$-\log K = 6.120 - 3 \log D + \log Q(b) \qquad \text{(at 25°)}$$

where

$$b = e^2/\mathring{a}DkT \qquad (7)$$

Substituting the value of $\mathring{a}$ = 4.00 Å. obtained for 100% methanol solution, eq. 7 gives the value of b = 4.263 and K = 0.0439, the latter being in good agreement with 0.041,[16] 0.056[17] and 0.068,[18] obtained for K from the determination of electric conductivity.

The apparent large salting-out effect may be partly due to the effect of ionic association, but is probably due to the increase of the dielectric constant of the solvent which occurs upon the breaking of the spheroidal long polymer chain of the alcohol[19] by the electrolyte.

The variation of $\mathring{a}$ of hydrochloric acid in methanol–water mixtures showed a maximum at around 90% methanol similar to the tendency for tetrabutylammonium bromide in the methanol–benzene and methanol–carbon tetrachloride systems which was observed by Fuoss, *et al.*[20] This resemblance is shown in Fig. 1.

V. Activity Coefficient of Hydrochloric Acid

The activity coefficient γ, based on molality in the usual sense, taking γ as 1 in the infinite dilute solution of hydrochloric acid in each solvent, may be calculated from the following equation, using the value of E^{0*}_{m} determined in the foregoing section and the electromotive force, E, of the cell (1)

$$\log \gamma = -(E - E_{\text{m}}{}^*)/2k - \log m \qquad (8)$$

Table V gives the values obtained at round concentration of m by the graphical method with log γ as the function of $\sqrt{m}$. The following Debye–Hückel equation, which includes the extended terms,[21] represents the experimental results

$$\log \gamma = -\frac{S_{(f)}\sqrt{C}}{1 + A'\sqrt{C}} + \frac{1}{2.3026}\left\{\left(\frac{4.6052S_{(f)}}{A'}\right)^3 \right.$$
$$[{}^1/_2\, X_3\,(\kappa a) - 2Y_3(\kappa a)] + \left(\frac{4.0652S_{(f)}}{A'}\right)^5$$
$$\left.[{}^1/_2\, X_5\,(\kappa a) - 4Y_5\,(\kappa a)]\right\} - \log\,(1 + 0.002M_{\text{XY}}m) \quad (9)$$

VI. Solvent Effect upon Activity Coefficient of Hydrochloric Acid

The activity coefficient, γ, calculated in the foregoing section is referred to a value of unity at infinite dilution of hydrochloric acid in each particular solvent. In the present experiments, the infinitely dilute state in pure water was taken as the sole standard state, then the infinitely dilute state in solvents other than water (reference state) was taken to possess the activity coefficient, y.

The difference of G^0 (the subscript s in $G_s{}^0$ will hereafter be omitted) in the first term of eq. 3 between the aqueous solution and other solutions will be represented by the equation

$$\Delta G^0 = -F(E^{\circ *} - E^\circ)$$
$$= 2RT \ln y \qquad (10)$$

where E° and $E^{\circ *}$ are the standard potentials of the silver–silver chloride electrode in aqueous and nonaqueous solutions, respectively.

The values of molality and mole fraction unit of y calculated from the above equation are given in the 2nd and 4th column of Table VI.

In order to make theoretical discussion on solvation effect possible, the mole fraction unit which does not contain the change of the number of sol-

---

[16] H. Goldschmidt and P. Dahl. *Z. physik. Chem.*, **A114**, 1 (1925).

[17] W. F. K. Wynne-Jones, THIS JOURNAL, **31**, 1647 (1927).

[18] D. M. Murray Rust and H. Hartley, *Proc. Roy. Soc.* (*London*), **A126**, 84 (1929).

[19] G. Oster and J. G. Kirkwood, *J. Chem. Phys.*, **11**, 175 (1943).

[20] R. C. Miller and R. M. Fuoss, *J. Am. Chem. Soc.*, **75**, 3076 (1953); H. Sadek and R. M. Fuoss, *ibid.*, **76**, 5897, 5902 (1954).

[21] T. H. Gronwall, V. K. LaMer and K. Sandved, *Physik. Z.*, **29**, 358 (1928).

vent molecule by different solvents[22] will be used.

Born[8d,23] has introduced the following equation for the relationship between the electrostatic part of ΔG^0, $\Delta G^0_{\text{elect}}$, and the dielectric constant D, of the solvent

$$\Delta G^0_{\text{elect}} = \frac{Ne^2}{2}\left(\frac{1}{D_2} - \frac{1}{D_1}\right)\left(\frac{1}{a_+} + \frac{1}{a_-}\right)$$
$$= 7.158\left(\frac{1}{D_2} - \frac{1}{D_1}\right)\left(\frac{1}{a_+} + \frac{1}{a_-}\right) \quad (11)$$

The sum of the reciprocal of the ionic radius $\Sigma 1/a_i$ will be 0.93, by adopting $\mathring{a} = 4.30$ Å. Thus, the activity coefficient over a wide range of aqueous solutions is represented by the Debye–Hückel equation, assuming that $a_+ = a_-$ as usual. This value closely agrees with the value of $\Sigma 1/a_i = 0.92$ calculated from the crystallographical ionic radius (1.81 Å.)[24] for the chloride ion and the diameter (2.76 Å.) of the water molecule for hydroxonium ion.

The values of $\Delta G^0_{\text{elect}}$ which were calculated from eq. 11 with the dielectric constant of water, D_1, are given in the 5th column of Table VI.

In Fig. 2, the curve is concave-up for the water-rich mixtures, and becomes convex-down at the methanol-rich side, with the inflexion point at 60% alcohol, *i.e.*, at a point where the molecular number of water and alcohol is approximately equal.

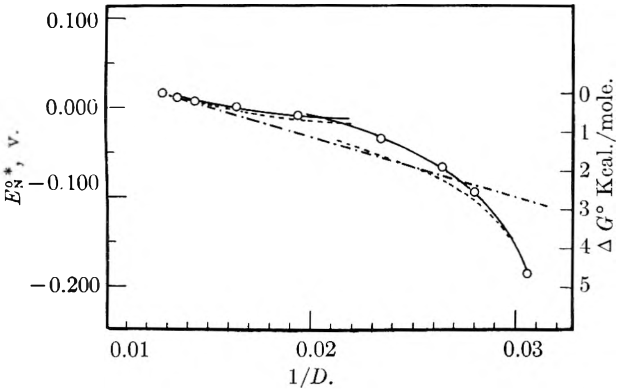

Fig. 2.—Standard electrode potentials (free energy of the transfer of unit activity HCl) *vs.* $1/D$: full line, observed; dotted line, calculated.

For the solutions containing less than 60% methanol it may be assumed that the dielectric constant in the neighborhood of ions is larger than that of the bulk solvent, due to the preferential solvation effect of the ions. This tendency must be more marked when a non-aqueous solvent of small polarity has been added. In fact, it entirely agrees with the order of glycerol < (methanol) < ethanol < isopropyl alcohol < dioxane.[8e,25] As for the free energy change, addition of a small amount of alcohol to the aqueous solution will only result in the disorder of alcohol outside the coördination sphere, because ionic charge will be shielded by the dipole of water; the entropy change, ΔS^0, becomes larger with decrease of ΔG^0 in proportion to $RT \ln a_w$. Taking this as ΔG^0_{solv}

$$\Delta G^0_{\text{solv}} = RT \ln a_w \quad (12)$$

Therefore, the total free energy change can be calculated from eq. 11 and 12 as

$$\Delta G^0 = \Delta G^0_{\text{elect}} + \Delta G^0_{\text{solv}} \quad (13)$$

The values calculated from the above equation are shown in the 6th column of Table VI[26] and agree with the experimental results within a difference of 2 mv. up to 40% of alcohol.

In 100% methanol solution, the presence of moderately strong alcoholation may be assumed because of the large positive value of the B-coefficient of viscosity[27] and the large negative value of the entropy of solution. The addition of a small amount of strongly polar water results in the hydration of ions with breaking of alcohol polymer chain, and ΔS^0 becomes suddenly large, probably with an attendant decrease of ΔG^0. In a similar way as in an aqueous solution ΔG^0_{solv} may be expressed by

$$\Delta G^0_{\text{solv}} = RT \ln a_{\text{alc}} \quad (14)$$

For consideration of the quantitative proton transfer from a water molecule to methanol the following equilibrium in which mole fraction g of proton is liberated from the hydroxonium ion to form the methyloxonium ion will be discussed.

$$\underset{1-g}{H_3O^+} + \underset{a_{\text{alc}}}{\text{MeOH}} \rightleftharpoons \underset{a_w}{H_2O} + \underset{g}{\text{MeOH}_2^+} \quad (15)$$

The equilibrium constant, K, of eq. 15 will be given as

$$K = g[a_w/(1-g)a_{\text{alc}}] \quad (16)$$

where a_w and a_{alc} are activities of water and methanol, respectively. Therefore, the standard free energy change of the proton transfer is equal to $-RT \ln K$. Since this corresponds to the difference between ΔG^0 and $\Delta G^0_{\text{elect}} + \Delta G^0_{\text{solv}}$ the reaction represented by eq. 15 is accompanied by the increase of free energy of 0.0834 e.v. (0.2024–0.1190), which, in turn, gives the value of $1/K = 25.7$.

On the addition of a_w of water to pure methanol, $(1 - g)$ mole fraction of proton is transferred from the methanol molecule to water molecule, and g mole fraction of proton remains as the methyloxonium ion, according to the equilibrium of eq. 15. The free energy change $\Delta G^0_{\text{p.t.}}$ of this process will be given by

$$\Delta G^0_{\text{p.t.}} = -gRT \ln K$$
$$= -\frac{a_{\text{alc}}}{Ka_w + a_{\text{alc}}} RT \ln K$$
$$= \frac{0.0834 a_{\text{alc}}}{25.7 a_w + a_{\text{alc}}} \text{ (in e.v.)} \quad (17)$$

By calculating the total free energy change from eq. 11, 14 and 17 (last column in Table VI), the values show the tendency of the ΔG^0 change near

---

[22] Accompanied by entropy change of $R \ln (M_{XY}/[H_2O])$ from aqueous solution to the solvent of a mean molecular weight of M_{XY}.

[23] M. Born, *Z. Physik*, **1**, 45 (1920).

[24] L. Pauling, "Nature of the Chemical Bond," Chap. X, Cornell University Press, Ithaca, N. Y., 1939.

[25] The question here is the tangent $(\alpha \Sigma 1/a_i)$ of the curve at aqueous solution. Excessive value of a from a straight line agreeing with measured values seems meaningless.

[26] a_w and a_{alc} were calculated from $a_w = p_w/p^0_w$ and $a_{\text{alc}} = p_{\text{alc}}/p^0_{\text{alc}}$ using p_w and p_{alc} (p^0_w and p^0_{alc} are the vapor pressures of pure water and of pure alcohol, respectively) in Table I.

[27] Viscosity $\eta = \eta_0(1 + A\sqrt{C} + BC)$ where η_0 is the viscosity of the solvent. *Cf.*, p. 178 of ref. 8.

pure methanol; these values approach Born's straight line.

By use of the existing theories regarding ΔG^0 of the methanol–water system, and consideration of the changes in ionic solvation, eq. 13, 12, 14 and 17 have been derived and found well able to explain the experimental results.

Acknowledgment.—The author expresses his deep gratitude to Prof. Emeritus Fusao Ishikawa and Prof. Nobuyuki Tanaka for their kind guidance and encouragement throughout the course of this work. He is also indebted to Mr. Akira Amano for the use of a part of the data of the electromotive force measurement.

STUDIES OF DIFFUSION FLAMES. I. THE METHANE DIFFUSION FLAME

BY S. RUVEN SMITH AND ALVIN S. GORDON

Chemistry Division, U. S. Naval Ordnance Test Station, China Lake, Calif.

Received September 6, 1955

Gaseous products from various regions inside and outside the glowing mantle of a methane diffusion flame in air have been analyzed with a mass spectrometer. The product analyses from the zones studied indicate that the methane is pyrolyzing in the inner mantle and the pyrolysis products are oxidized in the high temperature combustion zone at the edge of flame. The only oxygenate found in the flame is a trace of formaldehyde and this compound does not appear to be important in the combustion process.

Studies of the chemistry of flames have been reported by Faraday,[1] Eltenton,[2] Foner, Hudson and Avery,[3,4] Wolfhard and Parker,[5] and Smith and Gordon.[6] Faraday[1] examined the precombustion zone of a wax candle by removing gaseous products from the neighborhood of the wick and reigniting them. Eltenton[2] studied a methane flame with a mass spectrometer, with a view to identifying free radicals. Foner and colleagues[3] have used a mass spectrometer for the identification of free radicals in hydrogen–oxygen and methane flames and for the identification of chemical intermediates in the premixed propane–air flame. Wolfhard and Parker have examined the various zones of a diffusion flame spectroscopically on the basis of a deepening absorption as the flame was probed from the inside of the fuel toward the edge. They concluded that pyrolysis must play a role in the mechanism of burning, but they could not evaluate the importance of this process.

In the present work the chemistry of the combustion of a methane diffusion flame is followed by mass spectrometric analysis of samples from various regions of the flame. Our results show that pyrolysis is the only route for the disappearance of the methane.

Apparatus and Procedures.—A burner with a 27 mm. port was set up on a micromanipulator in a Plexiglas hood to eliminate the effects of air currents on the flame. A quartz probe 0.5 mm. o.d. at the tip with a constricted opening whose average diameter is 0.06 mm., is sealed into position above the burner so that any portion of the flame can be sampled by adjustment of the micromanipulator supporting the burner.

The samples from the flame are introduced into a previously purged and evacuated sample flask by rotating a three-way stopcock which diverts the flow of probed sample from the house-vac to the sampling manifold. The probe, which gives no visual disturbance of the flame in the process of sampling, permits a sample to be withdrawn in between 15 seconds and one minute.

Samples have been analyzed with a Consolidated Model 21-103 mass spectrometer. The identification of all the components in the mass spectrum was aided by use of thermal fractionation and high mass resolution.

One and three mil hairpin shaped Pt–Pt 10% Rh thermocouples, both bare and covered with a thin sheath of quartz tubing, were used for measuring the flame temperatures. In the case of the 1 mil coated couple the quartz tubing was 4 mil o.d. and 2 mil i.d.

Inside the luminous zone ($r = 0$ to $r \simeq 0.5$) where there are extremely low concentrations of oxygen and low temperature gradients, essentially the same temperatures are recorded by the one and three mil thermocouples, covered or bare. Toward the edge of the flame where the oxygen concentrations rapidly increase, the 1 and 3 mil bare wire thermocouples show a significantly higher temperature (~400°) than the coated thermocouples, indicating that oxidation reactions are being catalyzed. In the region where catalysis can occur the pyrolysis reactions are almost completed and there are only small concentrations of hydrocarbons.

The temperatures shown in the composition diagrams (Fig. 1–3) were obtained with the 1 mil quartz coated thermocouple, uncorrected for radiation and thermal conductivity. A series of experiments were made to determine the corrections for radiation and thermal conductivity of the thermocouples used in this work. It was shown that radiation corrections are quite unimportant even at the maximum temperatures of our flames. Thermal conductivity corrections are of much greater importance, but it has not yet been possible to design experiments to ascertain their magnitude. Inside the flame cone, where the pyrolysis reactions occur, the thermal gradients are relatively small and the conductivity corrections cannot be large.

Discussion

Probe techniques have been criticized because of the possibility of catalysis or of flame disturbance. To guard against these possibilities, extremely fine quartz probes were employed. They were about 0.5 mm. o.d. and about 0.3 mm. i.d. The end of the probe was sealed and ground to an extremely fine diaphragm opening. This probe design permitted sampling without any visible flame disturbance. The pressure was one atmosphere on the outside of the probe, and varied from 0 to 20 mm. on the inside as a sample was collected during an experiment.

---

(1) M. Faraday, "Chemical History of a Candle," 1861.

(2) G. C. Eltenton, *J. Chem. Phys.*, **15**, 455 (1947).

(3) S. N. Foner and R. L. Hudson, *ibid.*, **21**, 1374 (1953).

(4) R. Prescott, R. L. Hudson, S. N. Foner and W. H. Avery, *ibid.*, **22**, 145 (1954).

(5) W. G. Parker and H. G. Wolfhard, *J. Chem. Soc.*, 2038 (1950).

(6) S. R. Smith and A. S. Gordon, *J. Chem. Phys.*, **22**, 1150 (1954).

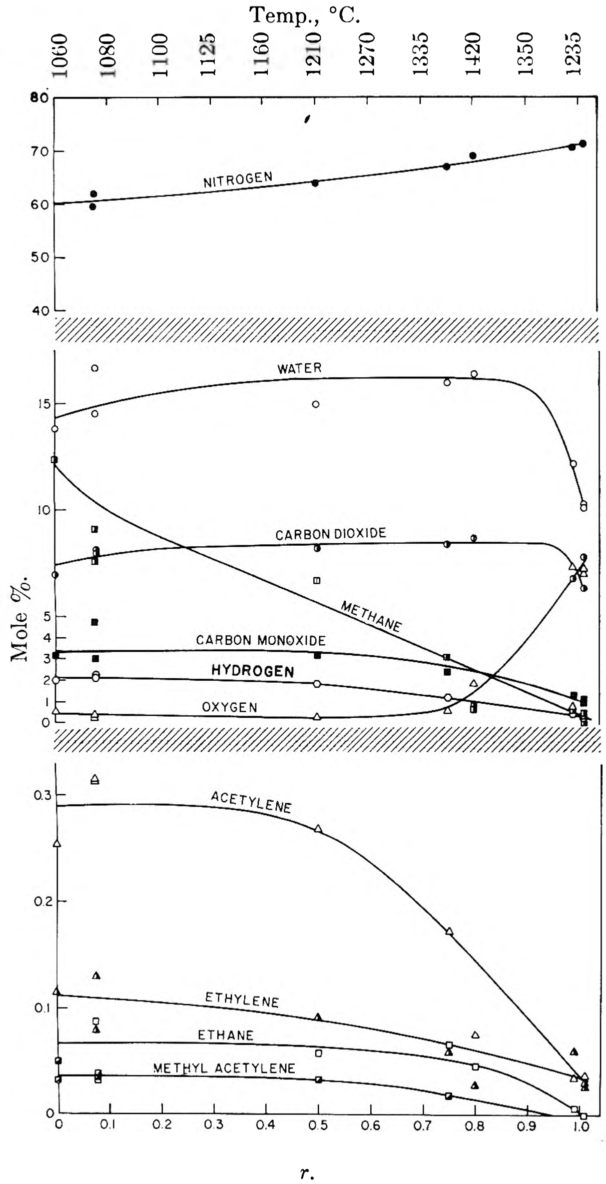

Fig. 1.—Composition of sample probed from flame 20 mm. above port. (r = ratio of distance of probe to central axis to radius of flame.)

From the sampling rate, the time inside the hot portion of the probe was calculated to be less than 0.5 msec. With this short residence time and low pressure, there does not seem to be much likelihood of catalysis. This was confirmed by increasing the residence time by a factor of 10 without appreciably disturbing the composition of the sample.

The compositions of the main constituents are presented in Figs. 1–3. Each figure shows the composition of the components as a function of the dimensionless coördinate r defined as the ratio of the distance of the probe to the central axis to the radius of the flame at a constant level above the port.

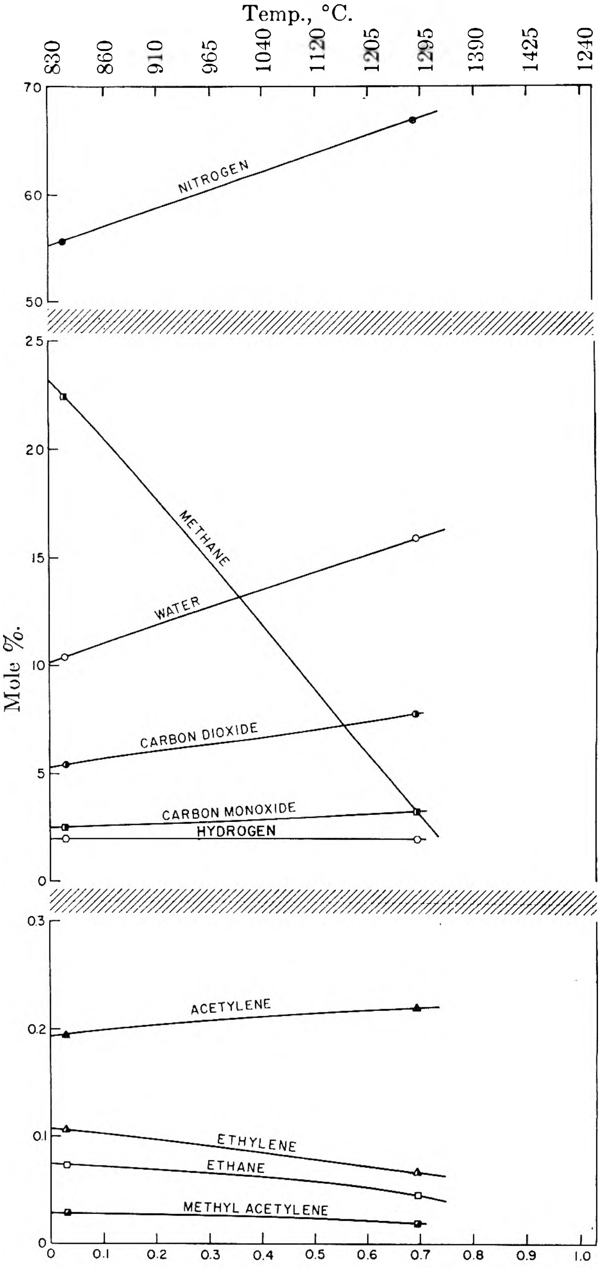

Fig. 2.—Composition of sample probed from flame 11 mm. above port. (r defined in Fig. 1.)

The constituents are essentially those found in the pyrolysis of methane[7] with superposition of argon, nitrogen, carbon monoxide, carbon dioxide, water and possibly traces of formaldehyde and methanol. With the exception of acetylene, which goes through a maximum, all the hydrocarbon constituents decrease with distance from the center of the flame toward the edge, as well as from the port outward parallel to the axis. This disappearance of the precursor hydrocarbon, methane, is especially dramatic.

Carbon monoxide first increases with distance from the axis, but goes through a maximum if the distance from the axis is relatively large.

Water, CO_2 and N_2 all increase from the axis and maximize toward the edge of the flame, indicating that these materials diffuse into the center of the flame from the edge.

The hydrogen is quite low and relatively constant inside the flame cone. Methane disappears quite rapidly within the cone, and the intermediate hydrocarbon products are present in only small and relatively constant concentrations. Thus,

---

[7] A. S. Gordon, *J. Am. Chem. Soc.*, **70**, 395 (1948).

about two moles of hydrogen should appear for every mole of methane which is decomposed. The lack of hydrogen, taken in conjunction with the maximizing of water vapor percentage at or near the edge of the flame, indicates that hydrogen rapidly diffuses from inside the flame cone to the edge where O_2 is available. Here the hydrogen is rapidly burned to water. The water diffuses in all directions, although the direction away from the flame is somewhat favored.

The ease of diffusion in the flame is shown by the fact that N_2 is almost 50 mole % of the gases 7 mm. above the port and 3 mm. from the axis of the flame.

The history of the methane carbon must be similar to the history of the hydrogen in methane. The methane carbon probably appears in the form of carbon or some compound which is mainly carbonaceous. Since the mechanism of formation must involve the hydrocarbon intermediates, the carbonaceous material must be built up from small units with concurrent dehydrogenation. Electron microscope studies[5] have shown the average diameter of soot particles derived from flames to be 200–500 Å. There are thus between 10^5 and 10^6 atoms in each soot particle. Since the possible generating species all have a low steady-state concentration, the reactions which form these particles must be quite efficient and the mechanism probably involves a chain process.

Porter[8] has postulated that in all flame and explosion processes, carbon particles are formed by the pyrolysis of acetylene. In many of the diffusion flames which we have examined, the sooting ability of the flame was reflected in the stationary concentration of acetylene in the flame mantle. However, a benzene diffusion flame, one of the prime sooting flames, had a stationary concentration of acetylene less than methane, a quite sootless flame. The benzene flame reflecting the thermal stability of the benzene, has relatively few constituents inside the flame mantle; acetylene, ethylene, methane and H_2 are the main pyrolysis products. The benzene persists in much higher concentration to the edge of the flame than does methane in the methane diffusion flame. The temperature inside the benzene diffusion flame cone is somewhat lower than that of the methane diffusion flame. Thus the lower stationary state of acetylene is not the result of more rapid acetylene pyrolysis than in the methane flame.

From the above, it is reasonable that carbon can be formed from other than acetylene. It is quite apparent that carbon may be formed from benzene or from the interaction of acetylene and benzene, as well as from acetylene alone.

Acetylene is singlet in its ground state and the ground state of C_2 has been identified as triplet from spectroscopic data, so that the reaction

$$1C_2H_2 \longrightarrow 3C_2 + 1H_2 \qquad (1)$$

is not possible because of multiplicity restrictions, although it is superficially attractive since it is exothermic.

A free radical mechanism involving polymer formation, accompanied by dehydrogenation is the most likely mechanism for carbon formation. Thus any hydrocarbon which can be easily polymerized by free radical initiation is a suitable intermediate for carbon formation.

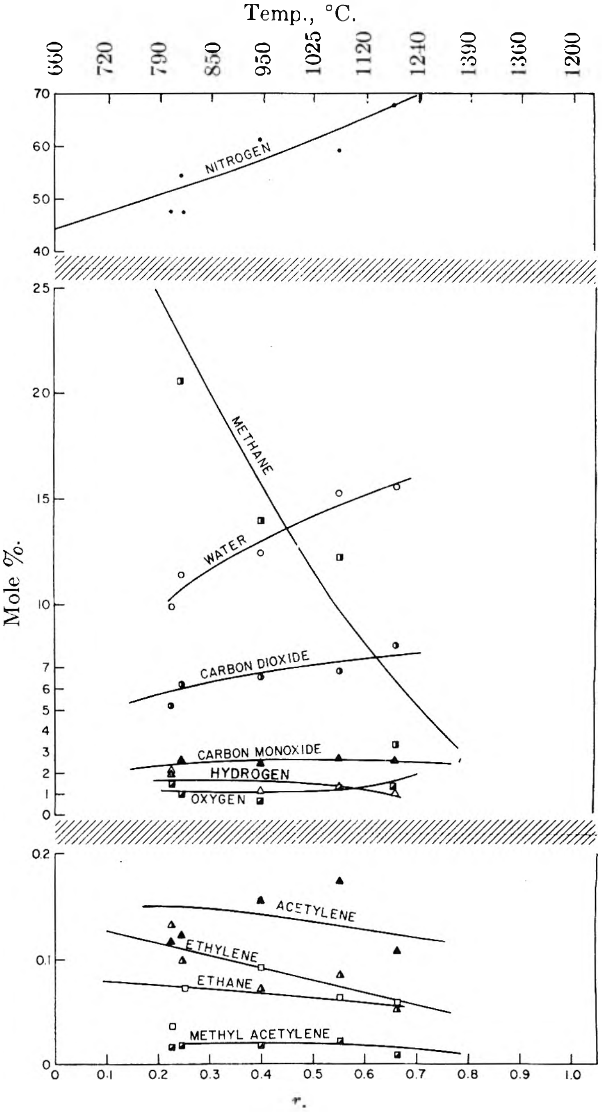

Fig. 3.—Composition of sample probed from flame 7 mm above port. (*r* defined in Fig 1).

The ratio of H/C inside the flame cone is calculated by summing all the H and C atoms in the sample. If all the products of the methane decomposition remained in the sample, the above ratio should be four. We find the ratio to hover around three, probably because the H_2O analyses are low. The H/C ratio is dominated by the ratio of H_2O to the sum of CO and CO_2 as the edge of the flame is approached.

Along the axis of the flame the free O_2 is of the order of one mole per cent. The free O_2 percentage along the axis decreases with increasing distance from the port. The free O_2 concentration also decreases for a considerable fraction of the distance from the axis to the edge of the flame. This type of distribution can result when air mixes with the fuel gas close by the port where the temperature at the edge is so cool that some free oxygen can penetrate the flame. At greater distances above the

---

[8] G. Porter, Agard Memorandum, AG13/M9, "The Mechanism of Carbon Formation."

port, the temperature at the edge is high enough so that the oxygen is effectively consumed before it can penetrate from the edge into the flame.

The small O_2 concentration inside the flame probably plays an important role in the primary process of the methane decomposition.

$$CH_4 + O_2 \longrightarrow CH_3 + HO_2 \qquad (2)$$

Pure methane is quite stable at temperatures up to 800°, while inside the flame we note considerable pyrolysis of methane at temperatures as low as 650°. Thus reaction (2) must play an important role in the methane pyrolysis.

The maximum temperature of about 1425° appears where the H_2O and CO_2 concentration has maximized.

Even though there are only small percentages of free oxygen inside the flame, the total bound plus free oxygen relative to N_2 is greater than in the air. Water analyses are the least reliable of all the constituents and the reported values are lower bounds. Thus the experimental values are upper bounds of the N_2/O_2 ratios.

Since N_2 and all the O_2 (free and bound) must get into the flame *via* diffusion, the enrichment of oxygen is of some interest. N_2 and O_2 probably have about the same diffusion constant. However, N_2 penetrates the flame edge, while O_2 is consumed forming H_2O, CO and CO_2. Thus the above ratio is probably determined by the ratio of the diffusion constants for H_2O, CO and CO_2 as contrasted to O_2.

The N_2/O_2 ratios also tend to increase as the gases move away from the port. As the gases move away from the port inside the burning cone, the N_2/O_2 ratio is determined in part by the ratio of the diffusion constant of N_2 as contrasted to those of CO, CO_2 and H_2O.

The $H_2O/(CO + CO_2)$ ratios at the various zones above the port were obtained. All the ratios show a small rise from the axis toward the edge of the flame. The zone at 20 mm. above the port was explored (out past the edge) of the flame and showed a sharp decrease after the initial slow rise. Thus the water diffuses more rapidly than the oxides of carbon.

The observed flame temperatures vary from about 650° at the central axis just above the port, to 1425° near the luminous edge. From the gas analyses water gas equilibrium constants were calculated. The temperatures corresponding to these equilibrium constants were 300–400° higher than the measured temperatures in the central cone, and 125–200° higher than the measured temperatures at the maximum temperature zone. As had been noted previously, the values reported for the mole percentages of water are probably low. Higher percentages of water would result in higher temperatures calculated from the water gas equilibrium constant. Thus the water gas constants calculated from the data in Figs. 1–3 correspond to lower bound temperatures.

As has been noted, the temperatures well inside the luminous cone are probably accurate, and our results indicate that the water gas equilibrium is not attained here. In the hotter regions of the flame the thermocouple temperatures must be corrected for thermal conductivity and the comparison of the observed and calculated temperatures cannot be made with confidence.

The measured maximum temperature of the flame falls about 550° short of the adiabatic flame temperature of a stoichiometric methane–air mixture. Although the thermocouple reading is somewhat low due to the thermal conductivity of the thermocouple, this cannot account for all of the difference. At the zone of maximum observed temperature there is still a fair percentage of CO and H_2 present; by the time these materials are oxidized an excess of air over stoichiometric is present which causes the temperature to decrease. Thus it should not be expected that the maximum flame temperature in these experiments will equal the adiabatic flame temperature.

The mass spectrometer identification of the components contributing to mass 30 was very difficult, since $C^{12}O^{18}$, $N^{14}O^{16}$, $C^{12}H_2O^{16}$ and $C_2{}^{12}H_6{}^1$ all have significant mass peaks at 30 and may all be present in the sample. The concentration of formaldehyde was checked by the Schiff base test on a large sample, and was shown to be less than 1 part in 10^5. The high mass resolution of about 800 mass units resolves the mass peak into two mass groups; $C^{12}O^{18}$, $N^{14}O^{16}$ and $C^{12}H_2{}^1O^{16}$ appear as one peak, and $C_2{}^{12}H^1{}_6$ appears as a second peak at a higher mass. The $C^{12}O^{18}$ contribution is calculated from the carbon monoxide and carbon dioxide present. Since the chemical tests indicated that formaldehyde is not present at the luminous edge of the flame, the residual of this peak is identified as NO. The temperature and the concentration of nitrogen and oxygen make the formation of NO reasonable. In several runs at the edge of the flame (not shown in the figures) relatively large mass 30 peaks are found where there is no methane, ethane or ethylene and essentially no hydrogen or carbon monoxide present. These samples indicate that as much as 0.05 mole % of NO can be formed at the edge of the flame. In the interior of the mantle

TABLE I

COMPARISON OF SAMPLES PROBED FROM METHANE DIFFUSION FLAME, WITH AND WITHOUT ADDED FORMALDEHYDE

	Sampled close to central axis		Sampled close to edge of flame	
	Normal Flame	Para-formal-dehyde added	Normal Flame	Para-formal-dehyde added
Benzene			0.006	0.007
Vinylacetylene			0.01	0.007
Diacetylene			0.005	0.004
Carbon dioxide	6.03	5.96	9.03	9.06
Propylene				0.004
Methylacetylene	0.03	0.01	0.03	.02
Argon	0.61	0.60	.75	.74
Oxygen	1.15	0.17	.42	.19
Formaldehyde		2.04	.01	.08
Ethane	0.08	0.05	.07	.05
Ethylene	0.12	0.24	.10	.11
Acetylene	0.22	0.22	.26	.29
Water[a]	...	...	...	...
Methane	27.82	21.12	7.55	5.46
Nitrogen	58.92	56.69	76.55	76.41
Carbon monoxide	2.79	8.73	3.30	5.11
Hydrogen	2.23	4.18	1.89	2.47

[a] Analysis on water free basis.

where the temperature is much lower and the concentration of oxygen is a few tenths of one per cent., the identity of the mass 30 is not certain and is probably due to both a trace of formaldehyde and NO which have diffused inward.

The effect of formaldehyde on the composition of the diffusion flame was obtained by placing pellets of paraformaldehyde on the grid of the burner port. Under these conditions, as may be seen in Table I a considerable concentration of formaldehyde results in higher concentrations of H_2 and of CO than in the normal flame. Also, the concentration of O_2 is lower than usual, presumably because of reaction with the formaldehyde vapor.

The formaldehyde concentration in the flame decreases sharply near the edge of the flame where higher temperatures and higher concentrations of oxygen are encountered.

Inside the luminous cone where practically al the methane disappears, it is most unlikely that formaldehyde plays any role in the chemistry of the methane disappearance. The primary reaction of methane is probably by oxygen and other free radical induced pyrolysis. At the edge of the flame, the importance of the role of formaldehyde in the combustion cannot be resolved by our experiments.

Acknowledgments.—The authors wish to acknowledge the assistance of Dr. Richard H. Knipe for many valuable discussions. Mr. Maynard Hunt gave considerable help in the temperature study. Mr. William Golyer aided in the experimental work and assisted in the operation of the mass spectrometer. Mr. Andreas V. Jensen also assisted in the operation of the mass spectrometer, and Mrs. Helen R. Young aided in the reduction of the mass spectral data.

ENERGIES AND ENTROPIES OF ASSOCIATION FOR AMIDES IN BENZENE SOLUTIONS. PART I

BY MANSEL DAVIES AND D. K. THOMAS

The Edward Davies Chemical Laboratories, University College of Wales, Aberystwyth, England

Received September 7, 1955

A precise isopiestic method has been used to study the association of trichloroacetamide and some anilides in benzene at temperatures 25–45°. The assumptions involved and the method of analyzing the simultaneously occurring association equilibria are discussed and illustrated for the solutes measured.

The structural character and the energy involved in the molecular association of the amides are of particular interest: the former has frequently been considered in relation to their infrared absorption spectra and has even been advanced as a criterion for deciding the geometrical ("*cis*" or "*trans*") structure of the monomeric molecules[1]; the energy involved is a prime factor in the H-bridge interaction which is so important in the various configurations of peptide and protein chains. Even so, there are very few adequate determinations of these factors, much of the data being of an essentially qualitative character over a limited range of conditions (concentration and temperature), or involving distinctly arbitrary elements in their interpretation.[2] The present account presents the results and analysis of systematic vapor pressure studies of amide solutions in benzene. As data have been obtained by two experimental methods, these have been segregated into Parts I and II: most of the results are in Part II, but the general assumptions and method of handling the data are given in the present Part I.

Experimental

A precise volumetric form of the isopiestic method has already been described.[3] The more rapid distillation and better draining of benzene compared with water improved both the speed and accuracy of the determinations. Thus the uncertainty of the apparent molecular weights of the solute was usually less than ±0.5% and results could be relied upon down to concentrations of 0.02*m*.

The standard solute chosen for benzene solutions was biphenyl. Of the many careful studies of this closely-ideal system we will quote only some of Tompa's results at 25°[4]: no departures from ideality could be established up to 0.25 *m*, whilst at 1.4 *m* the deviation from unity of the factor vapor pressure lowering/(v.p. solvent) (mole fraction solvent) was only 1.004. Accordingly, the mean apparent degree of association (*f*) of any non-volatile solute in benzene is closely approximated to by the ratio of its stoichiometric mole fraction to that of the biphenyl in the solutions which are isopiestic.

Materials. Benzene.—Analar solvent was well-dried ($CaSO_4$) and redistilled in an all-glass apparatus. When procurable Analar reagents were used in all the following preparations.

Biphenyl.—On distillation the middle fraction, b.p. 217° at 300 mm., was collected. This melted sharply at 71.0° (Heilbronn).

Acetanilide: twice recrystallized from benzene; m.p. 113.0°.

Formanilide: prepared from redistilled aniline and formic acid, excess of the product was treated with boiling petrol ether (60–80°) and after cooling the solid was filtered off and dried; m.p. 49°.

Trichloroacetamide.—The ethyl ester was first prepared and treated with excess of aqueous ammonia and the product recrystallized from benzene; m.p. 141°.

Trichloroacetanilide: twice recrystallized from benzene: m.p. 95°.

Results

A typical set of observations is shown in Table I. The temperature read on a thermometer calibrated at the N.P.L. to ±0.02° was 35.01°, the maximum fluctuations being ±0.002° (Beckmann). In this table, concentrations are in molalities, volumes in ml. The final volumes are those for which no change occurred on further equilibration for 4 to 6 hours and so are taken to give the isopiestic concentrations of the last column.

---

[1] M. Tsuboi, *et al.*, *Bull. Chem. Soc. Japan*, **22**, 215 (1949).

[2] Much of the earlier data is referred to in: W. E. S. Turner, "Molecular Association," Longmans Green and Co., London, 1915.

[3] M. Davies and D. K. Thomas, THIS JOURNAL, **60**, 767 (1956).

[4] H. Tompa, *J. Chem. Phys.*, **16**, 292 (1948).

TABLE I

BENZENE SOLUTIONS OF TRICHLOROACETAMIDE–BENZENE SOLUTIONS, BIPHENYL AT 35.01 ± 0.002°

Run no.		Initial concn.	Initial vol.	Final vol.	Vol. change	Mean change	Final concn.
1	Biphenyl	0.0172	5.812	6.122	+0.310	±0.312	0.0164
	Trichloroacetamide	.0165	5.900	5.586	−0.314		.0175
2	Biphenyl	.0265	5.869	5.894	+0.025	±0.025	.0264
	Trichloroacetamide	.0298	5.577	5.552	−0.025		.0300
3	Biphenyl	.0320	5.711	5.606	−0.105	±0.102	.0326
	Trichloroacetamide	.0386	5.818	5.917	+0.099		.0380
4	Biphenyl	.0393	5.456	5.372	−0.084	±0.083	.0399
	Trichloroacetamide	.0487	5.631	5.713	+0.082		.0480
5	Biphenyl	.0450	5.887	6.004	+0.117	±0.120	.0441
	Trichloroacetamide	.0529	5.749	5.626	−0.123		.0541
6	Biphenyl	.0480	6.231	6.341	+0.110	±0.111	.0472
	Trichloroacetamide	.0583	5.861	5.749	−0.112		.0594

TABLE II

(1) Formanilide in benzene at 24.98°

$10^3 \times N$	2.48	3.69	4.85	6.47	8.35		
f	1.13	1.19	1.24_5	1.32	1.38		
K_{12}	78	94	110	141	162		
$(f - 1)/\bar{N}$	59	61	63	65	63		

(2) Acetanilide in benzene

At 24.98°

$10^3 \times N$	0.88	2.22	2.39	3.54	4.28	5.78	
f	1.03_8	1.09	1.09_2	1.14	1.16_4	1.21_8	
K_{12}	48	54	51	61	64	75	
$(f - 1)/\bar{N}$	$44._6$	$44._0$	$41._8$	$46._6$	$44._5$	$45._9$	

At 35.01°

$10^3 \times N$	2.18	2.38	3.46	4.31	5.72		
f	1.07_3	1.08_2	1.11_3	1.14_0	1.18_6		
K_{12}	42	45	46	50	58		
$(f - 1)/\bar{N}$	$36._0$	$37._3$	$36._3$	$37._1$	$38._5$		

(3) Trichloroacetamide in benzene

At 24.98°

$10^3 \times N$	2.38	2.98	3.71	4.63	5.06		
f	1.19	1.23	1.27	1.32_5	1.35		

At 35.01°

$10^3 \times N$	1.42	2.29	2.93	3.72	4.26	4.57	
f	1.11_8	1.13_6	1.17	1.21	1.23_5	1.25	

At 45.05°

$10^3 \times N$	1.46	2.11	2.66	3.36	4.06	4.68	
	1.05_8	1.08_8	1.11	1.14	1.17	1.195	

(4) Trichloroacetanilide in benzene

At 24.68°

$10^3 \times N$	0.88	1.65	4.93	7.34	9.04	11.72	15.02
f	1.02_3	1.04_4	1.07_6	1.08_4	1.08_5	1.08_4	1.08_6

At 35.02°

$10^3 \times N$	0.81	1.56	4.78	7.20	8.95	11.58	14.95
f	1.01_4	1.02	1.05_4	1.07	1.06	1.07	1.07_2

Table II provides a summary of the isopiestic observations. N is the stoichiometric mole fraction of the solute in the solution. The mean degree of association for the solute (f) is obtained by dividing N by the effective mole fraction of the solute—in practice by the mole fraction of biphenyl in the isopiestic solution. This involves the major assumption that departures from ideality of the solute are due entirely to its association: the adequacy of this assumption is discussed later. A greater range of N values was precluded in some cases by limited solubility. $N = 10 \times 10^{-3}$ corresponds to 0.13 M. The factors K_{12} and $(f - 1)/\bar{N}$ are in mole fraction units.

Discussion

In 1943 Kreuzer[5] made a number of important general deductions by applying the Law of Mass Action to associative equilibria. Some similar

---

(5) J. Kreuzer, *Z. physik. Chem.*, **B53**, 213 (1943).

results have since been deduced by statistical methods. Firstly, we define Kreuzer's factors in terms of mole fractions—as he used the thermodynamically less acceptable molar concentration unit—and then quote those of his relations we shall use. N_n is the mole fraction of a n-mer in solution.

(1) $N = \sum_n nN_n$ = total concn. of solute in terms of mole fraction as monomer

(2) $\bar{N} = \sum_n N_n$ = total effective mole fraction of all n-mers

(3) $f = N/\bar{N}$ = mean degree of association

(4) $\alpha = N_1/N$ = stoichiometric fraction of solute present as monomer

(5) $\bar{\alpha} = N_1/\bar{N}$ = fraction of total independent molecular unit formed by monomer

(6) $K_{1n} = 1/k_{n1} = N_n/N_1^n$ = association constant for formation of n-mer from monomer: (k_n1 is the dissociation constant).

Without making any assumptions as to the number or nature of the associative equilibria involved, apart from their individual conformity to the Law of Mass Action in mole fraction units of the species directly involved, Kreuzer's general relations become

$$\bar{N} = \int_0^{N_1} (1/\alpha)\, dN_1 \qquad (7)$$

$$\ln (1/\alpha) = (f - 1)/f + \int_0^N (f - 1)/fN\, dN \qquad (8)$$

The exceptional value of these relations arises as follows: Absorption intensity or distribution data frequently give N_1 (or α), from which $\bar{N}$ (or f) is calculable by (7). From (8), osmotic data giving the dependence of f on N can be used to evaluate α (or N_1). It is useful to note that as $N \rightarrow 0$, the value of $(f - 1)/fN$ will approach, in general, the limit $1/K_{12}$. Kreuzer's subsequent use of these relations includes two special (arbitrary) cases. (i) If association of monomer to only one species of n-mer occurs, then $f = n - (n - 1)\bar{\alpha}$, so that n may be deduced from a plot of f against $\bar{\alpha}$. (ii) If a whole sequence of associates occurs with successive stages having the same equilibrium constant, *i.e.*, $K_{12} = K_{23} = K_{34} = \ldots \bar{K}$, then $(f - 1)/\bar{N} = \bar{K}$. This provides an easy means of determining $\bar{K}$ in this particular case.

In partial justification of the assumption that the departures from ideality are due to molecular association it can only be said that molecular association is undoubtedly a major factor in these cases: its occurrence can be "seen" in the infrared absorption changes[6] and, in a number of cases where those can be quantitatively followed, the equilibrium constants agree with those deduced from the simple osmotic basis.[7] The internal consistency and plausibility of the equilibria deduced on this assumption—and in particular, the practical constancy of the ΔH value for the association of any one solute—provide further criteria of the adequacy of the simple approach. For the amides we have studied the appearance of "association" bands in the infrared absorption, the anomalous variation of the molecular polarization[8a] and the departures from osmotic ideality are already so marked at low concentrations ($<0.05M$) that molecular aggregation is certainly a major factor. Only in such cases will the neglect of the many other factors[8b] which can contribute to non-ideality be even tentatively justified.

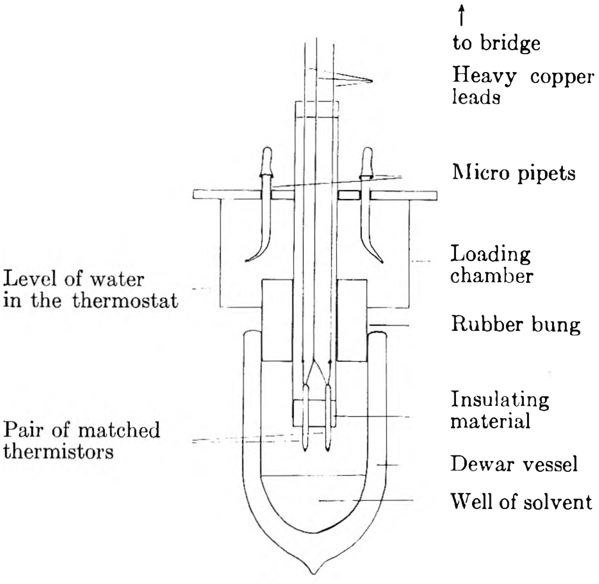

Fig. 1.

Kempter and Mecke[9] were the first to present a system—phenol in benzene—sensibly conforming to (ii) above. However, Hoffmann,[10] and later Coggeshall and Saier,[11] indicated that even for hydroxylic compounds, this was not the general occurrence but that much better conformity is obtained in these cases, which we designate as (iii), when $K_{12} < K_{23} = K_{34} = \ldots \bar{K}$. This condition, that two constants will usually be the minimum involved in successive association equilibria, has been clarified by a statistical treatment due to Saroléa-Mathot.[12] A simple model emphasizes that the entropy decrease on dimerization will generally be greater than in the subsequent stages in which only one monomer loses its translational and rotational degrees of freedom to an already existing complex: the model, in fact, leads to $K_{12}/\bar{K} = 1/p$ where p is the number of equivalent orientations which the monomer can take up in the medium.

An interesting example of these possibilities is provided by trichloroacetamide in benzene, Table II3. Although a plot of $(f - 1)$ against $\bar{N}$(*i.e.*, N/f) is, at 25°, fitted by a straight line through the origin and so conforms within experimental error to case (ii) above, at 35 and 45° a concavity toward the $\bar{N}$ axis is found at the lower concentrations before the points fall on a good straight line. This cor-

---

[6] (a) M. Davies and H. E. Hallam, *Trans. Faraday Soc.*, **47**, 1170 (1951); (b) M. Davies, J. C. Evans and R. L. Jones, *ibid.*, **51**, 761 (1955).

[7] Some (unpublished) instances of agreement between spectroscopic and osmotic association equilibrium constants found in these laboratories relate to $CH_3 \cdot CO \cdot NH_2$ in $CHCl_3$; $NH_2COOC_2H_5$ in $CHCl_3$; $CH_3 \cdot NH_2COOC_2H_5$ in CCl_4.

[8] (a) J. E. Worshaw and M. E. Hobbs, *J. Am. Chem. Soc.*, **76**, 206 (1954); (b) J. H. Hildebrand and R. L. Scott, "The Solubility of Non-electrolytes," 3rd Ed., Reinhold Publ. Corp., New York, N. Y., 1950.

[9] J. Kempter and R. Mecke, *Z. physik. Chem.*, **B46**, 229 (1940).

[10] E. G. Hoffmann, *ibid.*, **B53**, 179 (1943).

[11] N. D. Coggeshall and E. L. Saier, *J. Am. Chem. Soc.*, **73**, 5414 (1951).

[12] L. Saroléa-Mathot, *Trans. Faraday Soc.*, **49**, 8 (1953).

responds to case (iii). Although the data do not in this instance define the non-linear portion of the $(f - 1)$ *vs.* $\bar{N}$ plot as well as would be wished—owing to the approximate identity of K_{12} and $\bar{K}$ emphasized by the results at 25°—the problem of evaluating these two constants from the f and $\bar{N}$ values arises. Coggeshall and Saier have given a means of doing this when α and N are observed (*e.g.*, from infrared absorptions). We can proceed as follows.

Assuming

$$K_{12} \neq K_{23} = K_{34} = \ldots . K_{(n-1)n} = \bar{K}$$

then

$$K_{13} = K_{12}\bar{K};\ K_{14} = K_{12}\bar{K}^2;\ K_{1n} = K_{12}\bar{K}^{n-2}$$

$$\bar{N} = N_1 + N_2 + N_3 + \ldots N_n;$$

$$= N_1 + N_1^2K_{12} + N_1^3K_{12}\bar{K} + \ldots N_1^nK_{12}\bar{K}^{n-2};$$

This geometric series gives the sum

$$\bar{N} = N_1 + N_1^2 \times \frac{K_{12}(1 - N_1^n\bar{K}^n)}{1 - N_1\bar{K}}$$

and, provided[13] $-1 < N_1\bar{K} < 1$, as n becomes large it suffices to write

$$\bar{N} = N_1 + N_1^2K_{12}/(1 - N_1\bar{K}) \qquad (9)$$

Similarly, starting with the expression for N, one finds

$$(N - \bar{N}) = N_1^2K_{12} + 2N_1^3K_{12}\bar{K} + 3N_1^4K_{12}\bar{K}^2 + \ldots (n - 1)N_1^nK_{12}\bar{K}^{n-2}$$
$$= N_1^2K_{12}/(1 - N_1\bar{K})^2 \qquad (10)$$

From (9) and (10) we have

$$(N - \bar{N})(1 - N_1\bar{K}) = \bar{N} - N_1$$

which leads to

$$N_1 = \bar{N}(1 - b)/(1 - \bar{K}\bar{N}b)$$

where $b = (f - 1)$. Substituting for N_1, in (9) a quadratic equation for $\bar{K}$ is obtained which gives

$$\bar{K} = 1/\bar{N} \pm (2 - f)\{K_{12}/\bar{N}(f - 1)\}^{1/2} \qquad (11)$$

Equation 11 provides an explicit value for $\bar{K}$ from f and $\bar{N}$ provided K_{12} is known: the latter must be determined independently. Most simply, it is reasonable to assume that at the lowest concentrations for which association is detectable only the dimerization process will be significant, *i.e.*, as the concentration tends to zero the expression $f(f-1)/N(2-f)^2$ will become equal to K_{12}.

The results obtained in this way for trichloroacetamide are given in Table III

TABLE III

$CCl_3{\cdot}CONH_2$ IN C_6H_6

Temp., °C.	K_{12} in mole fraction units	$\bar{K}$	ΔH_{12} in kcal./mole	$\Delta\bar{H}$
24.98	93	93	−6.9	−3.6
35.01	64	77	−7.5	−3.8
45.05	43.5	63		

As already mentioned, the quantitative uncertainty in this instance arises from the approximate equality of K_{12} and $\bar{K}$ and the limited concentration range imposed by solubility, but our data leave no doubt that the association is not adequately represented as a simple dimerization and that $K_{12} < \bar{K}$. Although we have treated these results assuming the various equilibria of $K_{23} = K_{34} = \ldots \bar{K}$ were involved, the limited f-values can equally well be accounted for by only dimer and trimer formation, *i.e.*, $K_{12} \neq K_{23} = \bar{K}$. It is significant that the heat of dimerization, −7.2 ± 0.3 kcal./mole, is twice that for the subsequent stage, −3.7 ± 0.1 kcal./mole. These figures, supported by later data, strongly suggest that the initial dimerization is to a cyclic structure having two H-bridges per dimer, and as the net effect of the next stage is equivalent to the formation of one further H-bridge, the trimer must likewise be of a closed cyclic form. These conclusions essentially reproduce those found in a far more extensive study of acetamide itself in chloroform,[6a] although there is a marked solvent influence on the ΔH values.

Acetanilide associates somewhat less markedly than trichloroacetamide and our present data provide a shorter range of conditions over which to analyze the equilibria. Accordingly, in Table II2 we have given the individual values of K_{12} assuming simple dimerization to occur, and of $(f-1)/N = \bar{K}$ (case (ii)). It is clear that the former factor drifts markedly, whilst the second is constant to well within the experimental uncertainty. Accordingly, we deduce that the process is not limited to dimerization and appears to conform to case (ii) with $\Delta\bar{H} = -3.2 \pm 0.2$ kcal. per/mole of monomer added in association.

The results for formanilide at 25° follow the same pattern as those for acetanilide, *i.e.*, K_{12} more than doubles in a threefold concentration range but $\bar{K}$ is very steady at 63 ±2. It is clear from earlier ebullioscopic studies that the association of formanilide is greater than that of acetanilide and that it proceeds far beyond the dimer stage.[14] Although both for formanilide and acetanilide $(f - 1)$ is proportional to $\bar{N}$ over our measured range, the latter is too small adequately to establish model (ii) for the association: probably we really have to do with the early stages of model (iii).

The results for trichloroacetanilide (Table II4) show much smaller f values than those of the other solutes examined here and also the remarkable feature that these rise to a constant value of about 1.08 and then no longer increase with concentration. On any basis, it is difficult to explain these results, found at both 25 and 35°, but clearly they do not allow of any association pattern being deduced.

We wish to thank the D.S.I.R. for a Maintenance Award to one of us (D.K.T.) and the Shell Petroleum Co. for financial assistance.

---

(13) We have checked that the condition $N_1\bar{K} < 1$ does in fact apply in all those cases where we have used equation 11. A similar condition arises in deducing some of Kreuzer's relations.

(14) *Cf.* A. N. Meldrum and W. E. S. Turner, *Trans. Chem. Soc. (London)*, **97**, 1605 (1910); and E. Beckmann, *Z. physik. Chem.*, **6**, 437 (1890).

ENERGIES AND ENTROPIES OF ASSOCIATION FOR AMIDES IN BENZENE SOLUTIONS. PART II

BY MANSEL DAVIES AND D. K. THOMAS

The Edward Davies Chemical Laboratories, University College of Wales, Aberystwyth, England

Received September 7, 1955

A simple method based on the "thermoelectric osmometer" of Hill which uses single drops of solution and a pair of matched thermistors to compare vapor pressure lowerings is described. One-half per cent. or better accuracy can be attained readily for non-volatile solutes above 0.05 *M*. One N-propyl and four N-methyl amides were studied in benzene. After an initial dimerization, chain-association to high mean molecular weights occurs in dilute solutions except for trichloroacetamide and its N-methyl derivatives which produce cyclic dimers and trimers. The H-bridge energy in all these cases is 3.6 ± 0.2 kcal./mole. The entropies of association also are discussed.

The experimental method used in this Part stems from the "thermoelectric osmometer" due to Hill[1] and developed by Baldes.[2] McBain, Brady and Huff[3] described the use of matched thermistors for this method and it is essentially their arrangement which we have adapted to our needs. Nulkarni and, more particularly, Müller and Stolten[4] have given accounts of a similar procedure whilst the present work was in progress.

Experimental

The vapor pressure difference between solvent and solution is measured in terms of the temperature difference between individual isolated drops placed in the saturated solvent vapor. Condensation of the latter occurs on to the solution drop until its temperature rises so that the solvent partial pressure equals that of the pure liquid. For a 0.010 *M* ideal benzene solution this temperature difference is approximately 0.018° at 25°.

Our drops were placed on a matched pair of Stantel thermistors (type 2311/300), the resistance element being a minute bead having a very thin glass cover. At 20° each thermistor was of approximately 2000 ohm and maximum continuous power dissipation 10 milliwatt. Figure 1 shows the essential features of their mounting: in this the fixture of the leads in the glass tube was sufficiently rigid that no change in resistance occurred on raising and lowering the thermistors between the Dewar and the loading chamber. Care was taken to ensure maximum thermal insulation of the individual thermistors. The assembly was sunk in a thermostat controlled to ±0.01° and the silvered Dewar provided a well-defined vapor bath. At least 24 hours were needed for adequate temperature constancy to be attained within it. Observations were made with a simple Wheatstone bridge, each resistance being approximately 2000 ohm, and a moving coil lamp-and-scale galvanometer having a sensitivity of 218 mm. per μÅ. The applied e.m.f. could be reversed by a key and was tapped off a 2 volt battery *via* a potentiometer to ensure that excessive power was not developed in the thermistors.

With both thermistors bare, the bridge was balanced as nearly as the box resistances would allow: this gave the galvanometer zero. Drops of solvent were then placed on each thermistor and the steady galvanometer deflection on reversing the bridge e.m.f. noted: this provided the solvent reading, which was subtracted from subsequent readings when solvent and solution drops were equilibrated. The reversal of the e.m.f. which was always made, served *inter alia*, effectively to double the deflections. Steady readings were usually attained about four minutes after the thermistors had been lowered into the equilibrium chamber. Between any pair of solutions the galvanometer zero was checked to ensure constancy in the thermistor conditions: further, the "solvent reading" and that for standard (calibrating) solutions could be checked at frequent intervals in measuring new solutions.

The accepted deflections were the mean of five or six observations. Biphenyl was chosen as the standard, ideal, solute in benzene (see Part I) and the results for a typical calibration at 25.01° may be given. The deflections, Δ, recorded for the solutions are those obtained after subtraction of the (constant) solvent reading.

10^3 × mole fraction biphenyl (N_d)	3.75	7.30	9.39	11.92	16.07
Galvanometer deflection (Δ mm.)	34.0	66.5	85.5	108.0	147.0
$\Delta/(N_d \times 10^3)$	9.07	9.11	9.10	9.07	9.15

Not only are the deflections proportional to the mole fraction of the ideal solute, but the effective mole fraction ($\bar{N}$) of any non-volatile solute in a solution giving a deflection Δ is clearly the biphenyl mole fraction (N_d) giving the same deflection. Accordingly, the apparent mean degree of association of the solute is its stoichiometric mole fraction divided by N_d.

All solutions were made up by weight and samples kept in closely stoppered bottles in the thermostat for some time before use.

Two of the tests we made of the method may be briefly mentioned. We measured trichloroacetamide at low concentrations in benzene and compared the results with those of previous isopiestic determinations. The apparent molecular weights found for identical concentrations were

$10^3 \times N$	2.55	3.16	3.34	3.99	4.32
Thermistor mol. wt.	181.9	195.3	204.6	213.1	218.0
Isopiestic mol. wt.	190.8	199.4	203.0	212.4	218.8

The apparent molecular weights by the isopiestic method are certainly correct to better than one unit: the thermistor values are acceptable down to $N = 3.3 \times 10^3$ or 0.04 *M*.

We tested our whole procedure by determining the association constant, K_{12}, for benzoic acid in benzene at 25.0°: this is not a favorable case, as the dimerization is almost complete over the accessible concentration range. On a log K_{12} against $1/T$ plot our value at 25.01° ($K_{12} = 5.5 \times 10^3$ in mole fraction units) agrees excellently with the line defined by the recent ebullioscopic data of Allen and Caldin[5] at 54.1, 65.5 and 80.3° and the isopiestic data of Wall and Banes[6] at 32.5 and 43.3°.

Materials.—**N-Methylformamide**: prepared from formic acid and methylamine: b.p. 102–103° (20 mm.), n^{19}D 1.4313 (lit. n^{25}D 1.4310).

N-Methylacetamide.—The fraction boiling 108° (15 mm.) melted sharply at 28°.

N-Methylbenzamide: prepared by the Schotten–Baumann reaction, and recrystallized from alcohol; m.p. 82°.

N-Methyltrichloracetamide: prepared from methylamine and the ethyl ester: recrystallization from ether: m.p. 105°.

N-Propylacetamide: propylamine in aqueous acetic acid was treated with acetic anhydride, and the product fractionated; b.p. 223° (lit. 222–225°).

Owing to their hygroscopic nature, particular care was taken in storing and handling these amides. As for the

---

[1] A. V. Hill, *Proc. Roy. Soc.* (*London*), **A127**, 9 (1930).

[2] E. J. Baldes, *Biodynamica*, No. 46 (1939).

[3] J. W. McBain, A. P. Brady and H. Huff, THIS JOURNAL, **55**, 304 (1951).

[4] Nulkarni, *Nature* (*London*), **171**, 4344 (1953).

[5] G. Allen and E. F. Caldin, *Trans. Faraday Soc.*, **49**, 895 (1953).

[6] F. T. Wall and F. W. Banes, *J. Am. Chem. Soc.*, **67**, 898 (1945).

TABLE I

N-METHYLACETAMIDE IN BENZENE AT 24.57°

$10^3 \times \bar{N}$	1.00	2.00	4.00	6.00	7.00	8.00	9.00	10.00
f	1.07	1.18_6	1.49	1.84_5	2.05	2.28_6	2.52	2.76
$\bar{\alpha}$	0.946	0.881	0.748	0.638	0.593	0.551	0.515	0.482
$\bar{K}$ ($K_{12} = 69$)	...	152	154	148.5	147.8	148.3	148.1	147.6
$\bar{K}$ ($K_{12} = 60$)	...	173	161	149.8	147.5	146.8	145.5	144.4
$\bar{K}$ (from α)	...	...	...	145	144	146	145	145

isopiestic method, the non-volatility of the solute is a necessary condition in these studies: the practical limit was reached in the case of N-methylformamide which proved too volatile to give reliable results at 45°.

Results

The most obvious feature of the results is the pronounced abnormality of these solutes: for N-methylformamide at 25° and $N = 10 \times 10^{-3}$ (0.13 M), the apparent molecular weight is already three times that of the monomer. The infrared and dielectric polarization data[7] leave no doubt that the major source of the abnormalities is the molecular association of the solute. N-methylacetamide provides a pattern typical of a number of these amides. Representation of the results in terms of Kreuzer's relations (*e.g.*, f against $\bar{N}$ plot) shows the process to consist of an initial dimerization followed, even at our lowest concentrations, by further stages having higher association constants, *i.e.*, qualitative and quantitative considerations suggest type (iii) association where $K_{12} < K_{23} = K_{34} = \ldots \bar{K}$.

At the lowest concentrations the f—$\bar{N}$ curve for N-methylacetamide at 25° in benzene suggests the initial dimerization constant K_{12} is 70 ± 10 in mole fraction units. Using this value, one can then calculate $\bar{K}$ from equation 11 (Part I). This treatment is summarized in Table I for which, as in the other tables, f values have been read off a large scale plot of f against $\bar{N}$. The original curves have a minimum of six experimental points for the ranges quoted, the actual deviations from the smooth curves being usually less than 0.01 in the f values.

In Table I the $\bar{K}$ values are in mole fraction units, two of the sets corresponding to the different K_{12} values of 60 and 69. It is clear that the latter provides the better fit for the data and leads to $\bar{K} = 148 \pm 1$. In the last row some values of $\bar{K}$ have been calculated from the $\bar{\alpha}$ values using the relation deduced by Coggeshall and Saier.[8] Not only is the latter a cumbersome relation to evaluate but the $\bar{\alpha}$ values are, in this case, only obtainable indirectly, by graphical integration from the Kreuzer equation

$$\ln (1/\bar{\alpha}) = \int_0^{\bar{N}} (f - 1)/f\bar{N} \, d\bar{N}$$

The degree of agreement found suffices to establish the practical consistency of the relations used.

The experimental data for these systems are summarized in Table II and the association equilibrium data are collected in Table III. The equilibrium constants are in mole-fraction units, the enthalpies (ΔH) in kcal./mole, and the entropies (ΔS) in cal./mole per°K.

Discussion

The N-methyl derivatives of formamide, acetamide and benzamide and N-propylacetamide all show the same pattern, *i.e.*, they consistently provide apparent mean degrees of association (f) conforming to an initial dimerization constant followed by successive and approximately equal association constants: $K_{12} < K_{23} = K_{34} \ldots = \bar{K}$. The large f-values encountered (*e.g.*, $f \simeq 3.0$ at 0.12 M) suffice to establish that all associates up to at least a tetramer stage appear in dilute solutions. Although to within the experimental uncertainty, the data can be fitted by only two equilibrium constants that agreement, of course, only indicates the approximate equality of the association steps after the dimerization. For N-methylformamide it appears that $K_{12} \simeq \bar{K}$, the condition $K_{12} < \bar{K}$ being more pronounced for the acetamide and benzamide derivatives. Like trichloroacetamide itself, the N-methyl derivative does not follow a chain-association: the degree of association is now very much smaller: at 25° and $N = 4 \times 10^{-3}$, trichloroacetamide has $f = 1.38$, the N-methyl compound has $f = 1.05$. In fact, over the measured concentrations and especially at 35 and 49° the N-methyltrichloroacetamide is mainly involved in a monomer $\rightleftarrows$ dimer process. However, at the three temperatures, the data indicate that some further association does occur with $K_1 < K_{23}$. Marked differences from the preceding cases are also found for the corresponding heats.

Perhaps the most significant feature in these data is the approximate constancy in the heats of association: where dimerization is followed by chain-association these are all 3.6 ± 0.2 kcal. per mole of monomer added in the association. Clearly, this measures the energy of the "hydrogen bridge" in the polymolecular structures: in those cases where approximately the same value is found for ΔH_{12} it is suggested that only one hydrogen bridge is present in the dimers. This figure (3.6 kcal./mole) is probably the best available estimate of this interaction energy in amide structures, but it is important to remember that the solvent can have a considerable influence upon it.[9]

By the same criterion (the value of ΔH_{12}) it appears that both trichloroacetamide and its N-methyl derivative give rise to cyclic dimers in which, as for the carboxylic acid dimers, two hydrogen bridges are formed. These compounds are also unique in that there is no certainty that the association proceeds beyond the trimer, although there is some slight indication for N-methyl trichloroacetamide that this is so. The values of ΔH_{23} ($= \Delta H_{13} - \Delta H_{12}$) show that one further

---

(7) G. R. Leader and J. F. Gormley, *J. Am. Chem. Soc.*, **73**, 5731 (1951).

(8) N. D. Coggeshall and E. L. Saier, *ibid.*, **73**, 5414 (1951).

(9) E. A. Moelwyn-Hughes, D. Patraik, M. Davies and P. O. Jones, *J. Chem. Soc.*, 1249 (1951).

TABLE II

MEAN DEGREES OF ASSOCIATION (f) AND DEDUCED FRACTIONS OF SOLUTE PARTICLES FORMED BY MONOMER ($\bar{\alpha}$) IN BENZENE

Solute	$10^3 \times \overline{N}$	1.00	2.00	3.00	4.00	6.00	8.00	10.00	12.00	14.00	16.00	18.00	20.00
							At 24.92°						
N-Methyl-formamide	f:	1.10	1.31_5	1.59	1.84	2.37	2.90	...	...	...	...	...	...
	$\bar{\alpha}$:	0.944	0.847	0.749	0.665	0.539	0.451	...	...	...	...	...	...
							At 35.07°						
	f:	1.17_3	1.34	...	1.69_7	2.05	2.40_6	2.76	3.12	...	...	...	...
	$\bar{\alpha}$:	0.852	0.743	...	0.591	0.490	0.418	0.365	0.324	...	...	...	...
							At 24.57°						
N-Methyl-acetamide	f:	1.07	1.18_6	...	1.49	1.84_5	2.28_5	2.76	...	...	...	...	...
	$\bar{\alpha}$:	0.946	0.881	...	0.748	0.638	0.551	0.482	...	...	...	...	...
							At 35.07°						
	f:	1.06	1.13	1.22_6	1.34	1.63_6	1.94_5	2.26	2.56_6	...	...	...	...
	$\bar{\alpha}$:	0.951	0.899	0.847	0.795	0.698	0.615	0.546	0.492	...	...	...	...
							At 48.90°						
	f:	1.06	1.13	...	1.26	1.39	1.55	1.71	1.88	2.05_5	2.26	...	...
	$\bar{\alpha}$:	0.944	0.894	...	0.801	0.726	0.663	0.608	0.561	0.520	0.484	...	...
							At 24.92°						
N-Methyl-benzamide	f:	1.01	1.02	...	1.04	1.10	1.24	1.44	1.76	2.17	2.59_5	...	...
	$\bar{\alpha}$:	0.990	0.980	...	0.974	0.939	0.902	0.854	0.799	0.742	0.687	...	...
							At 35.07°						
	f:	...	1.01	...	1.03	1.06	1.11	1.19	1.30	1.57_6	1.91	2.27	...
	$\bar{\alpha}$:	...	0.992	...	0.981	0.969	0.945	0.918	0.887	0.851	0.810	0.765	...
							At 48.90°						
	f:	...	1.007	...	1.01_3	1.02	1.04	1.07	1.12	..	1.28	1.39	1.50
	$\bar{\alpha}$:	...	0.987	...	0.980	0.973	0.962	0.948	0.928	...	0.887	0.850	0.821
							At 24.57°						
N-Methyltri-chloro-acetamide	f:	1.01	1.02	...	1.05	1.11	1.20	1.32_5	1.50	1.63[a]	...	...	...
	$\bar{\alpha}$:	0.992	0.984	...	0.964	0.937	0.903	0.863	0.819	0.800[a]	...	...	...
							At 35.07°						
	f:	1.006	1.01	...	1.023	1.035	1.048	1.06_4	1.08	..	1.12	1.15	...
	$\bar{\alpha}$:	0.995	0.989	...	0.978	0.968	0.957	0.945	0.934	...	0.910	0.897	...
							At 48.90°						
(N-Methyl-trichloro-acetamide)	f:	...	1.007	...	1.013	1.02	1.026	1.03_2	...	1.045	1.05	1.065	1.08_3
	$\bar{\alpha}$:	...	0.993	...	0.987	0.980	0.974	0.969	...	0.957	0.951	0.944	0.938
							At 21.80°						
N-Propyl-acetamide	f:	1.04_6	1.09_5	...	1.19_5	1.297	1.40	1.50_7	1.61_6	1.72	1.83	...	...
	$\bar{\alpha}$:	0.957	0.916	...	0.842	0.778	0.723	0.674	0.632	0.594	0.560	...	...

[a] $\overline{N} = 13.00 \times 10^{-3}$.

TABLE III

Solute	t, °C.	K_{12}	$-\Delta H_{12}$	$\overline{K}$	$-\Delta\overline{H}$	$-\Delta S_{12}$	$-\Delta\overline{S}$
N-Methylacetamide	24.57	69 ± 3	3.45	148 ± 2	3.91	3.7 ± 0.7	2.7 ± 0.5
	35.07	$56._5$ ± 2	3.71	$118._5$ ± 2	3.64		
	48.90	$43._5$ ± 2		$91._7$ ± 2			
N-Methylformamide	24.92	213 ± 5	3.4_9	218 ± 4	3.8_7	1.3 ± 0.5	2.4 ± 0.7
	35.07	175 ± 3		175 ± 3			
N-Methylbenzamide	24.92	5.2_4 ± 0.1	3.57	$75._0$ ± 1	3.67	8.8 ± 0.6	3.9 ± 0.7
	35.07	4.2_9 ± 0.1	3.71	$61._3$ ± 1	3.75		
	48.90	3.3_0 ± 0.05		$47._0$ ± 0.5			
N-Propylacetamide	21.80	50		52 ± 2		...	...
N-Methyltrichloro-acetamide[a]	24.57	8.4_8 ± 0.2	...	$28._2$ ± 1.0	...	19.6 ± 1	5.5 ± 0.5
	35.07	5.5_6 ± 0.1	7.3_2	$23._4$ ± 1.0	3.2_6		
	48.90	3.4_0 ± 0.05	6.9_6	$17._8$ ± 0.5	3.9_2		
Trichloroacetamide[a]	See Part I		7.1 ± 0.4	...	3.7 ± 0.1	15.8 ± 0.4	8.6 ± 0.4

[a] For $\overline{K}$, $\Delta\overline{H}$, $\Delta\overline{S}$ read in these cases K_{23}, ΔH_{23}, ΔS_{23}.

"hydrogen bond" is probably formed in the trimer, *i.e.*, that the latter is also a cyclic structure.

The entropy changes on association also reflect these different categories. For an ideally simple process, (monomer) + (n-mer) → ($\overline{n + 1}$ mer), in which only translational and rotational energy changes occurred, one would expect $\Delta S \simeq -60$ cal./°K. per mole of monomer. However, to be set against this are the positive contributions to ΔS resulting from the conversion of the degrees of freedom of the monomer into low ("intermolecular") vibrational frequencies in the association complex. This condition is partly reflected in $\Delta S_{12} = -28$ e.u. for the gaseous dimerization of acetic acid[10] or in entropy of polymerization values, *e.g.*, for methyl methacrylate monomer,[11] $\Delta S = -28$ e.u. However, the values observed here, especially for $-\Delta \bar{S}$, are still very much smaller. This is almost certainly due to solvation changes which accompany association. If for each monomer molecule added to an existing complex, the net effect were to free one solvent molecule previously "frozen" in a solvation shell, the degrees of freedom changed for the monomer would be approximately balanced by those for the solvent. Some such compensation must certainly be involved as, were $\Delta S = -30$ e.u. and $\Delta H = -3.7$ kcal./mole, K would be c $\times 10^{-9}$ rather than of the order shown in Table III. This solvent factor plays an essential role in the association of these compounds, for only monomer can be detected spectroscopically in their saturated vapors.[12]

The larger values of $-\Delta S$ for the trichloroacetamide molecules conform well with the different (cyclic) structures found in these cases. The greater degree of order, or precision of orientation, probably involved in the cyclic structures relative to chain association makes $\Delta S = S(\text{dimer}) - 2S(\text{monomer})$ smaller than would otherwise be the case.

We may conclude with a reference to the frequently presented proposition that the chain-association often found for the amides is a consequence of the *trans*—configuration I of the monomers[13]—it being averred that the *cis*-form (II) would, for steric reasons, be essentially confined to cyclic dimerization. This argument is devoid of substantial foundation. Thus, if the free-energy changes in a simple representation are

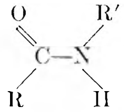
I

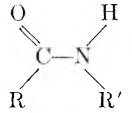
II

$$\begin{tikzcd}
\textit{cis}\text{-monomer} \arrow[r, "\Delta G_3"] \arrow[d, "\Delta G_1"'] & \text{cyclic association} \\
\text{trans-monomer} \arrow[r, "\Delta G_2"] & \text{linear (chain) association}
\end{tikzcd}$$

then if $(\Delta G_1 + \Delta G_2)$ has a larger negative value than ΔG_3, we would have a monomer stable in the *cis*-form leading to linear (*trans*) associated molecules. The converse relations may arise for N-methyltrichloroacetamide ($R = CCl_3$; $R' = CH_3$). As would be expected, accurate (Courtauld's) models show that the *trans*-configuration (I) is much easier to attain than the *cis* (II). The latter, although free from strain, requires coordinated packing of the $-CCl_3$ and H_3C- groups (so that on entropy considerations I is the favored form) which also results in the C=O and N—H groups of II being markedly exposed in fixed and adjacent positions on one side of the molecule. What is quite definite from our studies is that this molecule is almost restricted to cyclic dimer formation under conditions in which N-methylacetamide, for instance, shows marked chain association.

The absorption spectra for these different examples of association processes have not yet been reported.

We wish to thank the D.S.I.R. for a Maintenance Award (to D.K.T.) and the Shell Petroleum Co. for financial assistance.

---

[10] H. L. Ritter and J. H. Simons, *J. Am. Chem. Soc.*, **67**, 757 (1945).

[11] P. A. Small, *Trans. Faraday Soc.*, **49**, 441 (1953).

[12] J. C. Evans, *J. Chem. Phys.*, **22**, 1228 (1954); M. Davies, J. C. Evans and R. L. Jones, *Trans. Faraday Soc.*, **51**, 761 (1955), and unpublished observations in these laboratories.

[13] A. M. Buswell, J. N. Downing and W. H. Rodebush, *J. Am. Chem. Soc.*, **62**, 2759 (1940); M. Tsuboi, *Bull. Chem. Soc. Japan*, **22**, 215 (1949); J. E. Worsham and M. E. Hobbs, *J. Am. Chem. Soc.*, **76**, 206 (1954).

THE HEAT OF DECOMPOSITION OF TRICALCIUM SILICATE INTO β-DICALCIUM SILICATE AND CALCIUM OXIDE

By Stephen Brunauer, D. L. Kantro and C. H. Weise

Portland Cement Association Research and Development Laboratories, Chicago, Illinois

Received September 28, 1955

The paper presents the results of a redetermination, by an improved method, of the heat of the reaction $Ca_3SiO_5(c) = \beta\text{-}Ca_2SiO_4(c) + CaO(c)$. The heat of solution method was used, but equimolar mixtures of $\beta\text{-}Ca_2SiO_4$ and CaO were dissolved *together* rather than separately as in earlier investigations. The result was $\Delta H_{296} = -2100$ cal./mole. The estimated uncertainty was ±200 cal./mole.

Introduction

The decomposition of tricalcium silicate, Ca_3SiO_5, into β-dicalcium silicate, $\beta\text{-}Ca_2SiO_4$, and calcium oxide, is represented by the equation

$$Ca_3SiO_5(c) = \beta\text{-}Ca_2SiO_4(c) + CaO(c) \qquad (1)$$
$$\Delta H = -D \text{ cal.}$$

where D is the heat evolved in the decomposition of Ca_3SiO_5. There are three published values of D in the chemical literature: Johansson and Thorvaldson[1] obtained 470 cal. at 20°; King,[2] 3200 cal. at 25°; and Brunauer, Hayes and Hass,[3] 2400 cal. at 23°.

In all three investigations the same principle was used to obtain D. This is represented by the equation

$$D = H_{Ca_3SiO_5} - H_{Ca_2SiO_4} - H_{CaO} \qquad (2)$$

where $H_{Ca_3SiO_5}$, $H_{Ca_2SiO_4}$ and H_{CaO} are the heats of solution of Ca_3SiO_5, Ca_2SiO_4 and CaO, respectively. Johansson and Thorvaldson used hydrochloric acid, King, hydrofluoric acid, and Brunauer, Hayes and Hass, a mixture of nitric acid and hydrofluoric acid as their "solvents." Actually, the acids react with the solids; the heats liberated are, therefore, heats of reaction rather than heats of solution. Nevertheless, the traditional term, "heat of solution," will be retained throughout this paper.

All three published values of D were obtained by determining the three heats of solution *separately* and using eq. 2. This method, however, is valid only if the sum of the products obtained in the separate solution of Ca_2SiO_4 and CaO is identical with the products obtained in the solution of Ca_3SiO_5. This means absence of concentration effects, understood in a broad sense. The term "concentration effects" is used here to designate not only the changes in the states of the products of solution, but also the changes in the nature of the products caused by concentration changes. If such effects are present, the method of separate solutions does not give the right result, unless proper corrections are made.

In the present investigations the heats of solution of Ca_3SiO_5 and of equimolar mixtures of Ca_2SiO_4 and CaO were determined over a tenfold range of concentrations and D was obtained from the differences between the heat values at equal weights. This method leads to the correct value of D if the products obtained in the solution of equimolar mixtures of Ca_2SiO_4 and CaO are identical with the products obtained in the solution of Ca_3SiO_5. This requirement appeared to be fulfilled in the present experiments. The value of D obtained was 2100 cal., with an estimated uncertainty of ±200 cal.

Experimental

Preparation of Materials.—The Ca_3SiO_5 was prepared in the manner described by Brunauer, Hayes and Hass.[3] In the preparation of $\beta\text{-}Ca_2SiO_4$ the same materials were used, with the addition of boric oxide, the function of which was to prevent the inversion of $\beta\text{-}Ca_2SiO_4$ to the γ-form. The charge was heated to 1450 ± 20°, and this temperature was maintained for three hours. The first preparation of Ca_2SiO_4 was all in the β-form, and it contained 0.86% B_2O_3. We next attempted to prepare $\beta\text{-}Ca_2SiO_4$, using less B_2O_3. The second preparation contained 0.30% B_2O_3, but it "dusted," *i.e.*, most of it inverted to the γ-form. (The phase transition is accompanied by a large volume expansion, which causes the material to crumble to dust.) The third and final preparation was made by blending the first two preparations and reburning the blend at 1450 ± 20° for three hours. It contained no $\gamma\text{-}Ca_2SiO_4$, and its B_2O_3 content was 0.53%. The $\beta\text{-}Ca_2SiO_4$ was unusually hard and difficult to grind. After 40 hours of grinding in a porcelain jar mill containing flint pebbles, only about 10% of the charge passed a U. S. Standard No. 200 sieve, and this fraction was used in the present experiments. The grinding introduced about 0.4% SiO_2 into the sample, as shown in Table I.

The calcium oxide was prepared from "J. T. Baker Analyzed Reagent" calcium carbonate, low in alkali. The carbonate was heated in a platinum dish for four hours at 1050° in a globar furnace. The resulting cake was crushed to pass a U. S. Standard No. 100 sieve, and the powder was pressed into cylindrical pellets, $^1/_4''$ diameter and $^1/_8$ to $^3/_8''$ tall, in a Parr pellet press. The pellets were ignited for 72 hours at 1050° in the globar furnace and were stored in a desiccator over P_2O_5 until use. Ordinarily, they were used within the next few days, but one set of pellets was stored for six weeks prior to use. The heats of solution were not altered by the longer storage. Another set of pellets was ignited for seven days, instead of three days; this set also gave heats of solution in agreement with the others.

Mixtures of $\beta\text{-}Ca_2SiO_4$ and CaO were prepared by grinding equimolar quantities of the substances together in an agate mortar, thoroughly homogenizing the mixture, and pressing the powder into pellets. The pellets were stored in a desiccator over P_2O_5 until use.

The zinc oxide, used for the calibration of the calorimeter, was "J. T. Baker Analyzed Reagent" material and it was treated as prescribed in the ASTM standard test.[4] The acids used in the calorimeter were 2 N nitric acid, prepared by dilution of du Pont "C.P. Reagent" nitric acid with distilled water, and "J. T. Baker Analyzed Reagent" hydrofluoric acid, 49.4% solution. The heat of solution of ZnO was taken as 257.0 cal./g.[4]; and the standard error of the calibration measurements was ±0.11 cal./g.

Calorimetry.—The heat of solution calorimeter was similar to that used by Verbeck and Foster.[5] There were

---

[1] O. K. Johansson and T. Thorvaldson, *J. Am. Chem. Soc.*, **56**, 2327 (1934).

[2] E. G. King, *ibid.*, **73**, 656 (1951).

[3] S. Brunauer, J. C. Hayes and W. E. Hass, This Journal, **58**, 279 (1954).

[4] 1952 Book of ASTM Standards, American Society for Testing Materials, Philadelphia, 1953, Part 3, pp. 145–151.

[5] G. J. Verbeck and C. W. Foster, *Proc. Am. Soc. Testing Materials*, **50**, 1235 (1950).

TABLE I

ANALYSES AND COMPOSITIONS OF Ca_3SiO_5 AND β-Ca_2SiO_4

Ca_3SiO_5

Analysis Substance	%	Composition Substance	%
CaO	73.34	Ca_3SiO_5	99.07
SiO_2	26.04	$Ca_3Al_2O_6$[b]	0.27
Al_2O_3	0.10	CaO	.31
MgO	.23	MgO	.23
SO_3	.04	SiO_2	.04
Na_2O	.04	Na_2SO_4	.08
K_2O	nil	Total	100.00
Total[a]	99.79		

Free CaO 0.31

Free SiO_2 0.04

β-Ca_2SiO_4

Analysis Substance	%	Composition Substance	%
CaO	64.00	β-Ca_2SiO_4	97.15
SiO_2	34.73	$Ca_3Si_2O_7$[d]	1.25
Al_2O_3	0.11	$Ca_3Al_2O_6$[b]	0.29
MgO	.22	CaO	.05
SO_3	.03	MgO	.22
Na_2O	.03	SiO_2	.45
K_2O	nil	B_2O_3 (dissolved)	.53
B_2O_3	.53	Na_2SO_4	.06
Total[c]	99.65	Total	100.00

Free CaO 0.05

Free SiO_2 0.45

[a] The missing 0.21% was assumed to be Ca_3SiO_5. [b] Tricalcium aluminate, $3CaO \cdot Al_2O_3$. [c] The missing 0.35% was assumed to be Ca_2SiO_4. [d] Rankinite, $3CaO \cdot 2SiO_2$.

only two essential differences: the calorimeter head was fabricated from paper-based Bakelite, rather than Lucite, to obtain greater dimensional stability and mechanical strength, and the diameter of the sample funnel was increased from $^3/_{16}''$ to $^1/_2''$ to facilitate rapid introduction of the samples. The acid mixture was 8 ml. of 49.4% H_2F_2, with sufficient 2 N HNO_3 added to make the total weight 420 g.

Great difficulties were encountered in obtaining reproducible results, until extreme precautions were adopted to avoid carbonation and hydration of the samples. The Ca_3SiO_5 and Ca_2SiO_4 samples to be used during the day's experimental runs were ignited in the morning for one hour at 1050°, and were stored in a desiccator over P_2O_5. Then prior to the run each sample was re-ignited at 1050° for 15 minutes, cooled in a desiccator over P_2O_5, weighed, and immediately introduced into the calorimeter. For the CaO samples and for the pelletized mixture samples, a 30-minute ignition period was used prior to each run.

The temperatures were read on an N.B.S. calibrated Beckmann thermometer; ΔT, the temperature change caused by the solution of the sample, was determined by the method described by Weber.[6] The calorimeter constants were evaluated by the method of least squares from rating data obtained in a large number of runs. The graphical integration, required in the calculation of each ΔT, was performed by plotting the time–temperature data on a fine-grade coördinate tracing paper, cutting out the area and weighing. After the calculations, three small corrections were applied to ΔT: the stem correction, the calibration correction and the setting-factor correction.

Other Operations.—The ignition loss and carbon dioxide content were determined, the chemical analyses were performed, and the compositions of the substances were calculated according to the methods described by Brunauer, Hayes and Hass.[3] The analytical data and the calculated compositions of the Ca_3SiO_5 and Ca_2SiO_4 are given in Table I. The calculations were based on the method developed by Bogue.[7] The Ca_2SiO_4 was in the β-form; X-ray diffractometer charts and microscopical examination showed absence of γ-Ca_2SiO_4. The CaO contained only one impurity in more than trace amounts, namely, about 0.2% MgO. Since MgO has approximately the same heat of solution as CaO, no correction was made for this impurity.

Results and Discussion

Experimental Heat of Decomposition of Ca_3SiO_5.—The experimental heats of solution of Ca_3SiO_5 and those of equimolar mixtures of β-Ca_2SiO_4 and CaO are shown in Fig. 1. Each point represents an average heat of solution and an average sample weight for a narrow range in the weights of the samples. The number of runs averaged is given above the point for Ca_3SiO_5 and below the point for the mixture.

As seen in Fig. 1, the two curves run similar courses, the one being displaced from the other by approximately 9 cal./g. This difference is the experimental value of D, the heat of decomposition of Ca_3SiO_5, in cal./g., if the products of solution were the same at equal weights. *The similarity of the curves strongly indicates that this is the case here.* Actually, the two curves are not exactly parallel. This is caused mostly by experimental error in the determination of the heat of solution, but it is also possible that there were slight differences between the solution products obtained at equal weights. Averaging the differences takes care of random variations in both sources of error. If there was a slight systematic difference between the solution products obtained from Ca_3SiO_5 and from the mixture at equal weights, the error caused by this factor was overshadowed by the experimental error, because the difference between the heats of solution showed very slight or no trend with weight.

Both curves of Fig. 1 show a maximum in the vicinity of 1.3 g. of material dissolved. No attempt was made to ascertain the reason for the maximum, since an investigation of the nature of the dissolved ions and molecules at different concentrations was outside the scope of these investigations. The fact that in both curves the maximum appears in approximately the same weight range and has approximately the same shape is an added indication that the same products were obtained in the solution of Ca_3SiO_5 and the mixture at the same weights.

Dr. Paul Seligmann of this Laboratory developed a statistical method to obtain the mean value of D and its standard error. In the treatment, the experimental points shown in Fig. 1 were used and not the smooth curves. The data were grouped to obtain 16 sets of values for corresponding weight ranges of Ca_3SiO_5 and Ca_2SiO_4–CaO mixtures. It was assumed that the main source of error was in the reading of the temperature on the Beckmann thermometer and that this error was independent of the actual temperature rise. For a given material, an increase in weight of sample results in an increase in temperature rise, hence in a decrease in the relative error in the calculated heat. Thus, the error in the calculated heat may be taken to be inversely proportional to the sample weight with a propor-

---

(6) R. L. Weber, "Heat and Temperature Measurement," Prentice-Hall, Inc., New York, N. Y., 1950, pp. 174–177.

(7) R. H. Bogue, *Ind. Eng. Chem., Anal. Ed.*, **1**, 192 (1929).

tionality factor to be determined. It was further assumed that the proportionality factor for the error in the heat of solution of Ca_3SiO_5 would be different from that for the Ca_2SiO_4-CaO mixtures.

Let

w_i = mid-point of the ith wt. range
m_i = no. of Ca_3SiO_5 runs in the ith wt. range
n_i = no. of Ca_2SiO_4-CaO runs in the ith wt. range
H_{1i} = mean heat of soln. of Ca_3SiO_5 in the ith wt. range
H_{2i} = mean heat of soln. of Ca_2SiO_4-CaO in the ith wt. range.

The standard deviations of individual determinations may be written as

$$\sigma_{1i} = k_1/w_i$$

for the Ca_3SiO_5 and

$$\sigma_{2i} = k_2/w_i$$

for the Ca_2SiO_4-CaO mixtures, where k_1 and k_2 are the proportionality constants to be determined.

Equations were derived for the simultaneous determination of D, k_1 and k_2, and were solved by a method of successive approximations. After k_1 and k_2 had been found, the following equation gave the estimated weighted average for D

$$D = \frac{1}{C}\sum_{i=1}^{16} \frac{m_i n_i w_i^2}{k_1^2 m_i + k_2^2 n_i}(H_{1i} - H_{2i})$$

where

$$C = \sum_{i=1}^{16} \frac{m_i n_i w_i^2}{k_1^2 m_i + k_2^2 n_i}$$

The standard error was shown to be $1/\sqrt{C}$. *The mean experimental value of D thus obtained was 9.15 cal./g., with a standard error of ±0.23 cal./g.*

All the solutions obtained in the experiments represented by Fig. 1 were clear, with one exception. The 1.86-g. Ca_3SiO_5 sample gave cloudy solution, indicating some precipitation of calcium fluoride. This sample was not used in the evaluation of D.

The 52 experimental points on which the mixture curve in Fig. 1 is based include 35 points obtained with pelletized mixtures and 17 points obtained by adding the two constituents successively, CaO added first. In other experiments, Ca_2SiO_4 was added first and CaO afterwards. When CaO was added first, the final solutions were clear, and the sum of the heats of solution agreed with the heat of solution of a pelletized mixture of equal weight; but when Ca_2SiO_4 was added first, the solutions were cloudy, and the sum of the heats of solution was larger than the heat of solution of a pelletized mixture of the same weight. The cloudiness, caused by the precipitation of calcium fluoride, decreased with decreasing weight, and the sum of the heats of solution approached the heat values obtained when CaO was added first. The points obtained by successive additions, Ca_2SiO_4 added first, are not included in the curve. That the solution products obtained were not the same as those obtained in the solution of Ca_3SiO_5 was indicated both by the cloudiness of the solutions and by the trend with weight of the difference between the heats of solution of Ca_3SiO_5 and the mixture at equal weights. (The difference was 4.7 cal./g. at 1.6 g. and 7.3 cal./g. at 0.4 g.) These facts illustrate that care must be taken in heat-of-solution calorimetry to ascertain that the same final state is reached after the solution of both the reactants and the reaction products.

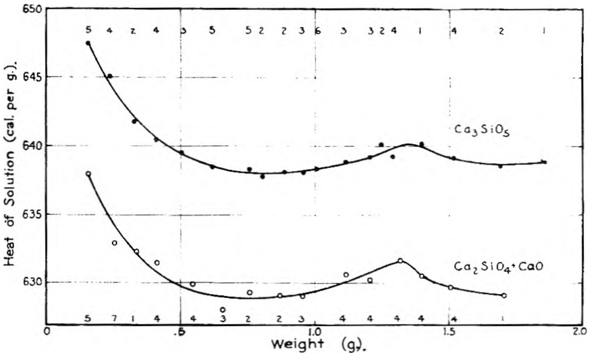

Fig. 1.—Heats of solution of Ca_3SiO_5 and of equimolar mixtures of β-Ca_2SiO_4 and CaO.

Correction for Impurities.—The initial compositions of our Ca_3SiO_5 and β-Ca_2SiO_4 are given in Table I. In spite of all precautions, both substances very slowly hydrated in the course of the months taken by the experiments. This was evidenced by the fact that the free lime content of ignited samples of Ca_3SiO_5 rose from 0.31 to 0.92%, and that of β-Ca_2SiO_4 from 0.5 to 0.19%. The corrections for the impurities were calculated on the basis of both the initial and final compositions, and the average was taken.

It was assumed that the contributions of the impurities to the heats of solution were additive. For the heats of solution of the impurities, the values of Brunauer, Hayes and Hass[3] were used, with the following changes and additions.

(1) The heat of solution of CaO is 861 cal./g., obtained by extrapolation of the experimental data shown in Fig. 3.

(2) The heat of solution of MgO is 862 cal./g. The 562 cal./g. in the paper of Brunauer, Hayes and Hass is a misprint. Both in that paper and in this, the correct value of MgO was used in the calculations.

(3) The heat of solution of Na_2SO_4, calculated from the N.B.S. Thermodynamic Tables,[8] is 3.9 cal./g. This correction term is negligible.

(4) The heat of solution of rankinite, $Ca_3Si_2O_7$, was estimated to be 537 cal./g. The estimate was based on the heats of formation and the heats of solution of β-Ca_2SiO_4 and β-$CaSiO_3$. The error in the estimate is likely to be less than 10 cal./g.; the uncertainty introduced by this term is, therefore, of the order of 0.15 cal./g.

For the heat of solution of B_2O_3 dissolved in β-Ca_2SiO_4, the heat of solution of crystalline B_2O_3 was used; in other words, the heat change occurring when B_2O_3 is dissolved in β-Ca_2SiO_4 was neglected. There is no value in the literature for this heat term, and its determination was beyond the scope of the present experiments. That the term is small is indicated by the fact that the presence of a small amount of B_2O_3 causes no distortion in the crystal lattice of β-Ca_2SiO_4; the X-ray diffraction line patterns of two samples of β-Ca_2SiO_4, one containing 0.25 and the other 0.53% dissolved B_2O_3, were identical.

(8) N.B.S Circular 500 (1952).

The correction term to be applied to the heat of solution of β-Ca_2SiO_4 was found to be -1.16 cal./g. on the basis of the initial composition, and -1.38 cal./g. on the basis of the final composition; the average was -1.27 cal./g. The weight ratio of Ca_2SiO_4 to CaO in the mixtures was 3.148. Since there was no significant correction term for the impurities in CaO, as stated earlier, the correction term to be applied to the heat of solution of the mixture was -0.96 cal./g. The correction for the heat of solution of Ca_3SiO_5 was -0.93 cal./g., based on the initial composition, and -1.22 cal./g., based on the final composition; the average was -1.07 cal./g. The correction to be applied to D, therefore, was -0.11 cal./g.

The corrected heat of decomposition of Ca_3SiO_5 was 9.04 cal./g., or 2100 cal./mole, rounding the value to the nearest 100 cal. We estimate the uncertainty to be ±200 cal./mole; and this is a generous estimate. The experimental uncertainty was ±0.23 cal./g., as was stated in the previous section, and the uncertainty in the correction for impurities may well be considerably less than ±0.64 cal./g.

Heats of Solution of β-Ca_2SiO_4 and CaO.—The method presented in this paper and the method of separate heats of solution, used by earlier investigators, lead to the same result if

$$H_{Ca_2SiO_4} + H_{CaO} = H_{Ca_2SiO_4 + CaO} \qquad (3)$$

To ascertain whether this condition was fulfilled, the heats of solution of Ca_2SiO_4 and CaO were determined separately. The results are given in Figs. 2 and 3. In these figures, as in Fig. 1, each point represents an average value, and the number of runs averaged is given under the point.

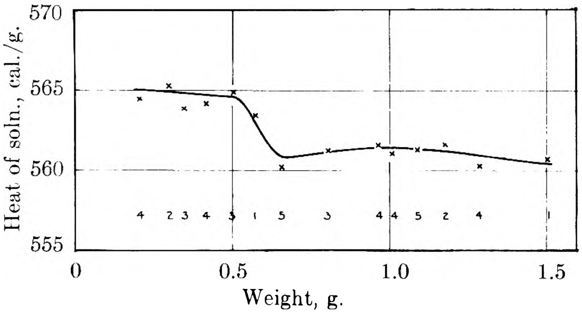

Fig. 2.—Heat of solution of β-Ca_2SiO_4.

The curve in Fig. 3 has a minimum at about 0.37 g. of CaO dissolved. All solutions obtained with smaller weights of CaO were clear, and those obtained with larger weights were cloudy, indicating precipitation of CaF_2. The cloudiness increased with increasing weights of CaO dissolved.

For purposes of the present investigations, the important part of Fig. 3 is the low-weight branch of the curve. At these weights the solutions were clear; consequently, the heats of solution could be used to calculate D by means of eq. 2. If $H_{Ca_3SiO_5}$ is taken from Fig. 1, $H_{Ca_2SiO_4}$ from Fig. 2, and H_{CaO} from the low-weight branch of the curve in Fig. 3, the values of D calculated for different weights are shown in column 2 of Table II. Column 3 of Table II shows the values of D calculated for the same weights from the two curves of Fig. 1. It will be seen that D values of the third column show very slight or no trend, whereas the D values of the second column decrease from 9.3 to 2.7 cal./g., then rise to 7.6 cal./g. The average of the D values of column 3 is 9.2 cal./g., and the highest value of D in column 2 is 9.3 cal./g. The latter value was obtained at the lowest weight, at which the solution products are most likely to be the same as those obtained from equimolar mixtures of β-Ca_2SiO_4 and CaO or from Ca_3SiO_5; consequently, this value of D should come closest to the true value.

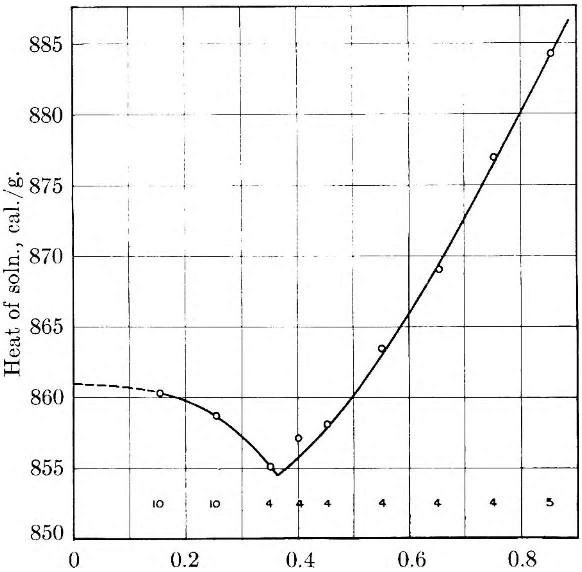

Fig. 3.—Heat of solution of CaO.

TABLE II

HEAT OF DECOMPOSITION OF Ca_3SiO_5

Wt. (g.)	D (cal./g.) Based on individual heats of soln.	D (cal./g.) Based on heats of soln. of mixtures
0.20	9.3	9.7
.30	6.4	9.8
.40	4.5	9.7
.50	3.3	9.7
.60	2.8	9.5
.70	2.7	9.2
.80	4.3	9.1
.90	5.3	9.1
1.00	5.4	9.2
1.10	5.9	8.7
1.20	6.4	8.4
1.30	7.3	8.4
1.40	7.6	9.5

Acknowledgments.—We wish to express our great indebtedness to Dr. Paul Seligmann for working out the statistical treatment used in the paper, to Dr. L. E. Copeland, Mr. Hubert Woods, Mr. T. C. Powers, Mr. G. J. Verbeck and Dr. H. H. Steinour for many helpful suggestions, and to Mr. C. L. Ford and his associates, Mr. E. LaBonde, Mr. E. E. Pressler, and Mr. W. G. Hime for the analytical work performed on the materials.

CONDUCTANCE AND OTHER PHYSICAL PROPERTIES OF UREA SOLUTIONS

BY V. K. VENKATESAN AND C. V. SURYANARAYANA

Physico-Chemical Laboratory, Annamalai University, South India

Received October 24, 1955

A systematic study of electrical conductance of aqueous solutions of urea has been made from 0.001 to 20 *N*. Viscometric and refractometric studies have been made at higher concentrations. Urea behaves as a weak electrolyte in aqueous solutions. At higher concentrations the variation of viscosity with concentration is best represented by an equation $\eta/\eta_0 = Ac^2 + B$ where η/η_0 is relative viscosity, C the concentration and A and B, constants. Electrolytic behavior of urea is best explained by a zwitterion structure.

Introduction

Aqueous solutions of urea are known to be electrolytically conducting.[1,2] The object of this investigation was to make a systematic study of electrolytic conductance of aqueous solutions of urea ranging from 0.001 to 20 *N*. Refractometric studies have also been made. At higher concentrations, ranging from 0.1 to 20 *N*, viscosity measurements have also been made.

Experimental Procedure

Purest E. Merck urea was used in these investigations. A platinized vertical cell with a cell constant value of 0.1845 was used for measuring conductance. Resistance of the solutions was measured with a Dawe's Impedance Bridge utilizing an amplifier detector instead of a telephone. The built-in microphone hummer supplied 1000 cycles per second. To eliminate stray capacitance a suitable part of the circuit was grounded by attaching firmly a copper wire to a cold water pipe. Temperature was controlled at 35 ± 0.05° using Townson and Mercer's thermostat S427. The same thermostat, being provided with glass panels was used for viscometric measurements with an Ostwald's viscometer. Hilger's Abbe Refractometer with Hoppler's ultra-thermostat was used for making refractometric measurements. Results obtained are recorded below. Conductivity water prepared with Vogel's[3] conductivity still was used for making solutions and the specific conductivity of it was subtracted from that of solution everytime.

Discussion

Column (3) of Table I shows the variation of equivalent conductance with concentration of urea solutions. With increase of concentration equivalent conductance falls off. It is clear from the results that in solutions urea behaves as a weak electrolyte, at all concentrations.

TABLE I

N	Specific conductivity	Equiv. conductance	Density	Viscosity, poises	Refractive index
0.0009165	0.00000176	1.9200			1.3323
.0018330	.00000678	3.6980			1.3324
.0045825	.00000566	1.2350			1.3333
.0091650	.00000366	0.3989			1.3323
.018330	.00000955	.5210			1.3324
.045825	.00000766	.16710			1.3325
.09165	.00001096	.11960			1.3330
.18330	.00001594	.08696	0.99580	0.007326	1.330
.45825	.00002366	.05163	0.99884	.007357	1.3345
.9165	.00003156	.03443	1.00828	.007515	1.3400
1.833	.00005925	.03232	1.00893	.007526	1.3400
5.000	.00012853	.02569	1.03394	.008128	1.3535
10.000	.00011183	.01118	1.07009	.009493	1.37375
15.000	.00010603	.07068	1.10423	.011380	1.39325
20.000	.00011813	.059065	1.14129	.01454	1.41400

Evidence was presented[4,5] that urea in solution is neither wholly nor in part amphoterically ionic and that it may be regarded as a weak base. Studies on the diamagnetic susceptibilities[6] of urea pointed to a resonating amphoteric ion changing through an amino–imino structure.

Reporting on the dielectric constants of amphoteric ions and polar molecules it was concluded[7] that urea is not amphoterically ionic, but rather is a very weak base with a very high permanent dipole moment.

A balanced view seems to be[8] that urea exists to a large extent as a zwitterion $NH_2^+:C(NH_2)O^-$. Dipole moment studies[9] strengthen the above view. Harris and Robson[10] also support the same view.

In summary[11] it is concluded that urea exists as a resonance hybrid of two zwitterion forms (1 and 2)

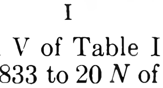

$$\overset{+}{N}H_2:\underset{\underset{-O}{|}}{C}-NH_2$$

I

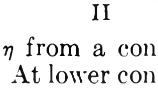

$$NH_2-\underset{\underset{O-}{|}}{C}:\overset{+}{N}H_2$$

II

Column V of Table I gives η from a concentration of 0.1833 to 20 *N* of urea. At lower concentrations of not more than 4 *N* many workers,[12-16] found η at different concentrations of urea solutions. Also data[17,18] are available up to a concentration of 5 *M*. Hence in the present investigation emphasis is laid on the η at higher concentrations.

Viscosity of dilute solutions of urea up to 0.1 *M* conformed[16] to an equation previously given on experimental basis by Jones and Dole[19] and Joy and Wolfenden[20] whereby the viscosities of solutions of strong electrolytes vary linearly with the square root of the concentration at high dilution. The equation given was

$$\eta/\eta_0 = 1 + A\sqrt{c} + Bc$$

---

[1] Trubsbach, *Z. physik. Chem.*, **16**, 709 (1918).

[2] T. N. Shivapuri, *Univ. Allahabad Studies, Chem. Sect.*, 1 (1950).

[3] A. I. Vogel and G. H. Jeffery, *J. Chem. Soc.*, 1201 (1931).

[4] J. Walker and J. K. Wood, *ibid.*, **83**, 490 (1903).

[5] J. Bell, W. A. Gillespie and D. B. Taylor, *Trans. Faraday Soc.*, **39**, 137 (1943).

[6] Archibald Clow, *ibid.*, **33**, 381 (1937).

[7] W. J. Dunning and W. J. Schutt, *ibid.*, **34**, 479 (1938).

[8] Ernest Bergmann and A. Weizmann, *ibid.*, **34**, 783 (1938).

[9] W. D. Kumler and Geo. M. Fohlen, *J. Am. Chem. Soc.*, **64**, 1944 (1942).

[10] J. O. Harris and A. H. Robson, *Nature*, **161**, 98 (1948).

[11] I. D. Morton and E. Hoggarth, "Chemistry of Carbon Compounds," Edited by E. H. Rodd, Vol. IB, Elsevier Press, New York, N. Y., p. 906, 1952.

[12] H. M. Chadwell and B. Agnes, *J. Am. Chem. Soc.*, **52**, 3507 (1930).

[13] G. Rudolf, *Z. Physik. Chem.*, **43**, 257 (1903).

[14] E. Fawsitt, *Proc. Roy. Soc. Edinburgh*, **25**, 52 (1904).

[15] C. Ranken and W. W. Taylor, *ibid.*, **45** [ii], 397 (1906).

[16] G. Jones and S. K. Talley, *J. Am. Chem. Soc.*, **55**, 624 (1933).

[17] A. N. Campbell and E. M. Kartzmark, *Can. J. Research*, **28B**, 161 (1950).

[18] N. D. Litvinov and A. I. Melnikova, *J. Appl. Chem.* (*U.S.S.R.*), **9**, 583 (in English) (1936).

[19] G. Jones and M. Dole, *J. Am. Chem. Soc.*, **51**, 2950 (1929).

[20] W. E. Joy and J. H. Wolfenden, *Proc. Roy. Soc.* (*London*), **A134**, 413 (1931).

where η/η_0 is relative viscosity and A and B are parameters to be obtained by plotting the left-hand member of the equation

$$\frac{\eta/\eta_0 - 1}{\sqrt{c}} = A + B\sqrt{c}$$

against $\sqrt{c}$. A becomes zero for non-electrolytes. Jones and Talley[16] found that for urea $\eta/\eta_0 = 1 + 0.03784C$, in dilute solutions up to a concentration of 0.1 M.

At higher concentrations, using the Jones and Dole equation for urea we have calculated η/η_0 using our results, and tabulated the values obtained in column 3 of Table II. As expected there is a wide divergence between observed and calculated values. Variation of relative viscosity with concentration of urea solutions is best represented by an extension of the Jones and Dole equation involving the square of concentration.

$$\eta/\eta_0 = AC^2 + B$$

where for urea A = 0.009971 and B = 1.02860. Observed and calculated values of η/η_0 based on the above equation are recorded in column 4 of Table II.

TABLE II

Concn., g. moles/l.	η/η_0 obsd. (I)	η/η_0 calcd. According to Jones and Dole eq. (II)	η/η_0 calcd. According to the extended form (III)	$\Delta(\eta/\eta_0)$ (I − II)	$\Delta(\eta/\eta_0)$ (I − III)
0.09165	1.0090	1.003468	1.02868	+0.005532	−0.01968
.22913	1.01407	1.00867	1.02912	+0.005400	−0.01505
.45825	1.0350	1.01735	1.0307	+0.01765	+0.0043
.91650	1.03700	1.03468	1.036975	+0.00232	+0.000025
2.5000	1.1200	1.09461	1.09096	+0.02549	+0.02904
5.000	1.3080	1.1892	1.2778	+0.1182	+0.0302
7.5000	1.5540	1.2839	1.5896	+0.2701	−0.0356
10.0000	2.004	1.3734	2.0257	+0.6306	−0.0217

Graph II (not given) shows the variation of equivalent conductivity (Λ) with η at higher concentrations above 0.1833 N. It is interesting that Λ falls off rapidly with increasing viscosity. The dipole moment of urea is high and is about 8.6 Debye units according to Bergmann and Weizmann.[8] A rapid fall of Λ in urea solutions of high viscosity must therefore be ascribed to dipole–dipole interactions of the zwitterions. This factor should contribute significantly to all abnormal behavior of highly concentrated urea solutions

Investigations[21] of refraction of urea solutions between 0.003 and 4.10 N showed that the refraction curve is very similar to that of strong electrolytes. Investigation[22] of the apparent molal refractivity of aqueous solutions of urea as a function of concentrations up to sufficiently high concentrations showed the same behavior as that of an electrolyte. From concentrations ranging between 0.001 to 20 N we have recorded in the last column of Table I the refractive index of urea solutions. At low concentrations values obtained by an interferometer[23] are more reliable and at higher concentrations Abbe refractometer is sufficiently reliable. We have therefore taken into consideration refractive index values of urea solutions ranging from 0.1833 to 20 N. A plot of refractive index against concentration (not given here) gives a straight line beyond 5 N solutions. From 0.1833 to 0.9165 N the curve rises continuously, short of linearity, and between 0.9165 and 5 N there is a sharp break in the curve intensifying at 1.833 N. In this connection it may be noted that the density values in column 3 of Table I when plotted against the respective concentrations give a similar curve (not given) as for refractive index with a break at the same concentration. A plot of viscosity against concentration of urea solutions (not given) also shows a break at identically the same concentration. Curve 2 in graph I also shows an inflection at concentrations round about 0.9165 and 1.833 N. Further from graph II (not given) it is clear that from about 1.833 N upwards to 10 N the fall in Λ with increasing η is less and becomes lesser from 10 N upwards. These observations point to the conclusion that at about 1.833 N in aqueous solutions of urea some notable intermolecular rearrangement is occurring manifesting itself in arresting the rate of growth of physical properties of the solutions. Both the solute and the solvent being polar, dipole–dipole interactions must be profoundly influencing the orientation of the solvent and solute molecules at different concentrations, perhaps with a noticeable transition occurring at a concentration of about 1.833 N. Gurney[24] discusses the various possibilities of orientation of molecules in solution taking into account different forces existing between them.

---

(21) J. M. Shershever and A. E. Brodskii, *Z. physik Chem.*, **B34**, 145 (1936).

(22) Biagio Pesce, *Atti V. Congr. nazl. chim. pura applicata, Rome*, 1935, Pt. I, 441 (1936).

(23) A. E. Brodskii, J. M. Shershever and N. S. Filippova, *Acta Physicochem. U.S.S.R.*, **3**, 685 (1935).

(24) R. W. Gurney, "Ionic Processes in Solution," McGraw-Hill Book Co., New York, N. Y., 1953.

A PHYSICO-CHEMICAL STUDY OF PYRIDINE-ACETIC ACID SYSTEM

BY V. K. VENKATESAN AND C. V. SURYANARAYANA

Physico-Chemical Laboratory, Annamalai University, South India

Received October 24, 1955

Equivalent conductivity, viscosity, contraction in volume and refractive index of mixtures of pyridine and acetic acid at different percentage compositions have been determined. In all cases the above properties exhibit a maximum at a composition of 83 mole % of acetic acid. Previous workers who investigated some of these properties ascribe the maxima to the formation of a complex. We have explained on a different basis that no such compound is formed, and that instead at that composition acetic acid attains maximum ionization. At least 17 mole % of pyridine has been shown to be necessary for complete ionization of acetic acid in pyridine.

Introduction

In studying the physico-chemical properties of mixtures of pyridine and acetic acid in different proportions formation of compounds has been reported by different workers based on different evidence—viscometric, cryoscopic, conductometric, Raman effect and magnetic susceptibility measurements. The over-all conclusions are conflicting and hence a systematic reinvestigation of electrical conductance, viscosity, volume contraction and refractometric measurements, has been made and reported herein.

Experimental Procedure

Purest Kahlbaum pyridine and glacial acetic acid were used. Pyridine and acetic acid were kept at 30° in a thermostat for several hours and by pipetting out the required volume of the two compounds totalling 50 cc. into 250-cc. glass stoppered Pyrex bottles different compositions of the mixtures differing by 10% were made ranging from 10 to 90%. Weight % or mole % composition could be computed by considering the density of pyridine (0.97301) and that of acetic acid (1.03777) and their respective molecular weights.

A platinized vertical cell with a cell constant value of 2.528 was used for measuring conductance. Resistance of the solutions was measured with a Dawe's Impedance Bridge utilizing an amplifier detector instead of a telephone. The built-in microphone hummer supplied 1000 cycles per second. To eliminate stray capacitance a suitable part of the circuit was earthed by attaching firmly a copper wire to a cold water pipe. Temperature was controlled at 30 ± 0.05° using Townson and Mercer's thermostat S427. The same thermostat, being provided with glass panels with suitable arrangement was used for viscometric measurements with an Ostwald viscometer. A Hilger Abbe refractometer with Hoppler ultra thermostat was used for making refractometric measurements. Results are recorded in Table I.

Discussion

Compound formation has been reported from measurements of electrical conductance,[1–4] viscosity,[5–8] boiling points,[9–11] freezing point depression[12,13] and heat of mixing,[14] at 83 mole % composition of acetic acid and also other compositions.

Raman spectra studies[15] indicated compound formation in a mixture of 40% pyridine.

Measurements of the depolarization of the scattered light, a study of the intensity–concentration curve and the magnetic susceptibilities[16] of the mixtures pointed to the existence of a complex at 60 mole % of acetic acid.

Table I gives results obtained in a very systematic investigation of the pyridine–acetic acid system. Column 4 of Table I shows the contraction in volume in cc. per 50 cc. of the solution, a plot of which against the mole % of acetic acid in the mixtures (not given) shows a maximum at about 83 mole % of acetic acid.

Column 9 represents values of equivalent conductance in the calculation of which the volume contraction of the mixtures has been taken into account. A plot of these values of equivalent conductance against mole % of acetic acid in the mixtures (not given) shows a maximum at about 83 mole % of acetic acid.

Column 10 shows the viscosity of mixtures of pyridine and acetic acid. A plot of viscosity against % composition of mixtures (not given) shows a maximum at 83.5 mole % of acetic acid.

Column 11 shows values of densities of the mixtures a plot of which against mole % composition (not given) indicates a maximum at 83 mole % of acetic acid.

The last column shows values of refractive index of the mixtures a plot of which against mole % composition (not given) shows the refractive index while falling linearly, abruptly breaks at a percentage composition of 83 mole % of acetic acid.

From the foregoing the most interesting observation is the conflicting and contradictory conclusions drawn so far. Various workers attribute the conductivity maximum and the viscosity maximum as occurring due to a compound formation. The only incontrovertible evidence for the existence of a compound of pyridine and acetic acid is at a composition of 40% of the former in a mixture of the two from the identical observations from Raman effect data, one by Roman Mierzecki[15] and the other by Venkataraman[16] corroborated by the magnetic susceptibility measurements by the latter. From conductometric, viscometric, refractometric and density determinations as detailed in Table I above or from the results of any other previous workers so far there is no evidence of compound formation at a composition of 40% of pyridine in the mixture. A

---

(1) A. N. Sackhanov, *J. Russ. Phys. Chem. Soc.*, **43**, 526 (1912).

(2) N. A. Trifonov and S. I. Cherbov, *Bull. inst. recherches biol. univ. perm (Russia)*, **6**, 313 (1929).

(3) Lloyd Swearingen and R. F. Ross, THIS JOURNAL, **38**, 395 (1934).

(4) A. S. Naumova, *Zhur. Obshchei Khim (J. Gen. Chem.)*, **2**, 1222 (1949).

(5) D. E. Tsakalatos, *Bull. soc. chim.*, [4] **3**, 235 (1908).

(6) O. Faust, *Z. physik. Chem.*, **79**, 97 (1911).

(7) A. E. Dunstan and F. B. Thole, *J. Chem. Soc.*, **95**, 1556 (1909).

(8) Lloyd Swearingen and Heck, THIS JOURNAL, **38**, 395 (1934).

(9) M. G. André, *Compt. rend.*, **125**, 1187 (1897).

(10) M. G. André, *ibid.*, **126**, 1105 (1898).

(11) J. A. Gardner, *Ber.*, **23**, 1587 (1890).

(12) Lloyd Swearingen and R. F. Ross, THIS JOURNAL, **38**, 1141 (1934).

(13) N. A. Pushin and I. I. Rikovski, *Z. physik. Chem.*, **A161**, 336 (1932).

(14) N. A. Pushin, A. V. Fedjushkin and B. Krogvie, *Bull. soc. chim. Belg.*, **11**, No. 1/2, 12 (1940–46) (Publ. 1947) (in Siberian).

(15) Roman Mierzecki, *Acta Phys. Polon.*, **11**, 329 (1953).

(16) S. Venkataraman, *J. Ind. Chem. Soc.*, **17**, 297 (1940).

TABLE I

PYRIDINE–ACETIC ACID

Vol. % of acetic acid (1)	Wt. % of acetic acid (2)	Mole % of acetic acid (3)	Contraction in vol. (in cc.) (per 50 cc.) (4)	Vol. containing 1 g. equiv. of AcOH without taking the contraction into account (v_1) (5)	Vol. containing 1 g. equiv. of AcOH taking the contraction into account (v_2) (6)	Sp. conductance (7)	Equiv. conductance $K \times v_1$ (8)	Equiv. conductance $K \times v_2$ (9)	Viscosity, poises (10)	Density (11)	Refractive index (12)
0	0	0	...	...	...	0.00001642	...	...	0.008354	0.97301	1.5040
10	10.59	13.50	0.31	578.80	575.30	.00001922	0.01113	0.01106	.009842	.98544	1.4904
20	21.05	25.99	0.55	289.50	286.20	.00004231	.01225	.01211	.011390	.99669	1.4790
30	31.37	37.56	0.79	193.00	189.90	.00010870	.02098	.02065	.013460	1.00864	1.4680
40	41.57	48.37	1.07	144.60	141.60	.0003831	.05540	.05424	.016480	1.02104	1.4560
50	51.60	58.41	1.39	115.80	112.60	.0014530	.16830	.16360	.020750	1.03369	1.4485
60	61.53	67.81	1.82	96.45	92.94	.0041450	.39970	.38520	.027040	1.04981	1.4395
70	71.36	76.60	2.14	82.64	79.11	.0071420	.59020	.56490	.033980	1.06407	1.4300
80	81.00	85.09	2.21	72.41	69.08	.0082880	.60010	.57250	.036240	1.07146	1.4175
90	90.55	92.66	1.58	64.31	62.22	.004980	.32030	.30980	.025580	1.06457	1.3985
100	100	100	...	...	...	...	...	...	.010400	1.03777	1.3700

maximum of equivalent conductivity as well as viscosity at a composition of 83 mole % of acetic acid noted by previous workers alone was their basis to conclude complex formation at that composition. Though our results are in agreement with theirs we hesitate to draw the same conclusion. It may be normal to expect a viscosity maximum to correspond to the formation of a complex, but it is unclear how at the same composition if a complex has really formed there should be a maximum of equivalent conductance instead of a minimum which should normally be expected due to the low mobility of a large sized complex even assuming it to be electrically conducting. So we believe, due to additional evidence of a density maximum and a break in the refractive index curve at the same composition that though not the formation of a complex, some other notable phenomenon must be occurring.

Conductivity studies[17] indicated that pyridine acts as a differentiating solvent toward "strong acids," HI, HNO_3, HBr, HCl whose relative strengths were determined by conductance measurements. Organic acids were found to be exceedingly conducting in pyridine. They point out that in pyridine these substances form pyridinium salts of the formula $C_5H_5NH^+, X^-$.

Pyridine being a proton accepting solvent, acetic acid must be expected, especially in view of the observations of Hantzsch and Caldwell[17] to be highly ionized in it. The nitrogen atom of the pyridine having a lone pair of electrons naturally attracts a hydrogen ion and forms a pyridinium ion.

As more and more pyridine is added to pure anhydrous acetic acid the latter ionizes to a greater extent, giving hydrogen ions and acetate ions. The hydrogen ions form pyridinium ions with pyridine molecules. Since each hydrogen ion requires one pyridine molecule for the formation of pyridinium ion, when the mole % of pyridine is less and the ionized acetic acid part is greater there must be, in addition to the pyridinium ions, some free hydrogen ions. As the percentage composition of pyridine increases, the ratio of free hydrogen ions to pyridinium ions must decrease progressively until 50% composition of the mixture, beyond which no free hydrogen ions can possibly exist. Now it is clear that as more and more pyridine is added to anhydrous acetic acid, for the equivalent conductivity to increase to a maximum, the ratio of free hydrogen ions to pyridinium ions must attain a maximum at 83 mole % of acetic acid which means that acetic acid requires at least 17 mole % of pyridine for complete ionization. At the composition at which equivalent conductivity is a maximum we must ascribe the effect to a large proportion of free hydrogen ions capable of high conductance existing. As pyridine concentration increases beyond 17 mole % of pyridine, the ratio of free hydrogen ions to pyridinium ions must naturally decrease progressively, resulting in a corresponding fall in equivalent conductance as is really the case in the graph (not given). Of course in the above arguments it is assumed that though electrically conducting, pyridinium ion has, due to its large size, very low mobility compared with the hydrogen ion. Thus at compositions containing more than 50% of pyridine all available hydrogen ions exist only as pyridinium ions and therefore it could be seen from the curve (not given) that the equivalent conductance is very low at 50% composition and goes on decreasing as pyridine content increases.

Addition of an electrolyte is known to increase the viscosity of a solution, from a consideration involving the dynamics of ionic atmospheres. Since at 83 mole % composition acetic acid is completely dissociated the ionic strength of the mixture must be a maximum at this composition and therefore the viscosity may be expected to be a maximum. As the percentage of pyridine increases, acetic acid content falls and as a result ionic strength decreases and therefore viscosity of the solutions falls progressively, as the results show.

The maximum density at the same composition may also be explained. The force of attraction between an ion and a dipole having the most favorable orientation is very strong, more so in systems of low dielectric constant. Gurney[18] states that in any ionic cosphere these molecular dipoles which have a

---

[17] Hantzsch and Caldwell, *Z. physik. Chem.*, **61**, 227 (1908).

[18] R. W. Gurney, "Ionic Processes in Solution," McGraw-Hill Book Co., New York, N. Y., 1953, p. 186.

favorable orientation will be attracted, while those that have the opposite orientation will be repelled. Since the former are more numerous the solvent in the cosphere is attracted toward the ion leading to a contraction in each cosphere. In any ionic solution the sum of the contractions that have taken place in the cosphere of the positive and negative ions will be apparent if we measure accurately the volume of the solution. Since at the density maximum the ionic strength is a maximum the contraction in volume must be a maximum and hence the density of the mixture a maximum.

From 100 mole % acetic acid to 83 mole % of acetic acid the refractive index curve (not given) rises rapidly but is short of linearity, perhaps showing increasing degree of ionization of acetic acid up to 83 mole % of acetic acid composition at which ionization is complete. Beyond that the ionic strength depends merely on the mole fraction and hence the curve is perfectly linear.

VISCOELASTICITY IN AQUEOUS SOAP SOLUTIONS

BY N. PILPEL[1]

Chemistry Department, University of London,
King's College, Strand, London, W.C. 2, England

Received November 4, 1955

Aqueous solutions of sodium and potassium oleate develop viscoelastic properties when electrolytes are added. This is thought to be due to a change in the shape of the soap micelles from small, detached spheres, to long interlinked cylinders. A study has been made of the onset of viscoelasticity under the influence of electrolytes. It is shown that over a limited range of soap concentrations the Law of Mass Action is obeyed and this is also true with small amounts of long chain alcohols present.

Introduction

It has been suggested[2] that the viscoelasticity which develops in aqueous solutions of sodium and potassium oleate on the addition of electrolytes is due to a change in the shapes of the soap micelles. At low concentrations of electrolyte the soap is believed to be in the form of small, spherical micelles, but at higher electrolyte concentrations these pack together into cylinders which then interlink to form a network structure. It is the existence of the network which appears to confer the property of viscoelasticity (but see ref. 3).

Maximum viscoelasticity does not develop suddenly at any one particular concentration of electrolyte, but builds up gradually, finally reaching the maximum value, after which further addition of electrolyte leads to coacervation and salting out. Although it has been possible to study certain rheological properties of soap–electrolyte systems in the regions of maximum viscoelasticity,[4–8] it is very much more difficult to do the same in the region when viscoelasticity first appears. Not only are such systems less stable but it is necessary to employ rather qualitative criteria for deciding when viscoelastic characteristics have, in fact, developed. On the other hand these systems are considered of interest since the transition from spherical to cylindrical micelles which is now postulated is, in some ways, an analogous process to the initial formation of micelles at the critical micelle concentration (C.M.C.) of a soap.

At the C.M.C. one may write

$$n\mathrm{M}^+ + m\mathrm{A}^- \rightleftharpoons \mathrm{M}_n\mathrm{A}_m{}^{-(m-n)}$$

where M^+ is the alkali metal cation. A^- is the long chain paraffin anion and $m > n$, and this expression reasonably predicts the relationship between the electrolyte concentration and the C.M.C.[9]

The present work has been undertaken to see whether any similar relationship can be discovered between the concentrations of soap and of electrolyte at the transition between spherical and cylindrical micelles, it being assumed that only when the latter type of micelles exist can interlinking take place and viscoelasticity develop.

Experimental

Preparation of Solutions.—Oleic acid was purified by fractional crystallization followed by molecular distillation at 10^{-3} mm. Long chain alcohols, kindly supplied by Messrs. Polak & Schwarz and Messrs. Price (Bromboro') Ltd., were purified by fractional distillation. All other reagents were of analar grade; distilled water was used throughout. The solutions were prepared in stoppered test-tubes by adding the oleic acid from an Agla syringe to enough NaOH or KOH solution to give a liquid having a *p*H of 10, then adding the appropriate quantity of the alcohol and of an $M/1$ solution of the electrolyte, agitating gently and allowing to stand for a few minutes at 20°.

Detection of Viscoelasticity.—The liquids were first tested for non-Newtonian viscosity by measuring the viscosity at mean rates of shear from about 5 up to about 20 sec.$^{-1}$ in a capillary tube viscometer fitted with a variable pressure head device. The rate of shear in such an instrument varies across the capillary, but by making simplifying assumptions a mean rate can be calculated. The method of calculation together with the technique of measurement have been discussed more fully elsewhere.[7] Liquids exhibiting a drop in viscosity as the rate of shear was increased were termed non-Newtonian, those whose viscosities remained sensibly constant were termed Newtonian. A further 5 to 10 cc. of each liquid was then subjected to torsional shear in the Weissenberg-Roberts rheogoniometer

---

[1] Research Organization, British Insulated Callender's Cables Ltd., 38 Wood Lane, London, W. 12, England.

[2] N. Pilpel, *J. Colloid Sci.*, **9**, 285 (1954).

[3] J. G. Oldroyd, *Proc. Roy. Soc.* (*London*), **A218**, 122 (1953).

[4] (a) H. G. B. de Jong and H. J. van den Berg, *Proc. Koninkl Nederland. Akad. Wetenschap.*, **52**, [15] 99 (1949); (b) *ibid.*, **53**, [7] 109, 233 (1950).

[5] H. G. B. de Jong, W. A. Loeven and W. W. H. Weijzen, *ibid.*, **53**, 743, 1122 (1950).

[6] H. G. B. de Jong, H. J. van den Berg, W. A. Loeven and W. W. H. Weijzen, *ibid.*, **54B**, 399, 407 (1951).

[7] N. Pilpel, *Trans. Faraday Soc.*, **50**, 1369 (1954).

[8] N. Pilpel, *ibid.*, **51**, 1307 (1955).

[9] W. D. Harkins, "Physical Chemistry of Surface Films," Chap. 4, Reinhold Publ. Corp., New York, N. Y., 1952.

and any rise of liquid in the capillary tubes, even though of short duration, taken to indicate the existence of elasticity. A full description of this instrument and of its method of operation has also been given elsewhere.[7,10,11] Finally a third portion of liquid was given an instantaneous swirl in a test-tube and any subsequent oscillation of entrapped air bubbles ascribed to elasticity. It was found that liquids exhibiting Newtonian flow in the viscometer did not exhibit elastic recoil in the test-tube or capillary rise in the rheogoniometer, while liquids in which either or both of these two phenomena occurred were invariably non-Newtonian. But a few of the liquids were non-Newtonian without being measurably elastic, while in other cases elasticity could only be detected by recoil but not by capillary rise in the rheogoniometer. In view of the experimental difficulties and the fact that the systems studied tended to lose their elastic properties when subjected to mechanical stress it was only possible to sort them rather qualitatively into two main categories. All liquids showing a viscosity independent of the rate of shear and no elasticity were termed Newtonian. All the other liquids were classified together as viscoelastic since the great majority of them were both elastic and non-Newtonian.

Results

In Fig. 1 curves have been drawn to show the division between Newtonian and viscoelastic systems. The positions of the dividing lines depended on the concentration of the soap and on the amounts of the different electrolytes that had been added. The divisions were not sharp and in general extended over an electrolyte concentration of about 0.03 M. But to avoid confusion they have been drawn as lines representing the approximate centers of zones in which viscoelasticity was first appearing. The region to the left of each curve was characterized by Newtonian behavior, that to the right by non-Newtonian viscoelastic behavior. It is seen that at soap concentrations below about 0.005 M viscoelasticity could not be produced by the addition of electrolytes alone while at electrolyte concentrations higher than that corresponding to the right-hand extremity of each curve coacervation and/or salting out took place.

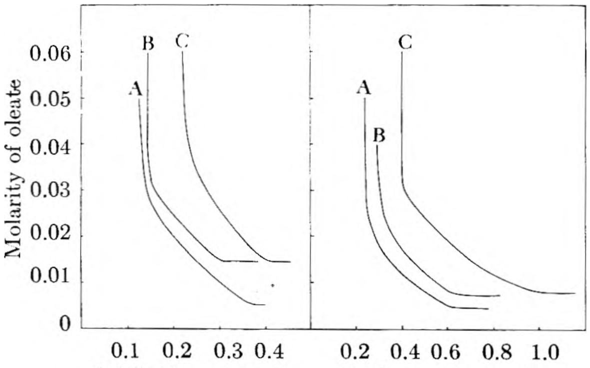

(a) Sodium systems. (b) Potassium systems.

Fig. 1.—Boundary curves: A, PO_4'''; B, CO_3''; C, Cl′.

As the concentration of soap was raised so the amount of electrolyte needed to produce viscoelasticity fell, but above about 0.05 M soap the curves became approximately asymptotic to the ordinate. (Clearly at considerably higher soap concentrations the curves must once more incline toward the ordinate since strong soap solutions with only traces of electrolyte present exhibit marked viscoelasticity.) For the systems now studied however it was found that the amount of electrolyte needed to produce viscoelasticity depended on the valency of the anion, less of a trivalent anion being needed than of a univalent anion. When the curves become asymptotic to the ordinate the ratios of the molarities of univalent to divalent to trivalent anions for the onset of viscoelasticity were found to be proportional very nearly to 1.56 to 1.40 to 1.00 and this proportionality held both for the sodium and for the potassium systems.

Discussion

This finding supports one reported previously,[2] namely, that the molarities of univalent, divalent and trivalent anions needed to produce maximum viscoelasticity in these systems are also very nearly in this ratio of 1.56:1.40:1.00. It enables the results for the three different anions to be treated by a common method. For the uni-univalent electrolytes the activity of the cation is taken as 1, for the uni-divalent electrolytes as 1.40 and for the uni-trivalent electrolytes as 1.56. The cation activity of the uni-univalent soaps is taken as 1.00.

Let us assume that the scheme currently accepted for the formation of spherical micelles at the C.M.C., namely

$$nM^+ + mA^- \rightleftharpoons M_nA_m^{-(m-n)} \qquad (1)$$

is also applicable to the conversion of spherical to cylindrical micelles on the addition of electrolyte. We may write

$$qM^+ + p(M_nA_m^{-(m-n)}) \rightleftharpoons M_q(M_nA_m)p^{-(p(m-n)-q)} \qquad (2)$$

where M^+ is the alkali metal cation, A^- is the long chain paraffin anion, and $p > q > m > n$. Rewriting equations 1 and 2 in terms of activities leads to

$$(a_{M^+})^n\,(a_{A^-})^m = K(a_{M_nA_m})$$

or

$$n \log a_{M^+} + m \log a_{A^-} - \log K = \log a_{M_nA_m} \qquad (3)$$

and

$$(a_{M^+})^q\,(a_{M_nA_m^-})^p = K^1(a_{M_q(M_nA_m)_p})$$

or

$$q \log a_{m^+} + p \log a_{M_nA_m^-} - \log K^1 = \log a_{M_q(M_nA_m)p} \qquad (4)$$

When cylindrical micelles, and hence viscoelasticity first develop $a_{M_q(M_nA_m)p}$ is a constant, and substituting for $\log a_{M_nA_m}$ from equation 3 into equation 4 gives

$$\log a_{M^+} = k - \frac{pm}{(pn + q)} \log a_{A^-} \qquad (5)$$

where k is a new constant. As a first approximation activities may be replaced by concentrations and it therefore follows that when viscoelasticity first appears the log of the concentration of the soap should be a linear function of the log of the concentration of the cation. The latter is obtained by summing the concentrations of cation contributed by the soap and by the electrolyte with due allowance made for cation activities in the different electrolytes.

Relevant data for 6 systems are given in Table I and plotted graphically in Fig. 2, where it is seen

---

(10) K. Weissenberg and S. M. Freeman, "Int. Congr. Rheology," North Holland Publishing Co., Amsterdam, 1949, Sept. 1948.

(11) J. E. Roberts, "2nd Int. Congr. Rheology," Butterworths, London, 1954, 1953, p. 91.

that between soap concentrations of about 0.01 and 0.04 *M*, the logarithmic relationship is reasonably obeyed for both the sodium and potassium soap. Above this concentration, however, departure from linearity occurs. There are several possible reasons for this, *e.g.*, anion adsorption onto the micelles, the development of a new type of cylindrical micelle, the breakdown of the assumption that activity is equal to concentration, etc., but it is not possible to be more specific at this stage. From the theory now employed one might also have expected the curves for the sodium and potassium systems to have coincided. That they did not is presumably due to the different numerical values of *n*, *m*, *p*, *q*, and the equilibrium constants for the sodium and potassium systems.

TABLE I

Concn. Na oleate, *M*	Concn. electrolyte, *M*	Concn. cation, *M*	log concn. Na oleate	log concn. cation
		Electrolyte NaCl		
0.04	0.24	0.28	−1.40	−0.553
.03	.27	.30	−1.52	−0.523
.02	.35	.37	−1.70	−0.432
.015	.40	.42	−1.82	−0.377
		Electrolyte Na_2CO_3		
0.04	0.14	0.24	−1.40	−0.620
.03	.16	.26	−1.52	−0.585
.02	.25	.37	−1.70	−0.432
.015	.30	.43	−1.82	−0.367
		Electrolyte Na_3PO_4		
0.04	0.13	0.24	−1.40	−0.620
.03	.14	.25	−1.52	−0.602
.02	.19	.32	−1.70	−0.495
.015	.25	.41	−1.82	−0.387
.01	.30	.48	−2.00	−0.319
		Electrolyte KCl		
0.03	0.40	0.43	−1.52	−0.367
.025	.50	.52	−1.60	−0.284
.020	.58	.60	−1.70	−0.222
.015	.70	.71	−1.82	−0.149
.010	.90	.91	−2.00	−0.041
		Electrolyte K_2CO_3		
0.025	0.32	0.47	−1.60	−0.328
.015	.43	.62	−1.82	−0.208
.010	.55	.78	−2.00	−0.108
		Electrolyte K_3PO_4		
0.030	0.24	0.40	−1.52	−0.398
.02	.27	.44	−1.70	−0.357
.015	.33	.53	−1.82	−0.276
.010	.46	.73	−2.00	−0.137
.005	.60	.94	−2.30	−0.027

Effect of Added Alcohol.—We consider now the effect of adding small amounts of alcohols on the development of viscoelasticity in soap–electrolyte systems.

In all the cases examined it was found that the presence of alcohol considerably reduced the amount of electrolyte needed for the first appearance of viscoelasticity, and the effect is thus similar to that at the C.M.C. of a soap when it is found that the alcohol is able partially to take the place of the electrolyte.[12]

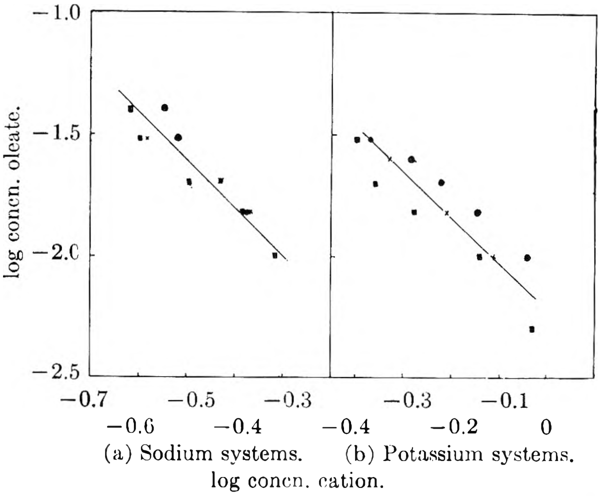

Fig. 2.—Log concn. oleate *vs.* log concn. cation: ●, Cl′; X, CO_3''; ■, PO_4''; slope of (a) −1.97, (b) −1.87.

In Table II data are given for the Na oleate, NaOH, alcohol system. The results were obtained by keeping the concentration of soap constant at 0.05 *M* and measuring the amount of electrolyte needed to produce viscoelasticity when different amounts of a series of alcohols had been added. It is seen that as the chain length of the alcohol was increased so the amount needed to produce viscoelasticity at a particular concentration of electrolyte was reduced and this was in agreement with expectation.[9]

TABLE II

0.05 *M* Na OLEATE

Concn. NaCl, *M*	Concn. cation, *M*	Concn. alcohol, *M*	log concn. cation	log concn. alcohol
		cis-9-Octadecen-1-ol		
0.22	0.27	0.0000	−0.569	0.00
.16	.21	.00125	− .678	−2.903
.11	.16	.00250	− .796	−2.602
		Dodecanol		
0.22	0.27	0.0000	−0.569	0.00
.16	.21	.00125	− .678	−2.903
.11	.16	.00250	− .796	−2.602
.08	.13	.00375	− .886	−2.426
		Decanol		
0.22	0.27	0.0000	−0.569	0.00
.17	.22	.00125	− .658	−2.903
.10	.15	.00375	− .824	−2.426
.08	.13	.00500	− .886	−2.301
		Octanol		
0.22	0.27	0.0000	−0.569	0.00
.14	.19	.0025	− .721	−2.602
.12	.17	.00375	− .770	−2.426
.10	.15	.00500	− .824	−2.301
		Hexanol		
0.22	0.27	0.0000	−0.569	0.00
.20	.25	.00125	− .602	−2.903
.13	.18	.00375	− .745	−2.426
.09	.14	.00750	− .854	−2.125

---

[12] S. H. Herzfeld, M. L. Corrin and W. D. Harkins, THIS JOURNAL, **54**, 271 (1950).

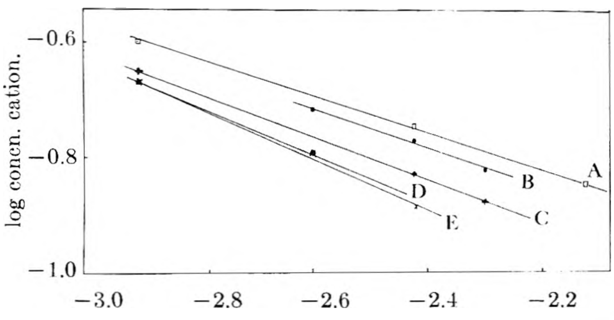

Fig. 3.—Log concn. cation *vs.* log concn. alcohol: ○, *cis*-9-octadecen-1-ol; ×, dodecanol; +, decanol; ●, octanol; □, hexanol.

When both alcohol and electrolyte are added to a soap solution, mixed micelles are formed in which the alcohol partially replaces the soap.[13,14] The schemes given by equations 1 and 2 must now be replaced by

$$sM^+ + rA^- + tL \rightleftarrows M_sA_rL_t^{-(r-s)} \quad (6)$$

and

$$yM^+ + x(M_sA_rL_t)^{-(r-s)}) \rightleftarrows M_y(M_sA_rL_t)_x^{-(x(r-s)-y)} \quad (7)$$

where M^+ is the alkali metal cation, A^- is the long chain paraffin anion, L is the un-ionized alcohol and $x > y > r > s > t$. Employing exactly similar reasoning to that for the soap–electrolyte system, it may be shown that at a particular activity of the soap

$$\log a_M = k^1 - \frac{xt}{y + xs} \log a_L \quad (8)$$

On equating activities to concentrations this leads to the prediction that when viscoelasticity first appears the logarithm of the concentration of the alcohol should be a linear function of the logarithm of the concentration of the cation. As before the cation concentration is obtained by summing the contributions of the soap and of the electrolyte.

Relevant data are included in Table II, and plotted in Fig. 3. It is seen that for alcohol concentrations between about 0.0012 and about 0.0075 *M* (depending on the solubility of the alcohol) the logarithmic relationship is reasonably obeyed. It breaks down however as the alcohol concentration → zero and this is presumably due to the fundamental difference between a simple micelle containing soap molecules only, and a mixed micelle in which both soap and alcohol are present.

Conclusions

It may be concluded, therefore, that over a limited region of concentrations the experimental results, both with and without alcohol present, are consistent with the assumption that viscoelasticity in soap–electrolyte systems develops as a result of a change in micelle shape. At low concentrations of electrolyte the soap is thought to be in the form of small spherical micelles but at higher concentrations these pack together into cylinders which are then able to interlink giving rise to viscoelasticity. The change from spherical to cylindrical micelles is brought about mainly by the added cation but there is also an anion effect as well as an effect due to the presence of un-ionized alcohol. The change obeys a simple form of the Law of Mass Action, but this is only true for a rather limited range of concentrations.

Acknowledgments.—The author wishes to thank Professor Sir Eric Rideal, F.R.S., for his interest and encouragement, and the Ministry of Supply for financial assistance.

[13] H. B. Klevens, *Chem. Revs.*, **47**, 1 (1950).

[14] W. D. Harkins, R. Mittlemann and M. L. Corrin, THIS JOURNAL, **53**, 1350 (1949).

POLYMER ASSOCIATION. III. MOLECULAR AGGREGATION AND INTRAMOLECULAR GROUP ASSOCIATION IN DILUTE SOLUTIONS OF STYRENE–METHACRYLIC ACID COPOLYMERS[1,2]

BY SHIH-YEN CHANG[3] AND HERBERT MORAWETZ

Contribution from Department of Chemistry, Polytechnic Institute of Brooklyn, Brooklyn, N. Y.

Received November 18, 1955

Seven styrene–methacrylic acid copolymers were studied in tetrachloroethane and carbon tetrachloride solution. The degree of molecular aggregation was determined by osmometry with and without added amine. The extent of carboxyl dimerization was measured by infrared spectroscopy and was found to be independent of the concentration of dilute polymer solutions, indicating that most of the carboxyl dimers form within single polymer coils. Two theoretical approaches to the degree of intramolecular group association in solutions of chain molecules carrying widely spaced interacting substituents are in satisfactory agreement with the experimental data. For any given degree of carboxyl association intermolecular aggregation was higher in the better solvent. The data indicate that the molecular chain configuration is independent of concentration in the dilute solution range.

Introduction

Carboxylic acids are known to be largely dimerized by hydrogen bonding in non-polar solvents[4] and, thus, polymers carrying carboxyl groups tend to form aggregates in suitable solvent media. A methyl methacrylate copolymer with 5 mole per cent. methacrylic acid was found to have an osmotic molecular weight of 184,000 in benzene solution at 49.7°, while in pyridine, which would be ex-

[1] Presented at the Meeting of the American Chemical Society, Minneapolis, September 15, 1955.

[2] Support by the Office of Naval Research is gratefully acknowledged. Reproduction in whole or in part is permitted for any purpose of the U. S. Government.

[3] Abstracted from a Ph.D. thesis submitted by S.-Y. Chang to the Graduate School of the Polytechnic Institute of Brooklyn, June, 1955.

[4] G. Allen and E. F. Caldin, *Quart. Rev.*, **7**, 255 (1953).

pected to suppress carboxyl dimerization, a value of 32,300 was obtained.[5] Osmotic and light scattering data indicated that the aggregates retained a constant size over the entire concentration range accessible to measurements. Interpretation of this surprising phenomenon suggested that only a small fraction of the carboxyl groups participate in intermolecular association, while the remaining carboxyls are either engaged in intramolecular group association or hidden in the interior of the polymer coil.[6]

The present investigation is concerned with the balance between intramolecular group association and molecular aggregation in solutions of polymers carrying varying densities of strongly interacting groups. Copolymers of methacrylic acid were used, since their carboxyl association equilibrium has been studied extensively and may be followed conveniently by infrared spectroscopy. Styrene was chosen as the comonomer because its copolymers are soluble in non-polar media and neither the solvent nor the styrene residues absorb strongly at wave lengths used for following carboxyl dimerization. As spectroscopic data do not differentiate between intramolecular and intermolecular group association, the extent of molecular aggregation was followed by osmometry. In addition, solution viscosity data were obtained to show the effect of strongly associating groups, spaced at varying intervals along the molecular chain, both on the molecular configuration at high dilution and on molecular interaction at higher solution concentrations.

Experimental

Preparation of Copolymers.—Methacrylic acid (Rohm and Haas), dried by sodium chloride and calcium chloride, and styrene (Dow Chemical Co.) were distilled at reduced pressure under nitrogen. Polymerization of the mixed monomers at 65°, after thorough degassing, in the presence of 0.025 to 1.84 weight per cent. azo-bis-isobutyronitrile (Eastman Kodak) was carried to roughly 10% conversion. The copolymer was precipitated twice from butanone solution into a large volume of methanol and dried *in vacuo* at 50° for 48 hours.

Analysis of Copolymer Composition.—Copolymer solutions in benzene containing 10 volume per cent. ethanol were titrated under nitrogen with sodium ethoxide in the same solvent mixture, using phenolphthalein as indicator. The sodium ethoxide was standardized against benzoic acid, recrystallized from ether (m.p. 122°). The methacrylic acid content of the copolymers was 3–4 times as high as that of the mixed monomers.

1,1,2,2-Tetrachloroethane (Eastman Kodak) was shaken with cold sulfuric acid until there was no discoloration, followed by washing with water until neutral to litmus. After drying over calcium chloride, the solvent was distilled twice under nitrogen at reduced pressure through a column equivalent to 20 theoretical plates (d_3 = 1.5807, b.p. 145.9–146.3°, n^{20}D 1.4954).

Carbon tetrachloride (Eimer and Amend, reagent grade) was dried over phosphorus pentoxide and distilled through a 40 cm. packed column (b.p. 76.7 ± 0.2°, d^4_{30} 1.5622).

Pivalic acid (Eastman Kodak, "white label") was purified by six fractional freezings.[7] The material, m.p. 35.4°, was distilled under reduced pressure before use, to free it from dissolved air.

Infrared Absorption Measurements.—A Perkin–Elmer Model 21 double beam spectrophotometer was used with the instrument settings recommended for quantitative analysis. The reproducibility is 0.5% in transmission and 0.005 μ in wave length. The optical densities were measured at the absorption maxima of the carbonyl stretching vibration at 5.70–5.75 μ and 5.85–5.88 μ for monomeric and dimeric carboxyls, respectively.[8] The effective resolution at these two bands was 0.051 and 0.063 μ. The pair of sodium chloride cells employed had an optical path length of 1 mm. The blank cell contained the solvent when studying the spectra of pivalic acid solutions; for studies of copolymer solutions, it contained a polystyrene solution of a concentration such as to compensate for the absorption due to styrene residues in the copolymer.

Osmotic Pressure Measurements.—Zimm–Myerson osmometers with Teflon gaskets and stainless steel plates were thermostated at 29.6 ± 0.005°. The height of the meniscus was located with a cathetometer reading to 0.01 cm. Wet regenerated cellulose membranes type 300 (Sylvania Division, American Viscose Co.) were conditioned by successive immersion, for 24 hours, in 50/50 water–acetone, 100% acetone (twice) 50/50 acetone–solvent, 25/75 acetone–solvent, 100% solvent (4 times). Solvents employed for the osmotic pressure measurements were 1,1,2,2-tetrachloroethane and carbon tetrachloride, with and without the addition of 1.6 volume % N,N-dimethylbenzylamine (Eastman Kodak, b.p. 179–180°) and a trace of *t*-butylcatechol to stabilize the amine. Combined capillary and membrane dissymmetry corrections were less than ±0.02 cm. Osmotic equilibrium was attained in 24 hours with carbon tetrachloride and in 48 hours with tetrachloroethane. Only with the lowest molecular weight copolymers was it necessary to allow for diffusion by extrapolation to zero time. The reduced osmotic pressure plots were linear with slopes and intercepts calculated by least squares. The true number average molecular weight $\bar{M}_n$ of the copolymers was obtained from osmotic data in solvents containing amine. In the absence of amine, higher apparent molecular weights were measured, giving a degree of aggregation D, defined as the ratio of the apparent to the true molecular weight.[5,6]

Viscosity Measurements.—Ostwald type viscosimeters with large wells for dilution of the solutions were used. Kinetic energy corrections were applied in calculating solution viscosities.

Results and Discussion

When a polymer solution is sufficiently dilute so that there is little interpenetration of the individual chain molecules, association equilibria involving groups attached to the macromolecular backbone will be governed by their local concentration in the swollen molecular coil, rather than the stoichiometric concentration in the body of the solution. This principle is strikingly illustrated in Fig. 1, which compares the dependence of the carboxyl association equilibrium on the solution concentration of pivalic acid and various styrene methacrylic acid

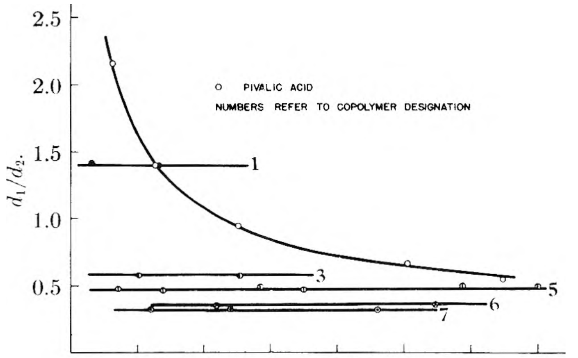

Fig. 1.—Carboxyl association of pivalic acid and styrene-methacrylic acid copolymers in tetrachloroethane.

---

(5) H. Morawetz and R. H. Gobran, *J. Polymer Sci.*, **12**, 133 (1954).

(6) H. Morawetz and R. H. Gobran, *ibid.*, **18**, 455 (1955).

(7) H. L. Ritter and J. H. Simons, *J. Am. Chem. Soc.*, **67**, 757 (1945).

(8) D. Hadzi and N. Sheppard, *Proc. Roy. Soc.* (*London*), **A216**, 247 (1953).

copolymers. The extent of carboxyl association is characterized by d_1/d_2, the ratio of the optical densities at wave lengths corresponding to free and dimerized carboxyls, respectively. As would be expected, this ratio decreases with increasing concentration of pivalic acid. However, with the methacrylic acid copolymers, d_1/d_2 depends merely on the copolymer composition and the nature of the solvent, remaining constant over the investigated range of concentrations. A slight decrease of d_1/d_2 with increasing solution concentration of the copolymer with lowest acid content was probably due to the very high solution concentrations (up to 8 g./100 ml.) used to obtain adequate absorption at wave lengths characterizing the carboxyl groups; interpenetration of molecular coils must have affected significantly the carboxyl association equilibrium.

Table I lists the mole fraction of methacrylic acid, F_A, and the true osmotic molecular weight $\overline{M}_n$, of seven styrene–methacrylic acid copolymers with their degree of aggregation, D, the second osmotic virial coefficient, B, the optical density ratio, d_1/d_2, and the intrinsic viscosities $[\eta]$ in tetrachloroethane or carbon tetrachloride solution. The extinction coefficients ϵ_1 and ϵ_2 of the free and dimerized carboxyl are required to obtain the degree of dissociation α of the carboxyl dimer. Assuming that pivalic acid has the same extinction coefficients as carboxyl groups of the copolymer, we have

TABLE I

SOLUTION PROPERTIES OF STYRENE–METHACRYLIC ACID COPOLYMERS AT 29.6°

Copolymer no.	Solvent	10^2F_A	$10^{-3}\ \overline{M}n$	D	10^6B[a]	d_1/d_2	$[\eta]$
1	$C_2H_2Cl_4$	0.79	26	1.07	8.7	1.42[b]	0.207
3	$C_2H_2Cl_4$	6.5	108	1.41	5.3	0.58	.773
4	$C_2H_2Cl_4$	7.3	57	1.46	5.8	.48	.525
5	$C_2H_2Cl_4$	8.9	102	1.51	−2.2	.48	.732
6	$C_2H_2Cl_4$	11.7	40	1.65	−4.1	.35	.480
7	$C_2H_2Cl_4$	15.2	142	1.80	−4.3	.32	.380
1	CCl_4	0.79	26	1.08	3.5	.49	.162
2	CCl_4	4.5	78	1.39	3.3	.20	.390
5	CCl_4	8.9	102	3.62	−2.6	.127	.356

[a] In g.$^{-1}$ cm.^{7} sec.$^{-2}$. [b] Obtained at a solution concentration of 2 g./100 ml.

$$d_1 = c\alpha\epsilon_1 \tag{1}$$

$$d_2 = c(1 - \alpha)\epsilon_2 \tag{2}$$

$$\frac{d_2}{c} = \epsilon_2 - \frac{d_1}{c}\frac{\epsilon_2}{\epsilon_1} \tag{3}$$

ϵ_1 and ϵ_2 may be obtained as the intercept of a plot of d_1/c against d_2/c. The experimental results led to values (l.-equiv.$^{-1}$-mm.$^{-1}$) of $\epsilon_1 = 37$, $\epsilon_2 = 41$ in 1,1,2,2-tetrachloroethane and $\epsilon_1 = 57$, $\epsilon_2 = 70$ in carbon tetrachloride. The apparent dimer dissociation constant K_d, given by

$$\frac{2c\alpha^2}{1 - \alpha} = K_d \tag{4}$$

tended to increase with rising acid concentration, as shown in Table II. A similar drift in the apparent equilibrium constant for acetic acid dimerization in carbon tetrachloride and chloroform has been reported by Barrow and Yerger.[9]

TABLE II

APPARENT DISSOCIATION CONSTANTS OF PIVALIC ACID DIMER IN CARBON TETRACHLORIDE AND 1,1,2,2 TETRACHLOROETHANE

	10^3K_d (moles/l.)	
10^3c	CCl_4	$C_2H_2Cl_4$
3.16	0.47	10
6.32	.52	11
12.64	.61	14
19.0	.81	
32.4		17

The dimerization equilibrium of carboxyls attached to a macromolecular chain may be represented formally by

$$\frac{2C_{\text{eff}}\alpha^2}{1 - \alpha} = K_d \tag{5}$$

where C_{eff} is the "effective concentration" of carboxyls in the swollen polymer coil and K_d is the dimer dissociation constant of a suitable monocarboxylic acid analog. Two approaches to an estimation of C_{eff} were considered.

(1) The C_{eff} of interacting groups attached to a flexible chain molecule may be approximated by a uniform distribution of these groups within a rigid sphere which is hydrodynamically equivalent to the polymer coil. Since $[\eta]/0.025$ is the volume in ml. of the equivalent sphere per gram of polymer[10,11]

$$C'_{\text{eff}} = 25z/M[\eta] \tag{6}$$

where z is the number of carboxyl groups per chain of molecular weight M and C'_{eff} is the equivalent concentration in equivalents per liter.

(2) In a second approach to the problem of estimating C_{eff}, z carboxyl groups are assumed to be attached at a constant spacing along the chain molecule. For flexible chains, the probability distribution of the end-to-end displacement r is

$$W(r)\text{d}r = (3/2\pi)^{3/2}(\overline{r^2})^{-3/2} \exp(-3r^2/2\overline{r^2})4\pi r^2\text{d}r \tag{7}$$

Kuhn[12] has pointed out that, for $r^2 << \overline{r^2}$

$$\frac{W(r)\text{d}r}{4\pi r^2\text{d}r} = (3/2\pi)^{3/2}(\overline{r^2})^{-3/2} = C \tag{8}$$

where C is the effective concentration determining the probability of ring formation from a flexible chain carrying a reactive group on each end. Since the mean square end-to-end displacement $\overline{r^2}$ is proportional to the chain length,[12] the association of the ith and the kth carboxyl group along a copolymer chain is determined by

$$C_{i,k} = (1000/N)(3/2\pi)^{3/2}[(k - i)(\overline{m^2})]^{3/2} \tag{9}$$

where $C_{i,k}$ is the effective concentration in equivalents per liter, N is Avogadro's number and $\overline{m^2}$ the mean square displacement of neighboring carboxyls on the copolymer. The concentration of a mono-

---

(9) G. M. Barrow and E. A. Yerger, *J. Am. Chem. Soc.*, **76**, 5248 (1954).

(10) H. Mark and A. V. Tobolsky, "Physical Chemistry of High Polymeric Systems," Second Edition, Interscience Publ., New York, N. Y., 1950, p. 295–296.

(11) P. J. Flory, "Principles of Polymer Chemistry," Cornell Univ. Press, Ithaca, N. Y., 1953, pp. 605–606, 611.

(12) W. Kuhn, *Kolloid-Z.*, **68**, 2 (1934).

TABLE III

COMPARISON OF CALCULATED AND EXPERIMENTAL VALUES OF C_{eff} AND α

Copolymer	Solvent	z	$f(z)$	$C_{\text{eff}} \times 10^2$	$C'_{\text{eff}} \times 10^2$	$C''_{\text{eff}} \times 10^2$	α	α'	α''
1	$C_2H_2Cl_4$	2	1.00	0.70	0.91	0.06	0.61	0.58	0.92
3	$C_2H_2Cl_4$	38	4.30	2.61	2.06	3.32	.49	.42	.36
4	$C_2H_2Cl_4$	40	4.03	3.50	3.37	3.92	.35	.35	.33
5	$C_2H_2Cl_4$	87	4.40	3.58	2.98	5.50	.34	.37	.29
6	$C_2H_2Cl_4$	43	4.07	6.02	5.98	6.88	.28	.28	.26
7	$C_2H_2Cl_4$	207	4.65	7.05	9.87	29.5	.25	.24	.14
1	CCl_4	2	1.00	0.13	1.16	0.08	.38	.15	.45
2	CCl_4	33	3.92	0.62	2.80	2.81	.19	.10	.10
5	CCl_4	87	4.40	1.38	6.14	11.3	.13	.07	.05

carboxylic acid resulting in the same probability of dimerization as that of the ith carboxyl group of a polymer with all the $(z - 1)$ other carboxyls is given by

$$C_i = \sum_{k=1}^{k=i-1} C_{i,k} + \sum_{k=i+1}^{k=z} C_{i,k} \qquad (10)$$

and the "effective concentration" C''_{eff} is obtained by averaging the C_i values. This leads to

$$C''_{\text{eff}} = (1000/N)(3/2\pi)^{3/2}(\overline{m^2})^{-3/2}f(z)$$

$$f(z) = \frac{2}{z} \sum_{i=1}^{i=z-1} \sum_{i=1}^{i=z-1} i^{-3/2} \qquad (11)$$

The values of $f(z)$ given in Table III show that the function tends rapidly to its asymptotic limit of 4.8. Since $\overline{r^2} = \overline{m^2}z$, we may utilize Flory's relation[13] between intrinsic viscosity and $\overline{r^2}$ to estimate $\overline{m^2}$ by

$$(\overline{m^2})^{3/2} = [\eta]M/z^{3/2}\,\Phi \qquad (12)$$

where Φ has a mean experimental value of 2.1×10^{21}. Substituting into (11) and evaluating the numerical factor

$$C''_{\text{eff}} = 1.15z^{3/2}f(z)/[\eta]M \qquad (13)$$

Estimates of the degree of dissociation of the carboxyl dimer α' or α'' were obtained from the calculated values of C'_{eff} and C''_{eff}, respectively, using for the dimer dissociation constant average pivalic acid values, 1.3×10^{-2} in tetrachloroethane and 5.8×10^{-4} in carbon tetrachloride. These results are compared in Table III with the spectroscopically determined value of α and the C_{eff} corresponding to it. The agreement of the observed and calculated values for copolymers 3, 4, 5 and 6 in tetrachloroethane is remarkably close. With copolymer 1 the average molecule carried only two carboxyls. The neglect of the statistical distribution of z, as well as that of intermolecular penetration at the high polymer concentration used, may account for the deviation of experimental values from theory. With copolymer 7, the spacing of the carboxyls is too close to justify the application of Kuhn's theory of chain configuration. Data obtained with copolymers 2 and 5 in carbon tetrachloride show also that the theory will fail when almost quantitative carboxyl dimerization is predicted, since some carboxyls attached to a copolymer coil will inevitably be isolated in positions inaccessible for association. Also, for small degrees of dissociation of the carboxyl dimer, C_{eff} is proportional to α^{-2}, so that C_{eff} becomes very sensitive to small errors in α.

The two treatments outlined above predict a different dependence of C_{eff} on z for a series of copolymers of constant composition but varying molecular weight. Using the conventional representation of intrinsic viscosity, $[\eta] = KM^a$, the "equivalent sphere" treatment leads to C_{eff} proportional to z^{-a}, while the second theory predicts C_{eff} proportional to $z^{0.5-a}f(z)$. Since $f(z)$ approaches a limiting value rather rapidly, the second theory would lead, in θ solvents,[13] to C_{eff} values independent of molecular weight, provided z is sufficiently large. This appears to be a much more reasonable result and the second treatment of C_{eff} is considered more exact, although the "equivalent sphere" approach gave, in the present study, somewhat better agreement with experiment.

For a given copolymer, both theories predict C_{eff} to be inversely proportional to the volume occupied by the macromolecule. Spectral determinations of the degree of group association should thus provide information about changes in polymer configuration, not only in the limit of infinite dilution, but at all concentrations at which the interpretation of the polymer coils has little effect on the association equilibrium. It has been pointed out that the decrease in the activity of the solvent should lead to a shrinking of the polymer coils with increasing solution concentration[14] according to

$$\frac{V_0 - V}{V_0} = \frac{3}{4}\frac{pV_0}{kT} + \ldots \qquad (14)$$

where V_0 and V are volumes of the molecular coil at zero concentration and finite concentration, respectively, and p is the excess osmotic pressure over the van't Hoff term. This equation would predict a shrinkage of copolymer 4 in tetrachloroethane by 7% at a concentration of 1 g./100 ml. and by 27% at a concentration of 2 g./100 ml. No change in the carboxyl dimerization equilibrium was observed, suggesting that equation 14 over-estimates considerably the concentration dependence of V.

In many of the solutions studied the degree of molecular aggregation D was quite low, although most of the carboxyls were dimerized. A typical case is that of copolymer 2 in carbon tetrachloride with $D = 1.39$, although an average of 83% of its 34 carboxyl groups were associated. The relation between molecular aggregation and $(1 - \alpha)$, the fraction of carboxyls associated, is shown in Fig. 2, which indicates that for a given degree of carboxyl association the molecular aggregation is higher in tetrachloroethane, the better solvent. Thermally

---

[13] Ref. 10, p. 611-612.

[14] S. G. Weissberg, R. Simha and S. Rothman, *J. Research Natl. Bur. Standards*, **47**, 298 (1954).

reversible gels may be formed by polymers with strongly interacting groups at widely separated points[15] and the equilibrium between intermolecular and intramolecular group association may determine whether a one phase gel will be stable, or whether group association will result in phase separation.

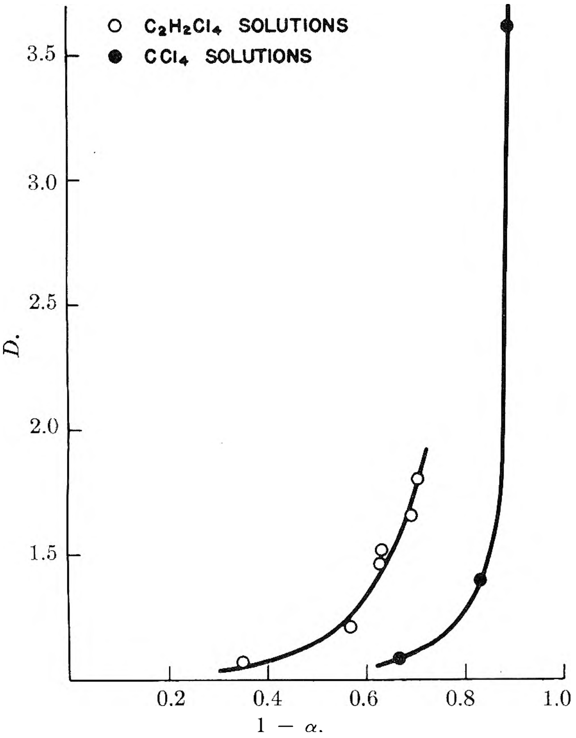

Fig. 2.—Molecular aggregation and carboxyl association in styrene–methacrylic acid copolymers.

Since both intermolecular and intramolecular carboxyl association may be eliminated by addition of a relatively small concentration of base, without altering substantially the nature of the solvent medium, it is interesting to compare the solution viscosity behavior of the acid copolymers in the presence and absence of 1.6 volume per cent. dimethylbenzylamine. Data listed in Table IV, where the subscript B refers to measurements in the presence of amine, show the effect of carboxyl association both on the intrinsic viscosity and the parameter k' defined by Huggins' relation[16]

TABLE IV

THE EFFECT OF 1.6 VOLUME % DIMETHYLBENZYLAMINE ON THE SOLUTION VISCOSITY OF STYRENE–METHACYRLIC ACID COPOLYMERS

Copolymer no.	Solvent	$[\eta]/[\eta]_B$	k'	k'_B
0[a]	$C_2H_2Cl_4$	1.23	0.24	1.11
3	$C_2H_2Cl_4$	0.85	.42	0.38
4	$C_2H_2Cl_4$	68	.63	.37
5	$C_3H_2Cl_4$	.73	.56	.38
6	$C_2H_2Cl_4$	.61	.90	.36
7	$C_2H_2Cl_4$	.37	1.87	.42
0[a]	CCl_4		0.54	[b]
1	CCl_4	.72	1.14	0.40
2	CCl_4	.71	1.64	.37
5	CCl_4	.43	2.24	.34

[a] Polystyrene, $\overline{M}_n = 40{,}000$. [b] Phase separation.

$$\eta_{sp}/c = [\eta] + k'[\eta]^2 c \qquad (15)$$

Intrinsic viscosities obtained in the absence of base reflect the hydrodynamic behavior of the molecular aggregates, which have been shown by osmometry to be stable within the experimental concentration range. The fact that all copolymers have $[\eta]/[\eta]_B < 1$ could be interpreted by side-by-side association of the molecular chains, but is more likely due to the strong contraction attending intramolecular carboxyl association, which overshadows any effect of molecular aggregation. The parameter k' has been postulated to contain a contribution due to the formation of doublets with intrinsic viscosities higher than those of the solute particles present at high dilution.[14,17,18] This concept is consistent with the observation that the values of k' were independent of the composition of the copolymer in the presence of amine, but rose sharply with the carboxyl content of the copolymer in solutions containing no base. It appears that at higher concentrations secondary aggregates are formed from the molecular association complexes characterized by the apparent osmotic molecular weight of the copolymers.

---

(15) J. D. Ferry, *Adv. Protein. Chem.*, **4**, 1 (1948).

(16) M. L. Huggins, *J. Am. Chem. Soc.*, **64**, 2716 (1942).

(17) V. Vand, THIS JOURNAL, **52**, 277 (1948).

(18) R. Simha, *J. Research Natl. Bur. Standards*, **42**, 409 (1949).

ULTRAVIOLET ABSORPTION STUDY OF PROTOLYSIS CONSTANTS OF SOME *PARA*-SUBSTITUTED PHENYLPHOSPHONIC ACIDS IN WATER

By WALTER J. POLESTAK AND HOWARD K. ZIMMERMAN, JR.

Department of Chemistry, Agricultural and Mechanical College of Texas, College Station, Texas

Received November 19, 1955

Ultraviolet absorption spectra have been observed for aqueous solutions of phenylphosphonic, *p*-bromophenylphosphonic, *p*-chlorophenylphosphonic and *p*-methoxyphenylphosphonic acids. The wave lengths for the secondary band maxima of the phenyl- and *p*-chlorophenylphosphonic acids agree closely with values earlier observed in 95% ethanol solutions, although the molar extinction coefficients are depressed by 10.9 and 15.5%, respectively, as a result of the solvent change. The absorption band for *p*-methoxyphenylphosphonic acid shows a small bathochromic shift with increasing *p*H. Stoichiometric ionization constants for both the first and second dissociations of all four acids are calculated from the spectral data and compared with values in the literature.

In recent years considerable data have been reported concerning both the ultraviolet absorption spectra and the stoichiometric dissociation constants of a variety of substituted arylphosphonic acids.[1-4] However, in surveying these data, one finds numerous gaps, as well as a few disagreements in the reported results. At the risk of adding to the discords, we undertook to carry out an independent study of the dissociation constants for four of these arylphosphonic acids. In our study of the dissociation constants, the spectrophotometric approach was chosen not only because it provided a method of attack entirely different from that used to obtain the majority of the literature data, but also because it could provide new information on the ultraviolet spectra of these acids in water as a solvent.

Experimental

Materials.—The compounds studied, namely, phenylphosphonic acid (m. 162.8–163°), *p*-chlorophenylphosphonic acid (m. 187–188.5°), *p*-bromophenylphosphonic acid (m. 201–202°) and *p*-methoxyphenylphosphonic acid (m. 164–164.5°) were obtained through the courtesy of Dr. L. D. Freedman. Their preparation has been described elsewhere.[5,6]

Acid solutions were prepared using stock solutions of reagent grade hydrochloric acid; carbonate-free sodium hydroxide stocks were used for solutions in the basic range. All solutions were made up from de-ionized distilled water.

Apparatus.—Spectra were recorded using the Beckman DU quartz spectrophotometer with silica cells of 1.000 cm. light path. The calibrated cell correction was 0.1% of measured absorbance. The spectrophotometer was calibrated with a Beckman 2260 mercury lamp as radiation source. For measurements, slit widths between 0.5 and 0.7 mm. were set as required.

In preliminary work, and for part of the final data, the Warren Spectracord attachment for the spectrophotometer was used.[7] The recording paper used for this portion of the work had a dimensional stability such that it suffered less than 0.25% change for relative humidities between 20 and 90%.

Measurements of *p*H employed the Beckman model G *p*H meter. In solutions of *p*H 10 or greater, the Beckman type B sealed glass electrode was used.

Procedure.—No stock solutions of the arylphosphonic acids could be kept for more than three days because of the development of a non-crystalline flocculation in them, probably as a result of mold growth.[8] Aqueous solutions of the four acids were prepared to 0.002 *M* by weighing all constituents. Desired amounts of HCl or NaOH solutions were added, and the result diluted to 0.001 *M*.

Spectra were recorded for each acid at approximate *p*H's of 1.5, 7, and 11 over the range from 220 to 360 mμ, using as comparison standard an aqueous solution of HCl or NaOH corresponding to the stoichiometric amount added to each test sample. From these spectra as obtained with the Warren Spectracord, wave lengths giving maximum light absorption were selected for further point-to-point study at additional *p*H values. Triple checks of absorption data obtained by the manual procedure showed a reproducibility of transmittance results within 0.5%.

Results

All acids showed a triple set of maxima in the plot of extinction *vs.* wave length except for *p*-methoxyphenylphosphonic acid. The results at these maxima are shown in Table I. For this latter acid, only the two peaks appeared.

TABLE I

EXTINCTION OF AQUEOUS *p*-SUBSTITUTED PHENYLPHOSPHONIC ACIDS

Compound	First max. λ_{max} mμ	First max. ϵ_{max}	Second max.[a] λ_{max}, mμ	Second max.[a] ϵ_{max}	Third max. λ_{max} mμ	Third max. ϵ_{max}
$C_6H_5PO_3H_2$	257.3	348	263.3	467	269.2	364
p-$BrC_6H_4PO_3H_2$	258.0	316	263.8	360	270.7	268
p-$ClC_6H_4PO_3H_2$	257.5	232	263.5	246	269.9	212
p-$H_3COC_6H_4PO_3H_2$			270	929	276	743

[a] This is the secondary band maximum according to the definition of Doub and Vandenbelt.[9]

The data of Table I apply to aqueous solutions of the acid compounds under study, with no additional acid or alkali. It is of some interest to notice that, although the wave length of the maximum for the secondary band is not shifted as one passes from alcoholic solution[1] to an aqueous one, the extinction coefficient for the band is depressed from a value of 524 in alcohol (95% EtOH) to a value of 467 in water in the case of the phenylphosphonic acid, while the extinction coefficient for *p*-chlorophenylphosphonic acid is depressed from 292 to 246 by the same solvent change. In view of the fact that the light absorption of each of the first three acids listed in Table I decreases with increasing *p*H of the solution, it is not unreasonable to suppose that this depression reflects an increasing

---

(1) H. H. Jaffe and L. D. Freedman, *J. Am. Chem. Soc.*, **74**, 1069 (1952).

(2) P. Lesfauries and P. Rumpf, *Compt. rend.*, **228**, 1018 (1949).

(3) C. V. Banks and R. J. Davis, *Anal. Chim. Acta*, **12**, 418 (1955).

(4) H. H. Jaffe, L. D. Freedman and G. O. Doak, *J. Am. Chem. Soc.*, **75**, 2209 (1953).

(5) G. O. Doak and L. D. Freedman, *ibid.*, **73**, 5658 (1951).

(6) R. W. Bost, L. D. Quinn and A. Roe, *J. Org. Chem.*, **18**, 362 (1953).

(7) Use of the Spectracord in this work resulted from the courtesy of the Fisher Scientific Company in loaning us the use of the instrument. This assistance is gratefully acknowledged.

(8) L. D. Freedman, private communication.

(9) L. Doub and J. M. Vandenbelt, *J. Am. Chem. Soc.*, **69**, 2714 (1947).

TABLE II

COMPARISON OF DISSOCIATION CONSTANTS[f]

Subst. phosphonic acid	$K_1 \times 10^2$ [b]				$K_2 \times 10^7$ [b]			
	A[b]	B[a]	C[a]	D	A[b]	B[a]	C[a]	D
Phenyl[c]	1.50	1.50	2.51	12.3[a] 11.0[b]	0.851	0.851	0.141	3.89[a] 3.09[b]
p-Bromophenyl[c]	2.14	...[e]	2.51		1.45	1.48	2.51	
p-Chlorophenyl[c]	2.51	2.19			2.04	1.78		
p-Methoxyphenyl[d]	0.832		0.955		0.955		0.795	

[a] Potentiometric measurements. [b] Spectrophotometric measurements. [c] Average deviation of *pK* values, present work, was ±0.06. [d] Average deviation of *pK* values, present work, was ±0.08. [e] Jaffe, Freedman and Doak state that this acid was insufficiently soluble in water to permit determination of this value by their potentiometric method. [f] A, This report; B, Jaffe, Freedman and Doak, ref. 4; C, Lesfauries and Rumpf, ref. 2; D, Banks and Davis, ref. 3.

ionizing influence which the water solvent exercises on the acid.

If from the spectral data, one plots the absorbance of a 0.001 *M* solution of acid against *p*H, a stepped curve is obtained having two regions of extreme sensitivity to *p*H changes. Such curves were plotted and treated by the method of Stenström and Goldsmith,[10] as modified by Irving, Rossotti and Harris,[11] making use of a differential plot of the data to locate the *p*H at which the ionized and un-ionized forms of the acidic species are of equal concentration. At such a point, the *p*H is numerically identical to the *pK* of the acid.

The two stoichiometric dissociation constants for the individual acids, as evaluated in this manner, are listed in Table II, where they are also compared with values reported by other investigators. As is to be seen from this comparison, our values for the dissociation constants are in good general agreement with those reported by both Jaffe, Freedman and Doak,[4] and by Lesfauries and Rumpf,[2] both of whose reports were based on potentiometric studies. Since our data derive directly from the spectral absorption characteristics of the test substance in solution, which in turn depend predominantly on stoichiometric concentrations, our constants are to be considered as "apparent dissociation constants," rather than thermodynamic ones. The results from the potentiometric method cited above were deduced on the same basis, so that the extent of agreement, particularly with the results of Jaffe, *et al.*, leads us to believe that the other constants (for other arylphosphonic and arylphosphinic acids) reported by them are to be preferred over others appearing in the literature.

Our findings are in complete disagreement with those of Banks and Davis.[3] Inasmuch as these investigators worked in ionic strengths corresponding to salt concentrations of the order of 1.0 *M*, we believe there is probably a high degree of uncorrected salt effect in the potentiometric results reported by them. Moreover, the molar extinction coefficients used by them in their spectrophotometric method were estimated on the basis of their potentiometric results. Consequently, we feel that their results are not reliable. Certainly the weight of the evidence supports this conclusion.

We experienced our greatest difficulty in the determination of the constants for the *p*-methoxyphenylphosphonic acid, and our results for this case are considerably less precise than are those for the other three cases. The difficulty arose from the fact that the differences in spectral transmission amounted to only about 8% in the *p*H range from zero to ten. As a result, the increment of absorption with change in *p*H (used in the differential plot) was not large anywhere in the range, and maximum precision was not possible. In addition the degree of resolution in the spectrum was poor. Optimum resolution appears to occur for these acids in the range of transmittance between 40 and 60%, whereas for the concentrations we had chosen for this substance, the transmittance was of the order of 20%. Solutions even more dilute than ours would probably lead to better values.

A further difficulty experienced in employing the spectrum of *p*-methoxyphenylphosphonic acid for dissociation constant calculations arises from the fact that the wave length of maximum light absorption undergoes a small bathochromic shift with increasing *p*H. This effect, together with the general increase in absorption as *p*H increases (contrary to experience with the other three acids) we believe to be attributable to the changing influence of the non-bonding valence electrons of the oxygen atom in the methoxy group on resonance within the phenyl ring. In acid solutions, the presence of a relatively high proportion of hydrogen ions in the solution makes probable a moderate degree of coördination of such ions with these non-bonding oxygen electrons, immobilizing them. With fewer hydrogen ions present, as in an alkaline solution, such non-bonding electrons are free to participate in a "quinoid" type of resonance with the ring, thereby lengthening the resonance path. This postulate raises the interesting question of whether or not this acid (as well as others of its type) exists to any extent in the form of "zwitterions." We have been able neither to find any mention of such a phenomenon in the literature nor to carry out experimental work to answer the question at the present time.

Insofar as the interpretation to be placed on the experimentally determined dissociation constants is concerned, the values we have obtained in agreement with the results of Jaffe, Freedman and Doak[4] lead us to concur in their conclusions. In particular, it appears from the fact that the *p*-bromo- and *p*-chloro- derivatives possess larger ionization constants (in the order which would be predicted from their well-known inductive influence—actu-

---

(10) W. Stenström and N. Goldsmith, THIS JOURNAL, **29**, 1477 (1925).

(11) H. Irving, H. S. Rossotti and G. Harris, *Analyst*, **80**, 83 (1955).

ally a perturbation of the resonance pattern in the phenyl group) than the unsubstituted phenylphosphonic acid, while the constant for the electron-yielding *p*-methoxy- derivative is depressed, that there is a very definite communication of electronic charges across the molecule to the site of ionization. Such a communication can only arise from the polarizability of the central phosphorus atom in the acid functional group, operating in concert with the resonance pattern within the phenyl ring.

Acknowledgment.—We wish gratefully to acknowledge the valuable consultations and many helpful suggestions contributed to us during this study by Dr. A. F. Isbell.

VISCOSITIES OF THE BINARY GAS MIXTURES, METHANE-CARBON DIOXIDE AND ETHYLENE-ARGON[1]

BY W. MORRISON JACKSON

Goodyear Atomic Corporation, Laboratory Division, Portsmouth, Ohio

Received November 25, 1955

Experimental viscosities at 25° are reported for the binary gas mixtures, methane-carbon dioxide and ethylene-argon over the composition range from 0 to 100 mole % of each component. The measured viscosities are compared with calculated values and their application to quantitative analysis of these gas pairs is discussed.

Introduction

Two inert binary gas mixtures for which no previous experimental viscosity data have been reported are methane-carbon dioxide and ethylene-argon. Calculations of the theoretical viscosities showed that for methane-carbon dioxide the change in viscosity with composition should deviate in a positive manner from the additivity of the individual viscosities, while for ethylene-argon the change in viscosity with composition should show a negative deviation. To verify this theoretical difference in behavior, the viscosities of these gas pairs were measured over the entire composition range using the capillary tube method, and the results were compared with the calculated values.

Experimental

Apparatus.—An automatic-reading capillary tube viscosimeter, previously described by Junkins,[2] was used for the determination of the viscosities of the gas pairs, methane-carbon dioxide and ethylene-argon. A straight platinum capillary with an internal diameter of 0.03 and 100 cm. in length was used in all of the measurements.

Materials.—The gases used to prepare the binary gas mixtures were obtained from commercial cylinders of methane, carbon dioxide, ethylene and argon. The impurities present in each gas as determined by mass spectrometer analysis are as follows. Methane: contained 0.1% oxygen, 0.1% propane and 0.7% ethylene; carbon dioxide: based upon a trace of argon observed a maximum of 0.1% oxygen and 0.4% nitrogen could have been present; ethylene: contained less than 0.17% propane and/or propene and a trace of air. Small amounts of acetylene would not have been detected; argon: contained 0.06% nitrogen and 0.01% oxygen, carbon dioxide and water.

The air used was medicinal quality "breathing air" which was dried by passing through a Dry Ice slush trap and drying towers of anhydrous calcium sulfate and anhydrous magnesium perchlorate.

Procedure.—Methane-carbon dioxide mixtures of the approximate composition desired were prepared by filling evacuated cylinders with one of the pure gases through a manifold to a predetermined pressure, and then adding the second pure gas at a higher pressure until the desired total pressure was obtained. To ensure thorough mixing, each cylinder was alternately heated and cooled several times and then allowed to stand about five days before sampling for analysis. The composition of the methane-carbon dioxide mixtures was determined by Orsat analysis. The chemical methods of analysis investigated were found to be unsatisfactory for ethylene-argon mixtures. Consequently, ethylene-argon mixtures were prepared in much the same manner as the methane-carbon dioxide mixtures except that they were mixed with extreme care using a specially designed manifold so as not to exceed a maximum error in composition of ±0.1%.

For the measurement of the flow time of a gas, whose viscosity was to be determined, the gas was admitted into the capillary forechamber until the pressure was greater than a reference pressure, P_1. As the gas flowed through the capillary into a container at a constant pressure, P_0, the forechamber pressure dropped until it was lower than a second reference pressure, P_2. The time required for the pressure to drop from P_1 to P_2 was recorded by a timer which was automatically turned on at P_1 and off at P_2. Measurements were repeated as necessary to establish the precision. After evacuation of the manifold and capillary, the reference gas was run in the same manner without changing the temperature or pressures P_1, P_2 and P_0. The temperature of the bath surrounding the forechamber and capillary and the pressures were noted for each measurement. Relative flow times under different pressure conditions were obtained by changing the reference pressures P_1, P_2 and P_0.

Results

Measurements of the viscosity of nitrogen at 65°, made under different pressure conditions of P_1, P_2 and P_0 to establish the precision of the viscosimeter and to determine the effect of varying Reynolds numbers, are shown in Table I.

TABLE I

VISCOSITY OF NITROGEN AT 65°

Mean pressure, P_m, cm.	Mean Reynolds no. Re_m	Exptl. viscosity of nitrogen, μpoise
16.64	16.5	195.3
18.87	15.3	195.4
25.29	40.3	195.4
31.91	58.3	195.5
37.71	85.7	195.4

Experimental viscosities of methane-carbon dioxide and ethylene-argon mixtures, for the composition range from 0 to 100 mole % of each component, are compared to calculated values in Tables II and III.

---

[1] Based on work performed for the U. S. Atomic Energy Commission by Union Carbide Nuclear Company, Union Carbide and Carbon Corporation, Oak Ridge, Tennessee.

[2] J. H. Junkins, *Rev. Sci. Instr.*, **26**, 467 (1955).

TABLE II

VISCOSITIES OF METHANE–CARBON DIOXIDE GAS MIXTURES AT 25°

Methane, mole %	Viscosity, μpoise		Methane, mole %	Viscosity, μpoise	
	Exptl.	Calcd.		Exptl.	Calcd.
0	151.0	151.0[a]	65.1	132.8	132.3
2.2	150.9	150.6	73.0	129.1	128.5
10.3	149.4	149.1	78.9	124.8	125.4
18.3	147.7	147.4	85.0	122.6	121.8
29.7	145.3	144.6	90.5	119.2	118.3
42.1	141.4	141.0	93.3	117.4	116.4
53.7	137.3	137.0	100	111.4	111.4[a]

[a] Experimental viscosities of pure gases used in calculating viscosities for mixtures.

TABLE III

VISCOSITIES OF ETHYLENE–ARGON GAS MIXTURES AT 25°

Ethylene, mole %	Viscosity, μpoise		Ethylene, mole %	Viscosity, μpoise	
	Exptl.	Calcd.		Exptl.	Calcd.
0	225.2	225.2[a]	60.0	147.0	145.6
10.0	211.1	210.1	70.0	135.0	134.5
20.0	196.3	195.9	80.0	124.2	124.0
30.0	182.7	182.3	90.0	113.6	113.8
40.0	169.8	169.5	100	104.2	104.2[a]
50.0	158.0	157.3			

[a] Experimental viscosities of pure gases used in calculating viscosities for mixtures.

Discussion

Myerson and Eicher[3] found that the differences between apparent viscosity values for uranium hexafluoride obtained by them and other investigators using the capillary tube method could be explained on the basis of Reynolds numbers. At pressures of one atmosphere or less, the viscosity is independent of pressure. However, Reynolds numbers are a function of pressure, and increase as the mean pressure

$$P_m = \frac{P_1 + P_2 + 2P_0}{4} \qquad (1)$$

increases, where P_1, P_2 and P_0 are initial, final and downstream pressures, respectively, of the gas flowing through the capillary. Since the critical Reynolds number, above which turbulent flow can be expected for metal capillaries,[4] is much less than for pipes, the possibility of exceeding it is present even at pressures below one atmosphere. This is especially true when the molecular weight of the gas is large. It is only when the critical Reynolds number is exceeded that the apparent viscosity varies with pressure.

Assuming viscous flow, the initial, final and mean Reynolds numbers for a given capillary can be calculated from

$$Re_i = \frac{2\rho rV}{\eta} = \frac{Mr^3(P_1 + P_0)(P_1 - P_0)}{8LRT\eta^2} \qquad (2)$$

$$Re_f = \frac{2\rho rV}{\eta} = \frac{Mr^3(P_2 + P_0)(P_2 - P_0)}{8LRT\eta^2} \qquad (3)$$

$$Re_m = \frac{Re_i + Re_f}{2} \qquad (4)$$

where ρ is the density, r the radius of the capillary, V the linear velocity, M the molecular weight of the gas, L the length of the capillary, R the ideal gas constant, T the temperature, η the viscosity, and P_1, P_2 and P_0 are initial, final and downstream pressures of gas flowing through the capillary.

As shown in Table I, changes in pressures P_1, P_2 and P_0 which changed the Reynolds number for nitrogen from 16.5 to 85.7 did not cause a significant change in the viscosities obtained. Thus, it is concluded that for light gases such as nitrogen, the critical Reynolds number of the capillary is not exceeded at pressures below one atmosphere, and that the viscosities for other light gases obtained with the same capillary should be independent of pressure.

From the viscosity of nitrogen at 23°, obtained by Yen,[5] the viscosity at 65° was calculated to be 195.2 μ poise. The average viscosity of nitrogen at 65° obtained during the present experiments was 195.4 μ poises, which is in good agreement with Yen's value.

The experimental and calculated viscosities for methane–carbon dioxide and ethylene–argon gas mixtures as shown in Tables II and III are in reasonably good agreement, thus verifying the initial assumption that the change in viscosity with composition, for the two gas pairs, should be different. The calculated values were obtained using an equation derived by Wilke[6]

$$\eta_m = \frac{\eta_1}{1 + \dfrac{(X_2/X_1)\,[1 + (\eta_1/\eta_2)^{1/2}(M_2/M_1)^{1/4}]^2}{(4/\sqrt{2})\,[1 + (M_1/M_2)]^{1/2}}} + \frac{\eta_2}{1 + \dfrac{(X_1/X_2)\,[1 + (\eta_2/\eta_1)^{1/2}(M_1/M_2)^{1/4}]^2}{(4/\sqrt{2})\,[1 + (M_2/M_1)]^{1/2}}} \qquad (5)$$

where η_1 and η_2 are the experimental viscosities, M_1 and M_2 the molecular weights, and X_1 and X_2 the mole fraction of the pure components.

The precision of the viscosity measurements using the capillary tube viscosimeter was approximately 1 part in 2000. Thus the chief source of error in the determination of viscosities *versus* composition was in the method of analysis to determine the composition. Check analyses indicated a maximum error of ±0.2% in the Orsat analysis of the methane–carbon dioxide mixtures. Since chemical analysis was found to be unsatisfactory for the analysis of ethylene–argon mixtures, the gases were mixed initially to a given composition. For this purpose a specially designed manifold, capable of mixing gases to a composition of ±0.1%, was used.

The difficulty of accurate analysis of a gaseous mixture such as ethylene–argon might be avoided by using viscosity values as a measure of composition. Application of such a method would require that there be a difference between the viscosities of the two gases and no maximum in the composition range of interest. Mixtures of methane–carbon dioxide and ethylene–argon satisfy these conditions as can be seen from Tables II and III. Having obtained a standard curve of viscosity *versus* composition, then the composition of any unknown mix-

---

(3) A. L. Myerson and J. H. Eicher, *J. Am. Chem. Soc.*, **74**, 2758 (1952).

(4) W. Ruches, *Ann Physik*, [4] **25**, 983 (1908).

(5) K. L. Yen, *Phil. Mag.*, **38**, 582 (1919).

(6) C. R. Wilke, *J. Chem. Phys.*, **18**, 517 (1950).

ture of the two gases could be determined quickly and accurately using an automatic-reading capillary tube viscosimeter to determine the viscosity.

Acknowledgment.—The author expresses his appreciation for the coöperation and assistance which he has received during the course of this work. Recognition is given to Dr. E. J. Barber for his direction of this work and to Mr. J. H. Junkins for his many helpful suggestions related to the design and operation of apparatus.

MOLTEN SALT MIXTURES. PART 2. THE REFRACTIVE INDEX OF MOLTEN NITRATE MIXTURES AND THEIR MOLAR REFRACTIVITIES

By H. Bloom and D. C. Rhodes

Department of Chemistry, Auckland University College, Auckland, New Zealand

Received November 28, 1955

A method has been developed for the accurate measurement of refractive index of molten salts. Measurements of refractive index have been carried out over a temperature range of about 100° for pure molten $NaNO_2$, $NaNO_3$, KNO_2, KNO_3 and $AgNO_3$. The molar refractivity of each salt has been calculated. The refractive indices of molten mixtures of $NaNO_3$–KNO_3, $NaNO_3$–$AgNO_3$ and KNO_3–$AgNO_3$ have similarly been investigated and their molar refractivities calculated. The plot of molar refractivity versus mole fraction is for the $NaNO_3$–$AgNO_3$ and KNO_3–$AgNO_3$ systems linear within experimental error. For the $NaNO_3$–KNO_3 system the deviations from the linear relation are slightly outside the limits of experimental error.

To explain the conductivity minima observed in isotherms of electrical conductivity of certain molten salt mixtures, such as the $CdCl_2$–KCl system, Bloom and Heymann,[1] Bloom, *et al.*,[2] and Harrap and Heymann[3] assumed that complex anions are present in such systems. Van Artsdalen and Yaffe[4] have pointed out, however, that a conductivity minimum is observed in the system LiCl–KCl in which the formation of complex ions is very unlikely. They drew attention to the danger of explaining such minima by the formation of complex ions, if there is no supporting evidence from other physical properties. In certain systems, *e.g.*, $PbCl_2$–KCl and $CdCl_2$–KCl the presence of complex ions has been qualitatively established by the large negative deviations from additivity, of electrical conductivity, together with a maximum value of the energy of activation for ionic migration, in the plot of property against composition. Such qualitative evidence, as well as that arising from considerable positive deviations of molar volume from additivity, does not yield quantitative information on the structure of the complex ions present.

The investigation of refractive index and molar refractivity of molten salt mixtures was undertaken in an attempt to find a physical property which is likely to be affected considerably by the presence of complex ions and which can give quantitative information about such complexes. Refractivities of ions both in the free gaseous state and in infinitely dilute aqueous solutions have been obtained by Fajans.[5] Similar data on molten salts can be used to give information about the mutual influence of ions in a melt.

In order to minimize experimental difficulties, the investigation of relatively low melting salts was first undertaken. For the systems selected, electrical conductivity and density studies have shown that their mixtures exhibit only minor departures from ideality.

No measurements of refractive index of molten salt mixtures have yet been published but there have been some determinations of the refractive index of pure fused hydroxides, nitrates and other fairly low melting salts. Meyer and Heck[6] determined the refractive indices of KNO_3, $NaNO_3$, KOH and NaOH and calculated their molar refractivities. Their method was to make cross-wires and their image coincide using an autocollimator. A beam of light illuminating the cross-wires was directed into the melt and made to strike an immersed inclined mirror. The angle of the mirror was adjusted so that the cross-wires and their real inverted image coincided. From the angle of the mirror and that of the measuring telescope, the refractive index could be evaluated. Wagner[7] modified the apparatus slightly and determined the refractive index of a number of alkali and silver nitrates and other oxy-salts. His results did not agree very well with those of Meyer and Heck.

Experimental

The chemicals used were all of analytical reagent quality and gave colorless clear melts. Silver nitrate was kept out of light to prevent photolysis. Mixtures of salts were made up by weighing lumps of the solidified previously fused salts, directly into the container.

Method.—Two sets of fine platinum cross-wires were rigidly supported at a distance of 2.5 inches apart by means of Pyrex glass rods. They were fixed firmly in a furnace which consisted of a stainless steel tube (3 inch diameter, 24 inches long) heated by a Nichrome V element fitted in an insulated case. The cross-wires were illuminated by light of a sodium vapor lamp just above the furnace tube and were viewed by means of a transit theodolite which was mounted about three feet from the furnace in such a way as to allow three dimensional adjustment. By alternately focussing the telescope on the upper and lower cross-wires and making suitable adjustments to the angle of inclination of the theodolite telescope, the angle of inclination of the cross-wires could be determined accurately. The melt which was contained in a Pyrex tube (2 inch diameter, 7 inches long) could be raised and lowered in the furnace. The surface of

---

[1] H. Bloom and E. Heymann, *Proc. Roy. Soc. (London)*, **188A**, 392 (1947).

[2] H. Bloom, I. W. Knaggs, J. J. Molloy and D. Welch, *Trans. Faraday Soc.*, **49**, 1458 (1953).

[3] B. S. Harrap and E. Heymann, *ibid.*, **51**, 259 (1955).

[4] E. R. Van Artsdalen and I. S. Yaffe, This Journal, **59**, 118 (1955).

[5] K. Fajans, *Z. physik. Chem.*, **24B**, 103 (1934).

[6] G. Meyer and A. Heck, *ibid.*, **100**, 316 (1922).

[7] O. H. Wagner, *ibid.*, **131**, 409 (1928).

the melt was initially situated below the lower cross-wire to enable the angle of inclination of the two sets of cross-wires to be determined in air. After this was done, the tube containing the melt was raised so that both sets of cross-wires were immersed. Owing to the refraction of light by the melt, the angle of inclination of the theodolite telescope had to be altered to bring both sets of cross-wires into focus in the line of the telescope. The angle of refraction was thus measured and found reproducible to better than 1′ in 15° (±0.1%). During the measuring process the temperature of the melt was measured by a chromel–alumel thermocouple and pyrometer (calibrated at the melting points of various metals and salts). Temperature was controlled by means of a "Simmerstat" to ±1°. The measurements were repeated at 20° intervals from about 20° above the melting point of the salt or liquidus temperature of a mixture to approximately 100° higher.

Results and Discussion

The refractive index, n, is defined by the equation

$$n = \frac{\sin\text{ (angle of incident beam)}}{\sin\text{ (angle of refracted beam)}}$$

The angles of incidence and refraction were determined directly so the refractive index at various temperatures could readily be calculated. In all cases the refractive index of pure salts and mixtures are linear functions of temperature (t°C.) so that results can be expressed in the form $n = a - bt$, where a and b are constants. All values of n are at the wave length of the sodium D line. Molar refractivity, R, is calculated from the Lorentz–Lorenz equation

$$R = \frac{n^2 - 1}{n^2 + 2} \times \frac{M}{d}$$

where M = molecular weight, defined in the case of mixtures as

$$M = M_1x_1 + M_2x_2 \quad (x = \text{mole fraction})$$

The density, d, of fused salts and mixtures was taken from published values; $NaNO_2$, $NaNO_3$ and KNO_3 by Bloom, *et al.*,[2] and $AgNO_3$ from Boardman, Dorman and Heymann.[8] As there are no reliable published results for KNO_2, density determinations were carried out, it being found by a sinker method that

$$d = 1.976 - 6.2 \times 10^{-4}t \quad (t \text{ in °C.})$$

Results of refractive index, molar refractivity and density are given in Tables I, II, III and IV.

Table I

Refractive Index, Density and Molar Refractivity (in cc.) of Pure Fused Salts

$n = a - bt$ (t in °C.)

Salt	Temp. range, °C.	a	$b \times 10^4$	Density	R, cc.
$NaNO_2$	315–400	1.476	2.0	$2.022-7.46\times10^{-4}t$	9.63
$NaNO_3$	320–460	1.495	2.0	$2.134-7.03\times10^{-4}t$	11.54
KNO_2	440–500	1.461	1.75	$1.976-6.2\times10^{-4}t$	11.67
KNO_3	345–480	1.473	1.7	$2.116-7.29\times10^{-4}t$	13.57
$AgNO_3$	260–365	1.706	1.55	$4.190-10.8\times10^{-4}t$	16.20

Table II

Refractive Index, Density[9] and Molar Refractivity (in cc.) of Fused Mixtures of $NaNO_3$ and KNO_3

Mole % $NaNO_3$	Temp. range, °C.	a	$b \times 10^4$	Density	R (exp.)	R (add.)
20	300–400	1.472	1.7	$2.126-7.44\times10^{-4}t$	13.07	13.16
40	280–400	1.465	1.5	$2.136-7.60\times10^{-4}t$	12.63	12.76
60	300–400	1.462	1.4	$2.132-7.40\times10^{-4}t$	12.18	12.35
80	300–400	1.459	1.2	$2.132-7.20\times10^{-4}t$	11.80	11.94

Table III

Refractive Index, Density[14] and Molar Refractivity (in cc.) of Fused Mixtures of $AgNO_3$ and $NaNO_3$

Mole % $AgNO_3$	Temp. range, °C.	a	$b \times 10^4$	Density	R (exp.)	R (add.)
20	310–380	1.504	1.0	$2.530-8.0\times10^{-4}t$	12.52	12.48
40	290–360	1.535	0.7	$2.906-8.3\times10^{-4}t$	13.47	13.42
60	270–350	1.576	0.6	$3.310-9.0\times10^{-4}t$	14.42	14.35
80	235–330	1.632	0.8	$3.734-9.7\times10^{-4}t$	15.33	15.29

Table IV

Refractive Index, Density[10] and Molar Refractivity (in cc.) of Fused Mixtures of $AgNO_3$ and KNO_3

Mole % $AgNO_3$	Temp. range, °C.	a	$b \times 10^4$	Density $\times 10^4 t$	R (exp.)	R (add.)
30	250–350	1.538	2.0	$2.669-9.4\times10^{-4}t$	14.40	14.37
55	150–300	1.588	1.9	$3.194-10.7\times10^{-4}t$	14.94	15.01
58	190–300	1.593	1.9	$3.259-10.8\times10^{-4}t$	14.96	15.06
70	170–300	1.614	1.4	$3.518-11.0\times10^{-4}t$	15.30	15.41

The maximum error involved in the measurement of refractive index is ±0.1% (being that involved in the measurement of angle by the theodolite). In the determination of molar refractivity, there is a more serious error, *i.e.*, that associated with density. The discrepancy between density measurements reported by different investigators may be as much as ±0.5%. Thus the possible error in refractivity due to density errors is estimated to be of the order of ±0.5%.

In all cases the molar refractivity calculated from the refractive index and density data were constant within 0.5% over the temperature ranges investigated. This compares favorably with the greater variation of values of R obtained by Meyer and Heck and Wagner. Our values of refractive index agree better with Meyer and Heck than with Wagner, whose results for $NaNO_3$, KNO_3 and $AgNO_3$, investigated also by us, are from 1 to 2% higher. The disagreement between the results of Meyer and Heck and those of Wagner is not systematic and is thus most likely due to random errors inherent in their experimental method. In their method which involved reflection of light from an inclined mirror immersed in a melt, unpredictable errors due to surface imperfections of the platinum mirror are possible. In addition, their investigations required the measurement of small angles (1–4°), in which an error of only 1′ would lead to an error of the order of 1% in refractive index. Neither Meyer and Heck nor Wagner investigated any mixtures.

The refractivity difference $R_{KNO_3} - R_{KNO_2}$ = 1.90 cc. while $R_{NaNO_3} - R_{NaNO_2}$ = 1.91 cc. Hence 1.905 represents the difference between the refractivities of O^{2-} in NO_3^- and $(e^-)_2$ in NO_2^-. It can also be seen that $R_{KNO_3} - R_{NaNO_3}$ = 2.03 cc. while $R_{KNO_2} - R_{NaNO_2}$ = 2.04 cc., hence $R_{K^+} - R_{Na^+}$ = 2.035. This value is identical (within experimental error) with the value of $R_{KNO_3} - R_{NaNO_3}$ for infin-

---

[8] N. K. Boardman, F. H. Dorman and E. Heymann, This Journal, **53**, 375 (1949).

[9] H. M. Goodwin and R. D. Mailey, *Phys. Rev.*, **25**, 469 (1907).

[10] H. Bloom, to be published.

itely dilute solutions: 13.25–11.21, determined by Fajans and Lühdemann.[11] Hence the effect of ionic interactions in molten KNO_3, KNO_2, $NaNO_3$ and $NaNO_2$ is either negligible or cancels out for the four salts.

Molar Refractivities of Mixtures of Molten Salts.—The measured values of molar refractivity (R exp.) of mixtures of $NaNO_3$-KNO_3, $NaNO_3$-$AgNO_3$ and KNO_3-$AgNO_3$ are given in Tables II, III and IV, respectively. These tables also give the calculated values (R add.) of molar refractivity from the usual additivity relation,[12] *i.e.*

$$R\ (\text{add.}) = R_1x_1 + R_2x_2$$

It can be seen from Tables II, III and IV that the differences between R(exp.) and R(add.) are small. The difference R(exp.) $-$ R(add.) is inside the limits of experimental uncertainty for the $NaNO_3$-$AgNO_3$ and KNO_3-$AgNO_3$ systems, but slightly outside these limits for the system KNO_3–$NaNO_3$.

The electrical conductivities of mixtures of KNO_3–$NaNO_3$ were measured by Goodwin and Mailey[9,13] and those of $NaNO_3$-$AgNO_3$ by Byrne, Fleming and Wetmore.[14] The surface tensions of the $NaNO_3$-$AgNO_3$ and KNO_3-$AgNO_3$ systems have been measured by Bloom,[10] while those of KNO_3–$NaNO_3$ were investigated by Boardman, Palmer and Heymann.[15] In these systems, isotherms of electrical conductivity and surface tension have small negative deviations from additivity while molar volumes have almost ideal values. Such behavior indicates that in the systems KNO_3–$NaNO_3$, $NaNO_3$-$AgNO_3$ and KNO_3–$AgNO_3$, little or no ionic interaction takes place. For these systems, the deviations from additivity of molar refractivity are very small.

Further investigations, including those on mixtures of $PbCl_2$–KCl and $CdCl_2$–KCl where strong interactions are expected, are at present being carried out in this Laboratory.

The authors are pleased to acknowledge a grant from the University of New Zealand Research Fund for the purchase of the apparatus used.

---

[11] K. Fajans and R. Lühdemann, *Z. physik. Chem.*, **B29**, 150 (1935).

[12] K. Fajans, in Weissberger "Physical Methods of Organic Chemistry," 2nd ed., Vol. 1, Interscience Publishers, New York, N. Y., 1949, p. 1170.

[13] H. M. Goodwin and R. D. Mailey, *Phys. Rev.*, **26**, 28 (1908).

[14] J. Byrne, H. Fleming and F. E. W. Wetmore, *Can. J. Chem.*, **30**, 922 (1952).

[15] N. K. Boardman, A. R. Palmer and E. Heymann, *Trans. Faraday Soc.*, **51**, 277 (1955).

MULTILAYER ADSORPTION ON PLANE SURFACES BY CAPACITY MEASUREMENTS. I. ADSORPTION ON GLASS AT HIGH RELATIVE PRESSURES

By U. Garbatski and M. Folman

Department of Chemistry, Technion, Israel Institute of Technology, Haifa, Israel

Received December 1, 1955

The adsorption of water vapor at relative pressures from 0.505 to 0.9976 and of isopropyl alcohol from 0.2 to 0.993 on glass plates is measured by change in electrical capacity. Layer thicknesses up to hundreds of Å. are found. Experimental details are given.

Introduction

The physical adsorption of vapors is generally explored on powders or other systems of high specific surface area. In the evaluation of the resulting isotherms generally there appear two difficulties of which one is the uncertainty about the state of the surface and the other the entering of capillary condensation into the picture besides adsorption on the surface in its strict sense.

For this reason, we sought a convenient method to use more defined plane surfaces of necessarily rather small areas of square centimeters instead of square meters as used generally (preliminary publication[1]).

Adsorptions on surfaces of small area have been measured in different ways among others by Iredale,[2] Cassel,[3] MacHaffie and Lenher,[4] Frazer,[5] Smith,[6] Latham,[7] Deryagin[8] and Bowden.[9] Iredale and Cassel used Gibbs' isotherm to calculate adsorption on mercury from the change in its surface tension. MacHaffie and Lenher, Smith and Latham measured the change of pressure with temperature, of vapors included in a vessel of the adsorbing material (*e.g.*, glass) and showed from the p–t curves obtained, that at cooling, condensation was preceded by multimolecular adsorption measurable up to 20 and even 200 layers. Frazer and later Deryagin used the change in polarization of plane polarized light reflected from glass covered with the adsorption layer.

The method chosen by us consists in measuring the change of capacity in a condenser consisting of two plates of the adsorbent kept at a fixed small distance by metallic holders cemented to their backs which constitute the plates of the condenser.

---

[1] U. Garbatski and M. Folman, *J. Chem. Phys.*, **22**, 2086 (1954).

[2] T. Iredale, *Phil. Mag.*, [6] **45**, 1088 (1923); **48**, 177 (1924); **49**, 603 (1925).

[3] H. Cassel, *Trans. Faraday Soc.*, **28**, 177 (1932).

[4] J. R. MacHaffie and S. Lenher, *J. Chem. Soc.*, **127**, 1559 (1925).

[5] J. H. Frazer, *Phys. Rev.*, [2] **33**, 97 (1929).

[6] J. W. Smith, *J. Chem. Soc.*, 2045 (1928).

[7] G. H. Latham, *J. Am. Chem. Soc.*, **50**, 2987 (1928).

[8] B. V. Deryagin, *et al.*, *C.A.*, **46**, 4881 (1952).

[9] F. P. Bowden and W. R. Throssel, *Nature*, **167**, 601 (1951).

The limits of sensitivity to the amounts adsorbed depend first of all on the sensitivity and constancy of the electrical system and the distance of the metal plates. Any material which may be produced in thin plates of a few square centimeters surface may be used as adsorbent. The sensitivity of our method at the present stage did not allow measuring layer thicknesses with more than a few Ångströms accuracy.

Experimental

Adsorption System.—The adsorbent was composed of two microscope cover glasses (non-corrosive Corning glass), 22 × 50 mm. and approximately 0.13 mm. thick. They were cemented each to a brass plate 22 × 54 × 5 mm. with Araldite and baked 4 hours at 170°. Afterwards the glass was cleaned with a detergent solution and dilute nitric acid and rinsed for hours with double distilled water. After drying the plates were clamped on two Teflon spacers (0.6 mm.) positioned at the ends beyond the glass. The brass clamps were insulated from the plates also by Teflon. Teflon was chosen as it is not wetted and is insoluble in the liquids used, it is also elastic enough to give under pressure good mechanical contact with the brass plates of the condenser and so no condensation will take place in the interstices. The distance between the glass plates was estimated by filling the space between them with amyl alcohol and weighing, giving an accuracy of 0.001 mm. The construction of the condenser was rather critical and this form was adopted after trying other models that showed mechanical deformation with pressure change.

The condenser was held in a glass vessel A that could be connected either to the vacuum line or to a glass vessel B containing a solution of known vapor pressure. By stopcocks it was possible to evacuate either one or both vessels or to add by distillation solvent to B in order to change the concentration.

Two leads through vacuum-tight seals connected the condenser to a concentric cable leading to the electrical measuring circuit.

The whole adsorption system was placed into a thermostat constant to 0.001°.

Electrical System.—The circuit used has been developed by Atree[10] and consists of a crystal controlled oscillator in which the capacity to be measured is part of the anode circuit. The anode current was measured to 5 × 10^{-8} after rectification and partial compensation. It depends on the resonance between the anode circuit containing the measured capacity and the grid circuit crystal controlled at 5.3 Mc. Changes in capacity were measured by compensating them with a precision condenser. The precision condenser was constructed according to Watson[11] and calibrated with a standard oscillator and condenser, and a Packard counter. The useful range of the precision condenser is 1 $\mu\mu$F., and its capacity linear with the readings on the micrometric movement to 0.001 $\mu\mu$F.

The whole oscillator uses a single miniature tube fed by batteries and dissipates less than a watt. It was put into a wide glass tube, closed at one end and submerged into the thermostat. Stability was reached after less than an hour. The stability of the system as a whole was better than 0.002 $\mu\mu$F. during 30 minutes, which was the maximum time of measurement.

Solutions of Known Vapor Pressure.—Relative pressures of water vapor from 0.985 to 0.9976 were obtained from solutions of mannitol. KCl solutions were used in the range p/p_0 0.86 to 0.98. Still lower relative pressures were obtained by connecting to the adsorption system a bulb with pure water at a fixed lower temperature.

Mannitol was prepared from chemically pure material by repeated crystallization from water. The melting point of the final product (162.2°) corresponded to that given in the literature. The concentrations of the solutions used were between 0.0024 and 0.014 m and an activity factor of unity was assumed. This assumption should introduce in $1 - p/p_0$ an error smaller than 1%. (Compare Frazer, *et al.*[12].) Potassium chloride of analytical grade was recrystallized and dried. The vapor pressure lowerings given by Robinson and Sinclair[13] were used. The solutions were prepared by introducing into the bulb B weighed amounts of the solute, to which water after degassing was added by distillation from a weighed vessel. Isopropyl alcohol (analytical grade) was twice distilled, dried over calcium oxide under reflux for 24 hours and distilled.

Dibutyl phthalate was used as the non-volatile solute. It was prepared from analytical material by two distillations *in vacuo*.

Solutions of different concentrations were prepared by a procedure similar to that of the aqueous solutions.

Lower relative pressures were obtained by connecting to the absorption vessel a bulb with isopropyl alcohol kept at a lower temperature.

Measurements.—The water isotherm was measured at 30.0° and that of isopropyl alcohol at 26.0°. After the electrical system and the thermostat reached equilibrium and the adsorption vessel was evacuated, the condenser was brought into contact with the vapor of the solution contained in bulb B. The oscillator was brought once more to resonance by changing the precision condenser. Final equilibrium of adsorption as shown by the capacity took, at lower vapor pressures a very short time. At relative pressures above 0.99 ten minutes and more were required for the last few percentages of adsorption to take place. The reason seems that the dissipation of the heat of adsorption needs time, and at relative pressures near to unity a very small rise in temperature becomes already significant. After constancy of the capacity had been reached the bulb containing the condenser was evacuated. Desorption was practically instantaneous and a constant capacity reading was reached in a few seconds. The difference between the final reading and that before adsorption was, in general, less than 0.003 $\mu\mu$F., and never more than 0.005 $\mu\mu$F. The change of capacity caused by the adsorption was calculated from the capacity value obtained after desorption.

At each point, two measurements were made that differed among them by at most 3%. In the following graphs (Fig. 1), the averages of the measurements are used.

Results and Discussion

The capacity changes ΔC plotted against p/p_0 are given in Fig. 1. The calculation of the thickness of the layers of adsorbate is based on the following considerations.

The condenser in our system is composed of plane parallel layers of glass, adsorbate and vapor and its capacity is given by the formula for a number of condensers in series

$$\frac{1}{C} = \sum_i \frac{1}{C_i} \tag{1}$$

where C is the capacity of the whole system and C_i the respective capacities of the various layers of dielectrica.

In vacuo there will be

$$\frac{1}{C} = \frac{1}{C_{gl}} + \frac{1}{C_v} \tag{2}$$

where C_{gl} is the fixed capacity of glass (plus cement) and C_v that of the free space *in vacuo*. In equilibrium with vapor, we obtain

$$\frac{1}{C'} = \frac{1}{C_{gl}} + \frac{1}{C_v'} + \frac{1}{C_a} \tag{3}$$

where C_a is the capacity of the adsorbed layers and C_v' that of the vapor filled space.

C_{gl}, C_v, C_v' are of the order of magnitude of 150–200 $\mu\mu$F. whereas C_a in our experiments was 3 × 10^6 $\mu\mu$F. at highest adsorptions and much greater at low adsorptions. In every case, the contribution of C_a to C' was at or below the accuracy of our measurements. Therefore practically

$$\frac{1}{C'} = \frac{1}{C_{gl}} + \frac{1}{C_v'} \tag{3a}$$

---

[10] V. H. Atree, *Electr. Eng.*, June (1952).

[11] H. E. Watson, *Proc. Roy. Soc. (London)*, **A143**, 558 (1934).

[12] J. C. W. Frazer, *et al.*, *J. Am. Chem. Soc.*, **42**, 1793 (1920).

[13] R. Robinson and O. Sinclair, *ibid.*, **56**, 1834 (1934).

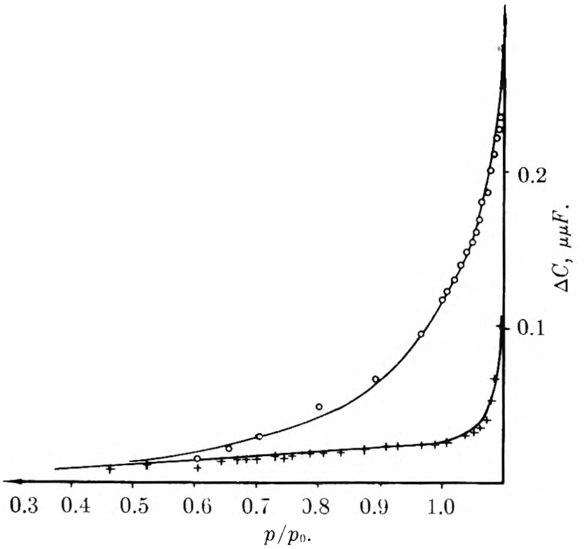

Fig. 1.—ΔC *versus* p/p_0: ○, water; +, isopropyl alcohol.

If A is the area of the condenser, d the distance between the glass plates, r the thickness of the adsorbed layer, and ϵ_v the dielectric constant of the vapor, we obtain

$$C_v = 0.0885 \frac{A}{d} \ \mu\mu\text{F}. \tag{4}$$

$$C_v' = 0.0885 \frac{A}{d - 2r} \ \mu\mu\text{F}. \tag{5}$$

From (2) and (3a) sufficient accuracy

$$\Delta C = C' - C = \frac{C_{gl}^2}{(C_{gl} + C_v)^2} (C_v' - C_v) = f(C_v' - C_v) \tag{6}$$

The factor f is found experimentally from the capacities *in vacuo* and in dry air, as r is negligible in this case, after measuring d directly.

The dielectric constants of air, water and isopropyl alcohol vapor at different pressures were taken from ref. (14) and (15).

The assumptions leading to equation 6 are too simplified as there is evidence to show that the surface active in adsorption is greater than the macroscopic surface of glass except in its virgin state.

It has been found severally[16] that the surface of glass treated under mild conditions, as used by us, is a few times greater than in the virgin state and a roughness factor of 3 to 5 seems indicated as a reasonable number.

A much higher factor than 5 could be possible only if capillaries or capillary cracks enter the picture, but as the following discussion of the isotherms will show, their existence seems excluded as no evidence of capillary condensation was found by us.

In such a case, the roughness should be in the nature of waves or pyramids where the height of the peaks is of the order of magnitude of their distance.

We used a model amenable to at least approximate calculation where for the waves or pyramids we substituted an array of cubes covering half the surface and in which the thickness of the adsorbed layers was much smaller than the dimensions of the cubes.

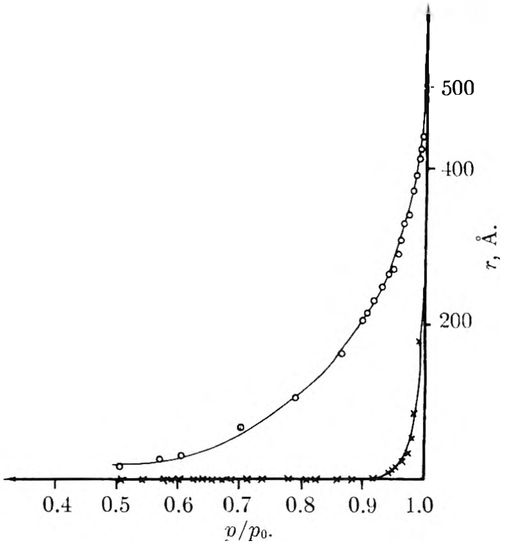

Fig. 2.—Adsorption isotherms: ○, water; +, isopropyl alcohol on glass; r, the thickness of the adsorbed layer in Angströms.

For such a geometry, a roughness factor of 3 is found. The change in capacity is obtained 3–4 times greater than for the same layer thickness on a plane surface.

A certain check on this model was given by the measurements with water vapor. Here, it is accepted that at $p/p_0 = 0.2$ to 0.4 a monolayer is formed. Extrapolation of our results to $p/p_0 = 0.4$ gives, monolayer being assumed, a roughness factor of 5.

Based on these considerations, we introduce this factor 5 into the calculation and the isotherms thus obtained are shown in Fig. 2.

Inspection of the isotherms shows that, at no relative pressure in our experimental range (up to 0.997 and 0.993 for water and isopropyl alcohol, respectively) is there a flattening out of the curves. This excludes the explanation of our isotherms by capillary condensation for the following reason. The shape of the curves requires that, even at the highest pressures, there are unfilled capillaries and these should have, according to Kelvin's law, diameters of 0.8 μ and much more if we take into account Shereshefsky's work[17] in which it was shown that at these relative pressures condensation takes place in capillaries tens of times wider than required by Kelvin's law. These are dimensions easily visible under the microscope, but no indications were found in a careful search.

It should be remarked here that uncertainties of the dielectric constants of the adsorbed layers are irrelevant as long as these are much greater than unity, as only C_a will be influenced, which may be neglected in the calculations (see above).

The isotherms show for both water and isopropyl alcohol, rather high adsorption near saturation pressure and indicate very strongly in their upper range continuous transition to condensation. This agrees with some earlier work[4] but stands in contradiction to the last results of Deryagin,[18]

---

(14) J. D. Stranathan, *J. Chem. Phys.*, **5**, 828 (1937).

(15) J. D. Stranathan, *Phys. Revs.*, **48**, 538 (1935).

(16) S. Brunauer, "The Adsorption of Gases and Vapors," Princeton Univ. Press, Princeton, N. J., 1945, p. 322, 343.

(17) J. L. Shereshefsky, *J. Am. Chem. Soc.*, **72**, 3682 (1950).

(18) B. V. Deryagin and M. Zorin, *Dokl. Ak. Nauk.*, **98**, 93, 96 (1954).

who found such curves only for non-polar liquids (CCl_4 and benzene), whereas the isotherms of water and polar organic liquids intersected the ordinate $p = p_0$ at a finite layer thickness.

Our isotherms both of water and of isopropyl alcohol fit, in the limits of experimental error, an equation 7 derived by Bradley[19] on the basis of the polarization theory of adsorption

$$\log \frac{p_0}{p} = K_1K_2^r + K_4 \tag{7}$$

or

$$\log \left[\log \left(\frac{p_0}{p}\right) - K_4\right] = r \log K_3 + \log K_1 \tag{8}$$

where r is the thickness of the layer in Å., adsorbed at p, and K_1, K_3, K_4, are constants. $K_1 = 0.275$; $K_3 = 0.991$; $K_4 = -0.004$ for water, and $K_1 = 0.026$; $K_3 = 0.966$; $K_4 = 0.004$ for isopropyl alcohol give straight plots for the left-hand expression of (8) against r as shown in Fig. 3.

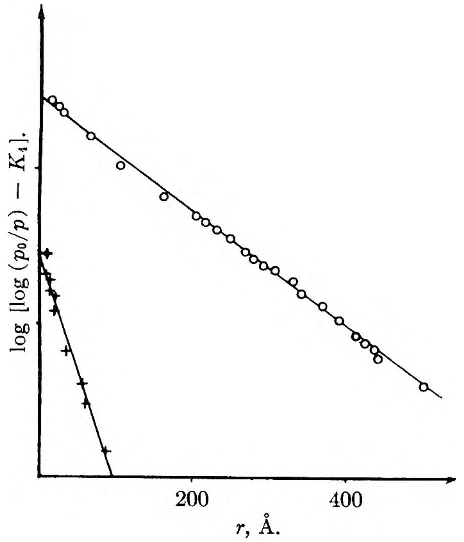

Fig. 3.—Adsorption plotted according to formula (8): O, water; +, isopropyl alcohol.

The constants have been chosen empirically to give optimum fit to a straight plot. No attempt has been made to deduce the constants from properties of the adsorbent surface and the adsorbate.

The thermodynamic meaning of (7) is that $\mu_a - \mu_L$, the chemical potential of the adsorbate minus the molar free energy of liquid in bulk, as given by

$$\mu_a - \mu_L = RT \ln p/p_0$$

decreases near exponentially with layer thickness. In our isotherms the term K_4 influences the function only very near to saturation. Such relationships have been found already in many cases. It is to be understood that (7) cannot be exactly correct as it gives in the limiting case $p = p_0$ the inequality $\log 1 = 0 \neq K_4$.

Bradley derives (7) from a molecular model based on electrostatic forces between an ionic adsorbent and polar adsorbate molecules. Brunauer, Emmett and Teller[20] criticize the polarization theory and show that, at least for non-polar adsorbates, this model gives far too small adsorptions. On the other side, they do not exclude the possibility that the interaction of permanent dipoles may give the energies required. Doubts have been expressed about the possibility of adsorption in so many molecular layers as found once more here, but the following considerations should be taken into account.

$\mu_a - \mu_L$ measures the free energy additional in the adsorption layer to that of the liquid in bulk, and Table I shows that with p/p_0 nearing unity, this additional amount allowing adsorption to take place is rather small indeed as compared, *e.g.*, to the energies indicated by heats of evaporation or heats of adsorption. Hennicker[21] collected the experimental evidence on the existence of long-range forces in liquids and our data in their order of magnitude are well in keeping with this evidence. As to the exact nature of these forces and their correlation to the structures of the adsorbent and the adsorbate, it seems to us that more experimental facts are needed. But even now one may say that $\mu_a - \mu_L$ decreases in many cases exponentially with layer thickness and that an explanation of this regularity seems easier on the basis of polarization effects than only with dispersion energies, which should decrease with the third power of the layer thickness.

TABLE I

p/p_0	$-(\mu_a - \mu_L)$, cal./mole	p/p_0	$-(\mu_a - \mu_L)$, cal./mole
0.998	1.2	0.95	30.9
.995	3.0	.93	43.7
.990	6.0	.90	63.3
.98	12.1	.85	97.7
.97	18.4		

We are pleased to acknowledge Mr. D. Fiat's work, who participated in the measurements on isopropyl alcohol.

---

(19) R. S. Bradley, *J. Chem. Soc.*, 1799 (1936).

(20) S. Brunauer, P. H. Emmett and E. Teller, *J. Am. Chem. Soc.*, **60**, 309 (1938).

(21) J. L. Hennicker, *Rev. Mod. Phys.*, **21**, 322 (1949).

PEROXYSULFURIC ACID AND PEROXYFORMIC ACID. EQUILIBRIUM AND FORMATION RATE

By J. M. Monger and Otto Redlich

Shell Development Company, Emeryville, California

Received December 2, 1955

The rates of formation of monoperoxysulfuric acid from hydrogen peroxide and sulfuric acid as well as the corresponding equilibria have been determined. Similar measurements have been carried out on peroxyformic acid. If the sulfuric acid concentration is increased from 5 to 12 *M*, the initial rate of reaction with hydrogen peroxide increases by a factor 120,000. It is concluded that hydrogen peroxide reacts only with the undissociated sulfuric acid, not with its ions. Equilibrium concentrations, half-conversion times and initial formation rates are given for various conditions.

Hydrogen peroxide reactions are often highly susceptible to catalysis. Oxidation with a peroxyacid as an intermediate is a quite well known type of application of hydrogen peroxide.

Numerous organic acids have been successfully used as peroxide catalysts.[1] It seems to be strange that sulfuric acid, as a rule, is not a suitable catalyst, in view of the fact that monoperoxysulfuric acid (persulfuric acid) is known to be quite reactive and also under certain conditions readily formed from sulfuric acid and hydrogen peroxide. A study of the equilibrium and formation of peroxysulfuric acid appeared therefore to be desirable. A parallel investigation of peroxyformic acid (performic acid) illuminated the behavior of peroxysulfuric acid by contrast.

Experimental Details

The reaction solutions were prepared by mixing aqueous solutions of acid and hydrogen peroxide of suitable concentrations so that the heat evolved was reduced to a minimum. The reaction was stopped by fifty-fold or higher dilution. Peroxyformic acid samples were at the same time quenched to ice temperature.

The samples were analyzed for hydrogen peroxide and peroxyacid according to one of the procedures suggested by Rius and Zulueta,[2] namely, titration of hydrogen peroxide by 0.1 *N* $KMnO_4$, addition of a drop of 10% KI solution, and titration of peracid with 0.05 *N* Na_2SO_3 to the starch-iodine end-point. In view of the small peroxyacid concentrations this procedure was more accurate than the titration of two separate samples, generally preferred by Rius and Zulueta.

In the analysis of peroxyformic acid mixtures the first titration was carried out at ice temperature. A second end point was determined after twice the titration time and the small difference was assumed to be equal to the loss of peroxyacid during the permanganate titration. The solution was then heated shortly to speed the hydrolysis of the peroxyacid, the liberated hydrogen peroxide was titrated with permanganate and any small remainder of peroxyacid was found by means of sulfite.

Peroxysulfuric Acid.—The initial concentrations of the reactants and the final concentration of peroxysulfuric acid in moles/liter are given in Table I. For the kinetic calculations the small losses of total peroxide found were corrected for by a proportionate increase in the concentrations of hydrogen peroxide and peroxysulfuric acid. The concentrations c_1 of H_2SO_4 and c_4 of H_2O were calculated from the analytical results for the concentrations c_2 of H_2O_2 and c_3 of H_2SO_5 and the initial concentrations.

One would expect that the quotient of the equilibrium concentrations (Table I)

$$K' = c_3c_4/c_1c_2 \qquad (1)$$

furnishes only a very crude estimate of the equilibrium constant *K*. This estimate can be slightly improved by introducing an approximate value for the ratio γ_4/γ_2 of the activity coefficients of H_2O and H_2O_2. We assume that this ratio is independent of the presence of H_2SO_4 and H_2SO_5 and depends only on the ratio of the concentrations c_4/c_2. Then we can estimate γ_4/γ_2 from the data for the binary system.[3] In the "adjusted equilibrium quotient" (Table I, Fig. 1)

$$L = K'\gamma_4/\gamma_2 \qquad (2)$$

the variation with c_2, clearly noticeable in K', is practically eliminated. The dependence of *L* on the total acid concentration indicates that H_2SO_5 is an appreciably weaker acid than H_2SO_4. Extrapolation furnishes the estimates $K = 0.1$ (25°) and $K = 0.2$ (75°) for the equilibrium constant.

It is obvious to try a representation of the rate measurements by means of a bimolecular rate constant k_1. Eliminating the constant of the back reaction

$$k_2 = k_1/K' \qquad (3)$$

by means of smoothed values of K', we obtain indeed satisfactory agreement for each individual run. But the values of the rate "constant" k_1 (Table I, Fig. 2) at 25° increase from 0.18×10^{-6} to 8700×10^{-6} l./mole minute when the acid concentration increases from 5.0 to 12.0 moles/l. The initial rate (at a constant hydrogen peroxide concentration of 1 mole/l.) increases therefore by a factor of 120,000 in the same range of acid concentration.

As far as we know, no similar concentration dependence of a reaction rate has been reported before. Yet the explanation is quite simple. The only quantity in sulfuric acid solutions which changes about as rapidly as the observed rate is the concentration of the undissociated acid.

In the concentration range of our measurements, unfortunately, there is not enough undissociated acid present to be detected by the determination of Raman intensities.[4] But the activity of the acid may be taken as a very crude measure of the concentration of the undissociated acid. The ratio of the activities of solutions containing 12 and 5 moles/l. can be estimated[5] to be about 240,000. For theoretical reasons and from results for nitric and perchloric acid[6] we should expect that the activity coefficient of the undissociated acid increases considerably with increasing concentration. For this reason, the concentration ratio of the undissociated acid should be considerably lower than 240,000. The observed ratio 120,000 of the reaction rates, therefore, may be interpreted as the concentration ratio.

The very high value of the temperature coefficient of the reaction rate obviously reflects the increase of the concentration of the undissociated acid.

At constant acid concentration, the bimolecular apparent rate constant k_1 is proportional to the initial hydrogen peroxide concentration. (Figure 2: The position of the broken line has been estimated from the total of the observed points.) We have not tried to represent the observations by a trimolecular rate law, though this probably would be possible.

Several ions (nickel, cadmium, fluoride, mercuric, tungstate) double the rate, if present at concentrations of 0.003 to 0.01 moles/l. without causing noticeable decomposition of hydrogen peroxide (measurements with 5 *M* H_2SO_4,

---

[1] *Cf.* D. Swern, *Chem. Revs.*, **45**, 1 (1949).

[2] A. Rius and C. Zulueta, *Anal. real. soc. espan. fis. y quim.*, **443**, 923 (1948).

[3] G. Scatchard, G. M. Kavanagh and L. B. Ticknor, *J. Am. Chem. Soc.*, **74**, 3715 (1952).

[4] L. F. Maranville, Thesis University of Chicago, 1949. Personal communication by Professor T. F. Young.

[5] Landolt-Börnstein, Tables, 3rd Suppl., p. 2145 (1936).

[6] G. C. Hood, O. Redlich and C. A. Reilly, *J. Chem. Phys.*, **22**, 2067 (1954).

Table I

Peroxysulfuric Acid

H_2SO_4	Initial concn., moles/l. H_2O_2	H_2O	Final concn. H_2SO_5, moles/l. Analysis	Cor.[a]	γ_4/γ_2[b]	K'	L	10^6k_1[c]
				At 25°				
5.00	1.012	40.0		0.01[d]	2.80	0.09	0.27	0.18
5.00	5.03	34.8		.09[d]	2.37	.13	.31	
5.00	5.03	34.8		.08[d]	2.37	.12	.28	0.34
5.00	9.90	28.2		.30[d]	1.88	.19	.36	1.8
8.00	1.98	27.8	0.138	.138	2.63	.27	.71	21
9.28	0.705	28.1			2.80			94
9.65	0.986	30.0	0.140	0.146	2.79	0.554	1.54	97
10.12	5.16	20.8	1.59	1.67	2.33	1.20	2.80	1220
12.0	1.00	19.8	0.518	0.566	2.82	2.32	6.54	8700
15.0	1.00	11.2	av.[e]	.72	2.83	3.4	9.6	
15.0	1.00	11.2	av.[e]	.71	2.83	3.3	9.4	
				At 75°				
4.85	0.911	39.0	0.016	0.019	2.81	0.17	0.49	97
4.85	4.82	33.7	.131	.133	2.38	.20	.48	430
4.85	9.59	27.4	.391	.395	1.89	.27	.51	1400
9.75	4.52	20.0	1.23	1.24	2.33	.93	2.71	

[a] Corrected for decomposition by assuming loss of H_2O_2 and H_2SO_5 proportional to their concentrations. [b] Calculated solely on basis of H_2O_2 and H_2O by assuming acid to have no effect. [c] Based on correlated values of K' and corrected H_2SO_5 values. [d] Values obtained after several days or weeks, extrapolated to infinite time. [e] The values of H_2SO_4, K', etc., are the averages of several samples. Small uncertainties exist due to diperoxysulfuric acid formation.

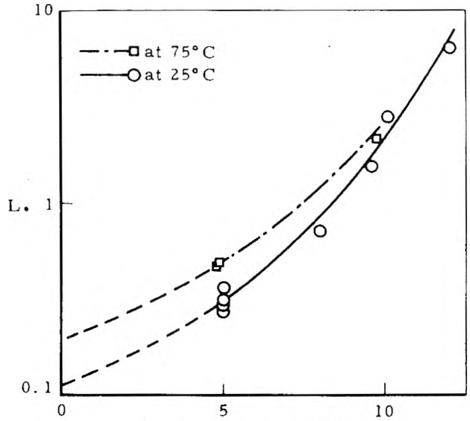

Fig. 1.—Adjusted equilibrium quotient of peroxysulfuric acid.

1 M H_2O_2 at 75°). At higher concentrations these ions catalyze the decomposition to a considerable extent.

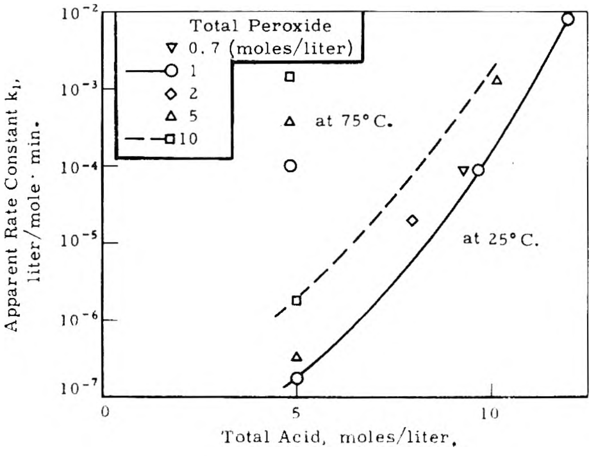

Fig. 2.—Rate of formation of peroxysulfuric acid.

Increase of the sulfate concentration of 5 M H_2SO_4 by saturation with ammonium, zinc and magnesium sulfates increases the formation rate of peroxysulfuric acid, as expected, but also causes fairly rapid decomposition.

Peroxyformic Acid.—The observations on the formation of peroxyformic acid are given in Table II in a similar manner as before. The concentration quotient K' (Fig. 3) and the specific reaction rate k_1 (Fig. 4) vary moderately with the concentrations of the reactants and the temperature. The agreement of the present results with previous work[7] is reasonably good in view of the different conditions.

Table II

Peroxyformic Acid

Initial concn., moles/l. HCOOH	H_2O_2	H_2O	Final concn. HCOOOH, moles/l. Analysis	Cor.[a]	K'	10^3k_1
			At 25° without H_2SO_4			
1.16	0.30	52.1	0.0036	0.0036	0.56	...
5.03	1.00	43.7	.060	.061	.57	0.23
10.0	1.00	33.3	.188	.188	.79	0.48
			At 25° with 0.1 M H_2SO_4			
1.00	1.02	51.8	0.010[b]	0.010	0.52	0.24
1.00	5.02	46.4	.69	.70	.71	.66
5.00	1.00	43.5	.068[b]	.068	.65	.46
5.00	4.92	38.3	3.52	3.86	.71	.80
10.0	1.02	33.0	0.201	0.207	.87	.77
19.5	5.12	6.6	3.65	3.80	1.9	7.6
			At 25° with 0.5 M H_2SO_4			
4.86	0.986	42.2	0.080	0.080	0.78	1.75
10.0	1.00	31.8	.232	.235	1.00	2.8
			At 75° without H_2SO_4			
5.00	1.00	43.8	0.050[b]	0.050	0.47	5.4
			At 75° with 0.1 M H_2SO_4			
5.00	1.00	43.8	0.064[b]	0.064	0.60	12.3

[a] Corrected for decomposition by assuming losses of H_2O_2 and HCOOOH are proportional to their concentrations. [b] Extrapolated.

---

(7) (a) J. d'Ans and W. Frey, *Z. anorg. Chem.*, **84**, 160 (1913); (b) W. H. Hatcher and G. W. Holden, *Trans. Roy. Soc. Canada*, **21**, 237 (1927).

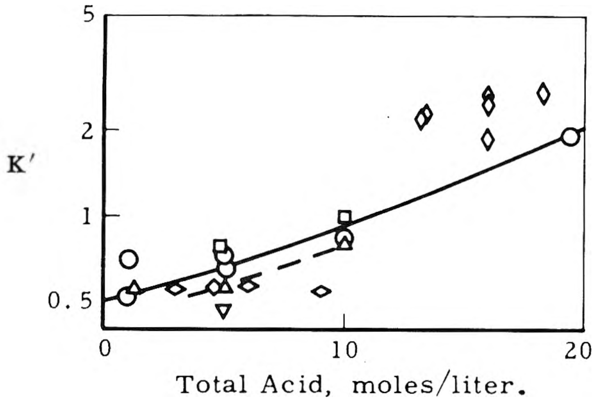

Fig. 3.—Equilibrium quotient of peroxyformic acid:
△, 0 H_2SO_4
○, 0.1 M H_2SO_4 at 25°
□, 0.5 M H_2SO_4
▽, 0 H_2SO_4
✧, 0.1 M H_2SO_4 at 75°
◇, D'Ans and Frey at 15°, 16–20 M H_2O_2
◇, Hatcher and Holden at 0°, 3–6 M H_2O_2.

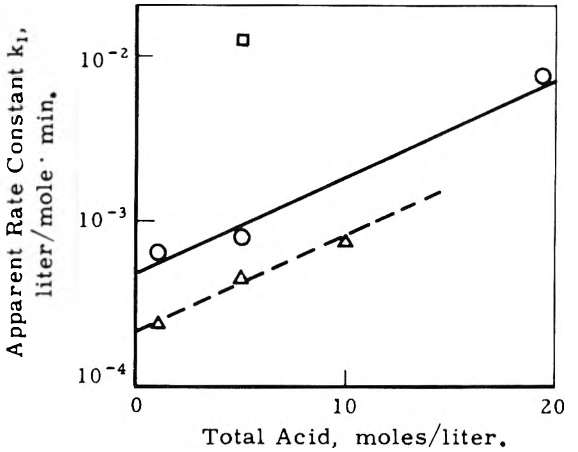

Fig. 4.—Rate of formation of peroxyformic acid:
- -△, 1 M H_2O_2 at 25°
—○, 5 M H_2O_2 at 25°
□, 1 M H_2O_2 at 75°
(with 0.1 M H_2SO_4).

The equilibrium constant, K = 0.5 at 25°, decreases slightly with increasing temperature (*cf.* Fig. 3).

The apparent bimolecular rate constant k_1 varies less with the hydrogen peroxide concentration than the rate constant for peroxysulfuric acid.

The catalytic effect of sulfuric acid (Fig. 5) and of a few other acids and salts has been previously reported by d'Ans and Frey.[7a] No new catalyst has been found.

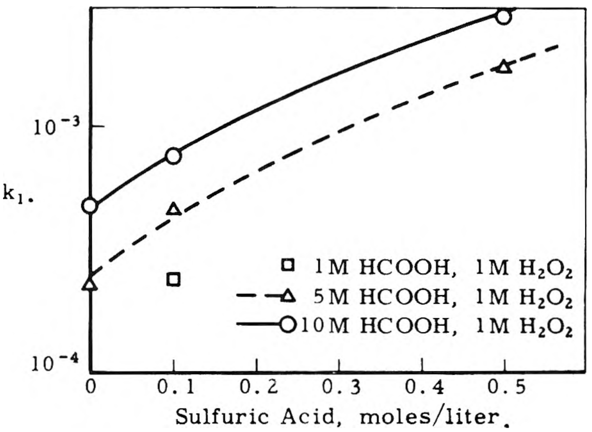

Fig. 5.—Effect of sulfuric acid on the rate of formation of peroxyformic acid.

Discussion

The formation of peroxyformic acid shows no surprising features. This result supports the conclusion that the seemingly anomalous behavior of sulfuric acid is due to its dissociation.

A reaction mechanism should explain the fact that the ions of sulfuric acid do not react with hydrogen peroxide. It should explain the higher than first order in hydrogen peroxide. Finally it should explain the influence of catalysts, especially the differences in the catalytic effect on the formation of the two peroxyacids. On the basis of the present results, we are not able to propose a satisfactory mechanism.

The usefulness of a peroxyacid as an intermediate under given conditions may be characterized by its equilibrium concentration and by the time required for reaching one half of this concentration or by the initial formation rate. Results calculated for a few sets of conditions are given in Table III. It is seen that the characteristic quantities for performic acid do not depend very much on the concentrations of the reactants. For a reasonably rapid formation of peroxysulfuric acid, high acid concentration is indispensable.

TABLE III

CALCULATED EQUILIBRIUM CONCENTRATIONS AND HALF-CONVERSION TIMES

			H_2SO_4			$HCOOH$[a]		
Temp., °C.	Initial acid, mole/l.	Initial H_2O_2, mole/l.	Equilibrium H_2SO_5, mole/l.	Time for 50% conversion	Initial formation rate, mole/l. min.	Equilibrium HCOOOH, mole/l.	Time for 50% conversion	Initial formation rate, mole/l. min.
25	12	1	0.597	3.2 min.	0.10			
25	10	1	.167	125 min.	0.001	0.207	19 min.	0.0077
25	5	1	.015	8.0 days	0.9×10^{-6}	.068	22 min.	.0023
25	5	5	.097	3.3 days	8.5×10^{-6}	.386	14 min.	.020
25	5	10	.415	1.4 days	0.09×10^{-3}			
25	1	1				.010	30 min.	.00024
25	1	5				.070	15 min.	.0033
75	5	1	.019	29 min.	0.5×10^{-3}	.064	45 sec.	.062
75	5	5	.135	10.4 min.	0.011			
75	5	10	.394	3.9 min.	0.072			

[a] Containing 0.1 M H_2SO_4 as catalyst.

NOTES

THERMAL EXPANSION OF CRYSTALLINE KHF_2[1]

By Richard W. Fink[2] and Edgar F. Westrum, Jr.[3]

Received October 3, 1955

In an approach to the study of the behavior of the $(F-H-F)^-$ ion in the soft, translucent, paraffin-like, high-temperature (β) phase of KHF_2, the volume increment on transition from the low-temperature (α) phase was determined. The existence of the beta-phase, stable from 196° to the melting point (239°C.) was first reported by Cady.[4] Westrum and Pitzer[5] demonstrated that the entropy increment of the $\alpha \rightarrow \beta$ transformation is nearly twice that involved in fusion, and that because the bonding is so largely ionic in the $(F-H-F)^-$ ion, the proton moves in a potential well having a single minimum in contrast to more typical hydrogen bonds with double minimum potential energy functions.

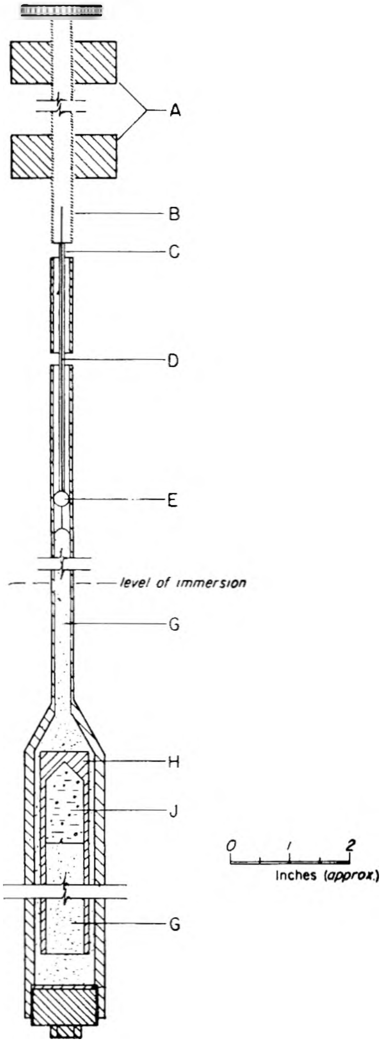

Fig. 1.—Diagram of the molybdenum float dilatometer described in the text.

The dilatometer is shown in cross-section in Figure 1. The sample (J) of KHF_2 is trapped within the float (H) machined from solid molybdenum stock. The body is machined from solid monel metal rod and provided with a monel tube of 0.636 cm. uniform bore which is silver-alloy brazed to the body (F) in such a manner that mercury (G) used as the dilatometric fluid does not contact the brazing alloy. The body is sealed with a molybdenum gasket seated by a threaded plug. The meniscus can be located to within about 0.006 cm. by closing an electrical circuit when incipi-

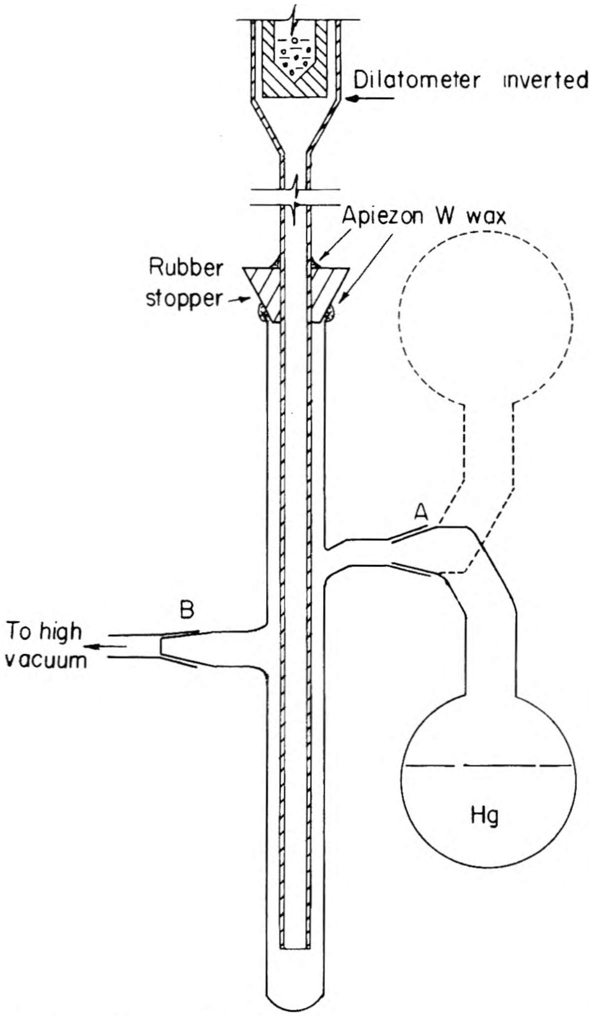

Fig. 2.—Technique of filling with mercury; prior to evacuation, the float was loaded with the KHF_2 sample.

---

[1] Experimental work performed at the University of California Radiation Laboratory under auspices of the U. S. Atomic Energy Commission. Preliminary measurements were made at the University of Michigan.

[2] Department of Chemistry, University of Arkansas, Fayetteville.

[3] Department of Chemistry, University of Michigan, Ann Arbor.

[4] G. H. Cady, *J. Am. Chem. Soc.*, **56**, 1431 (1934).

[5] E. F. Westrum, Jr., and K. S. Pitzer, *ibid.*, **71**, 1940 (1949); *J. Chem. Phys.*, **15**, 526 (1947).

ent contact with the mercury is made by the pointed tungsten rod (D). This rod, which is centered by the glass bead (E), is surrounded by an electrically-insulating sheath of polystyrene (C) and is activated by the shaft (B) which is threaded with a 0.006-cm. pitch and which engages two tapped brass blocks (A) mounted rigidly with respect to the body. Preliminary studies revealed that nickel, monel, and stainless steels react with β-KHF_2 with evolution of gas. No reaction with molybdenum was observed at temperatures as high as 260° over periods of several weeks.

The glass apparatus depicted in Fig. 2 illustrates the method of filling the dilatometer with mercury. After evacuation of the inverted dilatometer for several days at $<10^{-5}$ mm., the flask of mercury was rotated about point A. The pressure in the system was then gradually increased, forcing mercury into the instrument; after rotation about point B, the dilatometer could be removed in a normal, vertical position.

For measurements, a thermostated, stirred oil bath was used with an iron-constantan thermocouple placed close to the dilatometer body. The thermocouple was calibrated at the ice point, and the known transition and fusion temperatures of KHF_2. Determinations were made on approximately 17-gram samples of stoichiometric, spectroscopically-pure, anhydrous KHF_2. Correction for the thermal expansion of the apparatus under operating conditions was obtained from blank runs with only the empty float and mercury present. This correction amounts to about 50% of the observed value over the range of the α-phase and 25% of the observed value over the range of stability of the β-phase. Representative (corrected) data obtained in equilibrium observations both on increasing and decreasing temperatures are presented in Figure 3 for a KHF_2 sample which initially was finely divided. Identical results were obtained from a cast sample obtained upon pouring fused KHF_2 into the molybdenum float. The duration of a typical series of determinations was about 80 hours. No significant change in weight of the molybdenum float was detected. Calculations based on the Clapeyron equation indicate that the 0.5 atmosphere excess pressure of the mercury column does not cause appreciable shift in the transition temperature.

The mean molal values of the thermal expansion coefficients and of the volume increment on transition are:

$$\text{For } \alpha\text{-}KHF_2\text{:}\quad \left(\frac{\partial V}{\partial T}\right)_p^{\circ} = 0.0047 \pm 0.0005 \text{ cm}^3\text{-deg}^{-1}\text{-mole}^{-1} \quad 20° < T < 135°$$

$$\text{For } \beta\text{-}KHF_2\text{:}\quad \left(\frac{\partial V}{\partial T}\right)_p^{\circ} = 0.015 \pm 0.004 \text{ cm}^3\text{-deg}^{-1}\text{-mole}^{-1} \quad 196° < T < 239°$$

$$\Delta V°_{\alpha \rightarrow \beta} = 4.2 \pm 0.1 \text{ cm}^3\text{-mole}^{-1},\ 196°$$

Taking the density[6] of α-KHF_2 at 20° as 2.35 g.-cm.$^{-3}$, the data in Figure 3 yield a density of 2.25 g.-cm.$^{-3}$ for α-KHF_2 at the transition temperature and 2.02 ± 0.04 g.-cm.$^{-3}$ for the β-phase at this temperature. These values are in good accord with the recent data of Kruh, Fuwa and McEver[7] who find a value of 2.02 g.-cm.$^{-3}$ from X-ray diffraction measurements.

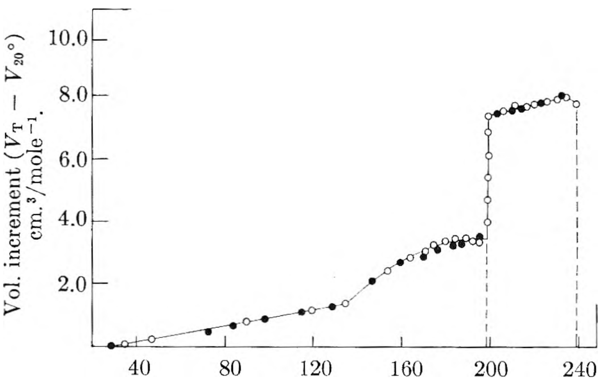

Fig. 3.—The curve shows representative (corrected) data for runs on a powdered 17.8-g. sample. Open circles are heating points; solid circles, cooling points. Runs on a cast 17.0 g. sample showed identical behavior. The pre-transition increase in volume is apparently real. Runs in which the sample was melted seemed to indicate a small volume contraction on fusion, but this effect was not conclusive from these experiments.

The pre-transition increase in the volume of α-KHF_2 observed between 135° and the transition temperature apparently is real and not the result of mechanical effects such as variations in interfacial tension, etc. Corresponding behaviour of the inter-planar distances have been observed by Kruh, Fuwa and McEver. Moreover, supercooling of the β-phase could be made to persist as low as 135° in this experiment. The large entropy and volume increments on transition suggest that the $(F-H-F)^-$ ion may exhibit a considerable measure of orientational freedom in the β-phase.

---

(6) L. Helmholz and M. T. Rogers, *J. Am. Chem. Soc.*, **61**, 2590 (1939).

(7) R. Kruh, K. Fuwa and T. E. McEver, THIS JOURNAL, **60**, Sept. (1956).

THE VOLUME OF MIXING OF BINARY MIXTURES. IV. BENZENE-2,2,4-TRIMETHYLPENTANE (ISOÖCTANE)[1]

BY SCOTT E. WOOD AND OSCAR SANDUS

Contribution from Department of Chemistry, Illinois Institute of Technology, Chicago, Illinois

Received October 22, 1955

The change of the entropy on mixing non-polar substances at either constant pressure or constant volume has been related qualitatively to orientation of the molecules in the pure liquids as well as in the solution.[2] Some progress might be made on this problem by studying a series of binary solutions having a common component, which would not have any orientation of the molecules in the liquid phase. Consequently, a program of research has been started to determine the thermodynamic properties of binary mixtures using isoöctane as the

---

(1) Taken in part from a thesis by Oscar Sandus, presented to the Graduate School, Illinois Institute of Technology, in partial fulfillment of the requirements for the degree of Doctor of Philosophy. The partial support of this research at different times by both the Atomic Energy Commission and the National Science Foundation is gratefully acknowledged.

(2) S. E. Wood, *J. Chem. Phys.*, **15**, 358 (1947); H. Goller and E. Wicke, *Angew. Chem.*, **B19**, 117 (1947); A. Münster, *Trans. Faraday Soc.*, **46**, 165 (1950); A. Münster, *Z. physik. Chem.*, **196**, 106 (1950); H. Tompa, *J. Chem. Phys.*, **21**, 250 (1953).

common component. The choice of isoöctane is a compromise between molecules whose potential field about the center of the molecule is spherically symmetrical and whose vapor pressures are of the proper magnitude for making measurements from approximately room temperature to about 100°. This paper reports the change of the volume on mixing at constant pressure for the benzene–isoöctane system over the entire range of composition and from 20 to 75°. The apparatus and procedure for the experimental measurements are identical to those described in the previous papers of this series.[3] The vapor pressures of this same system are being determined at the present time.

Materials.—The isoöctane was Phillips Petroleum Company pure grade, 99 mole % minimum. It was further purified by fractional distillation in a column similar to one previously described.[3a] The density of the purified product at 25° was 0.68774 g. cm.$^{-3}$ in comparison to 0.68775, determined by Kretschmer, Nowakowska and Wiebe[4]; 0.68776 determined by Brooks, Howard and Crafton[5]; and 0.68779 given in the Selected Values of Properties of Hydrocarbons.[6]

The benzene was also Phillips Petroleum Company pure grade, 99 mole % minimum. It was further purified as described previously.[3b] The density of the purified product at 25° was 0.87366 g. cm^{-3} identical to that given in the Selected Values of Properties of Hydrocarbons.

The water was the laboratory distilled water, which is obtained by redistilling condensed steam taken from the steam system of the building. The water was boiled before use to remove air and carbon dioxide.

The mercury used in the mixing bottles was triply distilled mercury. That used in the dilatometer was an especially pure grade purchased from Universal Scientific Industries and was reported to have "an impurity count less than 0.00001."

Density–Composition Curve at 25°.—Since the composition of the solutions used in the dilatometer could not be determined directly, it was necessary to establish the density–composition curve. The temperature used was 25 ± 0.01°. Determinations of the density were made at approximately each eighth mole fraction. Duplicate measurements, in which the order of weighing the components in making up the solutions was reversed, were made at each composition. All weighings were reproducible to ±0.03 mg. The observed weights were corrected to vacuum, for the evaporation loss from the time of weighing to the actual time of mixing, for the displacement of air by both the liquid and vapor phases and for the weight of each component in the vapor phase after mixing assuming equilibrium to be obtained. In making these last corrections, Raoult's law was assumed to be obeyed. In making all buoyancy corrections the true density of air was used as determined by the equation given in the International Critical Tables.[7] The temperature in the balance case was measured to 0.1°, the relative humidity to 1%, and the barometric pressure to 0.05 mm. The air inside the solution bottles and pycnometer was assumed to be dry because of the way in which they were cleaned and dried. The pycnometer was calibrated by the use of water, the density of the water being calculated from Tilton and Taylor's equation.[8] The conversion factor used in order to convert the density to units of g. cm.$^{-3}$ was 0.999973 ml. cm.$^{-3}$. In the actual determination of the density of the liquids it was found necessary to correct for the weight of vapor above the meniscus in the capillary. The atomic weights used are 12.010 for carbon and 1.0080 for hydrogen.

The densities thus observed were used to obtain the quantity, 100 $\Delta V^{\mathrm{M}}/V^0$, where ΔV^{M} equals $V - V^0$ and V is the volume of the solution and V^0 the sum of the volumes of the components. The equation

$$100\Delta V^{\mathrm{M}}/V^0 = Z_1Z_2[1.655 - 0.396(Z_1 - Z_2) + 0.200(Z_1 - Z_2)^2] \quad (1)$$

was obtained from these data. Table I gives, in order, the mole fraction of benzene,[9] the observed densities at 25°, $100\Delta V^{\mathrm{M}}/V^0$ determined from these densities, $100\Delta V^{\mathrm{M}}/V^0$ calculated from equation 1, and the difference between these two last values. The standard deviation in $100\Delta V^{\mathrm{M}}/V^0$ is ±0.002.

TABLE I

DENSITIES OF BENZENE–ISOÖCTANE MIXTURES AT 25°

x_1	d, g. cm.$^{-3}$	$100\ \Delta V^{\mathrm{M}}/V^0$		
		Obsd.	Calcd.	$\Delta(100\ \Delta V^{\mathrm{M}}/V^0)$
0.00000	0.68774	0.000	0.000	0.000
.12735	.70024	.148	.145	+ .003
.12838	.70037	.146	.146	.000
.25015	.71419	.260	.262	− .002
.25086	.71427	.260	.262	− .002
.37432	.73046	.352	.352	.000
.37148	.73005	.352	.350	+ .002
.49980	.74971	.408	.408	.000
.49802	.74941	.407	.407	.000
.62490	.77244	.414	.418	− .004
.62561	.77254	.420	.418	+ .002
.75176	.79998	.373	.370	+ .003
.75244	.80017	.369	.370	− .001
.87761	.83337	.244	.244	.000
.87685	.83316	.244	.245	− .001
1.00000	.87466	.000	.000	.000

The volume fraction, Z, of the solutions used in the dilatometer was determined by means of the equation

$$d = \frac{d_2 + (d_1 - d_2)Z_1}{1 + \Delta V^{\mathrm{M}}/V^0} \quad (2)$$

and equation 1. All densities used in equation 2 are those observed in the dilatometer. The densities of the pure liquids thus measured are greater than those measured in the pycnometer by 0.00005 g. cm.$^{-3}$ for benzene and 0.00011 g. cm.$^{-3}$ for isoöctane. This difference is presumably caused by the presence of air in the pycnometers but not in the dilatometers. These differences do not alter the values of $\Delta V^{\mathrm{M}}/V^0$ within 0.00005 assuming that the effect of air on the observed density is linear in the volume fraction.

---

[3] (a) S. E. Wood and J. P. Brusie, *J. Am. Chem. Soc.*, **65**, 1891 (1943); (b) S. E. Wood and A. E. Austin, *ibid.*, **67**, 480 (1945); (c) S. E. Wood and J. A. Gray III, *ibid.*, **74**, 3729 (1952).

[4] C. B. Kretschmer, J. Nowakowska and R. J. Wiebe, *ibid.*, **70**, 1785 (1948).

[5] D. B. Brooks, F. L. Howard and H. C. Crafton, *J. Research Natl. Bur. Standards*, **24**, 33 (1940).

[6] "Selected Values of Properties of Hydrocarbons," Natl. Bur. Standards Circular [illegible]461, Washington, D. C., 1947.

[7] "International Critical Tables," Vol. 1, McGraw-Hill Book Co., Inc., New York, N. Y., 1928, p. 71.

[8] L. W. Tilton and J. K. Taylor, *J. Research Natl. Bur. Standards*, **18**, 205 (1937).

[9] The mole fractions are accurate to one in the fourth place. The fifth place has been retained for purposes of calculation.

Coefficient of Expansion.—The specific volumes of the pure liquids and solutions were determined at 20° and each ten degree interval from 25 to 75°. These dilatometers were calibrated as formerly with water and mercury. The weight of the dilatometer and the expelled mercury at the end of an experiment agreed within 0.5 mg. with the original weight. This would give a total error of 0.00004 cc. in the change of the specific volume from 20 to 75°. The specific volumes in cm.^{3} g.$^{-1}$ were fitted to a cubic equation in the temperature by the method of least squares. Table II gives the mole fraction of benzene, the coefficients of the type equation

TABLE II

COEFFICIENTS OF THE EQUATION FOR THE SPECIFIC VOLUMES

x_1	a	$b \times 10^3$	$c \times 10^6$	$d \times 10^9$	$\Delta v \times 10^6$
0.00000	1.41195	1.6174	1.940	14.01	1.7
.11985	1.38816	1.5944	1.913	13.53	1.7
.12730	1.38649	1.6008	1.733	14.66	1.0
.25416	1.35841	1.5779	1.534	15.82	0.5
.37516	1.32876	1.5466	1.505	15.32	0.9
.49953	1.29495	1.5026	1.679	12.92	0.9
.62791	1.25561	1.4734	1.346	14.02	0.5
.75363	1.21239	1.4343	1.116	14.22	1.2
.87610	1.16510	1.3793	1.145	12.44	0.7
1.00000	1.11071	1.3145	1.327	9.12	2.1

$$v = a + bt + ct^2 + dt^3 \tag{3}$$

and the standard deviations of the calculated values from the observed values. The densities of the solutions at 25° were calculated from these equations and the compositions in the dilatometer were calculated in turn from equations 1 and 2.

The specific volume of benzene at 25°, as calculated from equation 3, is 1.14454 cm.^{3} g.$^{-1}$. Wood and Brusie[3a] report 1.14443; Wood and Austin,[3b] 1.14442; Burlew,[10] 1.14434; Scatchard, Wood and Mochel,[11] 1.14456; and Timmermans and Martin,[12] 1.14457. The density of isoöctane at 25°, as calculated from equation 3, is 0.68785 g. cm.$^{-3}$, in comparison to 0.68786 reported by Kretschmer, Nowakowska and Wiebe[4] after their value has been corrected for the effect of air as determined in this work.

The values of 100 $\Delta V^M/V^0$ have been calculated from equation 3 at 20° and each ten degree interval from 25 to 75°. The coefficients of the equation

$$100\Delta V^M/V^0 = Z_1Z_2[\alpha + \beta(Z_1 - Z_2) + \gamma(Z_1 - Z_2)^2] \tag{4}$$

were determined by the method of least squares at each temperature and these coefficients finally were fitted to equations in the temperature. These final equations are

$$\alpha = 1.6648 - 1.172 \times 10^{-3}t + 2.817 \times 10^{-5}t^2 \tag{5}$$

$$\beta = -0.3555 - 1.517 \times 10^{-3}t - 6.136 \times 10^{-6}t^2 \tag{6}$$

$$\gamma = 0.2228 - 9.022 \times 10^{-4}t \tag{7}$$

The curves in Fig. 1 represent the values of 100 $\Delta V^M/V^0$ at 25 and 75°. The circles represent the duplicate values obtained from the direct density measurements. Both $100\Delta V^M/V^0$ and ΔV^M increase slightly with the temperature. The former quantity is slightly asymmetric toward the benzene side but, if it is plotted against the volume fraction, it becomes asymmetric toward the isoöctane side. It is estimated that the uncertainty in $100\Delta V^M/V^0$ is less than ±0.005.

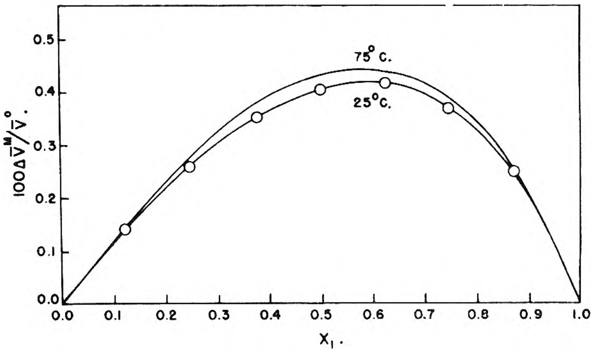

Fig. 1.—Percentage change of the volume of mixing *versus* mole fraction.

As a final check of equations 4, 5, 6 and 7, the densities of the solutions were calculated from these equations and equation 2 and compared to the original measurements. The deviations of these quantities are shown in Fig. 2. The over-all standard deviation is 1.3 × 10^{-5}.

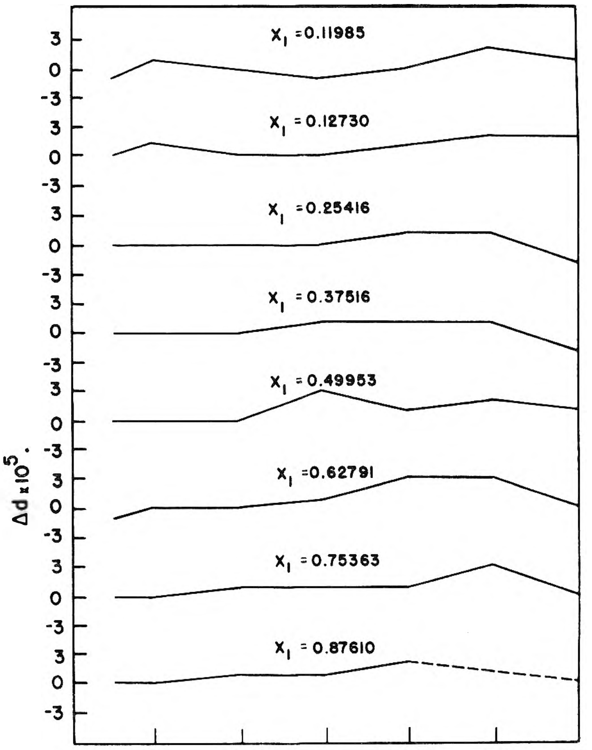

Fig. 2.—Deviations of experimental densities from calculated densities.

---

(10) J. S. Burlew, *J. Am. Chem. Soc.*, **62**, 690 (1940).

(11) G. Scatchard, S. E. Wood and J. M. Mochel, *ibid.*, **68**, 1957 (1946).

(12) J. Timmermans and F. Martin, *J. chim. phys.*, **23**, 750 (1926).

SOME THERMODYNAMIC PROPERTIES OF LIQUID CHLOROETHANE

By James W. Gilbert and Robert T. Lagemann

Contribution from the Department of Physics and Astronomy, Vanderbilt University, Nashville, Tennessee

Received November 18, 1955

Very little information is available on the thermodynamic properties of the rather important compound chloroethane (C_2H_5Cl) in the liquid phase. Certain of these, such as the specific heat at constant volume, are difficult to measure directly, but a determination of the velocity of compressional waves, which is relatively easy to carry out, enables one to calculate various properties if values of the density and specific heat at constant pressure are known. This has been done using reagent grade chloroethane purified in a 30-plate, low temperature column.

Experimental

The velocity of sound measurements were made by the interferometer method using equipment very similar to that described by McMillan and Lagemann.[1] Instead of being made of metal, the reservoir and reflector were fabricated from Fluorothene. The reflector was connected to the micrometer shaft by a ball and socket joint of Fluorothene which permitted easy alignment of the reflector when brought against the bottom of the liquid reservoir. Electrical contact to the top of the quartz crystal was effected by means of a thin, flexible strip of aluminum foil placed between the quartz crystal and the Fluorothene reservoir. An opening in the foil, smaller in size than the crystal, served to retain a drop of mineral oil which acted as a transducer.

Care was taken to maintain constant temperature by placing the interferometer in a thermostated water-bath. Also the frequency of the oscillator (500 kc./sec.) was checked by comparison with station WWV of the National Bureau of Standards. Several runs were made going from a high temperature of 12° to a low temperature of minus 14° (and return), with such good reproducibility that it is believed the samples remained pure while under study. Three different samples were used.

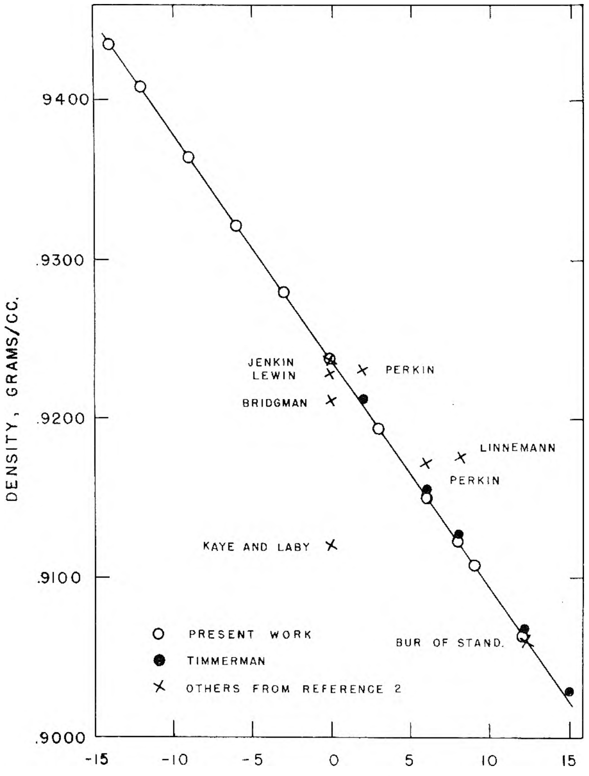

Fig. 1.—Density of liquid chloroethane as a function of temperature.

The density of liquid chloroethane had been measured before,[2] but because of the variation in the results of the various experimenters and because no values were available below 0°, new determinations have been made. Because of the high volatility of chloroethane, the picnometers (5 and 3 ml. capacity) used were equipped with capillary side arms. Even so, to avoid introducing significant errors due to evaporation losses, it was found necessary to make distinct mass measurements at each temperature at which the volume was determined. To prevent unduly large expansion and subsequent loss of liquid, as the picnometer was moved from ambient temperature into the bath, or *vice versa*, the density measurements were made in a cold room maintained at about 2°.

Results

The results of the density and velocity measurements are given in Table I. For comparison purposes Fig. 1 shows the values of density obtained by various workers. It can be seen that the present work is well substantiated.

Table I

Measured Values of the Density and Ultrasonic Velocity of Liquid Chloroethane

Temp., °C.	Density, g./cc.	Ultrasonic velocity, m./sec.	Temp., °C.	Density, g./cc.	Ultrasonic velocity, m./sec.
12	0.9063	1043	0	0.9237	1094
11	.9079[a]	1045	− 3	.9278	1109
10	.9094[a]	1050	− 6	.9321	1125
9	.9107	1054	− 9	.9364	1139
8	.9123	1059[a]	−12	.9407	1153
6	.9150	1068	−14	.9434	1162
3	.9193	1082			

[a] Obtained by interpolation.

The specific heat at constant pressure is known[3] over a range of temperatures, so that, combined with the density and velocity of sound measurements, it is possible to calculate certain other thermodynamic properties. The following well-known relations[4] were used for this purpose

$$\alpha = \frac{1}{V}\left(\frac{\partial V}{\partial T}\right)_p = -\frac{1}{d}\frac{\partial d}{\partial T} \tag{1}$$

$$V = (dB_{ad})^{-1/2} \tag{2}$$

$$B_{is} - B_{ad} = \frac{T\alpha^2}{dc_pJ} \tag{3}$$

$$\gamma = \frac{B_{is}}{B_{ad}} = \frac{C_p}{C_v} \tag{4}$$

In the above V is the ultrasonic velocity; d, the density; B_{ad}, the adiabatic compressibility; B_{is}, the isothermal compressibility; α, the volume coefficient of expansion; J, the mechanical equivalent of heat; γ, the ratio of specific heats; c_p, the specific heat at constant pressure; and c_v, the specific heat at constant volume; all measured at

---

(1) D. R. McMillan and R. T. Lagemann, *J. Acoust. Soc. Am.*, **19**, 956 (1947).

(2) See the summary by M. J. Timmermans and Mme. Hennaut-Roland, *J. chim. phys.*, **34**, 693 (1937); C. F. Jenkin and D. N. Shorthose, *Ice and Refrigeration*, **66**, 347 (1924).

(3) J. Gordon and W. F. Giauque, *J. Am. Chem. Soc.*, **70**, 1506 (1948).

(4) M. W. Zemansky, "Heat and Thermodynamics," 3rd ed., McGraw-Hill Book Co., New York, N. Y., 1951.

TABLE II

SOME THERMODYNAMIC PROPERTIES OF LIQUID CHLOROETHANE

Temp., °C.	Coefficient of expansion (°C.)$^{-1}$ × 10^3	c_p,[a] cal./g. deg.	B_{ad} (cm.^{2} dyne^{-1}) × 10^{12}	B_{is} (cm.^{2} dyne^{-1}) × 10^{12}	Ratio of specific heats	c_v, cal./g. deg.
12	−1.572	0.3805	101.5	148.3	1.461	0.2604
11	1.570	.3800	100.8	147.4	1.462	.2599
10	1.567	.3796	99.7	146.1	1.465	.2590
9	1.565	.3791	98.8	145.1	1.469	.2581
8	1.562	.3787	97.7	143.8	1.472	.2573
6	1.557	.3778	95.8	141.6	1.478	.2556
3	1.550	.3765	92.9	138.2	1.488	.2531
0	1.543	.3752	90.5	135.3	1.495	.2510
− 3	1.536	.3740	87.6	132.0	1.507	.2482
− 6	1.529	.3727	84.8	128.7	1.518	.2456
− 9	1.522	.3714	82.3	125.8	1.528	.2430
−12	1.515	.3702	80.0	123.0	1.538	.2408
−14	1.510	.3693	78.6	121.3	1.543	.2393

[a] Read from a curve constructed from data given by Joseph Gordon and W. F. Giauque, *J. Am. Chem. Soc.*, **70**, 1506 (1948).

the same temperature T. Values of the thermodynamic properties obtained for a range of temperatures by means of the foregoing relations are tabulated in Table II.

As might be expected, values of each of the properties appear to be linear functions of the temperature over the range of temperatures studied. In the case of the ultrasonic velocity a negative slope (or temperature coefficient) of 4.64 m./sec. deg. is obtained, in good agreement with a prediction made on the basis of an empirical formula discussed earlier.[5] The slope of the density-temperature curve is -1.425×10^{-3} g./cm.^{3} deg.

---

[5] R. T. Lagemann, D. R. McMillan, Jr., and W. E. Woolf, *J. Chem. Phys.*, **17**, 369 (1949).

THE REDUCTION OF URANIUM(VI) BY IRON(II) IN PHOSPHORIC ACID SOLUTION

By C. F. Baes, Jr.

Oak Ridge National Laboratory, Oak Ridge, Tennessee

Received November 14, 1955

Uranium(IV) in acidic sulfate solutions is rapidly oxidized to the hexavalent state by iron(III).[1] In the presence of 1–2 M added phosphoric acid, the oxidation, while slower, still proceeds to completion.[2] Some results of Quinn and Watts[3] at the Armour Fertilizer Works revealed, however, that uranium(VI) is slowly reduced by iron(II) in 6 M phosphoric acid at room temperature. More recently Canning and Dixon[4] have reported the quantitative reduction of uranium(VI) by iron(II) in hot 6 M phosphoric acid.

The following brief investigation of this oxidation–reduction system confirms the high dependence of the oxidation–reduction equilibrium on phosphoric acid concentration.

Experimental

Uranium(VI) sulfate and reagent grades of iron(II) sulfate, iron(III) sulfate, sulfuric acid and phosphoric acid were used to prepare the solutions used. Volumetric dichromate methods of analysis were used to standardize phosphoric acid stock solutions of uranium(VI),[2] iron(II) (stored under nitrogen) and iron(III).[5]

The extent of uranium(VI) reduction in phosphoric acid solutions containing iron(II) and iron(III) was determined by measuring the optical density at 630 and 670 mμ, using a Beckman model D.U. spectrophotometer. The molar extinction coefficients for uranium(IV) at these wave lengths were found to be 31.6 and 38.2, respectively, and were essentially constant over the phosphoric acid concentration range used (1.8–4.8 M). A small correction for the absorption of iron(III) was necessary, the molar extinction coefficient being 0.16 and 0.20 at 630 and 670 mμ, respectively.

Due to the slowness of the reduction at room temperature, several days were required to reach equilibrium in some cases. The total reducing power of typical solutions was determined by dichromate titration, the results indicating that air oxidation of these solutions (stored in 100-ml. volumetric flasks) was negligible. Since the solutions were stored at room temperature, the results correspond only approximately to 25°. The e.m.f. of the cell

$$\text{Pt}|\text{FeSO}_4\ (0.05\ M),\ \text{Fe}_2(\text{SO}_4)_3\ (0.025\ M),\ \text{H}_2\text{SO}_4\ (0.36\ M),\ \text{H}_3\text{PO}_4\ (C)|\text{S.C.E.}$$

under argon was measured with an L. & N. type K-2 potentiometer and a reflecting galvanometer at 24.7 ± 0.1°. In all cases constant readings were reached within 12 minutes. The precision of successive measurements on the same solution was usually 0.1 mv.

Results

Oxidation–Reduction Measurements.—The extent of uranium(VI) reduction by iron(II) was determined in two series of solutions, all of which were 0.36 M in sulfuric acid and initially *ca.* 0.01 M in uranium(VI). In the first series the phosphoric acid concentration was held constant at 3.68 M and the [Fe(II)]/[Fe(III)] ratio was varied at 0.05 M total iron. The results were consistent with the reaction

$$2\text{Fe(II)} + \text{U(VI)} = 2\text{Fe(III)} + \text{U(IV)}$$

$$K = \frac{[\text{Fe(III)}]^2\ [\text{U(IV)}]}{[\text{Fe(II)}]^2\ [\text{U(VI)}]} \quad (1)$$

the equilibrium quotient K being 13 ± 2 at *ca.* 25°, for equilibrium [Fe(II)]/[Fe(III)] ratios in the range 0.14–1.7.

In the second series of solutions the initial iron(II) and iron(III) concentrations were each 0.05 M

---

[1] I. M. Kolthoff and J. J. Lingane, *J. Am. Chem. Soc.*, **55**, 1871 (1933).

[2] J. M. Schreyer and C. F. Baes, Jr., *Anal. Chem.*, **25**, 644 (1953).

[3] Private communication from P. J. Quinn, 1952.

[4] R. G. Canning and P. Dixon, *Anal. Chem.*, **27**, 877 (1955).

[5] I. M. Kolthoff and E. B. Sandell, "Textbook of Quantitative Inorganic Analysis," Rev. Ed., The Macmillan Co., New York, N. Y., 1948, p. 609.

and the phosphoric acid concentration was varied. The results gave

$[H_3PO_4]$, M	1.85	2.59	3.33	3.68	4.81
K		0.047	0.54	4.8	13	173

at *ca.* 25°, K varying with approximately the eighth power of the phosphoric acid concentration.

Preliminary kinetic studies were carried out in which either the rate of appearance of uranium(IV) was followed spectrophotometrically or the rate of change of the [Fe(II)]/[Fe(III)] ratio was followed potentiometrically during the course of uranium(VI) reduction by iron(II) in 3.7 M phosphoric acid at 25 ± 2°. The half-time of reaction was found to be 160–170 min. One potentiometric rate measurement at 48° gave a half-time of approximately 14 minutes.

The introduction of fluorides into these solutions was found to increase both the extent and the rate of uranium(VI) reduction by iron(II). For a series of equilibrations in 3.7 M phosphoric acid, 0.36 M sulfuric acid, at 25° the results gave the following very approximate K values.[6]

$[F^-]$, M	0.08	0.16	0.24	0.4	0.8
K	100	300	1000	20,000	300,000

In these measurements, equilibrium was reached in a few minutes.

Fe(II)/(III) and U(IV)/(VI) Formal Electrode Potentials.—Measured values of the iron (II)/(III) formal electrode potential, $E'_{Fe(II)/(III)}$, in 0–7.4 M phosphoric acid are listed in Table I. Values of $E'_{U(IV)/(VI)}$ calculated from the equation

$$E'_{U(IV)/(VI)} = E'_{Fe(II)/(III)} - \frac{0.0591}{2}\log K \qquad (2)$$

are plotted *vs.* phosphoric acid concentration in Fig. 1. In using this equation, it was assumed that the presence of uranium(IV) and uranium(VI) in the oxidation–reduction equilibrium solutions did not appreciably alter the $E'_{Fe(II)/(III)}$ values, through change in ionic strength, the formation of uranium–iron complex species, or through the small change in the amount of uncomplexed phosphoric acid.

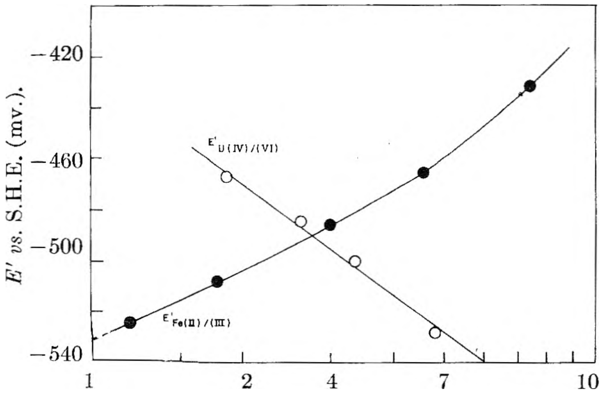

Fig. 1.—The uranium(IV)/(VI) formal electrode potential in phosphoric acid 0.36 M sulfuric acid solutions. The $E'_{U(IV)/(VI)}$ curve is drawn with a slope of $-(5/2) \times 59.1$ mv. The average slope of the $E'_{Fe(II)/(III)}$ curve over the same phosphoric acid concentration range is 1.6×59.1 mv.

TABLE I

FE(II)/(III) FORMAL ELECTRODE POTENTIALS IN PHOSPHORIC ACID SOLUTIONS AT 24.7°

0.05 M Fe(II), 0.05 M Fe(III), 0.36 M H_2SO_4

$[H_3PO_4]$, M	$E'_{Fe(II)/(III)}$ *vs.* S.H.E., v.	$[H_3PO_4]$, M	$E'_{Fe(II)/(III)}$ *vs.* S.H.E., v.
0	−0.6746	0.398	−0.5691
0.00994	.6697	.497	.5606
.01988	.6641	.795	.5413
.0398	.6539	1.182	.5248
.0596	.6440	1.774	.5082
.0994	.6285	2.956	.4869
.1988	.5985	4.55	.4665
.2982	.5811	7.40	.4322

The directions of the phosphoric acid concentration dependences of $E'_{Fe(II)/(III)}$ and $E'_{U(IV)/(VI)}$ are consistent with the more extensive complexing by phosphoric acid expected for the U^{+4} and Fe^{+3} ions as compared with UO_2^{++} and Fe^{++}.

---

[6] The screw cap polyethylene bottles used in these measurements contained enough air to result in appreciable oxidation (which apparently is catalyzed by fluoride).

EFFECT OF IODINE VAPOR ON SILVER IODIDE

BY JAMES E. MANSON

Geophysics Research Directorate. Air Force Cambridge Research Center, Air Research and Development Command, L. G. Hanscom Field, Bedford, Massachusetts

Received November 17, 1955

In a recent paper[1] it was suggested that iodine vapor might cause a preference of AgI for the hexagonal (H) modification. Prior to this Sieg[2] had reported this effect, but had not given data sufficient to enable repetition of his experiment. Therefore, several tests were run which substantiate the effect of I_2 vapor on the equilibrium phase of AgI and indicate that the equilibrium regions reported by Block and Moller[3] may be in error.

AgI was prepared by the method of Kolkmeijer and van Hengel[4] to be primarily the face centered cubic (C) modification. After grinding, this was analyzed to be approximately 12% (H) and 88% (C). The method of analysis has been described previously.[5]

One gram of this powder was placed in one arm of an inverted U-tube. The other arm contained a sample of I_2 crystals (C.P., resublimed) in an evacuated break-tip bulb. The U-tube was evacuated and the AgI out-gassed at 100° for one hour. The tube was sealed off at a pressure of 0.1 μ. The I_2 bulb tip was then broken and the tube thermostatted at 120° for 20 hours. During this time I_2 vapor diffused through the system, turning the AgI a dark brown. The I_2 was then recaptured by immersing the I_2 bulb in cold water inside the oven for nine minutes and in liquid N_2 for two minutes. The tube was then punctured, and the AgI analyzed by X-ray diffractometry. The first analysis started 30

---

(1) J. E. Manson, *J. Appl. Phys.*, **26**, 423 (1955).

(2) L. Sieg, *Naturwiss.*, **40**, 439 (1953).

(3) R. Block and H. Moller, *Z. physik. Chem.*, **152**, 245 (1930).

(4) N. H. Kolkmeijer and J. W. A. van Hengel, *Z. Krist.*, **88**, 317 (1934).

(5) J. E. Manson, *J. Appl. Phys.*, **26**, 1254 (1955).

minutes after puncture and lasted 25 minutes. A series of analyses was performed, as shown in Table I. A control sample was also run, differing only in that no I_2 crystals were used and a plain tube was substituted for the break-tip arm, the AgI being in equilibrium with its own vapor.

TABLE I

COMPOSITION FOR VARIOUS POST-EXPOSURE TIMES

Sample	Time, hr.	$(P_{10.3}/P_{11.0})$	Hex., % A	Hex., % B
(Before exposure)		0.06	12	
With I_2	1.0	1.14	?	
	1.5	1.04	?	
	2.0	0.93	96	70[a]
	75	0.71	83	
	147	0.70	82	
	9000	0.47	64	70
Without I_2	1.0	0.51	69	
	122	0.50	67	
	9190	0.31	48	50

[a] Poor over-all agreement; see Table II.

In Table I the figures under "% Hex." column A were calculated from the theoretical intensities of the 10·3 (H) line and the 11·0–220 (H + C) line, all based on the Zincite and Zincblende type structures of AgI. Under "% Hex." column B are the figures from a comparison of the observed and calculated intensities of a number of lines, as shown in Table II.

TABLE II

COMPARISON OF OBSERVED AND CALCULATED DIFFRACTION INTENSITIES[a]

Plane indices hex.	Plane indices cubic	With I_2 P_{obsd} (2 hr.)	With I_2 C^5_{70}	With I_2 P_{obsd} (9000 hr.)	Without I_2 C^5_{50}	Without I_2 P_{obsd} (9190 hr.)
10.0		67	64	72	34	36
00.2	111	100	100	100	100	100
10.1		48	44	43	24	23
10.2		19	22	26	12	7
11.0	220	67	90	76	79	71
10.3		62	46	36	25	22
20.0		14	7	11	4	4
11.2	311	38	50	45	44	44
20.1			6	12	3	4
20.2			4	6		
	400		6	4		
20.3			13	17	7	3
	331		8	4	9	5

[a] C_p^B refers to the calculated relative intensities for p% hexagonal AgI and $(1 - p)$% cubic AgI, with $B \times 10^{-16}$ cm.^{2} Debye–Waller temperature coefficient. P_{obsd} are normalized rate meter recording integrated areas under peaks.

Another set of samples was run keeping the AgI at 100° and the I_2 or blank bulb at 22°. In this case the 10·3 to 11·0–220 ratio was unaffected by the treatment, leading one to conclude that the structure was unchanged in both the sample and control. The AgI remained a bright yellow throughout these runs.

The data presented above were obtained during what were to be preliminary runs in a more thorough investigation of the factors influencing the structure of AgI aerosol particles. No satisfactory explanation of these effects has been developed. A lack of any line broadening discourages use of models containing random faulting,[6-8] and random interstitial addition of I atoms cannot cause the observed $(P_{10.3}/P_{11.0-220})$ behavior. However, several conclusions seem reasonable. The transformation from face centered cubic AgI to hexagonal AgI in equilibrium with its own vapor takes place rapidly at 120°, in conflict with the previously reported[3] very slow transition at 135°. After storage at laboratory temperature in a screw capped bottle for one year, this transformation was partially reversed. Addition of saturated I_2 vapor to the system at 120° caused severe disturbances in the crystal, with an increase in the proportion transformed to hexagonal.

---

(6) O. S. Edwards and H. Lipson, *Proc. Roy. Soc. (London)*, **A180**, 268 (1942).

(7) A. J. C. Wilson, *ibid.*, **A180**, 277 (1942).

(8) M. S. Paterson, *J. Appl. Phys.*, **23**, 805 (1952).

THE VAPOR PHASE INFRARED SPECTRA OF THE OZONIDES OF ETHYLENE, PROPYLENE AND ISOBUTYLENE[1]

By DAVID GARVIN AND CLARENCE SCHUBERT, S. J.

Frick Chemical Laboratory, Princeton University, Princeton, New Jersey

Received November 25, 1955

Current interest in the identification of products from ozone–hydrocarbon reactions[2] prompts this publication of the infrared absorption spectra of the ozonides of ethylene, propylene and isobutylene.

The ozonizations were carried out in inert solvents at −78°.[3] This method was adopted because higher ozonide yields generally are found at lower temperatures. For example, ozonization of isobutylene at 0° yielded appreciable quantities of high boiling material, acetone peroxide. Methyl chloride was used as solvent for ethylene and propylene, isobutane was used as solvent for isobutylene. After ozonization of the olefins, the crude products were freed from solvent and high boiling impurities by low temperature distillation *in vacuo*. Isobutylene ozonide was freed of water-soluble contaminants before distillation by washing with an equal volume of saturated sodium chloride solution. Prepared in this way the ozonides of ethylene, propylene and isobutylene are colorless liquids which explode violently when a drop is heated either unconfined or in a test-tube.

Ozonide samples which showed reproducible physical properties were used for spectral determinations. Successive portions withdrawn for analysis showed the same relative intensities of

---

(1) Supported jointly by Contract NOrd 7920 (USN Bureau of Ordnance, coördinated by APL Johns Hopkins University), Contract N6-ori-105 (ONR coördinated by Project Squid, Princeton University), and Contract AF 33(616)2411 (Power Plant Laboratory, WADC). Reproduction, translation, publication and use in whole or in part by the United States Government is permitted.

(2) See for example W. Schmitt, E. Moriconi and W. O'Connor, *J. Am. Chem. Soc.*, **77**, 5640 (1955); also P. Hanst, E. Stephens and Wm. Scott, Paper presented during the 20th Midyear Meeting of the American Petroleum Institute's Division of Refining, St. Louis, Mo., May 10, 1955.

(3) C. Harries and R. Koetschau, *Ber.*, **42**, [illegible]305 (1909); **41**, 3098 (1908).

infrared absorption bands, an indication of the homogeneity of the material. Physical constants are given in Table I.

Table I

	Mol. wt.	Vap. *P*, mm.	n_D
Ethylene ozonide	..	33 at 0°	1.386 at 20.0°
This work		77 at 16°	
Harries[2]	84.84[a]	16 at 18°	1.4099 at 17.5°
Propylene ozonide		11 at −12°	1.386 at 20.1°
This work	85.5[b]	80 at 22.5°	
Isobutylene ozonide			
This work	90.0[b]	25 at 18.4°	1.388 at 18.0°
Criegee[4]	..	143 at 43–43.5°	1.3872 at 20°

[a] F. p. depression in glacial acetic acid. [b] From vapor volume at room temperature.

The refractive index for isobutylene ozonide agrees with Criegee's determination. No comparisons are available for propylene ozonide. Our values for ethylene ozonide show a lower refractive index and a higher vapor pressure than obtained by Harries. His values, including a high molecular weight, 84.84, deviate from ours in the direction expected for material containing an appreciable amount of high boiling ozonization residue still present in his sample.

Vapor phase infrared spectra were taken at or below the vapor pressure of the ozonides with no added inert gas (10 cm. path) with a Perkin–Elmer Model 21 recording spectrophotometer. The spectra are shown in the figure. It will be noticed that any absorption in the 5.7 μ region is weak in comparison with the absorption at other wave lengths. Moreover, the absorptions which do appear in this region could be intensified by decomposing the ozonide vapors *in situ*, either thermally or by treatment with ozone. Also, the ozonization of isobutylene at 0° resulted in a product which manifested a relatively strong absorption at 5.75.

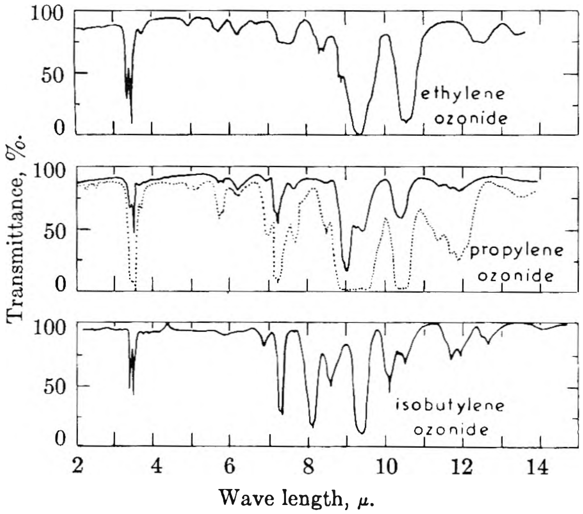

Fig. 1.

Briner[5] has assigned the prominent 5.62–5.95 μ absorptions that appear in the products of ozonization to the ozonide structure. Witkop[6] and Bellamy[7] have questioned this assignment. Goodwin, Johnson and Witkop[8] validly maintain that the 5.60 μ absorption of the crystalline ozonide of diphenyl fumarate is the ester carbonyl stretching frequency. However, it might be argued on the basis of Briner's work, that the ozonide structure also absorbs at this wave length. The three ozonide spectra presented here, which have no prominent carbonyl region absorption,[9] offer unambiguous support for Witkop's conclusion.

It is clear that the identification of ozonides should be based upon the characteristic bands in other spectral regions, such as 9–9.5, 10.5 and 12 μ.

---

[4] R. Criegee, G. Blust and H. Zink, *J. Chem. Phys.*, **87**, 766 (1954).

[5] E. Briner, B. Susz and E. Dallwigk, *Helv. Chim. Acta*, **35**, 341 (1952); E. Dallwigk, H. Paillard and E. Briner, *ibid.*, **35**, 1377 (1952); **36**, 1757 (1953); E. Dallwigk and E. Briner, *ibid.*, **36**, 1166 (1953); E. Dallwigk, *Arch. Sci.* (*Geneva*), **6**, 421 (1953).

[6] B. Witkop, J. Patrick and H. Kissman, *Ber.*, **85**, 961 (1952).

[7] L. Bellamy, "The Infrared Spectra of Complex Molecules," Methuen, London, 1954, p. 107.

[8] S. Goodwin, N. Johnson and B. Witkop, *J. Am. Chem. Soc.*, **75**, 4273 (1953).

[9] Note Added in Proof.—R. Criegee, A. Kerckow and H. Zinke, *Ber.*, **88**, 1878 (1955), report the absence of such absorptions by other ozonides.

MONTMORILLONITE COMPLEXES WITH SATURATED RING COMPOUNDS

By R. Greene-Kelly

Rothamsted Experimental Station, Harpenden, Herts, England

Received November 29, 1955

The sorption of aromatic compounds by montmorillonite has been shown[1] to produce complexes of two main types: the first giving a 001 spacing of 12.5 kX. which is generally independent of the type of ring system and the nature and position of substituents and the second which gives a 001 spacing which in contrast is markedly dependent on the shape, size and charge distribution of the molecule and which has a minimum value of about 15 kX. It was concluded that the first type of complex was one where the aromatic molecules were intercalated with their rings parallel to the planes of the silicate sheets and the second type where the molecules have reoriented so that their rings are now approximately perpendicular to the sheets. An analogous phenomenon has now been found with saturated ring compounds.

Experimental

The methods of preparation and examination by X-ray diffraction were identical to those described in an earlier paper.[1]

Results and Discussion

Tables I gives the 001 spacings of a selection of complexes of simple saturated ring compounds and sodium montmorillonite. They fall into two groups those of spacing 13.3–13.6 kX. (type A) and those of 14.6–14.8 kX. (type B).

Steric considerations suggest that a type A complex is one where the saturated and no longer planar molecule is oriented with its mean plane parallel to the silicate sheets. Figure 1 (a) shows the result of a one dimensional Fourier synthesis along the normal to the silicate sheets using the structure factors given in Table II. The method of carrying this out has been discussed elsewhere.[1] The electron density sketch appears to favor the above configura-

---

[1] R. Greene-Kelly, *Trans. Faraday Soc.*, **51**, 412 (1955).

TABLE I

MEAN 001 SPACINGS (CALCULATED FROM THE SPACINGS OF THE HIGHER ORDERS) OF A SELECTION OF COMPLEXES OF MONTMORILLONITE

Complexing substance	Obsd. d_{001} (±0.1 kX.)
Type A	
Tetrahydropyrrole	13.3
Piperidine hydrochloride	13.3
α-Methylpiperidine hydrochloride	13.5
α-Methylcyclohexanone	13.6
Type B	
Tetrahydrofuran	14.6
Piperidine	14.7
Cyclohexanol	14.6
Cyclohexanone	14.8

tion with an approximately coplanar arrangement of the ring atoms.[2]

TABLE II

OBSERVED STRUCTURE FACTORS OF THE 00l REFLECTIONS OF THE TETRAHYDROPYRROLE AND PIPERIDINE COMPLEXES THE SIGNS BEING ALLOCATED FROM CALCULATIONS ON TRIAL STRUCTURES

	Tetrahydropyrrole	Piperidine		Tetrahydropyrrole	Piperidine
001	24	27	007	$\overline{22}$	$\overline{13}$
002	6	0	008	8	$\overline{10}$
003	21	20	009	11	0
004	37	15	00, 10	17	8
005	12	24	00, 11	9	10
006	$\overline{14}$	0	00, 12	..	6

Type B complexes have similar 001 spacings to the corresponding aromatic complexes and this is consistent with a reoriented molecule with its plane perpendicular to that of the sheet. Figure 1 (b) shows an electron density sketch of the piperidine complex and whilst the details are not resolved it seems to confirm that the intercalated molecule is oriented with its plane perpendicular to the silicate sheets. The spacings of type B complexes are nearly constant and this clearly indicates that the oxygen atoms in the cyclohexanol and cyclohexanone complexes do not determine the separation of the silicate sheets. As with similar aromatic complexes it therefore seems unlikely that hydrogen bonding of the organic hydroxyl group takes place to the silicate oxygens. Attempts to produce type B complexes of more complex molecules (*e.g.*, α-methylpiperidine) were not successful as with aromatic molecules (*e.g.*, α-picoline) and in all cases type A complexes resulted.[1]

It is interesting to note that the calculated[4] 001 spacings of type A complexes of 14.4 kX. and type B of 16.0 kX. are over 1 Å. greater than the observed values. This effect has also been observed with aromatic complexes and is suggestive that the projected van der Waals contact distances[5] assumed between the silicate sheet oxygens and the organic molecules are too large.

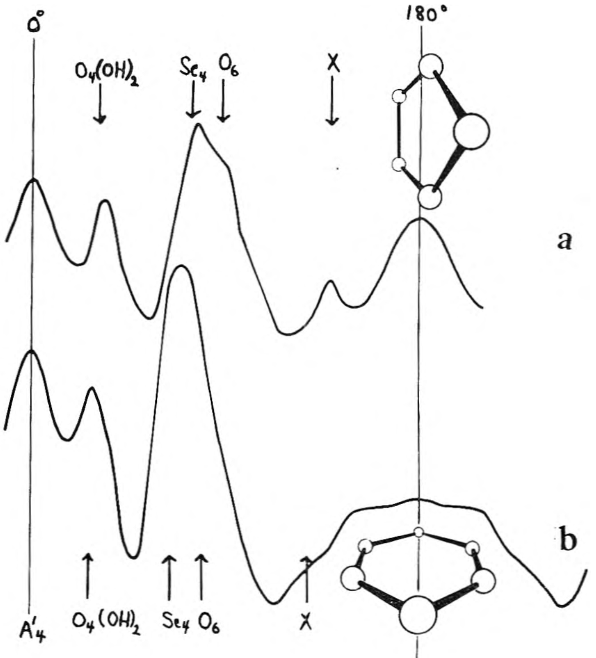

Fig. 1.—The result of a one-dimensional Fourier synthesis of: (a) tetrahydropyrrole complex d_{001} = 13.3 kX.; (b) piperidine complex d_{001} = 14.7 kX. Note the spurious peaks at X due to the short sequences used in the synthesis. The deduced orientation of the intercalated molecule is shown.

---

[2] The limited number of observed 00l reflections clearly do not permit any conclusions concerning ring puckering as suggested by Pitzer.[3]

[3] K. S. Pitzer, *Science*, **101**, 672 (1945).

[4] Assuming a random arrangement of molecules between the silicate sheets in orientations analogous to those of aromatic complexes.[1]

[5] L. Pauling, "Nature of the Chemical Bond," Cornell Univ. Press, Ithaca, N. Y., 1944.

A NOTE ON VISCOSITY OF MIXTURES. II. LIQUID-LIQUID TERNARY MIXTURES

BY R. P. SHUKLA AND R. P. BHATNAGAR

Department of Chemistry, Holkar College, Indore, India

Received December 5, 1955

The viscosity equation

$$(\eta_m)^{1/8} = \frac{d(x_1R_1 + x_2R_2 + \cdots\cdots + x_nR_n)}{M_n}$$

recently suggested[1] has been tested for ternary liquid–liquid mixtures.

Experimental.—All the liquids taken were of Analar quality of the British Drug House; however, they were distilled again and the fractions distilling at the correct boiling point were collected in glass-stoppered Pyrex flasks. Ethers and alcohols were kept over dry pure NaOH to keep them moisture free; the hydrocarbons were dried by keeping them over sodium wire.

The viscosity was determined by an Ostwald viscometer and was multiplied by the viscosity of water to get absolute viscosity. Table I gives the viscosity as calculated and determined. (η_{cal} is the calculated viscosity and η_{obs} is the viscosity observed, while x, d and M_m have usual meaning.)

Conclusion.—It will be seen from the table that the maximum error possible is of only 4% and hence it may be concluded that the viscosity of ternary mixtures can also be calculated from the equation suggested by us. Hence as there are no limitations for the number of components we can conclude that viscosity of any liquid mixtures can be cal-

---

[1] R. P. Shukla and R. P. Bhatnagar, THIS JOURNAL, **59**, 988 (1955).

TABLE I

System	Temp., °C.	x_1	x_2	x_3	"d"	M_m	$\eta \times 10^3$ cal.	$\eta \times 10^3$ obs.
(1) C_7H_8–CH_3OH–C_6H_6	35.0	0.1467	0.1506	0.7025	0.8618	73.10	5.187	5.10
(2) C_7H_8–C_2H_5OH–C_6H_6	35.0	.0905	.2524	.6572	.8549	71.20	5.556	5.60
(3) C_7H_8–C_6H_6–CCl_4	55.0	.7929	.1385	.0688	.8946	94.34	5.171	5.171
(4) CH_3OH–C_2H_5OH–C_7H_8	35.0	.1840	.1933	.6227	.8507	63.55	5.385	5.60
(5) CH_3OH–C_2H_5OH–CH_3COCH_3	45.0	.5048	.2541	.2413	.7874	41.83	4.948	4.82
(6) CH_3COCH_3–C_2H_5OH–CH_3OH	35.0	.0771	.0834	.8395	.7916	35.16	5.346	5.25
(7) CCl_4–C_6H_6–C_7H_8	35.0	.0688	.1385	.9046	.9046	94.34	5.515	5.64

(The Rheochor of substances taken in calculations were: toluene, 133.0; methyl alcohol, 49.9; benzene, 109.8; ethyl alcohol, 75.59; carbon tetrachloride, 122.0; acetone, 85.0.)

culated if the densities and viscosities of the component are known.

GASEOUS METAL NITRIDES. II. THE VAPOR PRESSURE OF GaN(S) AND EVIDENCE FOR A COMPLEX GASEOUS NITRIDE

By RODNEY J. SIME AND JOHN L. MARGRAVE

Department of Chemistry, University of Wisconsin, Madison, Wisconsin

Received December 1, 1955

In a previous paper[1] the importance of gaseous diatomic nitrides was discussed, and dissociation energies for diatomic metal nitrides were calculated. Recently, the chemistry and thermodynamic properties of the nitrides of the elements also have been reviewed.[2] In the description of methods for preparation of GaN(s) in the literature there are comments about the "volatility" of GaN in the NH_3 flow gas used during formation.[3] This behavior appears to be unusual since most solid nitrides presumably decompose to the elements on heating. A careful study of this vaporization phenomenon has been made.

GaN(s) is most conveniently prepared by passing $NH_3(g)$ over Ga(l) in a porcelain boat at 1000°. In many runs essentially quantitative conversion was obtained if one took into account the extensive transfer from the porcelain boat and the yellow-grey deposits of solid GaN (from X-ray patterns) found downstream from the boat. No GaN(s) is formed when $N_2(g)$ is passed over Ga(l) at 1000°. At 1000° the vapor pressure of liquid Ga is about 3×10^{-6} atm. and transfer of Ga by a non-reactive flow gas is slight.

To establish whether or not a gaseous nitride of Ga exists, the vaporization of Ga(l) in a helium and in a nitrogen flow system, and the vaporization of GaN(s) in a helium and in a nitrogen flow system were observed. It was found that Ga(l) is vaporized to an unexpected extent in a $N_2(g)$ flow and that GaN(s) vaporizes in either a N_2 or He flow at about the same rate without appreciable suppression by the N_2. Weight loss data for GaN vaporization are presented in Table I. The weight losses are reproducible and depend primarily on time and temperature with a small dependence on flow rate. Flow rates of oxygen-free, dry gases (passed over $Mg(ClO_4)_2$ and hot Cu or Ta) were varied and the weight losses extrapolated to zero flow rates for the calculation of vapor pressures listed in Table II where GaN(g) is assumed to be the vaporizing molecule.

TABLE I

VAPORIZATION OF GaN(s)

Temp., ° K.	Flow gas	Flow rate, ml./min.	Vol. of flow gas, l. at S.T.P.	Wt. loss, g.
1170	N_2	17	24.5	0.0008
1170	N_2	58	62.0	.0005
1353	N_2	50	21.3	.0178
1353	N_2	75	50.2	.0309
1353	He	200	136.0	.0423
1420	N_2	22	6.6	.0247
1430	N_2	36	14.0	.0562

TABLE II

VAPOR PRESSURE OVER GaN(s) ASSUMING GaN(g) AS THE VAPORIZING SPECIES

Temp., °K.	Pressure (extrapolated to zero flow rate), atm.
1170	4.8×10^{-5}
1353	5.4×10^{-4}
1425	1.7×10^{-3}

One may show from thermodynamic arguments, however, that GaN(g) is probably not the principal gaseous species. From available data,[1,2] one may estimate free energy functions and a heat of formation for GaN(g); the free energy function for GaN(s) is very likely close to that of ZnO(s), a compound of similar formula and of approximately the same formula weight. At 1500°K., for the reaction GaN(s) = GaN(g)

$$\Delta\left(\frac{F - H_0^\circ}{T}\right) = -58.8 - (-19.8) = -39.0 \text{ e.u., and}$$

$$\Delta H \approx 130 \text{ kcal./mole}$$

Thus, $P_{GaN} \approx 4 \times 10^{-11}$ atm. which is far lower than the observed pressure. Even a sizable decrease in the heat of vaporization would not make GaN(g) a very important molecule.

A possible explanation of the observed vaporization involves the formation of a polymer $(GaN)_x$. This behavior would be analogous to that found in studies of various gaseous halides where dimeric and even trimeric molecules were shown to be important vapor species.[4] The vapor pressures given in Table II need only be divided by x to give $P_{(GaN)_x}$. A log P vs. $1/T$ plot of these data gives a heat of vaporization of 62 ± 5 kcal./mole.

Attempts to obtain an absorption spectrum for

---

[1] J. L. Margrave and P. Sthapitanonda, THIS JOURNAL, **59**, 1231 (1955).

[2] R. J. Sime, B.S. Thesis, University of Wisconsin, 1955.

[3] W. C. Johnson, J. B. Parsons and M. C. Crew, THIS JOURNAL, **36**, 2651 (1932).

[4] (a) L. Brewer and N. Lofgren, *J. Am. Chem. Soc.*, **72**, 3038 (1950); (b) L. Friedman, *J. Chem. Phys.*, **23**, 477 (1955).

this gaseous nitride molecule at 600–900° were unsuccessful. No absorption was detected from 3000 to 7000 Å.

DENSITY, VAPOR PRESSURE AND HEAT OF VAPORIZATION OF 2,2,3-TRICHLOROHEPTAFLUOROBUTANE[1]

BY R. H. CAPPS AND W. MORRISON JACKSON

Electro Metallurgical Company, Niagara Falls, New York
Union Carbide Nuclear Company, Oak Ridge, Tennessee

Received December 5, 1955

The molar polarization, dipole moment and non-ideality coefficients of 2,2,3-trichloroheptafluorobutane have been determined by Magnuson.[2] Since other physical data were unavailable, work was undertaken to determine vapor pressure and liquid density data for this material. From these data and the non-ideality coefficients, the heat of vaporization at any temperature for which the data are valid can be calculated using the exact form of the Clapeyron–Clausius equation.

The 2,2,3-trichloroheptafluorobutane was obtained from the Hooker Electrochemical Company and was further purified by fractional distillation before use.

Density

Apparatus.—The orthobaric liquid density was determined as a function of the temperature by use of a glass dilatometer. A precision bored glass capillary of 1.4986 ± 0.0051 mm. i.d. connected the glass bulb to a small expansion bulb. Closure was made with a small metal valve instead of the standard glass stopcock so that the dilatometer could be used above atmospheric pressure and at temperatures above 60°. The apparatus weighed 72 g. and was 9.5 in. long.

Procedure.—The volume of the dilatometer was determined by distilling air-free water into the tared, evacuated instrument until the liquid level at 0° reached a uniform portion of the lower capillary. A line was established at this liquid level, and the gross weight taken at room temperature. Buoyancy corrections were made for the tare and gross weights in obtaining the weight of water. From the weight of water (20.4164 g.) and its known density of 0.999841 g. per cc. at 0°, the volume of the dilatometer to the established line was found to be 20.4196 ml. After the water was removed, the dilatometer was filled with air at atmospheric pressure and weighed. From the weight of air required to fill the instrument and the known density of air, the total volume was estimated to be 24.80 ml. The total volume above the calibration line on the capillary was 4.38 ml. This value was used in calculating the correction for the weight of the vapor over the liquid in density determinations.

After completion of the calibration, the water was removed and 2,2,3-trichloroheptafluorobutane admitted by distillation under vacuum. The same procedure was employed for obtaining densities as was used with water. When water or mineral oil-baths were used, the dilatometer was immersed in the fluid to a point above the valve seat, the open end of the valve being closed by a compression fitting with a Fluorothene seal. Since the coefficient of liquid expansion for chlorofluorocarbons is large, removal of some of the material by pumping between runs was necessary. The dilatometer was thoroughly degreased with acetone and dried before being reweighed.

Temperature control was maintained by suspending the dilatometer vertically in a thermostated water- or mineral oil-bath. The difference between the height of the liquid level in the capillary and the established calibration line was measured by use of a cathetometer readable to 0.002 mm. The volume of the liquid above the control line was estimated from the height of the liquid column and the bore of the capillary. The total volume of the liquid uncorrected for the expansion of glass is the sum of the calibrated volume and the volume in the capillary calculated as above.

Results.—The accuracy of the volume calibration was checked by determining the density of water at 24.4 and 39.0°. The data showed a small error in the fourth decimal place indicating that the desired accuracy to three decimal places could be attained.

TABLE I

ORTHOBARIC DENSITY OF 2,2,3-TRICHLOROHEPTAFLUOROBUTANE

Temp., °C.	Density expt., g./ml.	Density calcd. from eq. 1, g./ml.	Dev. of exptl. values from eq. 1
0	1.790	1.790	0.000
24.9	1.738	1.738	.000
61.2	1.655	1.656	− .001
70.5	1.634	1.634	.000
89.8	1.588	1.588	.000
98.3	1.568	1.567	+ .001
117.5	1.518	1.518	.000

The density values for 2,2,3-trichloroheptafluorobutane over the temperature range from 0 to 117.5° are presented in Table I. The data were fitted with the parabolic least squares equation

$$\rho = 1.7904 - 2.064 \times 10^{-3}t - 2.14 \times 10^{-6}t^2 \quad (1)$$

where ρ is the density in g. per ml., and t is the temperature in °C. Uncertainty of the equation, based on confidence limits at the 0.95 level, is ±0.07%. All experimental values were corrected for the cubical expansion of Pyrex glass with increased temperature by the equation

$$V = V_0(1 + 0.099 \times 10^{-4}t) \quad (2)$$

where V_0 is the volume at 0°, V is the volume at temperature t, and t is in °C.

The coefficient of liquid expansion, α, may be calculated in the temperature range 0 to 117.5° by the equation

$$\alpha = -\frac{1}{\rho}\frac{d\rho}{dt} \quad (3)$$

$$\alpha = \frac{2.064 \times 10^{-3} + 4.28 \times 10^{-6}t}{1.7904 - 2.064 \times 10^{-3}t - 2.14 \times 10^{-6}t^2}$$

Vapor Pressure

Apparatus.—Vapor pressures were determined by use of an all-nickel equilibrium still patterned after the high pressure still of Othmer and Morley.[3] The pot, vapor condensers and the lines connecting these to each other were insulated with about $^1/_2$ inch of glass wool which was retained by glass cloth. The condensation temperature of the vapor was measured by use of a 5-junction copper–constantan thermocouple which was calibrated from the melting points of uranium hexafluoride and benzoic acid. Electromotive force readings were made with a Rubicon potentiometer of accuracy comparable to that of the Leeds and Northrup type K-2 potentiometer. Pressure measurements below 4000 mm. of mercury were made using an open-end mercury manometer of 8 mm. bore attached to a Booth–Cromer pressure transmitter.[4] Pressures above 4000 mm.

---

[1] Based on work performed for the U. S. Atomic Energy Commission by Union Carbide Nuclear Company, Union Carbide and Carbon Corporation, Oak Ridge, Tennessee.

[2] D. W. Magnuson, Carbide and Carbon Chemicals Company, K-25 Plant Report No. K-1130, 1954.

[3] D. F. Othmer and F. R. Morley, *Ind. Eng. Chem.*, **38**, 751 (1946).

[4] S. Cromer, U.S.A.E.C. Declassified Report MDDC-803, April, 1947.

were read on a Wallace–Tiernan gage graduated in centimeters and having a precision of about ±1 mm.

Procedure.—In the determination of vapor pressures, about 25 ml. of 2,2,3-trichloroheptafluorobutane was admitted to the evacuated still and a small amount of nitrogen added as a confining gas. The temperature was then slowly raised until the condensed vapor was observed as a steady drip through a fluorothene observation window. After temperature–pressure equilibrium was established, the vapor pressure and temperature were recorded. An additional small amount of nitrogen (usually 1 to 5 cm.) was added to the still and the temperature raised as before until a second temperature–vapor pressure relationship was obtained. This procedure was continued until the vapor pressure was measured to 173°. The process of adding nitrogen was then reversed and small amounts of nitrogen were removed, with subsequent temperature decrease allowing vapor pressure readings to be made at various points as the temperature was lowered.

Results.—The vapor pressure equation

$$\log P_{\mathrm{mm}} = 6.69356 - \frac{1131.324}{t + 200} \tag{4}$$

was fitted to the experimental data for the range 29.58 to 172.68°. Uncertainty of the equation, based on confidence limits at the 0.95 level, is approximately ±1.1%. The experimental vapor pressures of 2,2,3-trichloroheptafluorobutane are presented in Table II. The boiling point at 760 mm. pressure calculated from equation 4 is 96.7°.

Table II

Vapor Pressure of 2,2,3-Trichloroheptafluorobutane

Temp., °C.	Vapor pressure, mm. Exptl.	Vapor pressure, mm. From eq. 4	Dev. of expt. from eq. values
29.58	58.5	58.3	+ 0.2
31.25	65.0	64.0	+ 1.0
42.15	104.4	105.0	− 0.6
55.01	178.1	178.5	− 0.4
62.66	240.5	243.4	− 2.9
73.33	355.0	358.5	− 3.5
78.40	424.5	426.5	− 2.0
94.99	714	721.8	− 7.8
98.23	809	794.5	+14.5
98.91	825	810.5	+14.5
103.47	908	923.9	−15.9
106.27	1012	999.3	+12.7
115.82	1293	1292	+ 1
121.37	1508	1490	+18
123.30	1545	1564	−19
138.29	2212	2235	−23
140.39	2317	2344	−27
145.53	2597	2627	−30
148.48	2822	2800	+22
166.66	4052	4056	− 4
170.02	4354	4326	+28
172.68	4632	4549	+83

Heat of Vaporization.—The heat of vaporization of 2,2,3-trichloroheptafluorobutane at various temperatures may be calculated from the exact form of the Clapeyron–Clausius equation given in equation 5 provided the vapor pressure, liquid density and deviation of the vapor from ideality are known for the given temperature range.

$$\Delta H = \frac{\mathrm{d}P}{\mathrm{d}T}\, t\Delta V \tag{5}$$

Differentiation of equation 4 gives

$$\frac{\mathrm{d}P}{\mathrm{d}T} = \frac{2604.964P}{(t + 200)^2} \tag{6}$$

Since

$$V = V_g - V_l = \frac{RT}{P(1 + AP)} - \frac{m}{\rho} \tag{7}$$

substitution of equations 6 and 7 into 5 yields

$$\Delta H_v = \frac{2604.964PT}{(t + 200)^2}\left(\frac{RT}{P(1 + AP)} - \frac{m}{\rho}\right) \tag{8}$$

where

ΔH_v = heat of vaporization per mole
P = vapor pressure
t = temperature, °C.
T = temperature, °K.
R = ideal gas constant
m = molecular weight
ρ = density
A = non-ideality coefficient (determined by Magnuson)[5]

Using equation 8, the heat of vaporization of 2,2,3-trichloroheptafluorobutane was calculated for the temperatures shown in Table III.

Table III

Heat of Vaporization of 2,2,3-Trichloroheptafluorobutane

Temp., °C.	Heat of vaporization, cal./mole
60	8207
80	7834
100	7487
120	7135
140	6728

Acknowledgments.—The authors wish to express appreciation to Mr. A. V. Faloon for purifying the 2,2,3-trichloroheptafluorobutane used in these studies and to Dr. E. J. Barber for directing the work.

---

[5] D. W. Magnuson, Carbide and Carbon Chemicals Company, K-25 Plant Report No. K-1130 (1954).

THE KINETICS OF THE REACTION BETWEEN Pu^{+3} AND PuO$_2^{+2}$ [1]

By A. E. Ogard and S. W. Rabideau

Los Alamos Scientific Laboratory, University of California, Los Alamos, New Mexico

Received December 5, 1955

In the course of the determination of the formal potential of the PuO$_2^+$–PuO$_2^{+2}$ couple in molar perchloric acid as a function of temperature,[2] it was noted that near 3°, following the addition of Pu^{+3} to the plutonyl ion, approximately one minute was required for the establishment of a stable potential. It was of interest to determine whether a detectable slowness in the reaction

$$\mathrm{Pu}^{+3} + \mathrm{PuO_2}^{+2} \underset{k_2}{\overset{k_1}{\rightleftharpoons}} \mathrm{Pu}^{+4} + \mathrm{PuO_2}^{+} \tag{1}$$

could be observed spectrophotometrically. Connick[3] has pointed out that this reaction usually can be considered to be in rapid reversible equilibrium. Heretofore no slowness has been detected in this reaction.

---

[1] This work was done under the auspices of the Atomic Energy Commission.

[2] S. W. Rabideau, *J. Am. Chem. Soc.*, **78**, June (1956).

[3] R. E. Connick, *ibid.*, **71**, 1528 (1949).

Experimental

The plutonium solutions were prepared by dissolving a weighed quantity of oxide-free metal in the required quantity of standardized J. T. Baker 71% perchloric acid. The plutonyl solutions were prepared by the prolonged ozonization of the Pu^{+3} solutions. Water redistilled from alkaline potassium permanganate was used in the preparation of all solutions. The spectrophotometric results were obtained with the Cary Model 14 recording spectrophotometer. Water at 5° was circulated through the walls of the cell compartment to minimize temperature changes of the solutions during the period of measurement. Dry helium was flushed through the cell, reference and phototube compartments to avoid condensation of moisture on the optical surfaces.

A double-chambered spectrophotometric mixing cell was used. Known weights of solutions of Pu^{+3} and PuO_2^{+2} were placed in their respective compartments. The cell was then immersed in an ice-bath for about an hour. At the end of this time the windows were dried, then the solutions were mixed in an atmosphere of helium which prevented the condensation of moisture on the cell windows. The first spectrophotometric readings were obtained approximately thirty seconds after mixing.

Results

From qualitative spectrophotometric observations of mixed solutions of Pu^{+3} and PuO_2^{+2} in molar perchloric acid at 3°, the gradual disappearance of Pu^{+3} (at 600 mμ) and the appearance of Pu^{+4} (at 652 mμ) were noted which demonstrated a measurable slowness in reaction (1). The rate law for this reaction can be written

$$-\mathrm{d}(Pu^{+3})/\mathrm{d}t = k_1(Pu^{+3}\ (PuO)_2^{+2})\{1 - K_{eq}/K^*\} \quad (2)$$

where K_{eq} is the equilibrium quotient, $(Pu^{+3})(PuO_2^{+2})/(Pu^{+4})(PuO_2^{+})$, and K^* is this quotient at any specified time, t. It has been found[2] that the value of K_{eq} at 3° is 4.3.

The value of k_1 was obtained from the slopes of the straight line plots of $\mathrm{d}(Pu^{+3})/(Pu^{+3})\mathrm{d}t$ *versus* $(PuO_2^{+2})\{1 - K_{eq.}/K^*\}$. The data for a typical experiment are given in Table I. The $\mathrm{d}(Pu^{+3})/\mathrm{d}t$ values were derived from measurements of slopes of plots of (Pu^{+3}) *vs.* time. As a test of the mechanism of the reaction, the initial concentrations of each of the plutonium solutions were increased by a factor of approximately three. A value of k_1 was obtained in this experiment which agreed with the previously determined rate constant within 11%. In another experiment the acidity was reduced to 0.50 *M*, but the ionic strength was maintained at unity with added sodium perchlorate. Rate determinations were also made at ionic strengths of 0.5 and 2. These results are summarized in Table II.

TABLE I

THE REACTION OF Pu^{+3} AND PuO_2^{+2} IN 1 *M* $HClO_4$ AT 3°

Time, min.	$(Pu^{+3}) \times 10^4$, moles/l.	$(PuO_2^{+2}) \times 10^{+3}$, moles/l.	$\mathrm{d}(Pu^{+3})/\mathrm{d}t \times 10^4$, moles l.$^{-1}$ min.$^{-1}$	$(1 - K_{eq.}/K^*)$
0	4.70	5.58	...	...
1.0	3.13	5.43	1.04	0.938
1.5	2.69	5.38	0.78	.879
2.0	2.34	5.35	.61	.809
3.0	1.84	5.30	.32	.637
4.0	1.59	5.27	.18	.503
5.0	1.45	5.26	.08	.405

TABLE II

SPECIFIC REACTION RATE CONSTANTS FOR THE REDUCTION OF PLUTONYL ION WITH Pu^{+3} IN PERCHLORIC ACID SOLUTIONS AT 3°

$(PuO_2^{+2})_i$, moles/l.	$(Pu^{+3})_i$, moles/l.	(H^+), moles/l.	μ	k_1, l. mole^{-1} min.$^{-1}$
1.488×10^{-2}	1.250×10^{-3}	1.00	1	80
5.583×10^{-3}	4.703×10^{-4}	1.00	1	90
4.099×10^{-3}	8.087×10^{-4}	0.50	1	72
3.838×10^{-3}	8.037×10^{-4}	0.50	0.5	52
5.108×10^{-3}	3.749×10^{-4}	2.00	2	..[a]

[a] Equilibrium essentially attained within the time of mixing.

From a comparison of the results obtained for k_1 at ionic strengths of 0.5, 1 and 2, it appears that an ionic strength dependence of k_1 is shown, and in agreement with the predicted rates for reaction (1) the value of k_1 is greatest in solutions of highest ionic strength. However, since the variation in the values of k_1 is rather large even at constant ionic strength and acidity, it is difficult to distinguish with a high degree of certainty between ionic strength and acidity effects from these data.

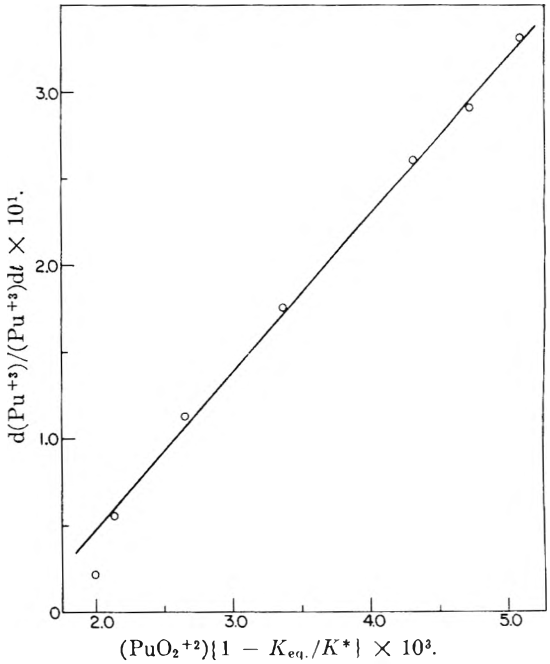

Fig. 1.—Evaluation of rate constant in molar perchloric acid at 3° for the reaction $PuO_2^{+2} + Pu^{+3} \rightarrow Pu^{+4} + PuO_2^{+}$.

THE REACTIONS OF AMMONIA AND HYDRAZINE WITH OXYGEN ATOMS AND HYDROGEN ATOMS IN ATOMIC FLAMES[1]

By Gordon E. Moore, Kurt E. Shuler,[1a] Shirleigh Silverman and Robert Herman

Contribution from the Applied Physics Laboratory, The Johns Hopkins University, Silver Spring, Maryland, and the Department of Physics, University of Maryland, College Park, Maryland

Received December 9, 1955

There has been much work reported in recent

---

[1] A portion of this work was supported by the Bureau of Ordnance, Department of the Navy, under Contract NOrd-7386 and by Guggenheim Brothers, New York, under Contract GU-1.

[1a] National Bureau of Standards, Washington, D. C.

years on the oxidation, pyrolysis and photolysis of NH_3 and N_2H_4. The results of these various studies have not as yet permitted the establishment of a consistent set of elementary mechanisms which adequately explains the experimental observations. There is thus a need to study in more detail the various elementary reactions which occur in these systems. In order to obtain some information along these lines we have studied, both spectroscopically and by the chemical analysis of the trapped products, the reactions of hydrogen atoms and oxygen atoms with NH_3 and N_2H_4 in atomic flames.

Experimental

The atomic flame apparatus which was employed is shown schematically in Fig. 1. The reaction chamber was provided with a quartz window which permitted spectrographic observations to be made perpendicular to the flow of the reactants. Power for the discharge was supplied from a 2$^1/_2$ kva. transformer with a 5000 volt secondary operated from a Variac. The concentrations of atoms issuing from the discharge were determined semi-quantitatively by the isothermal filament technique.[2] The filament was withdrawn from the reaction chamber before the runs were started. The pressure in the reaction vessel was measured by a tilt-type McLeod gage. The pressures employed were in the range ~0.5–1.0 mm. for most of the experiments described in this paper.

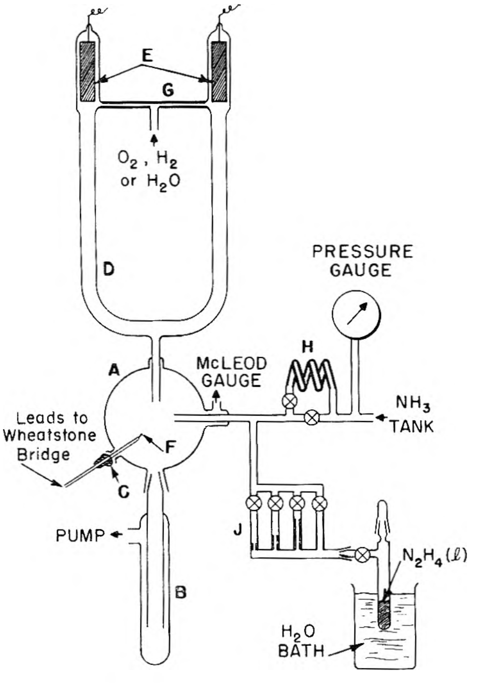

Fig. 1.—Schematic diagram of atomic flame apparatus showing: A, 1-l. reaction vessel; B, cold trap; C, ball and socket joint for inserting probes; D, discharge tube; E, tubular Al electrodes; F, platinum filament; and G, H and J, capillaries to control flow rates of reactants. Pumping speed ~3 l./sec.

All the spectrographic observations were made with a Bausch and Lomb medium quartz spectrograph on Eastman 103a-B plates. Slit widths from 100 μ to 1.0 mm. were employed in conjunction with exposure times ranging from 10 min. to about five hours. Commercial H_2, O_2 and NH_3, all stated to exceed 99.6% purity, were used for these experiments without further purification. The hydrazine assayed ~97%, the remainder being mostly water.

Chemical analyses for ammonia and hydrazine in the trapped products were carried out as follows: the total base was determined by titration with HCl to the methyl red end-point; the hydrazine was then determined by titration in ~5 HCl with KIO_3 solution using Brilliant Scarlet 3-R as an indicator.[3] The difference between the total base and the hydrazine was taken to represent the amount of ammonia present.

Results and Discussion

The chemical and spectroscopic data obtained in this study of the atomic flames of O or H atoms reacting with NH_3 and with N_2H_4 are summarized in Table I and discussed below.

TABLE I

SUMMARY OF EXPERIMENTAL RESULTS

Reactants	Emission bands[a] of NH_2	NH	OH	NO	Trap analysis
$O + NH_3$	..	vw	..	..	80–95% of NH_3 destroyed
$O + N_2H_4$	s	s	s	s	No NH_3 found, all of the N_2H_4 destroyed
$H + NH_3$	..	..	..	..	>95% of original NH_3 collected
$H + N_2H_4$	m	w	..	..	N_2H_4 mostly decomposed, 30–55% of max. possible NH_3 collected

[a] s, strong; m, moderately strong; w, weak; vw, very weak.

The band systems observed were the α-bands of NH_2 in the region from ~4000 Å. to the long wave length limits of the photographic plate at ~6500 Å., the $^3\Pi-^3\Sigma$ bands of NH at 3360 to 3370 Å., the $^2\Sigma-^2\Pi$ bands of OH, especially the (0,0) band at 3064 Å., and the γ-bands of NO, which were strongest in the region from 2250–2850 Å. An additional spectral feature observed in some of the atomic flames was the greenish-yellow air afterglow due to the recombination reaction[4]

$$NO + O = NO_2 + h\nu \qquad (1)$$

This continuum was found to be quite strong in cases where a large excess of atomic oxygen reacted with the nitrogen-containing fuels.[5]

Reactions with Atomic Oxygen. (a) $\mathbf{NH_3 + O}$.—The emission from the $NH_3 + O$ flame was very weak. Exposure times of about three hours with a slit of 100 μ were required to record even the strong central Q-branch of the NH band at 3360 Å. The OH bands also appeared weakly in such an exposure. However, a blank run with the same flow of oxygen and the same discharge voltage but with no ammonia present yielded the OH spectrum with even greater intensity. This indicates that the observed OH emission can be accounted for completely by the H_2O impurity in the oxygen. The other bands prominent in the premixed atmospheric pressure flame of ammonia and oxygen[6] (NH_2,NO) were not observed under our experimental conditions. It should be noted, however, that bands of NH_2 with intensity comparable to that found for NH could have been masked in these experiments by the overlapping emission of the air afterglow.

Since the reaction was non-luminous, we were

---

(2) See *e.g.*, J. R. Dingle and D. J. LeRoy, *J. Chem. Phys.*, **18**, 1632 (1950).

(3) R. A. Penneman and L. F. Audrieth, *Anal. Chem.*, **20**, 1058 (1948).

(4) A. G. Gaydon, "Spectroscopy and Combustion Theory," Chapman and Hall, Ltd., London, 1948, p. 101.

(5) The air afterglow is also obtained weakly in a discharge through commercial tank oxygen owing to the small amount of nitrogen impurities present.

(6) B. B. Fogarty and H. G. Wolfhard, *Nature*, **168**, 1122 (1951).

unable to observe directly the size of the reaction zone. However, the fact that some ammonia was always found in the trap, even in the presence of a considerable excess of atomic oxygen, suggests that the reaction is a fairly slow one.

(b) **N_2H_4 + O.**—The observed emission spectrum of the $N_2H_4 + O$ atomic flame consisted of bands of NH_2, NH, OH and NO. These bands were all at least two orders of magnitude more intense than their counterparts in the $NH_3 + O$ atomic flame in the same apparatus and under the same experimental conditions. Ten minute exposures with a 100 μ slit width gave well exposed plates for all these species.

The luminous zone of the $N_2H_4 + O$ atomic flame is very small compared with that of other atomic flames at the same pressure. The reaction volume is, for example, less than one tenth of the size of that for a comparable $C_2H_2 + O$ atomic flame. This shows that the reaction between N_2H_4 and O is a very fast one. When a small amount of N_2H_4 is added to a large excess of atomic oxygen, the air afterglow appears very strongly below the mixing zone. This indicates that the oxidation of hydrazine by atomic oxygen involves the formation of NO, a fact which is also borne out by the emission of the γ-bands of NO in the reaction zone.

The trap analysis showed that all the original hydrazine was destroyed in the reaction vessel. Since the thermal decomposition of hydrazine yields NH_3[7,8] and since no NH_3 was found in the trap, thermal decomposition of the N_2H_4 would seem to be ruled out. Qualitative analysis of the trap contents by the brown ring test indicated the presence of oxides of nitrogen.

Reactions with Atomic Hydrogen. (a) **NH_3 + H.**—In agreement with Dixon[9] no evidence was found which would indicate that NH_3 reacts with atomic hydrogen. No light emission was observed under our experimental conditions and with exposure times of ~3 hr., and the ammonia was recovered quantitatively in the trap. Our techniques could not, however, be expected to provide any direct evidence for possible exchange reactions or stripping-reforming reactions which may proceed without the formation of electronically excited intermediates.

It was found that the energy released by hydrogen atom recombination to a platinum filament inserted into the reaction chamber decreased with increasing partial pressure of ammonia under constant discharge conditions. This would seem to indicate that the presence of ammonia in the reaction system reduces the steady-state concentration of atomic hydrogen. Our observations can readily be accounted for on the basis that the NH_3 reacts with the H atoms only by an exchange reaction of the type proposed by Farkas and Melville[10]

$$NH_2H' + H \longrightarrow NH_3 + H' \qquad (2)$$

and that the decrease in the steady state concentration of H atoms is due to a recombination with NH_3 as the third body.

(b) **N_2H_4 + H.**—The reaction between hydrazine and atomic hydrogen took place with the emission of moderately strong NH_2 bands and relatively weak NH bands. Trap analyses showed, in agreement with Dixon's results,[9] that ammonia was a major reaction product. The ratio ρ = (moles of NH_3 formed/moles of N_2H_4 decomposed) was observed to depend on the partial pressure of the reactants and was found to vary from about 0.45 to about 1.14 ± 0.05. In general a higher ratio of hydrazine to atomic hydrogen at a given pressure favored the production of ammonia. The luminous reaction volume, although considerably larger than that for the reaction $N_2H_4 + O$ at the same pressure, did not fill the reaction chamber. Order of magnitude calculations show that the observed reaction volume is compatible with the rate constant for the hydrazine–atomic hydrogen reaction obtained by Birse and Melville.[11] The dependence of ρ on atomic hydrogen concentration suggests that the reaction between H atoms and N_2H_4 proceeds by at least two competing mechanisms of different order in H atoms.

---

(7) R. C. Murry and A. R. Hall, *Trans. Faraday Soc.*, **47**, 742 (1951).

(8) G. K. Adams and G. W. Stocks, "Fourth Symposium on Combustion," The Williams and Wilkins Co., Baltimore, 1952.

(9) J. K. Dixon, *J. Am. Chem. Soc.*, **54**, 4262 (1932).

(10) A. Farkas and H. W. Melville, *Proc. Roy. Soc. (London)*, **157A**, 625 (1936).

(11) E. A. B. Birse and H. W. Melville, *ibid.*, **175A**, 164 (1940).

APPEARANCE POTENTIAL STUDIES. I[1]

By Stephen S. Friedland[2] and Robert E. Strakna

Department of Physics, The University of Connecticut, Storrs, Connecticut

Received December 22, 1955

The measurement of appearance potentials of molecular fragments leads to some understanding of molecular structure (for example, see ref. 3). In addition, the magnitude of the appearance potential of polyatomic molecules, such as the esters and alcohols, may be used elsewhere. The proper combination of a polyatomic gas with an inert gas in a self-quenching Geiger–Muller counter is determined by the appearance potential of the polyatomic molecule. This is possible since the quenching process of the gas discharge in the counter depends upon the probability of electron transfer from the inert gas to the polyatomic molecule.[4] That is, the ionization potential of the inert gas has to be higher than the ionization potential of the polyatomic molecule or of the appearance potential of any of its fragments (if the fragment is to participate in the quenching action); the closer the two values, the higher the probability of electron transfer and thus the more effective quenching action. Further, the value of the appearance potential of the fragments may be utilized to determine whether the fragments formed in the discharge[5] will also act as quenching agents.

---

(1) Work supported by the Research Corporation, New York City.

(2) On leave with the Nuclear Development Corporation of America, White Plains, New York.

(3) (a) H. D. Hagstrum, *Rev. Modern Phys.*, **23**, 185 (1951); (b) H. B. Rosenstock, H. B. Wallenstein, A. L. Wahrhaftig and, H. Eyring, *Proc. Natl. Acad. Sci.*, **38**, 667 (1952).

(4) S. A. Korff and R. D. Present, *Phys. Rev.*, **65**, 275 (1944).

(5) S. S. Friedland, *ibid.*, **74**, 898 (1948).

With the above two points as a motivation, a systematic study of gases of interest has been undertaken. Methyl and ethyl alcohol and methyl and ethyl acetate are herein reported. Methyl and ethyl alcohol were reported on by Cummings and Bleakney[6] many years ago, but it was felt that the new techniques developed since their study warranted a re-investigation of these molecules.

Experimental

All measurements were made on a 90° sector type mass spectrometer. The electronics were of conventional design except for the ion gun control unit, which included a built-in potentiometric circuit for the measurement of the electron energy. The electron accelerating potential was obtained across a Leeds and Northrup precision resistance box of 0 to 10K ohms through which a constant current of 10 milliamperes was maintained. This current was continuously stabilized by use of a Weston standard cell as a reference. Simultaneously, the highly stabilized current was used to produce the potentials necessary to operate the other elements in the electron gun. The standardization circuit functioned by comparing the voltage drop across a resistor adjusted to 101.86 ohms with 1.0186 volt output, which is the same as the standard cell. If 10 milliamperes are flowing through the resistance box, the sum of the voltage drops across the 101.86 ohm resistor and the standard cell will be zero. However, if the current should depart slightly from its proper value, a resultant error voltage appears across the contacts of a Brown Converter and is chopped into a 60 cycle square wave by the motion of the armature contacts. The phase of the resulting voltage depends upon the polarity of the error. The error signal was amplified by a narrow band 60 cycle amplifier and was then fed into a phase sensitive detector which produced a d.c. output of similar polarity but of much greater size than the error signal. The output thus derived was used to correct the grid bias of a tube placed in series with the current to be regulated. The action was degenerative and hence tended to reduce the error to zero. A precaution taken to ensure stability of the system was that a d.c. feedback path was provided which was capable of correcting the system in the event of a major disturbance. This was necessary as the high gain of the a.c. amplifier tended to produce saturation and loss of phase sense when a sudden large signal was applied. A phase correction network was included to fulfill the Nyquist criterion for the frequency phase relations in any feedback circuit.

The unknown gas and the calibrating gas were admitted into the gas inlet simultaneously. The ion peak to be studied was adjusted in height to equal the ion peak of the calibrating gas with 50 volts supplied to the electron beam. The ionization efficiency curves for both gases were obtained rapidly and the method of initial breaks was used to determine the appearance potential. Reproducibility from day to day was better than 0.05 volt and all standards checked against each other were accurate within the same range.

The deviations indicated for the results are indicative of the reproducibility of the ionization efficiency curves from day to day. The accuracy of the ionization potentials, in terms of an absolute number, was approximately 0.2 of a volt for all values given.

If the ionization efficiency curve of the unknown turns out to be parallel to that of the calibrating gas and the points of initial break fall within 0.1 of a volt of each other, then it is possible to cite an accuracy less than the above value. However, in most cases, the two curves are not parallel, and it is difficult to find calibrating gases that have the proper appearance potential and therefore a value of 0.2 is most realistic.

The results of the measurements of the appearance potentials are as follows:

Methyl Alcohol.—Mass number 32, 11.36 ± 0.08 volt; 31, 12.26 ± 0.10 volt; 29, 14.26 ± 0.10 volt; 28, 14.31 ± 0.05 volt; 15, 14.96 ± 0.10 volt.

Ethyl Alcohol.—Mass number 46, 10.88 ± 0.15 volt; 45, 11.23 ± 0.08; 31, 12.28 ± 0.15; 29, 13.91 ± 0.15; 27, 15.31 ± 0.15.

Methyl Acetate.—Mass number 74, 10.95 ± 0.10 volt; 59, 12.31 ± 0.15; 43, 11.86 ± 0.10; 42, 11.81 ± 0.15; 31, 12.65 ± 0.20; 15, [illegible]4.26 ± 0.10.

Ethyl Acetate.—Mass number 88, 10.67 ± 0.05 volt; 61, 11.24 ± 0.10; 45, 11.44 ± 0.10; 43, 12.31 ± 0.20; 29, 12.47 ± 0.08; 27, 15.32 ± 0.20.

If we compare the values with the appearance potential of argon (15.77), krypton (14.01), xenon (12.14) and other inert gases, we see that all of the gases studied may be used as quenching vapor in conjunction with inert gases. However, as noted in the introduction, the smaller the difference of the potential, but with the polyatomic vapor having the lower value, the more positive will be the quenching action when used in a Geiger–Müller counter.

It will be noted that the criterion for good quenching is more closely satisfied by the fragments of the polyatomic molecules. Thus in the high counting rates where the fragment may be utilized in the quenching action, this factor should be considered.

Cummings and Bleakney[6] have analyzed the data of ethyl and methyl alcohol in terms of the structure of the molecule. The discrepancies introduced by their data, that is, the appearance potential of mass 45 in ethyl alcohol is lower than mass 46, is removed by these results. Similar analyses may be made for methyl and ethyl acetate and these will be the subject of a future publication.

LONGITUDINAL DIFFUSION IN ION EXCHANGE AND CHROMATOGRAPHIC COLUMNS. FINITE COLUMN

By W. C. Bastian and L. Lapidus

Contribution from the Department of Chemical Engineering, Princeton University, Princeton, N. J.

Received December 8, 1955

In a recent communication[1] the effect of longitudinal diffusion on the effluent concentrations from an ion-exchange column was considered. The equations developed, however, were only applicable to a column infinite in length. In the present note the authors present the equations for a column of finite length operating under equilibrium conditions. Consider a column of unit cross-sectional are and let

c = concn. of adsorbate in the fluid stream, moles/unit vol. of soln.
n = amount of adsorbate on the adsorbent, moles/unit vol. of packed bed
V = velocity of fluid through interstices of the bed
z = distance variable along the bed
D = diffusion coefficient of the adsorbate in soln. in the bed
c_0 = concn. of soln., admitted to the bed
α = fractional void vol. in the bed
k_1, k_2 = constants in equilibrium relation
L = length of bed

A material balance on an elemental section of the bed produces

$$D\frac{\partial^2 c}{\partial z^2} = V\frac{\partial c}{\partial z} + \frac{\partial c}{\partial t} + \frac{1}{\alpha}\frac{\partial n}{\partial t} \qquad (1)$$

The column is assumed to be operating under equilibrium conditions and to initially be free of adsorbate. This can be described by the equations

$$n = k_1 c + k_2 \qquad (2)$$

$$n = c = 0,\ t = 0 \qquad (3)$$

In addition the behavior of the fluid phase must be described at the inlet, $z = 0$, and at the outlet, $z = L$, of the bed. One may postulate a number of different representations at these two points but the recent and detailed work of Wehner and Wilhelm[2] has shown that those described by Dank-

---

(6) C. S. Cummings, II, and W. Bleakney, *Phys. Rev.*, **58**, 787 (1940).

(1) L. Lapidus and N. R. Amundson, This Journal, **56**, 984 (1952).

(2) J. F. Wehner and R. H. Wilhelm, personal communication.

werts[3] for a similar problem are correct. These are

$$Vc_0 = Vc - D\frac{\partial c}{\partial z}, z = 0 \qquad (4)$$

$$\frac{\partial c}{\partial z} = 0, z = L$$

Use of boundary conditions of this type were shown by Wehner and Wilhelm to be a consistent set which leads to plug flow of material at one extreme ($D = 0$) and perfect mixing of material at the other extreme ($D = \infty$). Making the change of variable

$$c - c_0 = we^{(Vz/2D\ -\ V^2t/4\gamma D)} \qquad (5)$$

Equations 1, 2, 3 and 4 become

$$\frac{D}{\gamma}\frac{\partial^2 w}{\partial z^2} = \frac{\partial w}{\partial t} \qquad (6)$$

$$-w = c_0e^{-Vz/2D}, t = 0 \qquad (7)$$

$$-\frac{\partial w}{\partial z} + \frac{V}{2D}w = 0, z = 0$$

$$\frac{\partial w}{\partial z} + \frac{V}{2D}w = 0, z = L \qquad (8)$$

If we now let $D/\gamma = k$ and $V/2D = h$ then the system of equations becomes identical to that describing one-dimensional heat flow in a plane with radiation from each face and an arbitrary initial distribution. From Carslaw and Jaeger[4] the solution can immediately be written as

$$w = 2\sum_1^\infty e^{-k\alpha_n^2 t}\frac{\alpha_n\cos\alpha_n x + h\sin\alpha_n x}{(\alpha_n^2 + h^2)L + 2h}$$

$$\int_0^L -c_0e^{-hx}(\alpha_n\cos\alpha_n x + h\sin\alpha_n x)\,dx \qquad (9)$$

where the α_n are the roots of

$$\tan\alpha_n L = \frac{2\alpha_n h}{\alpha_n^2 - h^2} \qquad (10)$$

Carrying out the indicated integration in equation 9, returning to the original variables (equation 5) and letting v = volume of solution = $Vt\alpha$ there finally results

$$\frac{c_0 - c}{c_0} = 2\sum_1^\infty \frac{\alpha_n L\sin\alpha_n L}{(\alpha_n L)^2 + \frac{v^2L^2}{4D^2} + \frac{vL}{D}}$$

$$e^{\left[\frac{vL}{2D} - \left(\frac{v^2}{4\gamma D} + \frac{D}{\gamma}\alpha_n^2\right)t\right]} \qquad (11)$$

where the α_n are the roots of

$$\alpha_n L\cot\alpha_n L + \frac{vL}{4D} = \frac{(\alpha_n L)^2}{vL/D} \qquad (12)$$

Equation 11 represents the effluent adsorbate concentration from the bottom of a column of length L as a function of the volume of solution into the column. While the roots of equation 12 are not readily available as such, Carslaw and Jaeger tabulate the first six roots of

$$\beta/2\cot\beta/2 + \frac{hL}{2} = 0$$

and of

$$\beta/2\tan\beta/2 - \frac{hL}{2} = 0$$

From these two sets of roots the first twelve roots of equation 12 may be obtained and all those following will increase by a factor of π.

The accompanying figure illustrates the use of equation 11. The effluent distribution is closer to perfect mixing than to plug flow. As also shown the finite column calculations do not deviate to any large extent from those for an infinite column. This cannot, however, be construed as a general situation.

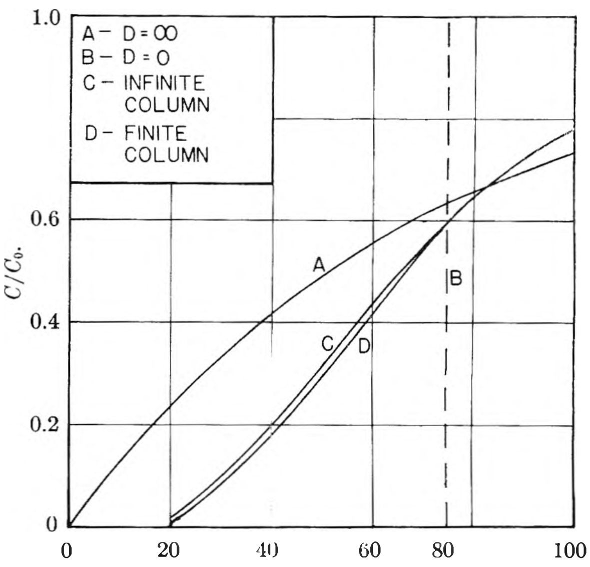

Fig. 1.—Values of C/C_0 *vs.* v, the volume of solution, L = 3 cm., V/D = 2.0 and γ = 25.

TEMPERATURE DEPENDENCE OF VISCOSITY OF LIQUIDS

By K. Keith Innes

Vanderbilt University, Nashville, Tenn.

Received December 23, 1955

Viscous flow of liquids is commonly interpreted as a rate process. Thus, the fluidity, ϕ, by analogy with the rate constant of chemical kinetics, is expected to show an exponential dependence on temperature. It has, indeed, been widely illustrated[1] that within the accuracy of most experimental data the viscosity, η, is given by

$$\eta = \frac{1}{\phi} = A'e^{B'/T} \qquad (1)$$

where A' and B' are taken as constants. Two of the few cases for which accuracy and sufficient range of temperature justify refinement of (1) are the interesting ones of water and mercury. Previous simple refinements for these substances have considered variation of B' with temperature.[2]

We wish to point out that further analogy with chemical kinetics,[3] particularly for low values of B', recommends the form

$$\eta = AT^ne^{B/T} \qquad (2)$$

where n is a third constant specific to the given liquid. In addition to relative simplicity, this form may offer information about temperature dependence of liquid structures.

It is our impression that equation 2 has not pre-

---

(3) P. V. Dankwerts, *Chem. Eng. Sci.*, **2**, 1 (1953).

(4) H. S. Carslaw and J. C. Jaeger, "Conduction of Heat in Solids," Oxford Press, 1947.

(1) See, as examples, E. N. da C. Andrade, *Nature*, **125**, 309 (1930); H. A. Kierstead and J. Turkevich, *J. Chem. Phys.*, **12**, 24 (1944).

(2) For example, T. A. Litovitz, *ibid.*, **20**, 1980 (1952).

(3) A. A. Frost and R. G. Pearson, "Kinetics and Mechanism," John Wiley and Sons, Inc., New York, N. Y., 1953, p. 24.

viously been employed from the above point of view, and, in fact, rarely at all.[4]

In Table I we have listed observed values of the viscosity of water from Dorsey's selection.[5] The uncertainties of values between 40 and 100° are thought[5] to be 0.5 to 1%. Below 40° the uncertainty is a few tenths of a per cent. We have shown in Table I the possibility of fitting the observations with equation 2, using $n = 5$ (found by trial and error), $A = 5.109 \times 10^{-17}$ and $B = 3337.7$. Calculated viscosities are correct from less than 40° to over 175°. Alternatively one could use $n = 10$ to improve the calculations from 0 to 100°, destroying, however, the fit above 100°. We prefer the equation with $n = 5$ because it is suitable for a wider temperature range. This rather arbitrary criterion is justified below for the case of water.

Data[6] and calculations for mercury are presented in a similar way in Table I, where we have used $n = {}^1/_4$, $A = 0.9827$ and $B = 393.1$. It is seen that the three constants are quite adequate over the available temperature range. Unfortunately, measurements have not been extended to the freezing point of mercury.

TABLE I

COMPARISON OF OBSERVED VISCOSITIES (MILLIPOISES) WITH THOSE CALCULATED USING EQUATION 2

	Water			Mercury	
t, °C.	η_{obsd}	η_{calcd}	t, °C.	η_{obsd}	η_{calcd}
10	13.10	12.20	−20	18.55	18.51
20	10.05	9.71	0	16.85	16.84
30	8.00	7.89	20	15.54	15.54
40	6.54	6.53	40	14.50	14.50
50	5.49	5.49	60	13.67	13.66
60	4.70	4.69	80	12.98	12.96
80	3.57	3.56	100	12.40	12.38
100	2.84	2.83	150	11.30	11.28
120	2.32	2.33	200	10.52	10.52
140	1.96	1.98	250	9.95	9.96
160	1.74	1.73	300	9.50	9.55
175	1.58	1.58	340	9.21	9.28
200	1.36	1.40			

Of other substances, for which accuracies and/or temperature ranges are much lower, we may mention, with less certainty: heptane,[7] for which we find, in the range −62 to +90°, $n = 1$, $A = 1.850 \times 10^{-4}$ and $B = 1266.7$; and methanol[8] for which, in the range −73 to +60°, $n = 0$, $A = 8.00 \times 10^{-2}$ and $B = 1262.0$. Observed viscosities may be calculated (millipoises) to within about 1% over the indicated temperature ranges. Within 25 to 30° of the melting points, the calculated viscosities are too low, much as in the case of water (Table I).

In interpreting the above results it is convenient to use the formulation of Eyring.[9] We have

$$B = \Delta H^*/R \text{ and } AT^n = \frac{\lambda_1 h}{\lambda_2 \lambda_3 \lambda} e^{-\Delta S^*/R}$$

where ΔH^* is the heat of activation for flow, ΔS^* is the entropy of activation, λ is the distance between equilibrium positions in the direction of motion, and the other three λ's are intermolecular distances in mutually perpendicular directions. It will be expected that the factor containing the λ's will change with temperature in approximately the same way as the reciprocal of molecular volume, that is, the factor should decrease by 9% for water and 6.5% for mercury for the temperature ranges of Table I. Using molecular volumes and the values of AT^n already quoted, entropies of activation for water and mercury are found to be positive and negative, respectively. In an entirely similar way, we conclude that ΔS^* is small and positive for methanol and small and negative for heptane. Only in the case of water does the entropy change strikingly in the temperature range considered.

These results are not entirely unexpected. For water and methanol, the formation of the activated state presumably involves, primarily, the breaking of a number of hydrogen bonds. In contrast, for the other two liquids, the mechanisms of flow are evidently coöperative ones. For example, one may note the possibility of viscous flow by the rotation of double molecules.[10]

The inadequacy of calculated values of the viscosities near the freezing points may be attributed to significant changes in heats of activation (and in the temperature dependencies of entropies) which, in turn, arise from major changes in the liquid structures. A rather definite illustration can be given according to the successful liquid water model of Bernal and Fowler,[11] who concluded that, in the approximate range 5 to 200°, a quartz-like structure predominates which, however, passes smoothly into a characteristic low temperature form, as well as a high temperature form. As we have pointed out, equation 2 with $n = 5$ gives an adequate representation of the viscosity of water over the range 35° to more than 175°, which is strikingly central to the Bernal–Fowler region. Evidently ΔH^* and ΔS^* are very sensitive to the appearance of both the low and the high temperature forms.

I am indebted to my wife, Ruth Craig Innes, for assistance with the calculations.

---

(4) The only references that have been found are: J. S. Dunn, *Trans. Faraday Soc.*, **22**, 401 (1926); F. Hovorka, H. P. Lankelma and S. C. Stanford, *J. Am. Chem. Soc.*, **60**, 820 (1938); H. G. de Carvalho, *Anais. assoc. quím. Brasil*, **2**, 21 (1943).

(5) E. N. Dorsey, "Properties of Ordinary Water Substance," Reinhold Publ. Corp., New York, N. Y., 1940, pp. 183–185.

(6) S. Erk, *Z. Physik*, **47**, 886 (1928).

(7) J. F. Johnson and R. L. LeTourneau, *J. Am. Chem. Soc.*, **75**, 1743 (1953), kinematic viscosities below 0°; G. Egloff, "Physical Constants of Hydrocarbons," Vol. I, Reinhold Publ. Corp., New York, N. Y., 1939, p. 41, densities below 0°; "International Critical Tables," Vol. 7, McGraw-Hill Book Co., Inc., New York, N. Y., 1929, p. 219, viscosities above 0°.

(8) "Handbook of Chemistry and Physics," 34th Ed., Chemical Rubber Publishing Co., Cleveland, Ohio, 1952, p. 1886; J. R. Partington, "An Advanced Treatise on Physical Chemistry," Vol. II, Longmans, Green and Co., New York, N. Y., 1951, p. 109.

(9) S. Glasstone, K. J. Laidler and H. Eyring, "The Theory of Rate Processes," McGraw-Hill Book Co., Inc., New York, N. Y., 1941, p. 484.

(10) J. O. Hirschfelder, C. F. Curtiss and R. B. Bird, "Molecular Theory of Gases and Liquids," John Wiley and Sons, Inc., New York, N. Y., 1954, p. 629.

(11) J. D. Bernal and R. H. Fowler, *J. Chem. Phys.*, **1**, 515 (1933).

THE EFFECT OF OPTICAL ISOMERS ON THE MELTING POINT OF GELATIN GELS

BY J. BELLO AND J. R. VINOGRAD

Gates and Crellin Laboratories of Chemistry, California Institute of Technology, Pasadena, California

Received January 5, 1956

It has long been known that certain compounds added to gelatin may raise or lower the melting point of gelatin gels. It has been suggested that the effect of these substances, or at least those ions that lower the melting point, is a result of binding of the additive by the gelatin[1] or due to other specific interactions.[2,3] The gelation of gelatin is accompanied by a large increase in the specific rotation; this has been reviewed by Ferry.[3] The change of specific rotation on gelation must certainly be the result of a change in the configuration of the gelatin molecule,[4] probably an increased ordering.

It has been reported that additives that lower the melting point of gelatin gels also lower the specific rotation of gelatin at temperatures at which gelation occurs in the absence of additive.[5-8] At sufficiently high additive concentrations, additives lower the specific rotation of gelatin to that of pure gelatin solutions at 35° or higher, where a limiting value of rotation is reached and no gelation occurs.[9] The decrease of rotation caused by additives that reduce the melting point represents a reversal of the configurational change attending gelation. At 35° or in the presence of 2 M potassium thiocyanate (one of the more effective melting point reducers), aqueous gelatin exists as discrete molecules[10] having the form of a random coil.[11,12] Additives that raise the melting point also raise the specific rotation.[4]

If the additives that raise or lower the melting point of gelatin gels do so by promoting or interfering, respectively, with the attainment of an ordered configuration necessary for gelation as a result of being bound by the gelatin or as a result of some other specific interaction at or near the asymmetric center it might be anticipated that optical isomers might exert different effects. A similar effect might be anticipated if additives act by being bound near asymmetric centers that are cross-linking sites in the gelation process. Alternatively, if the effect of additives is solely the result of changing the nature of the solvent, then D and L isomers will have identical effects on the melting point of gelatin gels since the effects of enantiomorphs on an optically inactive solvent must be identical. A DL mixture, however, might have a different effect from either pure enantiomorph as a result of formation of a racemic compound.

We have determined the melting point of gelatin gels in the presence of several sets of optical isomers, both melting point raisers and reducers. Included is sodium acetyltryptophan, one of the most effective melting point reducers reported.[13] The results are shown in Table I. The largest difference observed between isomers was 0.2°, a difference not larger than the experimental error.

TABLE I

MELTING POINTS OF 5% GELATIN GELS CONTAINING OPTICAL ISOMERS

Added substance	Concn., moles/l.	M.p., °C.
None	...	30.2
Disodium L-malate	0.5	32.1
Disodium DL-malate	.5	32.1
Disodium L-glutamate	.5	32.9
Disodium DL-glutamate	.5	33.0
Disodium L-aspartate	.5	32.9
Disodium D-aspartate	.5	32.9
Sodium acetyl-L-phenylalanine	.8	24.6
Sodium acetyl-D-phenylalanine	.8	24.8
Sodium acetyl-L-tryptophan	.5	19.1
Sodium acetyl-DL-tryptophan	.5	19.1
L-Arabinose	.91	30.5
D-Arabinose	.91	30.4

Had there been large differences between the effects of optical isomers, one could have attributed the melting point changes to binding of the additives at or close to asymmetric centers or to being bound at more distant sites which approach these centers during the configurational change attending gelation or to binding at non-asymmetric sites which react intermolecularly with asymmetric centers. None of these explanations for the effects of additives can be excluded if gelatin has a high degree of "configurational adaptability,"[14] being able to accommodate enantiomorphs equally well. There are other explanations for the effects of enantiomorphs which are not excluded by these data. Additives may act solely on the solvent, or they may occupy non-asymmetric sites which are involved in cross-linking or in the configurational changes.

Acknowledgment.—This work was performed under contract No. DA 49-007-MD-298 with the Office of the Surgeon General, Department of the Army. We wish to thank Miss Helene Riese for technical assistance.

Experimental

Sodium salts were prepared from the corresponding acids by reaction with sodium hydroxide, the final pH being between 8 and 9 to ensure complete conversion to the salt. The pH of pairs of isomers were adjusted to the same value to within 0.1 pH unit.

Acetyltryptophan and acetylphenylalanine were prepared according to du Vigneaud and Sealock[15] and du Vigneaud and Meyer,[16] respectively. The remaining amino acids were the best quality sold by the California Foundation for Biochemical Research.

The gelatin used was Wilson Laboratories' U-COP-CO, Special Non-Pyrogenic Gelatin, an acid extracted pigskin gelatin of isoelectric point 9.2.

---

(1) J. Bello and J. R. Vinograd, Paper No. 10 presented before the Division of Colloid Chemistry at the 127th Meeting of the American Chemical Society, Cincinnati, Ohio, March 29–April 7, 1955.

(2) G. A. Feigen and I. L. Trapani, *Arch. Biochem. Biophys.*, **53**, 184 (1954).

(3) J. D. Ferry, "Advances in Protein Chemistry," Vol. IV, M. L. Anderson and J. T. Edsall, editors, Academic Press, Inc., New York, N. Y., 1948, p. 1.

(4) C. Robinson and M. V. Bott, *Nature*, **168**, 325 (1951).

(5) E. Stiasny, *Kolloid Z.*, **35**, 353 (1924).

(6) A. B. Manning, *Biochem. J.*, **18**, 1085 (1924).

(7) J. R. Katz and J. F. Wienhoven, *Rec. trav. chim.*, **52**, 36 (1933).

(8) D. C. Carpenter and F. E. Lovelace, *J. Am. Chem. Soc.*, **57**, 2337 (1935).

(9) This is restricted to the commonly investigated concentration range, up to 10% gelatin. At higher concentrations the melting point increases sharply: J. Russel, "The Theory of the Photographic Process," C. E. K. Mees, editor, The Macmillan Co., New York, N. Y., 1954, p. 63.

(10) E. O. Kraemer, THIS JOURNAL, **45**, 660 (1941); **46**, 177 (1942).

(11) J. W. Williams, W. M. Saunders and J. S. Cicirelli, *ibid.*, **58**, 774 (1954).

(12) H. Boedtker and P. Doty, *ibid.*, **58**, 968 (1954).

(13) R. S. Gordon, Jr., and J. D. Ferry, *Federation Proc.*, **5**, 136 (1946).

(14) F. Karush, *J. Am. Chem. Soc.*, **72**, 2705 (1950).

(15) V. du Vigneaud and R. R. Sealock, *J. Biol. Chem.*, **96**, 511 (1932).

(16) V. du Vigneaud and C. E. Meyer, *ibid.*, **98**, 295 (1932).

Melting points were measured as follows. About 10 ml. of solution in a 150 × 20 mm. loosely stoppered test-tube was warmed at 50° for ten minutes to erase the sample's thermal history, stoppered tightly and stored at 0 ± 0.01° for 20 hours. A Neoprene ball, d_{20}^{20} 1.17, and diameter 0.5 cm. was inserted under the surface of the gel, the stopper replaced and the tube heated at the rate of 5° per hour. The melting point was taken as the temperature at which the ball reached the bottom of the tube. The reproducibility of the method is about ±0.3°.

THERMAL DIFFUSION NEAR THE CRITICAL SOLUTION TEMPERATURE[1]

By L. J. Tichacek and H. G. Drickamer

Department of Chemistry and Chemical Engineering, University of Illinois, Urbana, Illinois

Received January 13, 1956

The thermal diffusion ratio α for a binary system is defined by the flux equation

$$\vec{J}_1 = -\rho D\,[\overrightarrow{\text{grad}}\,X_1 - \alpha X_1(1 - X_1]\,\frac{1}{T}\,\overrightarrow{\text{grad}}\,T] \qquad (1)$$

From the thermodynamics of irreversible processes it is possible to derive an expression for α[2] where

$$\alpha = \frac{\bar{V}_1\bar{V}_2}{\bar{V}}\left[\frac{Q_2^*}{\bar{V}_2} - \frac{Q_1^*}{\bar{V}_1}\right]\frac{1}{X_1\dfrac{\partial\mu_1}{\partial X_1}} \qquad (2)$$

the $\bar{V}_i$'s are partial molar volumes, $\bar{V}$ is the average volume and O_i^* is the heat of transport of component i. For our present purposes, the factor in the denominator $X_1\,\partial\mu_1/\partial X_1$ is of most interest. In an ideal solution it equals RT. It approaches zero as one approaches the critical solution temperature.[3] Since there is no necessity for the numerator to go to zero at this point, α should increase greatly in magnitude as we approach the critical solution temperature.

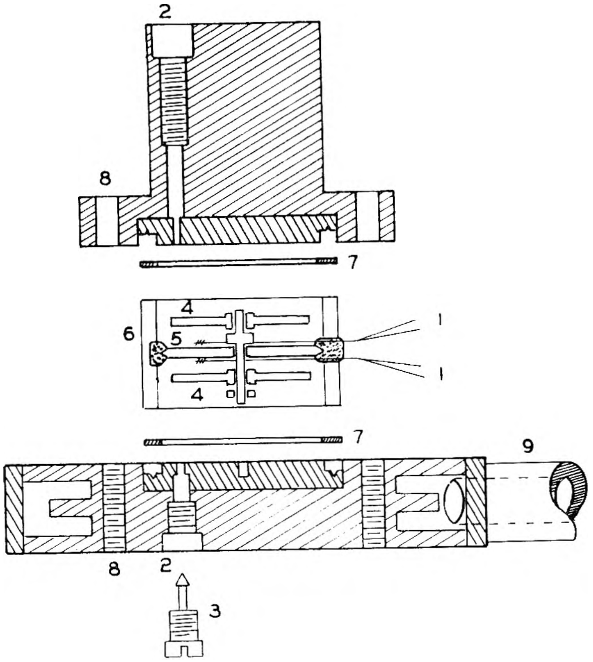

Fig. 1.—Glass walled thermal diffusion cell: 1,1, thermocouples; 2,2, sample taps; 3, sample tap scaling screw; 4,4, agitators; 5, fritted glass diaphragm, cemented in; 6, wall of cell chamber—glass tubing; 7,7, Teflon gaskets; 8,8, holes for connecting screws; 9, coolant takes.

To test this hypothesis thermal diffusion measurements were made on the system isoöctane (2,2,4-trimethylpentane) perfluoroheptane. The isoöctane was Phillips pure grade. The perfluoroheptane was obtained from Minnesota Mining and Manufacturing Co. It was carefully redistilled and a cut boiling from 82.2 to 83° was retained.

In order to operate with a ΔT of 1-2°, a special cell was designed as a modification of our standard cell.[4] The cell is shown in Fig. 1, and is largely self-explanatory. The fritted glass was seated in a groove etched in the glass body of the cell and sealed in with sauereisen. The ΔT was measured using iron–constantan thermocouples. The cell is in many ways more useful than our standard cell.

The results are shown in Fig. 2. Because of the small ΔT's used, considerable scatter was inevitable. $X\,(\partial\mu/\partial X)$ can be written using Scatchard-Hildebrand theory.[3]

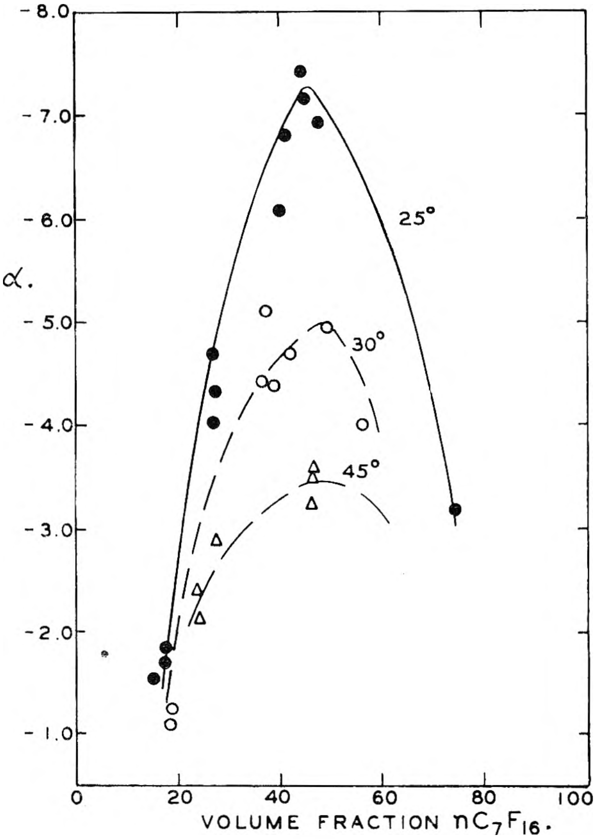

Fig. 2.—Thermal diffusion ratio α *vs.* composition system *n*-perfluoroheptane (2,2,4-trimethylpentane).

$$X_1\frac{\partial\mu}{\partial X_1} = RT\left[1 - \frac{\varphi_{1R}\varphi_{2R}}{V_R T_R}\right] \qquad (3)$$

where

φ_i = volume fraction i

$\bar{V}$ = average molar volume. The subscript R refers to the value relative to the value at the C.S.T.

---

[1] This work was supported in part by the AEC.

[2] L. J. Tichacek, W. S. Kmak and H. G. Drickamer, This Journal, **60**, 660 (1956).

[3] J. H. Hildebrand and R. L. Scott, "Solubility of Non-Electrolytes," 3rd Ed., Reinhold Publ. Corp., New York N. Y., 1950, p. 253.

[4] R. L. Saxton, E. L. Dougherty, Jr., and H. G. Drickamer, *J. Chem. Phys.*, **22**, 1166 (1954).

It can be shown that use of a Flory–Huggins type entropy correction would not affect the calculations materially for this system.

If one assumes, quite rashly, that the heats of transport (and partial molar volumes) are independent of temperature and composition in this range then relative values of α can be calculated

$$\frac{\alpha}{\alpha_{\mathrm{A}}} = \frac{T_{\mathrm{A}}\left[1 - \frac{\varphi_{\mathrm{R}}\,\varphi_{2\mathrm{R}}}{\bar{V}_{\mathrm{R}}\,T'_{\mathrm{R}}}\right]_{\mathrm{A}}}{T\left[1 - \frac{\varphi_{\mathrm{R}}\,\varphi_{2\mathrm{R}}}{\bar{V}_{\mathrm{R}}\,T'_{\mathrm{R}}}\right]} \qquad (4)$$

Using $T_c = 23.2°$ $(\varphi_c)_{C_7F_{16}} = 0.45$ as the best estimated values and using 25° and $\varphi_{C_7F_{16}} = 0.45$ as the fiducial state (A), the calculated ratios vary in the same manner as the experimental ratios, but considerably more rapidly with temperature and composition. If T_c were about 10–12°, the agreement would be substantially better, but there is no justification for using this latter value.

TABLE I

CALCULATED AND EXPERIMENTAL VALUES OF α/α_A

T, ° C.	$\varphi_{C_7F_{16}}$	(α/α_A) exp.	(α/α_A) calcd.	$(\alpha/\alpha_A)^a$
25	0.18	0.21	0.036	0.17
30	.45	.63	.28	.72
45	.45	.43	.10	.42

[a] Using $T_c = 10°$.

Part of the discrepancy is probably caused by averaging properties even over 1–2° in a region where they vary rapidly with temperature, and by the approximate solution theory used. Doubtless the major error is the assumption that the heats of transport are independent of temperature and composition in this region.

THE CRYSTAL STRUCTURE OF SODIUM AMIDE[1]

BY ALLAN ZALKIN AND DAVID H. TEMPLETON

University of California Radiation Laboratory and Department of Chemistry, Livermore and Berkeley, California

Received January 7, 1956

In a recent note, Juza, Weber and Opp[2] described the crystal structure of sodium amide. We studied the structure independently and arrived at the same arrangement of sodium and nitrogen atoms, but found slightly different values for the cell dimensions and atomic coördinates.[3,4]

Sodium amide was prepared by Dr. W. L. Jolly at the Livermore laboratory by the direct combination of molten sodium and ammonia gas at 300°.[5] The resulting material was a fused yellowish mass covered by a layer of unreacted sodium. The product was removed from its crucible for investigation in an argon-filled dry box. The yellowish white and opaque material when crushed was found to be very fragile and brittle. The resulting fragments were irregular with no apparent cleavage planes.

The search for a single crystal was a hit-or-miss affair. The material was ground and sieved; particles that would pass a 50-mesh sieve but not a 100-mesh one were collected. These chunks were sealed in capillaries of 0.2 to 0.3 mm. diameter and manipulated under a binocular microscope (36×) until an isolated fragment could be fixed in place by being jarred into a constricted portion of the capillary. Three suitable single crystals, isolated in this way, were mounted on a Weissenberg camera and photographed using Cu Kα radiation. By chance the three rotation axes were [110], [101] and [011].

A face-centered orthorhombic cell was obtained from the Weissenberg patterns. More precise dimensions for this cell were then derived from a powder pattern taken with Cr Kα radiation. These dimensions are compared in Table I with the data of Juza, Weber and Opp,[2] who chose a different orientation of the axes. Also listed in the tables are experimental densities and densities which we calculated for the two sets of data with 16 molecules per unit cell.

TABLE I

CELL DIMENSIONS AND DENSITY OF SODIUM AMIDE

	This work	Juza, Weber and Opp[2]
	$a = 8.964 \pm 0.003$ Å.	$b = 8.929$ Å.^{a}
	$b = 10.456 \pm 0.003$	$c = 10.427$
	$c = 8.073 \pm 0.003$	$a = 8.060$
Density		
(expt.)	1.40^b	1.39^c
(calcd.)	1.37	1.38

[a] Converted from kX. units; last digit in doubt. [b] By flotation. [c] By pycnometer.

The systematic absences correspond to certain special positions in space group Fddd--D^{24}_{2h}. It was easy to show, as described elsewhere,[4] that the sodium and nitrogen positions are

16 Na in (f): $\pm(0, y, 0;\ 1/4, 1/4 + y, 1/4) + F$
16 N in (g): $\pm(0, 0, z;\ 1/4, 1/4, 1/4 + z) + F$

in agreement with Juza, Weber and Opp, taking account of the different assignment of axes. Approximate values of y and z from inspection of the intensities were 0.15 and 0.25. The structure was refined by one-dimensional Fourier calculation of the electron density along $(0,y,0)$ and $(0,0,z)$. The intensities used were obtained mostly from the best set of Weissenberg patterns, which were for rotation about [011], by visual comparison with a set of standard exposures. Layers zero through three were used. They were normalized to a common basis by means of equivalent reflections which fell in different layers for this orientation.

Figures 1 and 2 show the electron density along the b- and c-axes, respectively. The parameters chosen, after a minor backshift correction, are $y = 0.146$ and $z = 0.236$, compared with 0.142 and 0.233 by Juza and co-workers.[2] The structure factors calculated for this final structure using Na^+ and N atomic form factors,[6,7] were also used to calculate

---

(1) This research was performed under the auspices of the U. S. Atomic Energy Commission.

(2) R. Juza, H. H. Weber and K. Opp, *Naturwissenschaften*, **42**, 125 (1955).

(3) A. Zalkin and D. H. Templeton, Abstracts, Summer Meeting American Crystallographic Association, Pasadena, California, 1955.

(4) A. Zalkin and D. H. Templeton, U. S. Atomic Energy Commission Report UCRL-4557 (1955).

(5) L. M. Dennis and A. W. Browne, "Inorganic Syntheses," Vol. 1, McGraw-Hill Book Co., New York, N. Y., 1939.

(6) "International Tabellen zur Bestimmung von Kristallstrukturen," Vol. II, Bornträger, Berlin, 1935.

(7) J. A. Hoerni and J. A. Ibers, *Acta Cryst.*, **7**, 744 (1954).

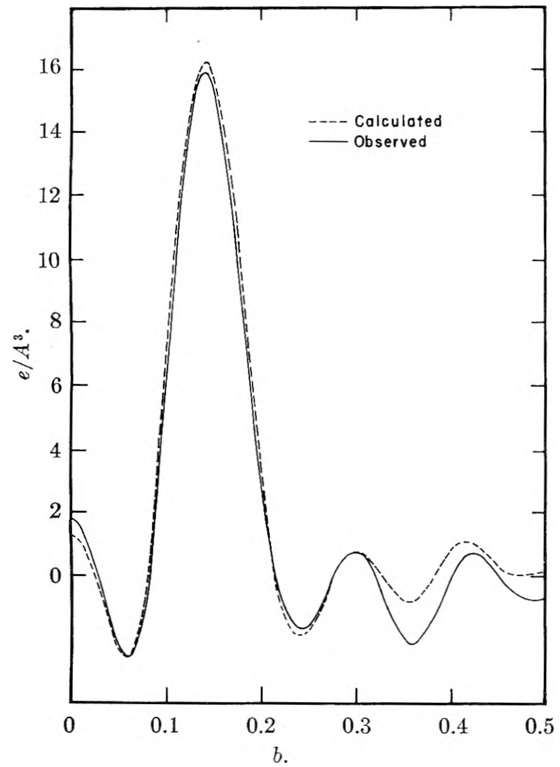

Fig. 1.—Electron density distribution along the *b* axis.

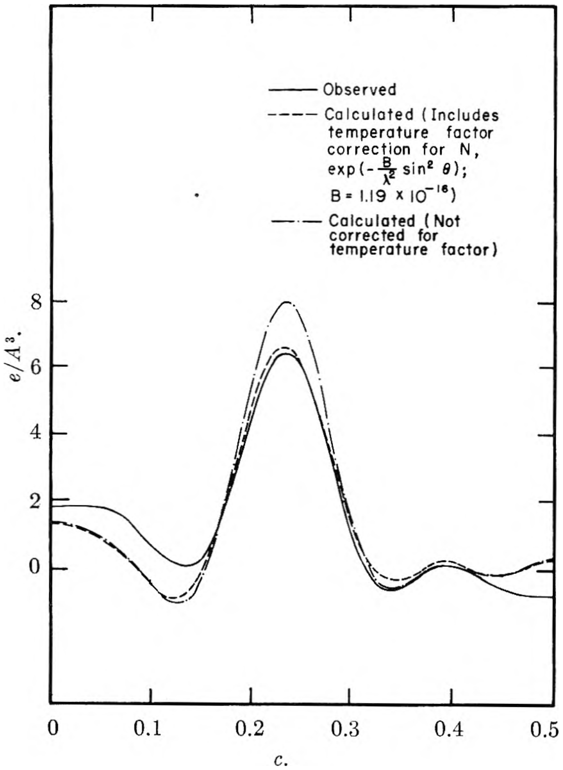

Fig. 2.—Electron density distribution along the *c* axis.

electron densities, which are included in the figures for comparison. In order to get coincidence of the curves it was necessary to include a temperature factor, exp $(-B \sin^2\theta/\lambda^2)$ with $B = 1.19 \times 10^{-16}$ for nitrogen, but a factor of unity for sodium. For 126 reflections permitted by the reflection rules, including zero ones, R is calculated as 26.5.[8] The standard errors in y and z, by the method of Cruikshank,[9] are 0.001 and 0.005, respectively. The complex shape of the anhedral crystal made absorption correction prohibitively difficult; this was not attempted, although it is recognized as an important omission.

We calculate the following interatomic distances

2 Na–N	2.44 Å.	(2.38, ref. 2)
2 Na–N	2.49	(2.50, ref. 2)
2 Na–Na	3.05	
1 Na–Na	3.06	
1 N–N	3.81	
2 N–N	3.88	
4 N–N	3.99	
2 N–N	4.11	

The minimum nitrogen–nitrogen distance of 3.81 Å. is much longer than that of the weak hydrogen bonds in solid ammonia, 3.38 Å. or the even shorter hydrogen bonds observed in other compounds.[10] Thus there are no hydrogen bonds in this structure, as is also true of lithium amide.[11]

Each sodium atom has four nitrogen nearest neighbors and *vice versa*. The four nitrogen neighbors have a nearly regular tetrahedral arrangement around the sodium atom as shown in Fig. 3A, but the four sodium neighbors of a nitrogen have a highly distorted tetrahedral arrangement as shown in Fig. 3B. These sodium atoms are concentrated toward one side of the nitrogen, and the packing in a model shows vacant holes on the opposite side of the nitrogen. It is suggested that the hydrogen atoms, being less negative than the nitrogen, will be located on the side away from the sodium neighbors, in positions described below.

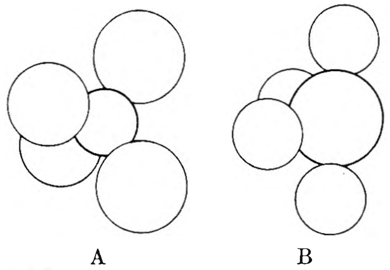

Fig. 3.—Coördination geometry in sodium amide: A, nitrogen configuration about sodium; B, sodium configuration about nitrogen.

The sodium–nitrogen distances correspond to a radius of about 1.60 Å. for the amide ion, corrected to coördination six by Zachariasen's[12] method. This value is reasonable but not necessarily very significant because of the peculiar coördination geometry.

Since the amide ion is isoelectronic with water, it is expected to have a bond angle slightly greater than a right angle. Thus the two hydrogen atoms must be in general positions related by the twofold axis, since special positions would require the molecule to be linear. With reasonable estimates of

---

[8] A table of calculated and observed structure factors is available upon request from the authors; it is also given in ref. 4.

[9] D. W. J. Cruikshank, *Acta Cryst.*, **2**, 65 (1949).

[10] J. M. Robertson, "Organic Crystals and Molecules," Cornell University Press, Ithaca, N. Y., 1953, p. 244.

[11] R. Juza and K. Opp, *Z. anorg. allgem. Chem.*, **266**, 313 (1951).

[12] W. H. Zachariasen, "American Crystallographic Association Meeting Abstracts," Pennsylvania State College, April 1950.

the dimensions of the amide ion, we investigated the packing of the hydrogen atoms with those from the neighboring amide ions and with the neighboring sodium atoms. For reasonable interatomic distances free rotation is impossible. The best packing was achieved with hydrogen parameters

$$x = 0.08$$
$$y = -0.03$$
$$z = 0.32$$

This arrangement gives for the minimum distances

H-N = 1.01 Å. (covalent bond, assumed)
H-H = 1.6 Å. (hydrogens of same amide ion, assumed)
H-H = 2.3 Å. (hydrogens of neighboring amide ions)
H-Na = 2.2 Å.

Figure 4 illustrates the hydrogen atom packing.

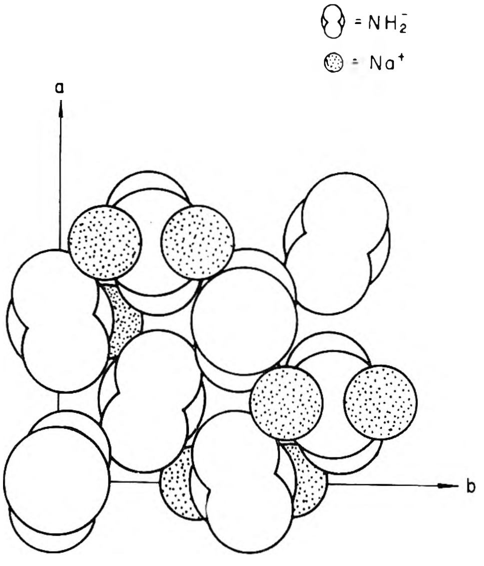

Fig. 4.—Hydrogen packing in sodium amide.

Powder patterns of this material photographed at approximately −120 and 160° indicated no structural change from room temperature.

We are indebted to Dr. W. L. Jolly and Mr. Saul Siegel for providing the pure samples and to Dr. E. R. Bissell for the density measurements.

DIFFUSION-RECOMBINATION IN DECOMPOSITION OF ACETYL PEROXIDE[1]

By James R. Nash, William H. Hamill and Russell R. Williams, Jr.

Contribution from the Radiation Project, Department of Chemistry, University of Notre Dame, Notre Dame, Indiana

Received January 9, 1956

It has been suggested by Levy and Szwarc[2] and further demonstrated by Rembaum and Szwarc[3] that ethane production in thermal decomposition of acetyl peroxide in various solvents results from a "cage" recombination of methyl radicals produced in dissociation of a single molecule of peroxide. The ratio C_2H_6/CO_2 is independent of the concentration of scavenger solutes, *e.g.*, iodine, at moderate concentrations in solution, but strongly dependent in gas phase decompositions.

It appeared to us that the production of ethane in solution is an example of diffusion recombination such as we have studied in other systems and that at higher concentrations of iodine a decrease in ethane yield should occur and be susceptible to treatment by our semi-empirical equation.[4]

Acetyl peroxide, obtained as a 25% solution in dimethyl phthalate, by courtesy of the Buffalo Electrochemical Co., was decomposed at *ca.* 0.01 *M* in toluene at 70 and 85°. Initial concentration of peroxide was determined by iodometry.[5] Product gases were collected, measured and subjected to mass spectrometric analysis. In several experiments, with and without added iodine, the first-order rate of production of carbon dioxide was verified. A rate constant of 1.53×10^{-5} sec.$^{-1}$ at 70° and an activation energy of 30.4 kcal./mole were obtained, in satisfactory agreement with previous work.[6]

The ratio of ethane to carbon dioxide was determined at iodine concentrations up to 0.1 *M*. The ratio decreased with increasing iodine concentration but showed no measurable change with temperature.

Since we have shown that carbon dioxide production is not affected by iodine, it follows that the efficiency of the "cage" recombination of methyl radicals is being diminished by iodine. The diffusion-recombination equation previously developed[4] has been applied to this phenomenon by taking $2C_2H_6/CO_2$ to be the efficiency of recombination of methyl radicals, $W_\infty(X)$. Figure 1 shows that log $(1 - W_\infty(X))$ is a linear function of $(X_{I_2})^{1/2}$ as indicated by the equation. Assuming that no primary (*i.e.*, non-diffusive) recombination occurs, the intercept yields $P_1\ (5.75\ \gamma\rho_0)^{-1} = 0.033$ and the slope yields $P_1P_2^{1/2}\ (3.24\ \gamma^2) = 0.17$, where γ is the mean free distance of diffusion and ρ_0 the distance of

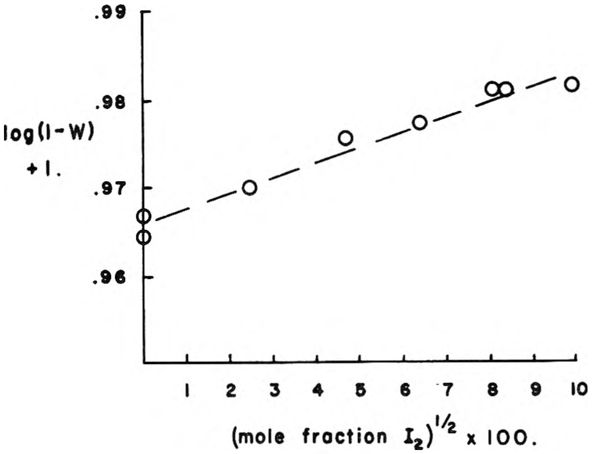

Fig. 1.—Decomposition of acetyl peroxide in toluene solution; $W = 2C_2H_6/CO_2$.

---

[1] Work supported in part by the U. S. AEC under contract At(11-1)-38 and U. S. Navy equipment loan contract Nonr-06900. Presented at the 129th Meeting of the American Chemical Society, Dallas, Tex., April 8-13, 1956.

[2] M. Levy and M. Szwarc, *J. Am. Chem. Soc.*, **76**, 5981 (1954)

[3] A. Rembaum and M. Szwarc, *ibid.*, **77**, 3486 (1955).

[4] (a) J. C. Roy, R. R. Williams, Jr., and W. H. Hamill, *ibid.*, **76**, 3274 (1954); (b) J. C. Roy, W. H. Hamill and R. R. Williams, Jr., *ibid.*, **77**, 2953 (1955).

[5] C. D. Wagner, R. H. Smith and E. D. Peters, *Ind. Eng. Chem., Anal. Ed.*, **19**, 976 (1947).

[6] M. Levy, M. Steinberg and M. Szwarc, *J. Am. Chem. Soc.*, **76**, 5978 (1954).

initial displacement of the radicals in units of collision diameters of the radicals. P_1 and P_2 are the probabilities of reaction between, respectively, two free radicals and free radical with iodine upon encounter. While we have no independent evaluation of these factors, they are not likely to be much less than unity. Taking $P_1 = P_2 = 1$ we find $\gamma = 1.35$ and $\rho_0 = 3.9$. These values are larger than those observed in some other systems[4,5,7] but are consistent with the configuration of the acetyl peroxide molecule and the size of the solvent molecule, since the unit of measurement refers to the methyl radical.

(7) J. C. Roy, J. R. Nash, R. R. Williams, Jr., and W. H. Hamill, *J. Am. Chem. Soc.*, **78**, 519 (1956).

ADSORPTION OF NITROGEN ON PURE SODIUM CHLORIDE

BY DONALD S. MACIVER AND PAUL H. EMMETT[1]

Contribution from Multiple Fellowship of Gulf Research & Development Company, Mellon Institute, Pittsburgh, Pa.

Received January 14, 1956

The Brunauer–Emmett–Teller[2] method of determining the surface area of solids by means of isothermal gas adsorption measurements has been found to be applicable to a wide variety of adsorbent–adsorbate systems. Recently, however, Young and Benson[3] have reported that the BET plot of nitrogen adsorption at −195° on very pure sodium chloride exhibits a negative intercept. This effect, if real, would seem to indicate a breakdown of the BET equation when applied to this system. Therefore, in order to determine the reality of the effect reported by Young and Benson and to explain their results, we have studied the adsorption of nitrogen on sodium chloride at −195° in the pressure region in which the BET equation should be applicable.

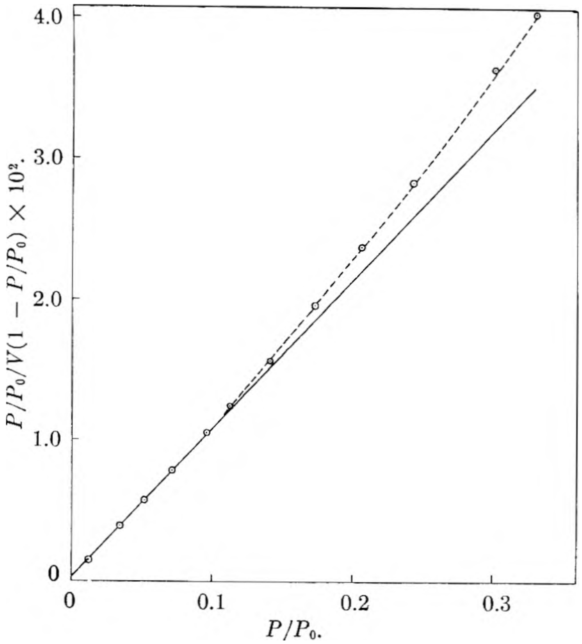

Fig. 1.—BET plot of nitrogen adsorption on sodium chloride at −195°.

Experimental

The sodium chloride employed in this work was provided by Dr. G. C. Benson and was prepared by electrostatically precipitating the fumes from molten sodium chloride.[4] Prior to the adsorption measurements the adsorbent was transferred in an atmosphere of dry nitrogen from the evacuated, sealed-off bulb in which it was received to a suitable sample tube.

The volumetric adsorption apparatus employed in the present work was similar to the one described frequently in the literature.[5-7] The nitrogen used for adsorption measurements was of high purity grade from Linde Air Products Company and was freed of condensable impurities by passage over glass beads at −195°; the helium, for calibrational purposes, was from the Air Reduction Company and was purified by passage over degassed charcoal at −195°.

Prior to the adsorption measurements the sample was evacuated at room temperature to a pressure of 10^{-5} mm.; the evacuation was continued until such time as the rate of gas evolution from the sample was negligible. It was necessary to avoid the use of high temperatures in the degassing process in order to prevent any sintering of the sample. A nitrogen adsorption isotherm was then run at −195°. The BET plot of the adsorption data is given in Fig. 1. The straight line obtained up to a relative pressure of about 0.1 had an intercept of 3×10^{-4} and a slope of 0.105. From these, a "c" value of 351 and a V_m of 9.49 cc. (STP)/gram was calculated. The latter value corresponds to a surface area of 41.7 m.^{2}/gram, if the adsorbed nitrogen molecule has a cross-sectional area of 16.2 Å.^{2}.

Discussion

It is obvious from Fig. 1 that the BET plot for this system tends to deviation from linearity at a fairly low relative pressure. Instead of the customary linear portion extending from relative pressures of 0.05 to 0.35 we find one extending from relative pressures of 0.01 to 0.10. Young and Benson made their adsorption measurements at relative pressures of 0.06 to 0.28. As can be seen from Fig. 1 the points from 0.06 to 0.20 lie in a fairly straight line due to the small second derivative of the broken curve. Consequently, if one had only those points measured by Young and Benson one would naturally take the 0.06 to 0.20 region as linear and conclude from this that the plot had a negative intercept. From the curve in Fig. 1, however, one can say that the linear part of the BET plot between relative pressures 0.01 and 0.1 gives a positive intercept and a reasonable surface area. Furthermore, this linear part of the curve extends as it should from a little below to a little above the relative pressure (0.05 in this case) corresponding to a monolayer. It would appear that on certain crystals having smooth faces with very little heterogeneity, adsorption data tend to deviate from the behavior expected, in the direction of tending to give a stepwise adsorption isotherm. This reflects itself in the BET plots by a departure from linearity at relative pressures that are considerably lower than those at which the BET plots ordinarily cease to be linear when nitrogen is used as the adsorbate. In systems of this nature it therefore seems advisable to extend the adsorption measurements to relative pressures low enough to make sure that one is deal-

---

(1) Johns Hopkins University, Baltimore, Md.

(2) S. Brunauer, P. H. Emmett and E. Teller, *J. Am. Chem. Soc.*, **60**, 309 (1938).

(3) D. M. Young and G. C. Benson, private communication.

(4) D. M. Young and J. A. Morrison, *J. Sci. Instr.*, **31**, 90 (1954).

(5) P. H. Emmett, "Am. Soc. Testing Materials, Symposium on New Methods for Particle Size Determination," 1941, p. 95.

(6) P. H. Emmett, *Advances in Coll. Sci.*, **1**, 1 (1942).

(7) P. H. Emmett and S. Brunauer, *J. Am. Chem. Soc.*, **56**, 35 (1934).

ing with the linear portion of the BET plot that includes the relative pressure at which a statistical monolayer is obtained.

THE DECOMPOSITION OF MALONIC ACID IN GLYCEROL AND IN DIMETHYL SULFOXIDE

By Louis Watts Clark

Contribution from the Department of Chemistry, Saint Joseph College, Emmitsburg, Maryland

Received January 18, 1956

A number of investigators have made kinetic studies on the thermal decomposition of malonic acid alone and in solution.[1] Although it is well known that malonic acid, like oxalic acid, is smoothly decarboxylated in glycerol, the kinetics of the reaction in that solvent have not been previously reported.

Preliminary studies in this Laboratory revealed the interesting fact that the solvent, dimethyl sulfoxide, likewise promotes the decomposition of malonic acid, and does so even more efficiently than glycerol.

The kinetics of the decomposition of malonic acid in these two solvents have been carefully studied in this Laboratory, and results of this investigation are reported herein.

Experimental

Reagents.—C.P. malonic acid was further purified by recrystallization from ether. The purity of the reagent was demonstrated by the fact that the volume of carbon dioxide evolved from every quantitative sample in the decarboxylation experiments was invariably stoichiometric.

Dimethyl Sulfoxide (99.9% pure), and glycerol, Analytical Reagent Grade, 95% by volume, were also used in these experiments.

Apparatus and Technique.—The apparatus and technique used in these experiments have been previously described.[2]

Decomposition of Malonic Acid in Glycerol.—At the beginning of each experiment 100 ml. of glycerol was placed in the dry reaction flask in the thermostated oil-bath. A 0.1671-g. sample of malonic acid (sufficient to yield 36.0 ml. of CO$_2$ at STP on complete reaction) was placed in a thin glass capsule (blown from 6 mm. soft glass tubing and weighing approximately 0.2 g.) and introduced at the proper moment into the solvent in the manner previously described. The rapidly rotating mercury seal stirrer immediately crushed the capsule, the contents were dissolved and mixed in the solvent, and reaction began. The evolved carbon dioxide was measured at constant pressure.

The above procedure was repeated at eight different temperatures between 150–160°. Every sample of malonic acid yielded the stoichiometric volume of carbon dioxide within experimental error. For example, the final observed volume of gas at STP produced by one sample at 154.3° was 35.6 ml.; at 156.0°, 36.0 ml.; at 156.3°, 35.9 ml.; at 159.9°, 36.0 ml.; at 161.0°, 36.0 ml. Duplicate and triplicate runs at the same temperature showed excellent reproducibility.

Decomposition of Malonic Acid in Dimethyl Sulfoxide.—At the beginning of each experiment 100 ml. of dimethyl sulfoxide was saturated with dry carbon dioxide gas and placed in the reaction flask in the thermostated oil-bath. Samples of malonic acid weighing 0.1671 g. were added to the solvent and the evolved gas measured as described above. The experiment was repeated at five different temperatures between 130–140°. Every sample invariably yielded the stoichiometric volume of carbon dioxide allowing for the experimental error. For example, the final observed volume at STP produced by one sample at 129.8° was 36.1 ml.; at 134.3°, 35.5 ml.; at 138.8°, 36.0 ml. Reproducibility was excellent.

Results and Discussion

The experimental data were converted to standard conditions and milliliters of evolved gas was plotted against time for each temperature. Values of x corresponding to different values of t were obtained from the resulting isotherms. Log $(a - x)$ was then plotted against t (a is the theoretical stoichiometric volume of carbon dioxide, 36.0 ml.). The points thus obtained for the middle 80% of the reaction fell on perfectly straight lines in every experiment. This fact indicates that the decomposition of malonic acid in glycerol, as well as in dimethyl sulfoxide, is a first-order reaction.

From the slopes of the lines thus obtained the specific reaction velocity constants for the decomposition of malonic acid in the two solvents were calculated for the various temperatures.

For the case of the decomposition of malonic acid in glycerol, the temperatures studied, as well as the corresponding specific reaction velocity constants in sec.$^{-1}$, were as follows: 152.2°, 0.00364; 154.1°, 0.00413; 155.7°, 0.00470; 156.3°, 0.00483; 158.1°, 0.00513; 159.0°, 0.00570; 159.9°, 0.00578; 161.0°, 0.00666. Results for the case of the decomposition of malonic acid in dimethyl sulfoxide were as follows: 129.8°, 0.00416; 131.3°, 0.00490; 134.3°, 0.00618; 137.0°, 0.00740; 138.8°, 0.00845.

A straight line was obtained in each case when log k was plotted against $1/T$ according to the Arrhenius equation. From the slopes of the lines thus obtained the energy of activation and the frequency factor for the reaction in each solvent was calculated. For the decomposition of malonic acid in glycerol these were found to be 25,500 cal., and 5.3×10^{10}, respectively; for the decomposition of malonic acid in dimethyl sulfoxide corresponding values were 23,350 cal., and 2.3×10^{10}, respectively.

The temperature coefficient for the reaction in glycerol was found to be 2.11, in dimethyl sulfoxide 2.26.

The enthalpy of activation, entropy of activation and free energy of activation at 140°, according to the Eyring equation, were found to be as follows: for the decomposition of malonic acid in glycerol, 24,600 cal., −12.2 e.u., and 29,650 cal., respectively; for the decomposition of malonic acid in dimethyl sulfoxide, 22,300 cal., −15.0 e.u., and 28,350 cal., respectively.

It is of interest to compare the rate of reaction in the two solvents at some particular temperature. At 140°, k for malonic acid in glycerol is 0.0013, for malonic acid in dimethyl sulfoxide it is 0.0092. Therefore, malonic acid decomposes seven times as fast in dimethyl sulfoxide as it does in glycerol at this temperature.

It is also of interest to ascertain how the values of k in these two solvents compare with that for the pure acid for a given temperature.

By melting one-half mole (53 g.) of the pure acid

---

[1] (a) J. Laskin, *Trans. Sib. Acad. Agr. For.*, **6**, No. 1 (1926); *C.A.*, **23**, 1804 (1926); (b) J. Bigeleisen and L. Friedman, *J. Chem. Phys.*, **17**, 998 (1941); (c) G. A. Hall, Jr., *J. Am. Chem. Soc.*, **71**, 2691 (1949); (d) J. G. Lindsey, A. N. Bournes and H. G. Thode, *Can. J. Chem.*, **29**, 192 (1951); (e) J. G. Lindsey, A. N. Bournes and H. G. Thode, *ibid.*, **30**, 163 (1952).

[2] (a) H. N. Barham and L. W. Clark, *J. Am. Chem. Soc.*, **73**, 4638 (1951); (b) L. W. Clark, *ibid.*, **77**, 3130 (1955); (c) **77**, 6191 (1955).

and measuring the evolved gas at 140° a value of k of 0.00025 sec.$^{-1}$ was obtained, a result which agrees with that reported by J. Laskin.[1a] Therefore, at this temperature, malonic acid decomposes about five times as fast in glycerol, and 37 times as fast in dimethyl sulfoxide, as it does alone.

BOILING POINT-COMPOSITION DIAGRAM FOR THE SYSTEM 1,4-DIOXANE-n-BUTYL ALCOHOL

By James B. McCormack, John H. Walkup and R. I. Rush

Chemistry Laboratory, Centre College of Kentucky, Danville, Ky.

Received January 23, 1956

In order to extend information previously obtained in this Laboratory[1] the boiling point-composition diagram for the system 1,4-dioxane-n-butyl alcohol has been determined. The dioxane and n-butyl alcohol were purified by methods described elsewhere,[1] and the determinations were carried out in an Othmer equilibrium still.[2] The pressure was maintained at 760 mm. of mercury by means of a Cartesian manostat.[3] Equilibrium was assumed to be attained when samples checked on the refractometer had a constant reading, and the composition of the samples was determined from a refractive index-composition curve.[1] The boiling point was read with an accuracy of ±0.05°. The data secured are given in Table I and also presented graphically.

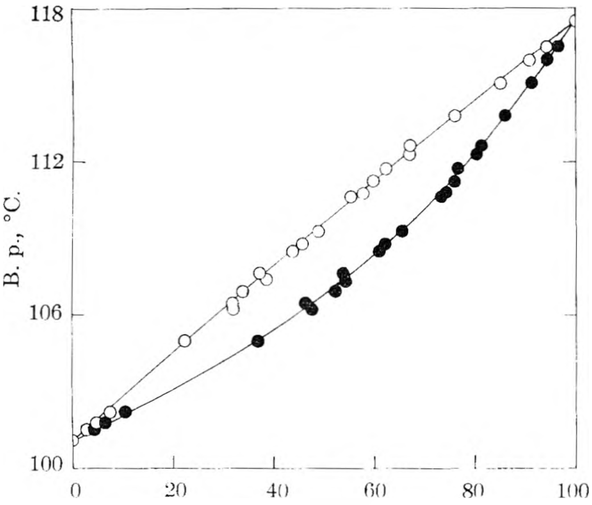

Fig. 1 —Boiling point-composition diagram for the system 1,4-dioxane-n-butyl alcohol.

TABLE I

BOILING POINT-COMPOSITION DATA FOR THE n-BUTYL ALCOHOL-1,4-DIOXANE SYSTEM AT ONE ATMOSPHERE PRESSURE

B.p., °C.	Composition (wt. % alcohol)		B.p., °C.	Composition (wt. % alcohol)	
	Vapor	Liquid		Vapor	Liquid
101.1	0.0	0.0	109.3	48.9	65.4
101.5	3.0	4.5	110.55	55.4	73.2
101.8	4.9	6.7	110.8	57.8	74.2
102.2	7.5	10.7	111.25	59.8	75.8
105.0	22.2	36.8	111.65	62.3	76.3
106.25	31.9	47.5	112.3	67.0	80.1
106.5	31.6	46.1	112.65	67.0	81.1
106.95	33.8	52.1	113.8	75.8	85.9
107.35	38.0	54.4	115.1	85.0	91.2
107.4	38.8	54.4	116.0	90.6	94.2
107.55	37.2	53.6	116.5	94.2	96.4
108.5	43.8	60.8	117.5	100.0	100.0
108.8	45.6	62.2			

---

[1] R. I. Rush, D. C. Ames, R. W. Horst and J. R. McKay, THIS JOURNAL, in press (1956).

[2] D. F. Othmer, *Anal. Chem.*, **20**, 763 (1948).

[3] R. Gilmont, *Ind. Eng. Chem., Anal. Ed.*, **18**, 633 (1946).

RADIOLYSIS OF ETHANE: MOLECULAR DETACHMENT OF HYDROGEN

By Leon M. Dorfman

General Electric Research Laboratory Schenectady, New York

Received January 24, 1956

The chief products in the radiolysis of ethane are hydrogen and a polymeric liquid,[1,2] the yield for hydrogen formation being approximately 3.9 molecules/100 e.v.[2,3] This note reports the results of experiments which show that a large fraction of the hydrogen is formed intramolecularly by direct detachment of molecular hydrogen without the apparent intermediate formation of single atoms of hydrogen.

Molecular detachment of hydrogen is inherent in one of the seven primary processes suggested by Williams and Essex,[4] namely, direct formation of hydrogen and ethylene ion, based on the observed[5] mass spectral pattern of ethane. The hydrogen may be released from an excited ethane molecule or ion. It may originate from more complex ions which can be formed in ion-molecule reactions which occur with high efficiency as shown recently by Stevenson and Schissler.[6]

The data which follow provide no information concerning the nature of the transitory entity from which the hydrogen is released. They indicate only the fraction of the total hydrogen formed by molecular detachment.

In these experiments a number of mixtures of deuteroethane and normal ethane have been irradiated in a 1 Mev. electron beam and the hydrogen isotope fraction analyzed mass spectrometrically. The degree of isotopic randomization of the hydrogen is a measure of the relative occurrence of single-atom reactions and molecular detachment if it is known that secondary exchange produces no appreciable isotopic mixing.

Experimental

The deuteroethane was obtained from Tracerlab, Inc. It contained 98 ± 1 isotopic per cent. deuterium as determined mass spectrometrically. The deuteroethane was degassed at $-195°$, then fractionated twice by bulb-to-bulb

---

[1] W. Mund and W. Koch, *Bull. soc. chim. Belg.*, **34**, 119 (1925).

[2] S. C. Lind and D. C. Bardwell, *J. Am. Chem. Soc.*, **48**, 2335 (1926).

[3] L. M. Dorfman, F. J. Shipko and C. F. Pachucki, to be published.

[4] N. T. Williams and H. Essex, *J. Chem. Phys.*, **17**, 995 (1949).

[5] J. A. Hipple, Jr., *Phys. Rev.*, **53**, 530 (1938).

[6] D. P. Stevenson and D. O. Schissler, *J. Chem. Phys.*, **23**, 1353 (1955).

TABLE I

ELECTRON IRRADIATION OF C_2H_6–C_2D_6 MIXTURES

Run no.	Total press (mm.)	Mole fraction C_2H_6	Mole fraction C_2D_6	Irradiation time (min.)	Hydrogen, micromoles	Isotopic analysis H_2	Isotopic analysis HD	Isotopic analysis D_2	$x = 1 - \left[\frac{(HD)^2}{[(H_2)(D_2)K_e]}\right]^{1/2}$
1	743.2	0.519	0.481	2.0	3.6	0.481	0.260	0.259	0.59
2	692.6	.468	.532	1.0	2.1	.427	.273	.300	.58
3	690.0	...[b]	...	3.0	5.1	.433	.251	.316	.62
4[a]	683.7	.506	.494	2.0	7.4	.492	.226	.282	.66
5	720.5	.413	.587	0.25	5.4	.371	.255	.374	.62
6	720.0	...[b]	...	0.25	0.7	.395	.247	.358	.64
7	546.2	.498	.502	0.25	0.6	.480	.246	.274	.62

[a] 10 microns of oxygen added. [b] Hydrocarbon mixture from previous run used again after removing H_2.

distillations at −140 to −150°. The presence of any higher hydrocarbons was not detectable in a mass spectrometric analysis. The normal ethane used was Phillips' research grade. It was similarly degassed and distilled.

Two separate radiation cells were used. Each was a cylindrical glass cell with a 2 mil thick stainless steel window fastened to a Fernico seal. The cells were 20 mm. in diameter with over-all volumes of 49.0 and 60.2 cc. Each cell was closed off by a vacuum stopcock. The irradiations were carried out by placing the cell in a collimated electron beam emitted from a resonant transformer which has been described.[7] The electron energy within the tube was 1 Mev. The beam traversed two 2 mil steel windows, that of the exit tube and of the cell, so that the energy of the electrons incident on the gas was approximately 0.8 Mev.

The irradiation times were varied from 15 seconds to 3 minutes. The conversion of the ethane in any run was always less than 0.3%. The actual amount of hydrogen formed varied from 0.6 to 7 micromoles. After the irradiation the ethane was condensed at −195° and the small amount of hydrogen removed by means of a toepler pump. The pressure was measured and the gas analyzed in a General Electric analytical mass spectrometer. Samples of the hydrocarbon mixture were also analyzed before and after two of the runs.

Results and Discussion

The details of seven runs are given in Table I. The composition of the ethane–deuteroethane mixtures is indicated in cols. 3 and 4. In runs no. 3 and 6 the hydrocarbon mixture remaining from the previous runs was used again. In run no. 4, oxygen, at a pressure of 10 μ, was deliberately added as an inhibitor to reduce the rate of any chain exchange reaction which might conceivably occur. The actual amounts of hydrogen isotopes formed in the radiolysis are shown in col. 6. In runs no. 6 and 7 the amount of hydrogen was so small that separation by means of a toepler pump was not carried out. Instead the irradiation cells were connected to the mass spectrometer manifold, the ethane frozen at −195°, and the hydrogen released directly into the manifold. For these two analyses the conventional expansion bulb of the mass spectrometer was replaced by a suitably small bulb.

As may be seen from the isotopic analysis, the hydrogen formed in the radiolysis shows a marked preponderance of the unmixed molecules. There is thus a wide deviation from a randomized mixture. This can be interpreted most simply in terms of hydrogen formation by single-atom reactions and by a molecular process. For the case of a mixture of ethane and completely deuterated ethane the HD will be formed intermolecularly by reactions involving intermediate formation of atoms. The H_2 and D_2 will result from both inter- and intramolecular reactions. For the case of detachment from an ethane molecule or ion the fraction of these formed intramolecularly may be calculated from the deviation from equilibrium. This fraction will be given by

$$x = 1 - \left[\frac{(HD)^2}{(H_2)(D_2)K_e}\right]^{1/2}$$

where K_e is the equilibrium constant for the H_2–D_2 system and has the value[8] 3.25 at 25°. The values of x are given in the last col. of Table I. An average value in excess of 0.6 is obtained. This means that almost half the total hydrogen is formed in a molecular process. There is a small correction since the deuteroethane used is not completely deuterated and some HD can be formed molecularly. Thus, the fraction of the total hydrogen formed molecularly is at least 0.5, and even if some exchange occurs we can write

$$H_m \geq 0.5\,(H_m + H_a)$$

where H_m and H_a represent the fraction of hydrogen formed in molecular and atom reactions, respectively, since exchange will reduce the value of x.

All indications, however, seem to point to the fact that with the extremely small degree of conversion of the ethane, exchange did not play an important role. The fraction of HD formed did not change materially over a 12-fold variation in the amount of hydrogen formed and in the irradiation time. The addition, in run no. 4, of 10 μ of oxygen as an inhibitor did not drastically lower the fraction of HD formed, although it is possible that some atomic hydrogen did interact with the oxygen. And, finally, sampling of the hydrocarbon mixture after runs no. 1 and 3 indicated no measurable exchange according to mass spectrometer analysis. Thus for the simplest case, that of detachment from an ethane molecule or ion, one can justifiably write the equality

$$H_m = 0.5(H_m + H_a)$$

It is of interest in this connection to point out that the system $C_2H_4 + H_2$ is lower in energy than the system $C_2H_5 + H$ by over 2 e.v. And in general, systems resulting from molecular detachment of hydrogen will be lower in energy than those in which only atomic hydrogen is formed.

For the case of detachment from a more complex ion the interpretation of the foregoing data will be altered only in degree, to the extent that molecular detachment of hydrogen will be even more predominant over atom formation. If, for example, hydrogen were released from the mixed onium ions,

---

[7] E. E. Charlton and W. F. Westendorp, *Electronics*, **17**, 128, December (1944).

[8] H. C. Urey, *J. Chem. Soc.*, 562 (1947).

$C_2H_6D^+$ and $C_2D_6H^+$ this would lead to the possibility of HD formation by a molecular as well as single atom reaction. If the extreme assumption is made that all the hydrogen results from such an intermediate, the fraction of hydrogen formed intramolecularly is changed from 0.5 to 0.7. Any interpretation will lead to the conclusion that in the radiolysis of ethane, at least 50% of the hydrogen formed is detached molecularly.

From the data in Table I the relative rates of radiolysis of C_2H_6 and C_2D_6 can be deduced. Runs no. 1, 4 and 5 are most accurate for this purpose since the mass spectral sensitivities of the isotopes were determined on the same day the analyses were carried out. The rate of radiolysis of ethane to that of deuteroethane is found to be 1.5.

Acknowledgment.—I am indebted to Mr. P. C. Noble for carrying out the mass spectrometer analyses and to Mr. G. Schacher of the G. E. General Engineering Laboratory for analyzing the very small hydrogen samples.

HEAT CAPACITIES OF MULTIMOLECULAR LAYERS OF NITROGEN TRIFLUORIDE ADSORBED ON ANATASE[1]

By A. R. Siebert and E. L. Pace

Morley Chemical Laboratory, Western Reserve University, Cleveland 6, Ohio

Received January 28, 1956

In recent years, the detection of phase transitions in adsorbed films by heat capacity measurements has received considerable attention. Frederikse,[2] Morrison,[3] and Dennis[4] have reported transitions for helium, argon, nitrogen and methane, respectively, in the multimolecular region. In each case the phase transition appeared as maxima in the heat capacity *vs.* temperature curve.

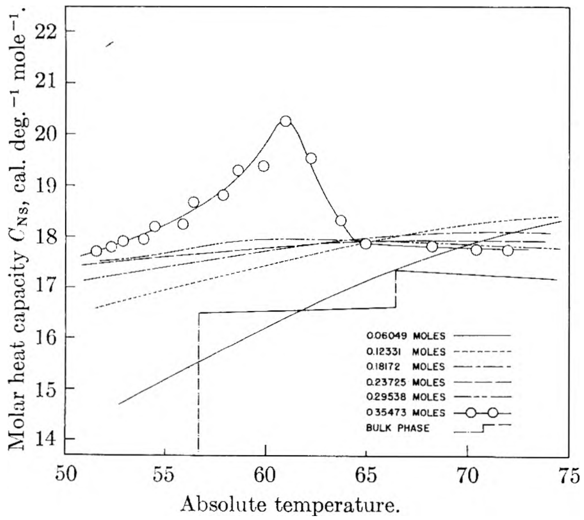

Fig. 1.—Multilayer heat capacities of nitrogen trifluoride adsorbed on anatase.

The present work describes the multimolecular heat capacities of nitrogen trifluoride adsorbed on anatase. Two regions of special interest are the solid transition (56.62°K.) and the triple point (66.37°K.). The range of temperatures therefore used for most of the measurements was 50 to 75°K. Coverages of 1.0 to 5.9 monolayers were run in this range. In order to investigate in more detail the nature of the transition corresponding to the solid transition in the bulk, one series of heat capacity measurements at a coverage of 4.0 monolayers was extended to 10°K. The calorimeter and procedure have been described.[5]

The surface area was obtained by the B.E.T. method using krypton; 0.05977 mole was found to constitute a monolayer. As the vapor pressures of nitrogen trifluoride[6] were negligible in the temperature range used, no desorption or heat of compression corrections were necessary.

The results of the heat capacity measurements are plotted in Fig. 1. The results are in general agreement with those reported by Dennis,[4] Morrison,[3] and Frederikse.[2]

The curves show a maximum near the triple point only for the coverage of 5.9 monolayer. Therefore, bulk behavior for nitrogen trifluoride begins between 4.9 and 5.9 monolayers. Bulk properties begin between 1.6 and 2.9 monolayers for argon and between 3 and 4 monolayers for methane. The heat capacity for lower coverages appears to be more similar to those for methane than those for argon. The heat capacity curves for argon, methane and nitrogen trifluoride in the monolayer region are above or nearly the same as those of the liquid phases, but the heat capacities of nitrogen in the monolayer region are decidedly below those of the bulk liquid phase.[7]

The partial molar heat capacities at 5.4 monolayers have been calculated using the data of the

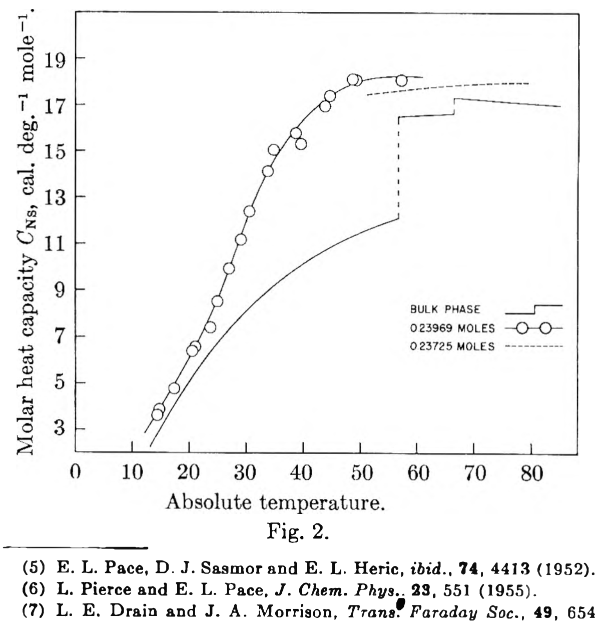

Fig. 2.

---

[1] This work was supported by the U. S. Atomic Energy Commission under Contract No. AT (30–1)-824. Some of the equipment used was loaned by the U. S. Office of Naval Research under Contract No. 182(00).

[2] H. P. R. Frederikse, *Physica*, **XV**, No. 10, 860 (1949).

[3] (a) J. A. Morrison and L. E. Drain, *J. Chem. Phys.*, **19**, 1063 (1951); (b) J. A. Morrison, L. E. Drain and J. S. Dugdale, *Can. J. Chem.*, **30**, 890 (1952).

[4] K. S. Dennis, E. L. Pace and C. S. Baughman, *J. Am. Chem. Soc.*, **75**, 3269 (1953).

[5] E. L. Pace, D. J. Sasmor and E. L. Heric, *ibid.*, **74**, 4413 (1952).

[6] L. Pierce and E. L. Pace, *J. Chem. Phys.*, **23**, 551 (1955).

[7] L. E. Drain and J. A. Morrison, *Trans. Faraday Soc.*, **49**, 654 (1953).

4.9 and 5.9 monolayer curves. The integral

$$\int_{50}^{66} (\bar{C}_{N_s} - C_p \text{ solid})\, dT = 120.9 \text{ cal.}$$

This is approximately of the order of the heat of fusion of 95.11 cal.[6] for nitrogen trifluoride. If the bulk liquid heat capacity is assumed to extend over the region from 50 to 66°K., then the integral is equal to 96.2 cal., a value nearly equal to the heat of fusion.

No transition in the adsorbed phase corresponding to the solid transition was observed. This result is of special interest as the heat of transition for nitrogen trifluoride is approximately four times as great as the heat of fusion.[6] Pierce[8] attempted to supercool the high temperature crystalline form of nitrogen trifluoride to 10°K. without success. It is apparent from the heat capacity curve at a coverage of 4 monolayers shown in Fig. 2 that it was possible to accomplish this supercooling for the nitrogen trifluoride as a physically adsorbed phase.

(8) Louis Pierce, Doctoral Thesis, Western Reserve University, 1954.

ON THE AGGREGATION OF BOVINE SERUM ALBUMIN IN ACID *p*H

BY MARTIN J. KRONMAN, MALVIN D. STERN[1] AND SERGE N. TIMASHEFF

Department of Chemistry, Temple University, Philadelphia, Pennsylvania
Eastern Regional Research Laboratory[2]
Philadelphia 18, Pennsylvania

Received February 8, 1956

The effects of low and high *p*H on the state of aggregation of bovine serum albumin have been the subject of a number of recent publications.[3–5] It is the purpose of this communication to report on some light scattering and ultracentrifugal measurements carried out on crystallized Armour bovine plasma albumin (BSA) in the *p*H range of 3 to 5 as a function of ionic strength, *p*H, preliminary deionization of the protein solution,[6] and length of time that the protein solution was permitted to remain at room and refrigerator temperatures.

The light scattering data obtained as a function of angle were measured on an instrument whose calibration was described in a recent publication,[7] while the light scattering experiments carried out as a function of concentration at 90° were performed in the previously used photometer[8,9] with a 3-ml. cell[10] on solutions cleared for light scattering as previously described.[11] The ultracentrifugal measurements were carried out at room temperature in a Spinco Model E analytical ultracentrifuge at 59,780 r.p.m.

The results of the multiangle light scattering experiments as a function of time are shown in Figs. 1 and 2. The curves in Fig. 1 were obtained using non-deionized BSA in *p*H 4.0 acetate buffer of 0.20 ionic strength. Curves A and B were obtained with a 2.1% protein solution, A at 325 to 650 sec. after dilution, and B at 4,500 to 4,600 sec. This solution was then diluted in the cell with clean buffer and filtered. The light scattering results obtained with the resulting 0.78% protein solution are shown by curves C and D, obtained at 8,000 and 20,000 sec., respectively. While curves A and B indicate an increasing molecular weight[12] and dissymmetry with time, curves C and D show a disaggregation and disappearance of very large aggregates upon dilution as evidenced by the great reduction of dissymmetry in these measurements. Similar results were obtained with another non-deionized solution at *p*H 4.0 which, however, had not been filtered after dilution, as well as with a non-deionized BSA solution in *p*H 5.0 acetate buffer of 0.20 ionic strength.

When an experiment was carried out with deionized BSA in *p*H 4.5 acetate buffer of 0.20 ionic strength no change in turbidity or appearance of dissymmetry occurred upon standing for close to 4.5 hours at room temperature.

In Fig. 2 are presented the low *p*H multiangle light scattering results obtained with two deionized preparations of BSA. The stock solution of protein was deionized at room temperature and lyophilized prior to use. In the first experiment, shown by curves A and B of Fig. 2, the lyophilized protein was dissolved in a 0.20 *M* NaCl solution of *p*H 3.0 and permitted to stand overnight at refrigerator temperature. This was then brought to room temperature, filtered and diluted to the concentration of the measurement. The results indicate that a considerable degree of aggregation occurs with standing at room temperature. The angular envelope, however, shows little dissymmetry.[16] Thus, immediately after dilution, the molecular weight was 100,000. This value had increased to 111,000 after 3.5 hours of standing

---

[1] The research work reported here from Temple University was supported by a grant to M. D. Stern from the Research Corporation, New York, New York.

[2] One of the laboratories of the Eastern Utilization Research Branch, Agricultural Research Service, U. S. Department of Agriculture.

[3] M. E. Reichmann and P. A. Charlwood, *Can. J. Chem.*, **32**, 1092 (1954).

[4] H. A. Saroff, G. I. Loeb and H. A. Scheraga, *J. Am. Chem. Soc.*, **77**, 2908 (1955).

[5] P. Bro, S. J. Singer and J. M. Sturtevant, *ibid.*, **77**, 4924 (1955).

[6] H. Dintzis, Doctoral Dissertation, Harvard University, 1952.

[7] M. J. Kronman and M. D. Stern, THIS JOURNAL, **59**, 969 (1955).

[8] B. A. Brice, M. Halwer and R. Speiser, *J. Optical Soc. Am.*, **40**, 768 (1950).

[9] M. Halwer, G. C. Nutting and B. A. Brice, *J. Am. Chem. Soc.*, **73**, 2786 (1951).

[10] H. M. Dintzis, in press.

[11] F. F. Nord, M. Bier and S. N. Timasheff, *J. Am. Chem. Soc.*, **73**, 289 (1951).

[12] Since all multiangle light scattering measurements were taken at a single concentration, the assumption was made that the second virial coefficient is very small at an ionic strength of 0.20 and can be neglected. This assumption has been shown experimentally to be valid as a close approximation.[13] It was also assumed that the thermodynamic interaction term contribution to the intercept in multicomponent light scattering measurements[14] was negligible in the case of BSA.[15]

[13] R. J. Gibbs and S. N. Timasheff, to be submitted for publication to the *Arch. Biochem. and Biophys.*

[14] J. G. Kirkwood and R. J. Goldberg, *J. Chem. Phys.*, **18**, 54 (1950).

[15] H. M. Dintzis, S. N. Timasheff, J. G. Kirkwood and B. D. Coleman, Abstracts, 126th Meeting of the American Chemical Society, New York, Sept., 1954.

[16] If the solution was filtered and used immediately after adjustment of *p*H to 3.0, a large dissymmetry appeared. This was followed by the precipitation of the residual bound ketone[17] liberated from the protein.

[17] P. Bro, private communication to S. N. Timasheff.

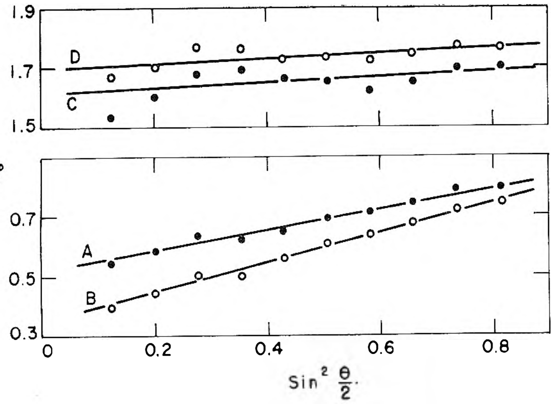

Fig. 1.—Angular scattering envelope for non-deionized BSA solutions in pH 4.0 acetate buffer ($\Gamma/2$ = 0.20): A, 2.1% protein, 325–650 sec; B, same, 4,500–4,600 sec.; C, solution diluted to 0.78%, 8,000 sec.; D, same, 20,000 sec.

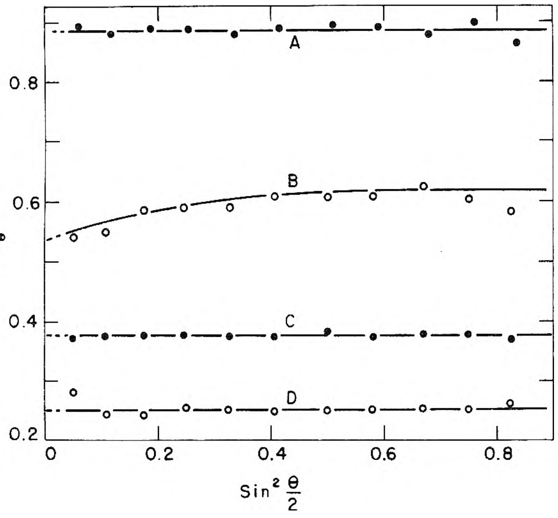

Fig. 2.—Angular scattering envelope for deionized BSA solutions in pH 3.0 HCl–NaCl (0.20 M NaCl): A, 0.72% protein, 13,000–14,000 sec.; B, same, 75,300–76,100 sec.; C, 0.68% protein, 100–800 sec.; D, same, 62,000–63,000 sec. (All times are from the moment of dilution. The concentrated stock solutions had remained overnight at refrigerator temperature.)

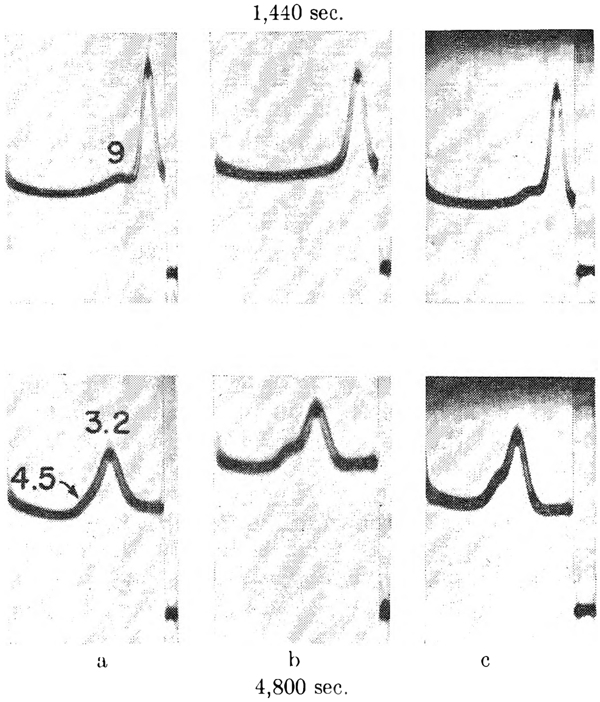

Fig. 3.—Ultracentrifugal patterns of deionized BSA in pH 3.0 HCl–KCl ($\Gamma/2$ = 0.20): a, solution deionized at 25° and lyophilized; run immediately after light scattering (curve B of Fig. 2); b, solution deionized at 4° and used fresh; analyzed in ultracentrifuge after standing 5 days at 25° and 21 days at 4° at pH 3.0; c, solution deionized at 4°, frozen for 6 weeks; analyzed after standing 5 days at 25° at pH 3.0. (In all cases, sedimentation proceeds from right to left.)

and to 182,000 after 21 hours. Ultracentrifugal analysis[18] of this solution at the end of the light scattering experiment showed the presence of two heavy components (10% of $S_{20,w}$ = 4.55, 15% of $S_{20,w}$ = 8.97) in addition to the normal albumin boundary ($S_{20,w}$ = 3.18) (Fig. 3a). Such a composition of the solution corresponds well to a weight average molecular weight of 182,000.

Another run done under similar conditions and shown by curves C and D of Fig. 2, indicates that a protein solution which had aggregated to a molecular weight of 400,000 after standing for 20 hours after dilution at room temperature (curve D) displayed no angular dissymmetry. This would indicate that extensive aggregation can occur in BSA at pH 3.0 without increasing drastically the length of the kinetic unit. Such a case would be possible only if the aggregation were mostly of a side-by-side rather than end-to-end type. The difference in the extent of aggregation observed with these two similarly treated solutions is a good example of the observed variation[17] in the extent and rate of aggregation of BSA in acid pH.

Another set of light scattering measurements was carried out with a BSA solution which had been deionized at 4°. In this case, light scattering measurements, reported in detail elsewhere,[13] were carried out in the pH range of 2.6–3.2 in HCl–KCl media of 0.01 and 0.20 ionic strengths. The solutions were measured both immediately after deionization and also after six weeks storage in a frozen condition. The deionized protein was adjusted to the conditions of the experiment and then permitted to stand overnight at refrigerator temperature. Each solution was then brought to 25°, filtered and used immediately in 90° light scattering measurements as a function of concentration. In view of the complete symmetry obtained in the multiangle experiments described above, no dissymmetry measurements were made. The results obtained yielded molecular weight values of a magnitude similar to that normally obtained for BSA at isoionic pH's (72,000–80,000).[15,20] Ultracentrifugal analyses carried out on these solutions immediately after the light scattering measurements showed no differences from pictures obtained at pH 5.6 in 0.1 M KCl.

When the solutions used in the last light scatter-

---

[18] All values of sedimentation constants and area analysis are those measured at a total protein concentration of 0.7–0.8%. They are not corrected for the Johnston and Ogston anomaly.[19]

[19] J. P. Johnston and A. G. Ogston, *Trans. Faraday Soc.*, **42**, 789 (1946).

[20] S. N. Timasheff, H. M. Dintzis, J. G. Kirkwood and B. D. Coleman, *Proc. Nat. Acad. Sci. U. S.*, **41**, 710 (1955).

ing experiments were permitted to stand for five days at 25°, no change was observed in the ultracentrifugal patterns in the case of the 0.01 ionic strength solutions. In the case of the 0.20 ionic strength solutions, however, various degrees of aggregation were found, depending on the treatment of the deionized stock BSA solution. Thus, when the experiments were done on a freshly deionized BSA solution, the ultracentrifugal analyses, taken after five days at 25° followed by 21 days at 4° showed the presence of only 18% of the "dimer" (Fig. 3b), but no heavier (8.97 *S*) component. The deionized solution that had been kept for six weeks in a frozen condition prior to adjustment of the *p*H to 3.0, after standing for four days at room temperature in *p*H 3.0 KCl–HCl of 0.20 ionic strength, yielded ultracentrifugal pictures which showed the presence of equal amounts (*ca.* 15%) of the "dimer" and of the heavier (8.97 *S*) component (Fig. 3c).

These results, which indicate that aggregation occurs in BSA at *p*H 3.0 at high ionic strength, are in good agreement with recent reports.[4,5] The observed dependence of the aggregation on pretreatment of the BSA is also consistent with the findings of Halwer, *et al.*[9] Furthermore, the low values of the sedimentation constants of BSA obtained at *p*H 3 are in complete agreement with those reported by Bro, Singer and Sturtevant[5] and, as proposed by these authors, they "provide additional evidence" for the reversible expansion of BSA in acid solution, described by Yang and Foster[21] and by Tanford, *et al.*[22]

It would appear from the above observations that deionization in the cold followed by immediate use of the protein solution results in a preparation which is fairly resistant to aggregation at acid *p*H's. Freezing of the deionized solution or deionization at room temperature followed by lyophilization results in a more labile material. The data obtained in the *p*H region of 4.0 to 5.0 with deionized and non-deionized preparations indicate that in the latter case complications arise due to the presence of an ionic "impurity." This leads to the formation of very heavy aggregates which, however, can be dissociated by dilution. Since the dilution also reduces the concentration of the free "impurity" in the solution, it might possibly lead to a shift in the equilibrium toward disaggregation. That the size of the aggregate in the last case is very large and its concentration is small can be concluded from the pronounced dissymmetry of light scattering and also from the fact that ultracentrifugal analyses of BSA under similar conditions give no evidence for the presence of significant amounts of very large components.

Summary.—Light scattering and ultracentrifugal measurements have been carried out on deionized and non-deionized solutions of BSA in acid *p*H's. It was found that while the non-deionized solutions aggregated readily, the deionized protein aggregated only at the lower *p*H's (∼3) in high salt concentration. The rate and extent of aggregation were erratic. No appreciable dissymmetry was observed with the deionized protein, indicating that the associated units are compact.

Acknowledgment.—We would like to thank Dr. P. Bro and Dr. S. J. Singer for discussing our data and making their paper[5] available to us prior to publication.

---

[21] T. J. Yang and J. F. Foster, *J. Am. Chem. Soc.*, **76**, 1588 (1954).

[22] C. Tanford, J. G. Buzzell, D. G. Rands and S. A. Swanson, *ibid.*, **77**, 6421 (1955).

A PRELIMINARY LIGHT SCATTERING STUDY OF THE ENZYMATIC DEGRADATION OF DESOXYRIBOSE NUCLEIC ACID

BY M. E. REICHMANN[1]

Contribution from Gibbs Laboratory, Harvard University, Cambridge Massachusetts

Received February 9, 1956

With the demonstration that the weight and shape of molecules of desoxyribose nucleic acid (DNA) can be determined by light scattering methods[2] and with the Watson–Crick model[3] available for describing the detailed structure of DNA it appeared of interest to examine the nature of the enzymatic degradation using the specific enzyme DNase. In this way the initial stages of the attack could be examined in contrast to the later stages that have been the subject of much investigation and one might hope to learn in some detail how the enzyme degrades the native DNA structure. One possibility would be that the enzyme is end-selective, that is, that it dislodges fragments from the ends of the DNA molecule. Another is that the enzyme breaks the double chain at random either because it can bring about the simultaneous scission of two juxtaposed ester bonds or because its action is so rapid that it tends to destroy a number of ester bonds in any locale before it diffuses away. Still a third possibility is that the enzyme breaks only one ester bond at a time and does this at random. In this case the molecular weight decay would be retarded: the details would be similar to the analysis made by Thomas and Doty[4] in a recent study of acid degradation of DNA. The study of the fall in molecular weight with time will have a quite different pattern for each of the three cases mentioned here and for others not enumerated. Consequently, our attention focused on finding the conditions under which the light scattering observations could be carried out on a degrading system and then in observing the pattern of molecular weight decay.

Experimental.—DNA prepared by Dr. R. Varin and described previously[5] was employed together with DNase from the Worthington Biochemical Sales Co. (2 × recrystallized). It was found necessary to add the magnesium salt activator to the enzyme and then add this mixture to the DNA solution. Using this procedure angular intensity measurements (30–135°) were made on three very dilute DNA solutions to which different amounts of DNase had been added. A borate buffer of *p*H 7.4 served as solvent and both the DNA and enzyme–magnesium salt solution

---

[1] Science Service, Canada Agriculture, Ottawa, Ontario, Canada.

[2] See for example, M. E. Reichmann, S. A. Rice, C. A. Thomas and P. Doty, *J. Am. Chem. Soc.*, **76**, 3047 (1954).

[3] F. H. C. Crick and J. D. Watson, *Proc. Roy. Soc.* (*London*), **A223**, 80 (1954).

[4] C. A. Thomas, Jr., and P. Doty, *J. Am. Chem. Soc.*, **78**, 1854 (1956).

[5] M. E. Reichmann, R. Varin and P. Doty, *ibid.*, **74**, 3203 (1952).

were centrifuged at about 100,000 *g* for 30 minutes before beginning the experiment.

The slowest reaction, employing 0.08 *M* buffer in 0.1 *M* NaCl, enzyme at 2.2 γ/ml., $MgSO_4$ at 2.6 γ/ml. and DNA at 150 γ/ml., was perhaps the most interesting. The Mg^{++} concentration in this experiment is lower than the phosphorus concentration in order to slow down the rate of reaction. Plotting the scattering data as Kc/R_0 against $\sin^2/\theta/2$ it was found that the plots were translated upward as a function of time with practically no change in slope. This is directly interpreted as showing that the mean square end-to-end dimension of the DNA molecules was decreasing in proportion to the molecular weight. This indicates that the structural features of the double chain remain intact even though a degradation into smaller units occurred.

The molecular weight as a function of time showed a marked retardation before undergoing a substantial decline. No change in molecular weight occurred during the first 50 minutes. After this period the molecular weight decreased, reaching 20% of its original value in 10 hours. Thus the double chain scission is preceded by a period in which no dissociation of the DNA molecule into small segments occurred.

In a fast reaction carried out at six times the enzyme concentration only one point could be measured which showed the retardation effect. The reaction proceeded roughly 10 times faster and after 3 hours slowed noticeably.

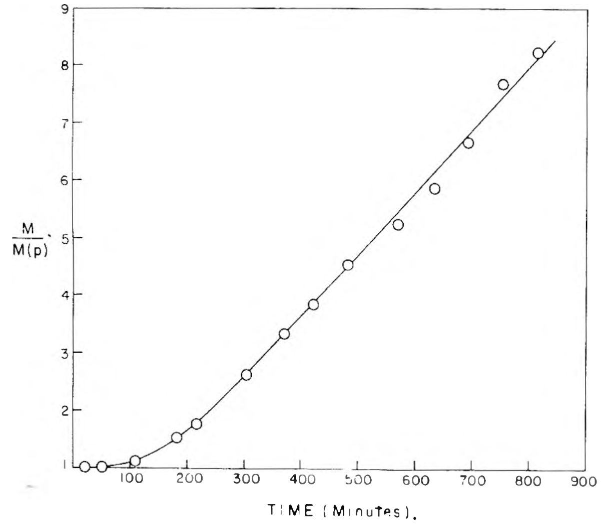

Fig. 1.—Enzymatic degradation of DNA reciprocal of the relative decrease in weight average molecular weight with time.

The third experiment aimed at producing the maximum degradation consistent with this type of conditions. The enzyme and $MgSO_4$ concentration were similar to the first experiment but no NaCl was present since it inhibits the enzyme. Because of the low ionic strength in this case the value of Kc/R_0 can no longer be taken as a good approximation to the reciprocal weight average molecular weight. The much larger value of the virial coefficient raises Kc/R_0 and therefore indicates a lower apparent value for the molecular weight. Thus under these conditions the *apparent* molecular weight initially was 3.3 million rather than the known value of 6.8 million. Within 1.5 hours this had fallen to an apparent value of 285,000. It was unchanged 15.5 hours later when double the initial amount of DNase was added. After four days the apparent molecular weight was only slightly lower: 190,000.

Discussion.—These results point to three conclusions regarding the enzymatic degradation of DNA: (1) There is initially a retardation in the molecular weight decay. (2) While the molecular weight falls the configurational properties of the fragments seem to be the same as original material. (3) The reaction slows down long before it reaches the stage of mono and dinucleotides.

With regard to the first point it is of interest to note evidence[6,7] that ester bonds are broken at a uniform rate. If this is the case here then it appears that many single bond scissions occur before there is a break in the double chain. Further support for this suggestion comes from plotting the reciprocal of the weight average molecular weight against time as suggested by Thomas and Doty.[4] When this is done random scission of the double chain should produce data falling on a straight (or nearly straight) line with a positive slope. Degradation occurring through the coincidence of single bond cleavages which are themselves random should produce a curve with an initial slope of zero. The data of the first experiment are plotted in this way in the figure. It is seen that indeed the initial slope is zero: the remainder of the curve is consistent with the theoretical predictions of this model. Consequently it appears likely that this represents the principal feature of at least the early stages of enzyme attack. It is of interest to note that the delay in the molecular weight decay observed here and its interpretation explains at once a similar delay in the viscosity decay recently reported by Zamenhof, *et al.*[8]

The second observation, that the configuration is unchanged during the early stages of degradation, indicates that the Watson–Crick structure remains intact except where double chain scission occurs. This same conclusion is reached from the recent observations of the retardation in optical density changes during the reaction.[9]

The third observation is the least original since it has been observed for some time[10] that non-dialyzable fragments remain after exhaustive enzyme attack. The slowing down of the reaction as early as observed in our second experiment, however, indicates other possibilities than the occurrence of enzyme resistant "cores." For example this may be due to inhibition of the enzyme by-products or a gradual aggregation of the fragments to produce what has been called a core.

It is obvious that all of the points mentioned above deserve further investigation of a quantitative manner. Nevertheless, these preliminary results do show the time-dependent light scattering measurements offer a unique attack on this problem and that in this initial application evidence has been found to suggest the general outlines of the degradation reaction.

Acknowledgment.—The collaboration of Professor Paul Doty in this work and useful discussions with Dr. Charles A. Thomas, Jr., are greatly appreciated. This investigation was supported by a research grant (C-2170) from the National Cancer Institute of the National Institutes of Health, Public Health Service.

(6) J. Gregoire, *Bull. soc. chim. biol.*, **34**, 284 (1952).

(7) L. F. Cavalieri and B. Hatch, *J. Am. Chem. Soc.*, **75**, 1110 (1953).

(8) S. Zamenhof, G. Griboff and N. Marullo, *Biochim. Biophys. Acta*, **13**, 459 (1954).

(9) C. A. Dekker and H. K. Schachman, *Proc. Natl. Acad. Sci.*, **40**, 894 (1954).

(10) S. Zamenhof and E. Chargaff, *J. Biol. Chem.*, **178**, 531 (1949).

ORDER THESE SPECIAL PUBLICATIONS FOR YOUR PERMANENT RECORDS

Selected For Reprinting Solely On The Basis Of Their Importance To You

UNIT OPERATIONS REVIEWS

1st Annual Review	$0.50
2nd Annual Review	0.50
4th Annual Review	0.50
5th Annual Review	0.50
6th Annual Review	0.50
7th Annual Review	0.75
8th Annual Review	0.75
9th Annual Review	0.75

FUNDAMENTALS REVIEWS

1st Annual Review	0.75
2nd Annual Review	0.75

UNIT PROCESSES REVIEWS

1st Annual Review	0.50
5th Annual Review	0.75
7th Annual Review	1.50

MATERIALS OF CONSTRUCTION REVIEWS

3rd Annual Review	0.50
4th Annual Review	0.75
5th Annual Review	0.75
6th Annual Review	0.75
7th Annual Review	0.75
8th Annual Review	1.50

ANALYTICAL CHEMISTRY REVIEWS

2nd Annual Review	1.50
3rd Annual Review	1.50
5th Annual Review	0.75
7th Annual Review	1.50

INDUSTRIAL & ENGINEERING CHEMISTRY REVIEWS

March 1955 edition includes: 3rd Fundamentals Review 10th Unit Operations Review	2.00
September 1955 edition includes: 9th Annual Materials of Construction Review 8th Unit Processes Review	2.00

RESOURCES SYMPOSIA

Southwest	0.50
Far West	0.50
New England	0.75
Mid Atlantic	0.75
Rocky Mountain—Part 1	0.75
East North Central States	0.75
West North Central States	0.75
South Atlantic States	0.75

MISCELLANEOUS REPRINTS

Raman Spectra	0.35
Corrosion Testing in Pilot Plants	0.25
Atmospheric Contamination and Purification Symposium	0.75
Titanium Symposium	0.50
Adsorption Symposium	0.50
Careers in Chemistry & Chemical Engineering	1.50
Information Please Symposium	0.50
Dispersion in Gases	0.50
Statistical Methods in Chemical Production	0.50
Liquid Industrial Wastes Symposium	0.75
Nucleation Phenomena	0.75
Chemical Facts and Figures—1952	1.00
Corrosion Data Charts	0.75
Synthetic Fibers	1.00
Chemical Progress in 1952	0.75
Chemical Facts and Figures 1954	1.50
Process Kinetics Symposium	0.75
X-Ray Symposium	0.75
Emulsion Paints	0.75
Industrial Process Water Symposium	0.75
Symposium on Pilot Plants	0.75
Symposium on Boiler Water Chemistry	0.75
Flow through Porous Media	0.75
Process Instrumentation Symposium	0.75
First Air Pollution Review	0.50
Jet Fuels Symposium	0.75
Symposium on Application of Silicones	0.75
Pulsatory and Vibrational Phenomena	1.25
Plastics as Materials of Construction	1.75

ADVANCES IN CHEMISTRY SERIES

No. 4, Searching the Chemical Literature	2.00
No. 5, Progress in Petroleum Technology	4.00
No. 6, Azeotropic Data	4.00
No. 7, Agricultural Applications of Petroleum Products	1.50
No. 8, Chemical Nomenclature	2.50
No. 9, Fire Retardant Paints	2.50
No. 10, Literature Resources for Chemical Process Industries	6.50
No. 11, Natural Plant Hydrocolloids	2.50
No. 12, Use of Sugars and other Carbohydrates in the Food Industry	3.00
No. 13, Pesticides in Tropical Agriculture	2.50
No. 14, Nomenclature for Terpene Hydrocarbons	3.00
No. 15, Physical Properties of Chemical Compounds	5.85

MISCELLANEOUS

Seventy-Five Eventful Years (History of the ACS)	5.00
Chemistry—Key to Better Living	4.00
Combination of Seventy-Five Eventful Years and Chemistry—Key to Better Living	7.50
List of Periodicals Abstracted by Chem. Abs.	3.00
10 Years Numerical Patent Index (1937–1946)	6.50
27 Year Collective Formula Index	80.00
2nd Decennial Index to Chemical Abstracts	100.00
3rd Decennial Index to Chemical Abstracts	150.60
4th Decennial Index to Chemical Abstracts	120.60
Directory of Chemical and Chemical Processing Plants in the South Atlantic States	1.00

Supply of the above items is limited, and each will be sold only until present stock is exhausted.

Order from: Special Publications Department, American Chemical Society
1155 Sixteenth Street, N.W., Washington 6, D. C.